creative commons
COMMONS DEED

저작자표시-비영리-변경금지 2.0 대한민국

이용자는 아래의 조건을 따르는 경우에 한하여 자유롭게

- 이 저작물을 복제, 배포, 전송, 전시, 공연 및 방송할 수 있습니다.

다음과 같은 조건을 따라야 합니다:

저작자표시. 귀하는 원저작자를 표시하여야 합니다.

비영리. 귀하는 이 저작물을 영리 목적으로 이용할 수 없습니다.

변경금지. 귀하는 이 저작물을 개작, 변형 또는 가공할 수 없습니다.

- 귀하는, 이 저작물의 재이용이나 배포의 경우, 이 저작물에 적용된 이용허락조건을 명확하게 나타내어야 합니다.
- 저작권자로부터 별도의 허가를 받으면 이러한 조건들은 적용되지 않습니다.

저작권법에 따른 이용자의 권리는 위의 내용에 의하여 영향을 받지 않습니다.

이것은 이용허락규약(Legal Code)을 이해하기 쉽게 요약한 것입니다.

Disclaimer

dCollection

이학박사 학위논문

Cretaceous ankylosaurs of Mongolia

: implications for paleobiogeography, paleoecology, and evolution, with a taxonomic review of Mongolian armored dinosaurs

백악기 몽골 갑옷공룡 연구와 이들의 고지리학적, 고생태학적, 진화적 고찰, 그리고 몽골 갑옷공룡의 분류학적 리뷰

2022년 8월

서울대학교 대학원

지구환경과학부

박 진 영

Cretaceous ankylosaurs of Mongolia

: implications for paleobiogeography, paleoecology,

and evolution, with a taxonomic review of

Mongolian armored dinosaurs

지도 교수 이 융 남

이 논문을 이학박사 학위논문으로 제출함

2022년 8월

서울대학교 대학원

지구환경과학부

박 진 영

박진영의 이학박사 학위논문을 인준함

2022년 8월

위 원 장 _____ (인)

부위원장 _____ (인)

위 원 _____ (인)

위 원 _____ (인)

위 원 _____ (인)

ABSTRACT

Ankylosaurs are a group of dinosaurs that are quadrupedal, herbivorous, and have a heavily ornamented skull and parasagittal rows of osteoderms covering the dorsolateral surfaces of the body. Additional ankylosaur specimens were discovered in the Gobi Desert of Mongolia by the Korea-Mongolia International Dinosaur Expedition between 2007 and 2008. They were excavated from the Upper Cretaceous Bayanshiree (Cenomanian−Turonian), Baruungoyot (middle−upper Campanian), and Nemegt (upper Campanian−lower Maastrichtian) formations. Based on the three new skulls from the Bayanshiree Formation of Bayan Shiree cliffs, the diagnosis of *Talarurus plicatospineus* is revised. A new skull with a partial postcranial skeleton collected from the Nemegt Formation in Hermiin Tsav turned out to be a new taxon, *Tarchia tumanovae* sp. nov. A new articulated postcranial specimen from the Baruungoyot Formation in Hermiin Tsav is classified as an indeterminate ankylosaurid dinosaur. The phylogenetic analysis showed that *Talarurus* is sister to the clade that includes the derived Asian ankylosaurines (*Saichania chulsanensis*, *Tarchia kielanae*, and *Zaraapelta nomadis*). It also showed that there was the dispersal of ankylosaurines from Asia to western North America before the Cenomanian. The rostral differences between *Talarurus* and *Tsagantegia*, another ankylosaurine from the Bayanshiree Formation, suggest possible niche partitioning among these taxa. The squamosal horns of *Tar. tumanovae* are divided into the external dermal layer and the underlying squamosal

horn proper. The irregular ventral margin of the base of the upper dermal layer may represent a resorption surface, suggesting that the squamosal horns of some ankylosaurines underwent extreme ontogenetic remodeling. Localized pathologies on the dorsosacral ribs and the tail provide evidence of agonistic behavior. The tail club knob asymmetry of *Tar. tumanovae* resulted from restricted bone growth due to tail club strikes. Furthermore, ankylosaurid diets shifted from low-level bulk feeding to selective feeding during the Baruungoyot and the Nemegt "age" (middle Campanian–lower Maastrichtian). This ankylosaurid niche shifting might have responded to habitat change and competition with other bulk-feeding herbivores. Asian ankylosaurids evolved rigid bodies with a decreased number of pedal phalanges. There were also at least two forms of flank armor within Ankylosauridae, one with spine-like osteoderms and the other with keeled rhomboidal osteoderms. Unique anatomical features related to digging are present in Ankylosauridae, such as dorsoventrally flattened and fusiform body shapes, extensively fused series of vertebrae, anteroposteriorly broadened dorsal ribs, a robust humerus with a well-developed deltopectoral crest, a short and robust ulna with a well-developed olecranon process, a trowel-like manus, and decreased numbers of pedal phalanges. Although not fossorial, ankylosaurids were likely to dig the substrate, taking advantage of it for self-defense and survival. Moreover, all ten ankylosaur species known in Mongolia are reviewed in this dissertation.

Keywords: Ankylosauridae, Ankylosaurinae, *Talarurus plicatospineus*, *Tarchia tumanovae*, niche partitioning, Mongolia

Student Number: 2017-34699

TABLE OF CONTENTS

LIST OF FIGURES

LIST OF TABLES

1. INTRODUCTION

Ankylosauria (Osborn, 1923) is a clade of herbivorous quadrupedal dinosaurs that can be defined as all thyreophorans closer to *Ankylosaurus* than to *Stegosaurus* (Carpenter, 2007; Sues, 2019). They are characterized by a heavily ornamented skull and transverse rows of osteoderms that cover the dorsolateral surfaces of the body (Vickaryous et al., 2007). These dinosaurs are known from the Middle Jurassic to the end of the Late Cretaceous (Brown, 1908; Dong, 1993; Carpenter, 2007) and were distributed on every continent (Vickaryous et al., 2007; Arbour and Currie, 2016; Maidment et al., 2021). Ankylosaurs are subdivided into two major groups, the Nodosauridae (Marsh, 1890) and Ankylosauridae (Brown, 1908). Nodosaurids are defined as all ankylosaurs closer to *Panoplosaurus* than to *Ankylosaurus*, whereas ankylosaurids are defined as vice versa (Sereno, 1998).

Since the discovery of *Pinacosaurus grangeri* by Gilmore (1933), abundant remains of ankylosaurs have been excavated from Mongolia. A total of ten taxa are currently known, and all are placed in the Ankylosauridae (Table 1). The Mongolian taxa are assigned to two subfamilies within the ankylosaurids, the Shamosaurinae (Tumanova, 1983) and Ankylosaurinae (Nopcsa, 1918). The Shamosaurinae are ankylosaurs that are more basal than the Ankylosaurinae. However, the evolution of Mongolian ankylosaurines has been poorly understood, and their interrelationships are still debated among researchers (Carpenter, 2001;

Hill et al., 2003; Vickaryous et al., 2004; Thompson et al., 2012; Arbour and Currie, 2016). It may be because Mongolian ankylosaur taxa mainly were diagnosed based on skull materials, and only a handful of postcranial materials were described in detail.

Additional specimens of ankylosaurs have been excavated from Mongolia during the Korea-Mongolia International Dinosaur Expedition between 2007 and 2008. These specimens include three new skulls of *Talarurus* from the Upper Cretaceous Bayanshiree Formation (Cenomanian–Turonian), an articulated postcranial skeleton of an indeterminate ankylosaurid from the Upper Cretaceous Baruungoyot Formation (middle–upper Campanian), and a new skull with a partial postcranial skeleton of a new taxon from the Upper Cretaceous Nemegt Formation (upper Campanian–lower Maastrichtian). In this dissertation, the newly discovered specimens are described and discussed. The new skulls of *Talarurus* from the Bayanshiree Formation provide new information on their phylogeny, intercontinental exchange of ankylosaurines between Asia and North America during the Cretaceous, and implications for understanding nich partitioning among armored dinosaurs.[1] The new articulated postcranial skeleton from the Baruungoyot Formation provides valuable insight into the postcranial evolution of

[1] This contents was published in the following publication:
Park, J.-Y., Lee, Y.-N., Currie, P.J., Kobayashi, Y., Koppelhus, E., Barsbold, R., Mateus, O., Lee, S., Kim, S.-H., 2020. Additional skulls of *Talarurus plicatospineus* (Dinosauria: Ankylosauridae) and implications for paleobiogeography and paleoecology of armored dinosaurs. Cretaceous Research 108, 104340.

ankylosaurids, and insight based on anatomical features into the possibility of ankylosaurid digging behavior.[2] The skull and postcranial skeleton of the new taxon from the Nemegt Formation provides further evidence of ontogeny, agonistic behavior, and suggestions of niche shifting in Mongolian ankylosaurids.[3] Additionally, all ten Mongolian ankylosaur taxa are reviewed in this dissertation.

[2] This contents was published in the following publication:
Park, J.-Y., Lee, Y.-N., Currie, P.J., Ryan, M.J., Bell, P., Sissons, R., Koppelhus, E.B., Barsbold, R., Lee, S., Kim, S.-H., 2021. A new ankylosaurid skeleton from the Upper Cretaceous Baruungoyot Formation of Mongolia: its implications for ankylosaurid postcranial evolution. Scientific Reports 11, 4101.

[3] This contents was published in the following publication:
Park, J.-Y., Lee, Y.-N., Kobayashi, Y., Jacobs, L.L., Barsbold, R., Lee, H.-J., Kim, N., Song, K.-Y., Polcyn, M.J., 2021. A new ankylosaurid from the Upper Cretaceous Nemegt Formation of Mongolia and implications for paleoecology of armoured dinosaurs. Scientific Reports 11, 22928.

Table 1. Ankylosaur taxa of Mongolia.

Taxa	Occurrence
Ankylosauria Osborn, 1923	
Ankylosauridae Brown, 1908	
Shamosaurinae Tumanova, 1983	
Shamosaurus Tumanova, 1983	
Sh. scutatus Tumanova, 1983	Zuunbayan Formation (Aptian–Albian)
Ankylosaurinae Nopcsa, 1918	
Minotaurasaurus Miles and Miles, 2009	
M. ramachandrani Miles and Miles, 2009	Djadokhta Formation (Campanian)
Pinacosaurus Gilmore, 1933	
P. grangeri Gilmore, 1933	Djadokhta Formation (Campanian)
Saichania Maryañska, 1977	
Sa. chulsanensis Maryañska, 1977	Baruungoyot Formation (middle–upper Campanian)
Talarurus Maleev, 1952b	
Tal. plicatospineus Maleev, 1952b	Bayanshiree Formation (Cenomanian–Santonian)
Tarchia Maryañska, 1977	
Tar. kielanae Maryañska, 1977	Baruungoyot Formation (middle–upper Campanian)
Tar. teresae Penkalski and Tumanova, 2017	Nemegt Formation (upper Campanian–lower Maastrichtian)

(continued)

Taxa	Occurrence
***Tar. tumanovae* sp. nov.**	Nemegt Formation (upper Campanian–lower Maastrichtian)
Tsagantegia Tumanova, 1993	
Ts. longicranialis Tumanova, 1993	Bayanshiree Formation (Cenomanian–Santonian)
Zaraapelta Arbour et al., 2014b	
Z. nomadis Arbour et al., 2014b	Baruungoyot Formation (middle–upper Campanian)

II. MATERIALS AND METHODS

All ankylosaur specimens used in this study were collected during the Korea-Mongolia International Dinosaur Expedition between 2007 and 2008. Fossil preparation was done at the Hwaseong City laboratory of South Korea between 2007 to 2013. All specimens are now permanently held in the Institute of Paleontology, Mongolian Academy of Sciences in Ulaanbaatar, Mongolia. Measurements of the specimens were taken using a measuring tape and a digital caliper. Comparisons to other ankylosaur taxa were made by examining some MPC specimens and published literature. Adobe Illustrator CC (version 24.0.1, https://www.adobe.com/kr/products/illustrator.html) was employed to produce most of the figures.

The Mongolian geographic and stratigraphic names were based on Benton et al. (2000), and the chronostratigraphic framework followed those of Jerzykiewicz and Russell (1991). The term ‘caputegulum’ (*sensu* Blows, 2001) was used herein to refer to the cranial ornamentation of ankylosaurs. Armor terminology followed those of Maryañska (1969) and Arbour et al. (2013), while phalangeal formulae were based on Padian (1992).

For the phylogenetic analysis, the skull-related characters of *Talarurus* were re-coded into the data matrix of Zheng et al. (2018), with the addition of *Akainacephalus* (Wiersma and Irmis, 2018). “*Zhejiangosaurus*” and all

nodosaurids, except for *Gargoyleosaurus* and *Nodosaurus*, were excluded for improved consistency index. One error was also corrected in the data matrix of *Tsagantegia* (character state 15:1 was changed to 15:0). It should note that the data matrix of Zheng et al. (2018), which is based on Arbour and Currie (2016), includes *Minotaurasaurus ramachandrani* within *Tarchia kielanae*, *Tarchia teresae* within *Saichania chulsanensis*, and *Oohkotokia horneri* within *Scolosaurus cutleri*. The revised dataset of 177 characters and 27 taxa (25 ingroup and two outgroup taxa) was analyzed using TNT (Tree Analysis Using New Technology) version 1.1 (Goloboff et al., 2008). All characters were treated as unordered and of equal weight. A traditional search (Wagner trees; swapping algorithm: tree bisection-reconnection; random seeds: 1; replicates: 1000; trees to save per replication: 10) was performed, and the 'Bremer.run' script was used to calculate the Bremer support values on each node of the strict consensus tree.

For the phylogeny of the new taxon from the Nemegt Formation, the character list and data matrix used in this study was modified from Penkalski and Tumanova (2017) (see Supplementary data VIII-2). The modifications include the following: modified one character (5); added two new characters (22 and 23); revised a few character states of *Pinacosaurus grangeri* (character state 5:0 to 15:1) and PIN 3142/250 (holotype of *Tarchia teresae*) (5:? to 5:1, and 6:0 to 6:?). Including the new taxon, seven taxa with 23 characters were analyzed in TNT version 1.1 (Goloboff et al., 2008). A traditional search was performed, using implied character weighting and a k-value of 3.

III. GEOLOGICAL SETTING

The studied specimens are from the Upper Cretaceous Bayanshiree (Cenomanian–Turonian), Baruungoyot (middle–upper Campanian), and Nemegt (upper Campanian–lower Maastrichtian) formations. The Bayanshiree Formation is widely distributed in the Eastern Gobi Basin (Jerzykiewicz and Russell, 1991; Hicks et al., 1999), whereas the Baruungoyot and Nemegt formations are distributed within the Nemegt Basin (Gradziński and Jerzykiewicz, 1974a, b; Gradziński et al., 1977; Jerzykiewicz and Russell, 1991; Jerzykiewicz, 2000; Eberth et al., 2009a, 2018; Fanti et al., 2018; Jerzykiewicz et al., 2021).

III-1. Bayanshiree Formation

The Bayanshiree Formation is a terrestrial sedimentary succession up to 300 m thick (Martinson, 1982; Jerzykiewicz and Russell, 1991; Hicks et al., 1999; Jerzykiewicz, 2000). The formation conformably overlies the Sainshand Formation and unconformably underlies the Javkhlant Formation (Eberth et al., 2009b) (Fig. 1). It is comprised by multi-colored clays with fine-grained fluvial sandstones with calcareous concretions (Vasiliev et al., 1959) and conglomerates (Sochava, 1975; Martinson, 1982; Jerzykiewicz, 2000). Various fossils have been discovered from the Bayanshiree Formation, including freshwater ostracods, mollusks, fishes,

mammals, and an abundance of reptiles, including dinosaurs (Table 2). Comparisons to vertebrate faunas of North American non-marine units, which are well confined by ammonite zonation and palynology, yield a late Cenomanian–Coniacian to early Santonian age (Jerzykiewicz and Russell, 1991). Whereas magnetostratigraphic and palynological analysis suggests a deposit age between Cenomanian to no later than the Santonian (Hicks et al., 1999). Recent calcite U-Pb analyses obtained 89.6 ± 4.0 and 95.9 ± 6.0 Ma between Cenomanian and Turonian (Kurumada et al., 2020). Additional specimens of ankylosaurs have been excavated from Mongolia during the Korea-Mongolia International Dinosaur Expedition between 2007 and 2008. These specimens include three new skulls of *Talarurus* from the Upper Cretaceous Bayanshiree Formation (Cenomanian–Turonian), an articulated postcranial skeleton of an indeterminate ankylosaurid from the Upper Cretaceous Baruungoyot Formation (middle–upper Campanian), and a new skull with a partial postcranial skeleton of a new taxon from the Upper Cretaceous Nemegt Formation (upper Campanian–lower Maastrichtian).

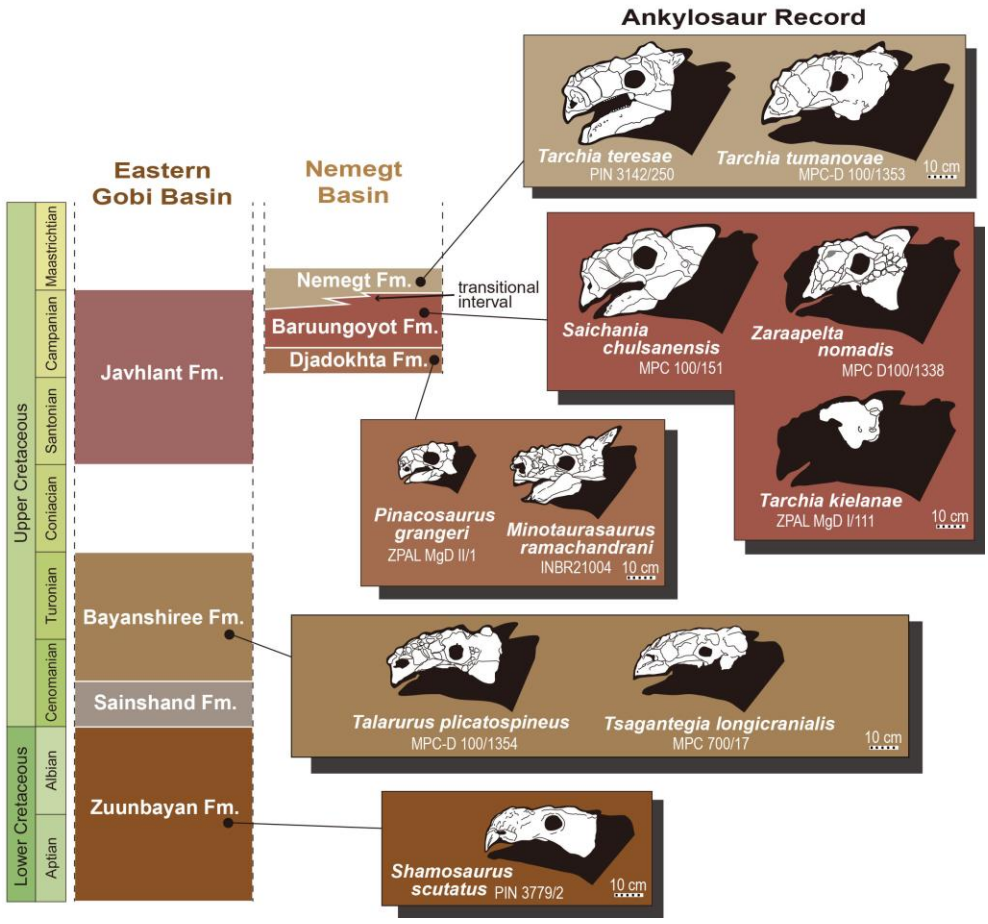

Figure 1. Stratigraphy and ankylosaur record of Eastern Gobi and Nemegt basins.

Table 2. Various fossils reported from the Bayanshiree Formation.

Fossils	References
Freshwater ostracods and mollusks	Barsbold (1972) Sochava (1975) Hicks et al. (1999)
Fishes	Efremov (1949)
Mammals	Rougier et al. (2015)
Turtles	Młynarski and Narmandach (1972) Sukhanov and Narmandach (1975) Chkhikvadze and Shuvalov (1980) Jerzykiewicz and Russell (1991) Sukhanov (2000) Danilov et al. (2014)
Neosuchian crocodyliforms	Efimov (1983) Jerzykiewicz and Russell (1991) Turner (2015) Lee et al. (2019)
Pterosaurs	Watabe et al. (2009)
Dinosaurs	
Ankylosaurs	Maleev (1952b) Tumanova (1987, 1993) Arbour and Currie (2016)
Pachycephalosaurs	Watabe et al. (2011)
Ceratopsians	Maryañska and Osmólska (1975) Jerzykiewicz and Russell (1991)

(continued)

Fossils	References
Hadrosauroids	Maryañska and Osmólska (1975, 1981a) Tsogtbaatar et al. (2019)
Sauropods	Martinson (1982)
Tyrannosaurids	Perle (1977)
Ornithomimosaurs	Jerzykiewicz and Russell (1991) Makovicky et al. (2004)
Therizinosaurids	Jerzykiewicz and Russell (1991) Russell and Dong (1993)
Dromaeosaurids	Barsbold (1983)

III-2. Baruungoyot Formation

The Baruungoyot Formation comprises clastic continental sediments and is up to 135 m thick (Gradziński and Jerzykiewicz, 1974a; Eberth, 2018). The formation conformably overlies the Djadokhta Formation and underlies the Nemegt Formation (Gradziński and Jerzykiewicz, 1974a, b; Gradziński et al., 1977; Jerzykiewicz and Russell, 1991; Jerzykiewicz, 2000; Eberth et al., 2009a, 2018; Fanti et al., 2018) (Fig. 1). This unit is dominated by fine-grained, red-brown, poorly cemented sandstones and siltstones (Gradziński et al., 1977; Jerzykiewicz, 2000; Eberth, 2018). Although rare, red-colored claystone is also present (Gradziński and Jerzykiewicz, 1974a; Gradziński et al., 1977). These sediments are deposited in fluvial, alluvial fan, paludal, lacustrine, and eolian environments (Eberth et al., 2009a; Eberth, 2018). Fossils from the Baruungoyot Formation include invertebrates, fishes, frogs, mammals, turtles, and various squamates and dinosaurs (Table 3). The age of the Baruungoyot Formation was variously suggested. Comparisons of mammalian taxa yield a possible early Campanian (Kielan-Jaworowska, 1974a, 1974b) or questionably mid-Campanian age (Kielan-Jaworowska, 1975a, 1975b; Kielan-Jaworowska and Trofimov, 1980), or late Campanian, and/or early Maastrichtian age (Lillegraven and McKenna, 1986). A Santonian–Campanian age was proposed based on turtle taxa (Shuvalov and Chkhikvadze, 1975) and a Santonian–Maastrichtian age ostracod records (Stankevich and Khand, 1976). Whereas a study on charophytes suggested a late Santonian age (Karczewska and Ziembińska-Tworzydło, 1983). However, based on

the correlations of vertebrate records with those of North American rock units, the Baruungoyot Formation is regarded as the middle–late Campanian in age (Jerzykiewicz and Russell, 1991).

Table 3. Various fossils reported from the Baruungoyot Formation.

Fossils	References
Diplopods	Dzik (1975)
Invertebrate traces	Eberth et al. (2009a) Eberth (2018)
Fishes	Kurzanov (1987)
Frogs	Borsuk-Bialynicka (1978) Špinar and Tatarinov (1986)
Mammals	Kielan-Jaworowska (1969, 1974a, 1974b, 1975a, 1975b) Gradziński et al. (1977) Kielan-Jaworowska and Trofimov (1980) Kurzanov (1987) Jerzykiewicz and Russell (1991) Kielan-Jaworowska et al. (2000, 2003) Kielan-Jaworowska (2013)
Turtles	Młynarski (1972) Jerzykiewicz and Russell (1991)
Squamates	Gilmore (1943) Sulimski (1975) Gradziński et al. (1977) Sulimski (1978, 1984) Borsuk-Białynicka (1984) Borsuk-Białynicka and Moody (1984) Borsuk-Białynicka (1985, 1988) Jerzykiewicz and Russell (1991) Norell et al. (1992) Norell and Gao (1997)

(continued)

Fossils	References
	Gao and Norell (1998) Alifanov (2000) Conrad et al. (2011) Tałanda (2017)
Dinosaurs	
Pachycephalosaurs	Maryańska and Osmólska (1974) Perle et al. (1982) Sereno (2000) Sullivan (2006)
Protoceratopsids	Maryańska and Osmólska (1975) Kurzanov (1987, 1990) Sereno (2000) Alifanov (2003, 2008) Matsumoto and Saneyoshi (2010) Kim et al. (2019) Czepiński (2019)
Ankylosaurs	Maryańska (1977) Tumanova (2000) Carpenter et al. (2011) Kielan-Jaworowska (2013) Arbour et al. (2014) Penkalski and Tumanova (2017)
Sauropods	Kurzanov and Bannikov (1983) Weishampel et al. (2004)
Ornithomimids	Jerzykiewicz and Russell (1991)
Alvarezsaurs	Karhu and Rautian (1996)

(continued)

Fossils	References
	Alifanov and Barsbold (2009)
Oviraptorosaurs	Barsbold (1981, 1986) Currie (2000) Kundrát and Janáček (2007) Longrich et al. (2010) Fanti et al. (2012)

III-3. Nemegt Formation

Exposed in the northern and central parts of the Nemegt Basin, the Nemegt Formation is the youngest rock unit of the Cretaceous of Mongolia (Gradziński, 1970; Gradziński and Jerzykiewicz, 1974b) (Fig. 1). It is composed of clastic continental sediments and is about 235 m thick (Gradziński and Jerzykiewicz, 1974a; Eberth, 2018). The formation conformably overlies the Baruungoyot Formation, and an approximately 25 m thick interfingering interval is present between the two units (Gradziński, 1970; Gradziński and Jerzykiewicz, 1974a, b; Gradziński et al., 1977; Jerzykiewicz and Russell, 1991; Jerzykiewicz, 2000; Eberth, 2009a, 2018; Fanti et al., 2018). It is dominated by light grey to tan colored, poorly cemented sandy mudstones and sandstones, which were deposited in fluvial, lacustrine, and paludal environments (Gradziński and Jerzykiewicz, 1974a; Gradziński et al., 1977; Eberth, 2009a, 2018). The Nemegt Formation is considered as the most fossiliferous among the Cretaceous rock units of Mongolia (Jerzykiewicz, 2000). A variety of fossils have been discovered, including invertebrates, fishes, frogs, mammals, and dinosaurs (Table 4). A Maastrichtian age was proposed for the Nemegt Formation based on gastropod and bivalve records (Barsbold, 1972; Martinson, 1975), while the studies on charophytes suggested a Campanian–Maastrichtian age (Karczewska and Ziembiúska-Tworzydło, 1970; Kjansep-Romaschkina, 1975). A late Campanian to early Maastrichtian age was proposed based on taxonomical similarity of the Mongolia hadrosaur *Saurolophus angustirostris* with the North American *Saurolophus osborni* (Rozhdestvensky,

1971, 1974). This proposal is supported by correlations of vertebrate records with those of North American rock units (Jerzykiewicz and Russell, 1991). Recently, Jerzykiewicz et al. (2021) proposed that Djadokhta, Baruungoyot, and Nemegt formations are coeval, based on a number of overlapping fossil taxa, and the Upper Cretaceous Gobi Basin can be visualized as an ephemeral lake surrounded by semi-arid alluvial plains and arid dune fields.

Table 4. Various fossils reported from the Nemegt Formation.

Fossils	References
Charophytes	Karczewska and Ziembiúska-Tworzydło (1970) Kjansep-Romaschkina (1975) Gradziński et al. (1977) Karczewska and Ziembiúska-Tworzydło (1983)
Ostracods	Szczechura and Błaszyk (1970) Stankevitch and Khand (1976) Gradziński et al. (1977)
Branchiopods	Novojilov (1954)
Gastropods	Barsbold (1971, 1972) Martinson (1975)
Bivalves	Barsbold (1972) Martinson and Kolesnikov (1974)
Invertebrate traces	Eberth et al. (2009a) Eberth (2018)
Fishes	Jerzykiewicz and Russell (1991) Sereno et al. (2009) Fowler et al. (2011) Newbrey et al. (2013) Kim et al. (2022)
Frogs	Gubin (1993)
Mammals	Clemens et al. (1979) Suzuki and Watabe (2000)

(continued)

Fossils	References
Squamates	Alifanov (1993a, b, c, 2000)
Turtles	Khosatzky and Młynarski (1971) Młynarski and Narmandakh (1972) Shuvalov and Chkhikvadze (1975, 1979) Jerzykiewicz and Russell (1991) Khosatzky (1999) Sukhanov (2000) Suzuki and Narmandakh (2004) Danilov et al. (2014)
Neosuchian crocodyliforms	Konzhukova (1954) Efimov (1983) Jerzykiewicz and Russell (1991) Storrs and Efimov (2000) Turner (2015)
Pterosaurs	Tsuihji et al. (2017)
Dinosaurs	
Ankylosaurs	Maleev (1956) Maryañska (1969) Tumanova (1977, 1987) Arbour et al. (2013, 2014) Penkalski and Tumanova (2017) Paulina-Carabajal et al. (2018)
Pachycephalosaurs	Maryañska and Osmólska (1974) Sullivan (2006) Evans et al. (2011, 2018)
Hadrosaurids	Rozhdestvensky (1952)

(continued)

Fossils	References
	Gradziński et al. (1977)
	Maryańska and Osmólska (1979, 1981a, b)
	Norman and Sues (2000)
	Bell (2011)
	Dewaele et al. (2015)
	Bell et al. (2018)
Sauropods	Nowinski (1971)
	Borsuk-Białynicka (1977)
	Barsbold et al. (2000)
	Maryańska (2000)
	Wilson (2005)
	Currie et al. (2018)
	Averianov and Lopatin (2019)
Tyrannosauroids	Maleev (1955, 1965, 1974)
	Kurzanov (1976)
	Carpenter (1992)
	Olshevsky (1995a, b)
	Osmólska (1996)
	Carr (1999)
	Currie (2000)
	Hurum and Sabath (2003)
	Saveliev and Alifanov (2007)
	Brusatte et al. (2009)
	Sereno et al. (2009)
	Fowler et al. (2011)
	Tsuihiji et al. (2011)
	Brusatte et al. (2012)
	Bever et al. (2013)
	Owocki et al. (2020)

(continued)

Fossils	References
Ornithomimosaurs	Osmólska and Roniewicz (1970) Osmólska et al. (1972) Pawlicki and Bolechała (1987) Barsbold (1988a) Hurum (2001) Norell et al. (2001) Barrett (2005) Kobayashi and Barsbold (2006) Phil and James (2010) Bell et al. (2012) Lee et al. (2014) Lee et al. (2018)
Alvarezsaurs	Perle et al. (1993, 1994) Zhou (1995) Novas (1996) Chiappe et al. (1998) Kurochkin (2000) Senter (2005) Lee et al. (2019a)
Therizinosaurs	Maleev (1954a) Osmólska and Roniewicz (1970) Rozhdestvenskii (1970) Barsbold (1976) Perle (1982) Phil and James (2010)
Oviraptorosaurs	Gradziński et al. (1977) Kurzanov (1981) Osmólska (1981)

(continued)

Fossils	References
Dromaeosaurids	Barsbold (1986a, 1988b, 2000 Lü et al. (2004, 2005) Currie et al. (2015) Tsuihiji et al. (2016) Funston et al. (2018) Lee et al. (2019b)
	Barsbold (1983) Jerzykiewicz and Russell (1991)
Troodontids	Barsbold (1974) Osmólska (1987) Kurzanov and Osmólska (1991) Norell et al. (2009)
Birds	Nessov and Borkin (1983) Kurochkin (1988a, b, 1999, 2000)
Eggs	Sochava (1969) Mikhailov (1991) Sabath (1991) Mikhailov (2000) Weishampel et al. (2008) Montanari et al. (2013)
Tracks	Currie et al. (2003) Ishigaki (2010) Eberth (2018) Lee et al. (2018) Nakajima et al. (2018) Stettner et al. (2018)

IV. RESULTS

IV-1. Systematic paleontology

Dinosauria Owen, 1842; *sensu* Padian and May, 1993

Ornithischia Seeley, 1887; *sensu* Padian and May, 1993

Thyreophora Nopcsa, 1915; *sensu* Sereno, 1986

Ankylosauria Osborn, 1923; *sensu* Carpenter, 2007

Ankylosauridae Brown, 1908; *sensu* Sereno, 1998

Ankylosaurinae Nopcsa, 1918; *sensu* Sereno, 1998

Talarurus Maleev, 1952b

Talarurus plicatospineus Maleev, 1952b

Type specimen. PIN 557/91, an incomplete posterior portion of the skull (Maryañska, 1977).

Type locality and horizon. Upper Cretaceous (Cenomanian–Turonian) Bayanshiree Formation, Bayan Shiree, eastern Gobi Desert, Mongolia.

Studied specimens. MPC-D 100/1354, a nearly complete cranium except for the damaged right dorsal surface. MPC-D 100/1355, a skull (lacking the nasal area) with one partial left mandible, one partial cervical half ring, one dorsal vertebra, one dorsal rib piece, and other postcranial fragments. MPC-D 100/1356, a cranium lacking the nasal area (Figs. 2–10). All specimens are from the type locality.

Revised diagnosis. An ankylosaurid distinguished by the following unique set of characters (autapomorphies with an asterisk): an anteriorly protruded single internarial caputegulum*; around 20 flat or concave caputegulae surrounded by a broad sulcus present in the nasal region*; a vertically oriented, elongate loreal caputegulum with pitted surface*; an elongate lacrimal caputegulum positioned above the posterodorsal border of the maxilla*; two longitudinally arranged large frontoparietal caputegulae surrounded by smaller rhomboid caputegulae*; small but elongate medial supraorbital caputegulae*; a posterior supraorbital caputegulum that is four times larger than the anterior one*; up to three transverse parallel grooves on the dorsal surface of the posterior supraorbital caputegulum*; a "neck" present at the base of the quadratojugal horn (shared with *Pinacosaurus mephistocephalus* and *Minotaurasaurus*); postocular caputegulae ventral to the posterior rim of the orbit extend almost to the anteroventral margin of the squamosal horn*; a longitudinal furrow tapering towards the apex of the squamosal horn*; a lateral nuchal caputegulum four to five times larger than surrounding nuchal caputegulae*; ventral margin of the pterygovomerine keel positioned dorsal to the alveolar ridge*; paired basal tubera of basisphenoid medially divided (shared with *Akainacephalus* and *Gobisaurus*); short paroccipital span that does not reach the squamosal horns (shared with *Akainacephalus* and *Minotaurasaurus*).

Remarks. Numerous specimens of *Talarurus* have been collected, including partial postcranial skeletons of six individuals from the Bayan Shiree cliffs and many fragmentary specimens from nearby localities (Tumanova, 1987, 2000; Arbour and

Currie, 2016). However, cranial elements of *Talarurus* are rare, and only two incomplete skulls, including the holotype, were described in the scientific literature (Maleev, 1952b; Tumanova, 1987). The holotype skull (PIN 557-91) only includes the frontal, parietal, and occipital regions with partial squamosal horns (Maleev, 1952b). Another partial cranium (PIN 3780/1) includes the skull roof, occipital regions, and a nearly complete braincase (Tumanova, 1987). Both specimens lack the premaxillae and maxillae, ventral rami of the jugals, the ventral postorbital regions (including the quadratojugal horns), most of the palatal elements, and the mandibles. The three new additional skulls of *Talarurus* described herein are much more complete than the previously reported materials (Figs. 2–10).

All known skull materials of *Talarurus* (PIN 557, 3780/1 and MPC-D 100/1354, 100/1355, 100/1356) share the following characters: polygonal nasal and frontal caputegulae with wide sulci between each; no lacrimal incisure (*sensu* Arbour et al., 2014b); large frontoparietal caputegulae surrounded by smaller caputegulae; small but elongate medial supraorbital caputegulae; laterally protruding large posterior supraorbital caputegulae; no overlap between the posterior border of the supraorbital caputegulum and the anterior border of squamosal horn in lateral view; transverse frontoparietal depression (*sensu* Godefroit et al., 1999); large lateral nuchal caputegulum that is four to five times larger than the medial ones; nuchal caputegulae slightly overhang the posterior margin of the skull; nuchal shelf ventrally fused with the supraoccipital and the paroccipial processes; anterolaterally projected short and stout basipterygoid

processes; medially divided and rounded rugose basal tubera on basisphenoid; posteroventrally directed reniform occipital condyle; foramen magnum wider than high; sagittal nuchal ridge on supraoccipital that increases in transverse width ventrally and dorsally; short paroccipital span that does not reach the squamosal horns; paroccipital process tapers in height towards the lateral terminus and curves ventrally. Among these features, the overall morphology of the caputegulae in general and the supraorbital and nuchal caputegulae, in particular, are considered diagnostic. Therefore, it is apparent that all three new specimens are *Talarurus* (Figs. 2–10).

Talarurus was previously diagnosed by Arbour and Currie (2016) based on a single autapomorphy, which is the presence of a unique V-shaped upraised area, anteromedial to the transverse frontoparietal depression (*sensu* Godefroit et al., 1999). This V-shaped area is observable in PIN 557-91. Although Penkalski (2018) considered this a possible result of taphonomic alteration, it is evident that it is the anterior boundary of the posteriorly situated large frontoparietal caputegulum. However, this boundary is transversely linear in PIN 3780/1 and MPC-D 100/1355. It also appears to be W-shaped in MPC-D 100/1356. Therefore, this seems to vary intraspecifically.

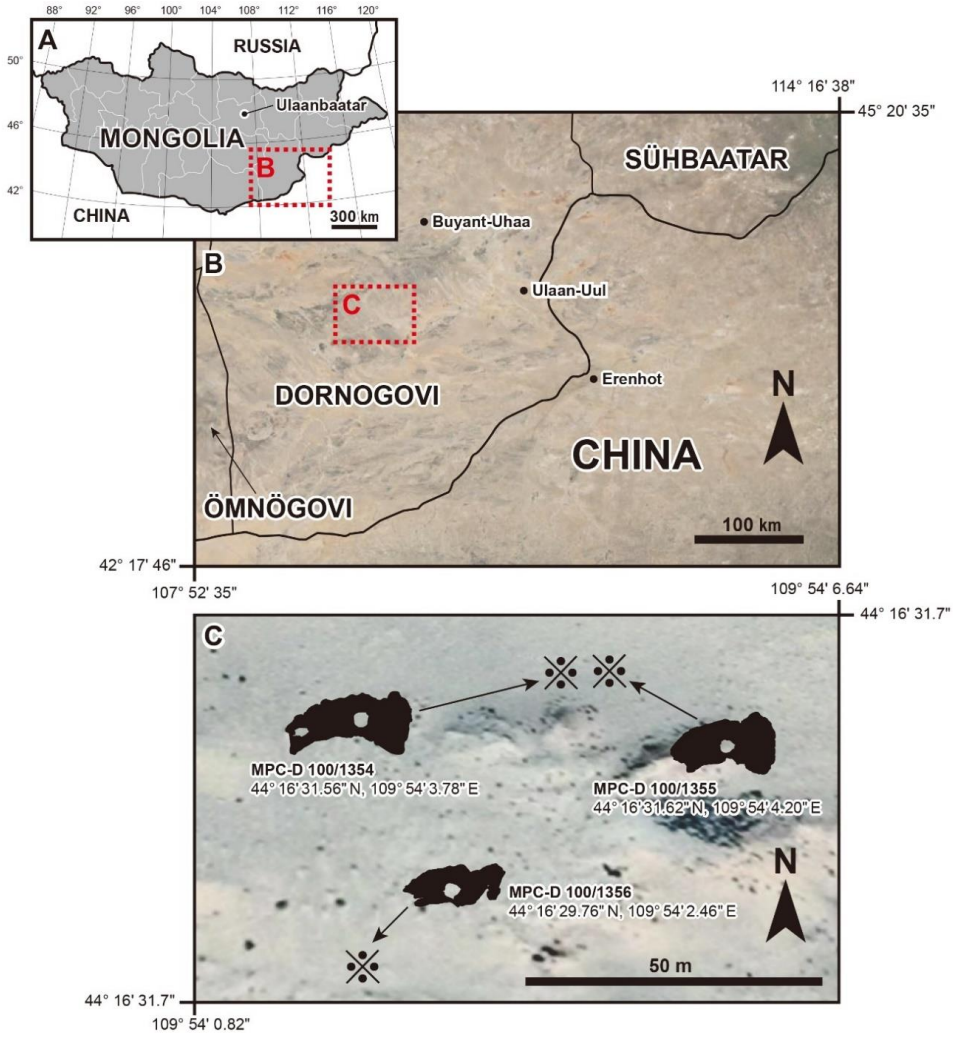

Figure 2. Map showing the locality where the new skull specimens of *Talarurus plicatospineus* were discovered. (A) Map of Mongolia. (B) Magnified map from A (surrounded by the dotted lined rectangle). (C) Magnified map from B (surrounded by the dotted lined rectangle) with the locality marked by the reference mark (※).

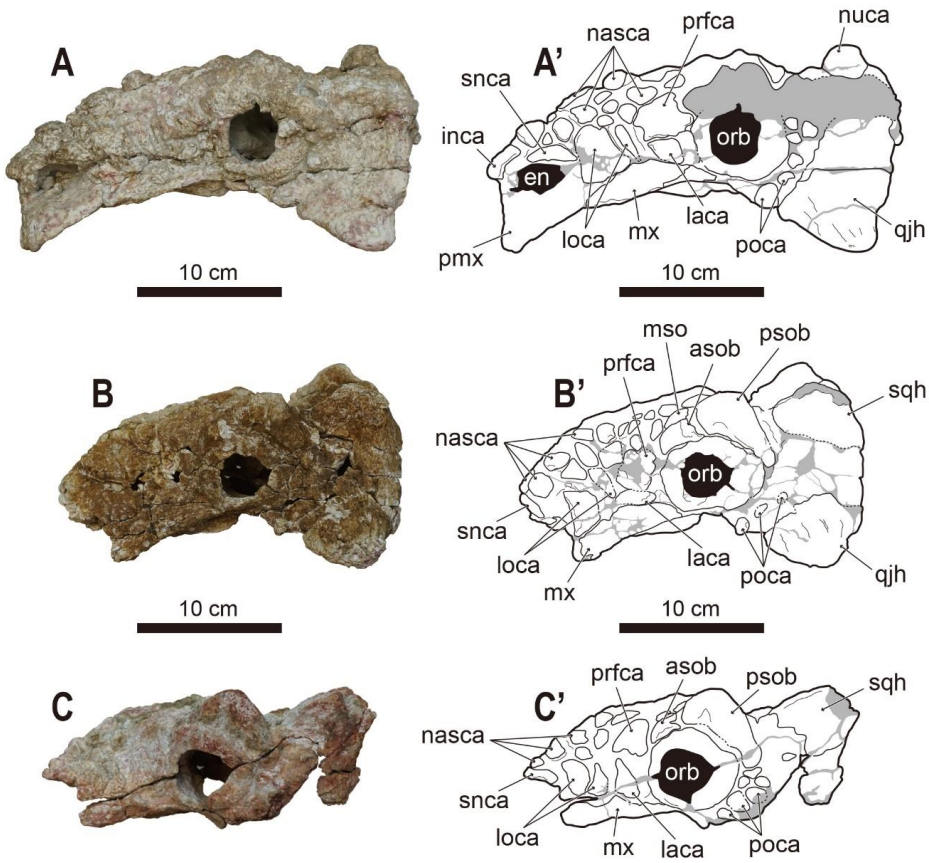

Figure 3. Photographs (A–C) and line drawings (A′–C′) of new skull specimens of *Talarurus plicatospineus* in left lateral view. (A–A′) MPC-D 100/1354. (B–B′) MPC-D 100/1355. (C–C′) MPC-D 100/1356. Grey area indicates a damaged surface.

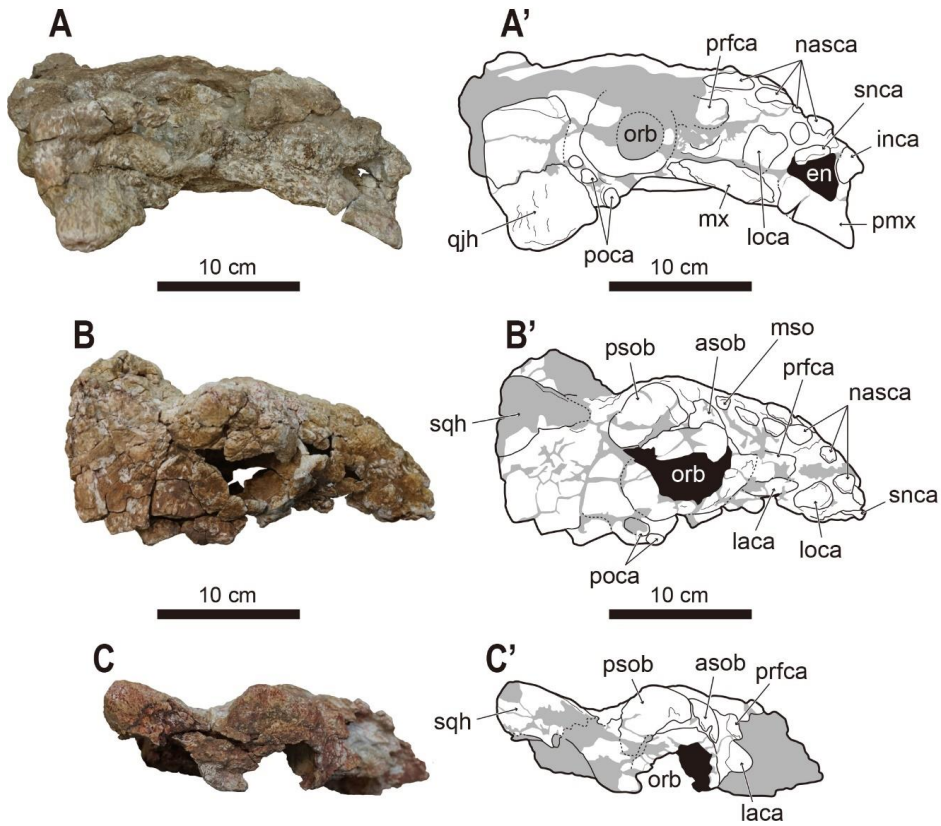

Figure 4. Photographs (A–C) and line drawings (A′–C′) of new skull specimens of *Talarurus plicatospineus* in right lateral view. (A–A′) MPC-D 100/1354. (B–B′) MPC-D 100/1355. (C–C′) MPC-D 100/1356. Grey area indicates a damaged surface.

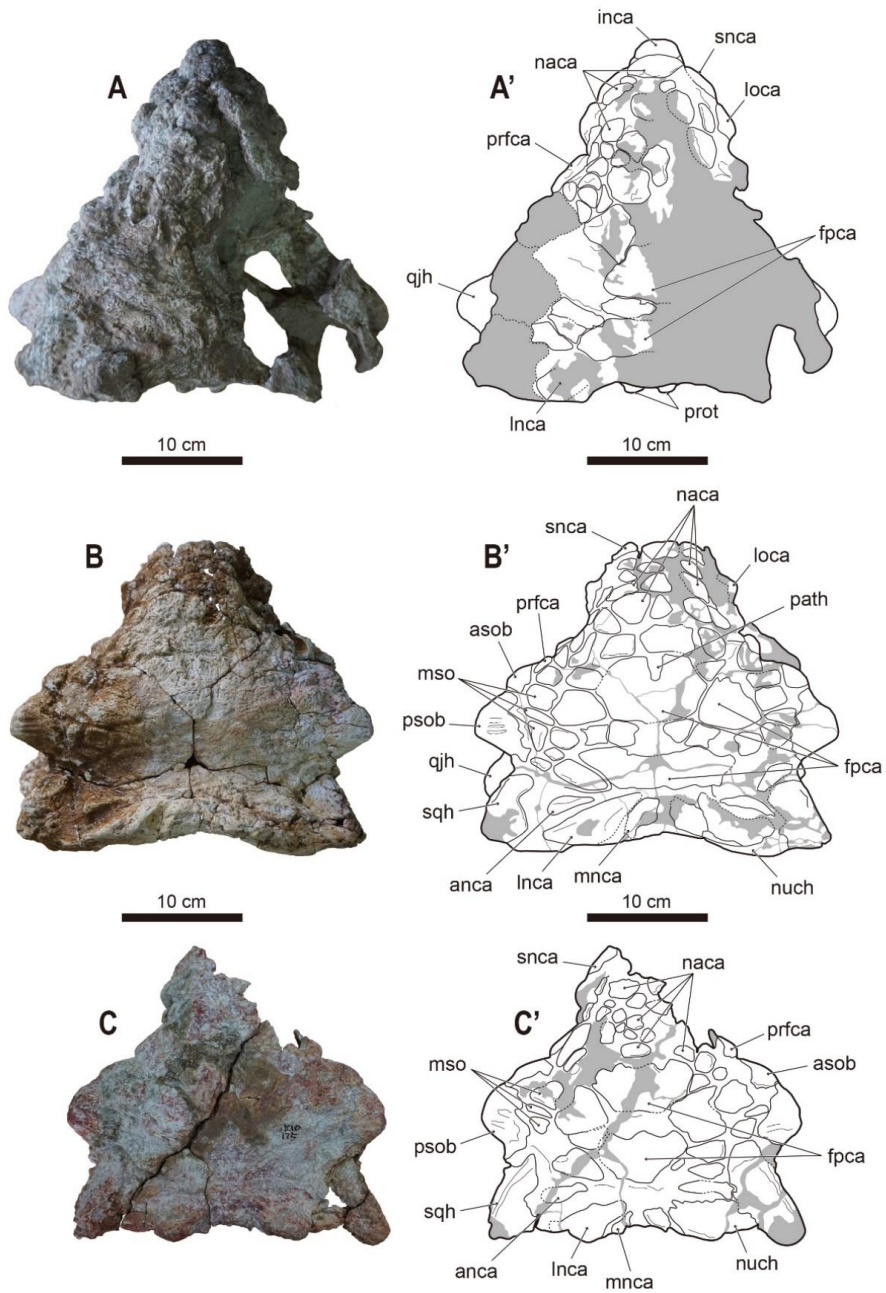

Figure 5. Photographs (A–C) and line drawings (A′–C′) of new skull specimens of *Talarurus plicatospineus* in dorsal view. (A–A′) MPC-D 100/1354. (B–B′) MPC-D 100/1355. (C–C′) MPC-D 100/1356. Grey area indicates a damaged surface.

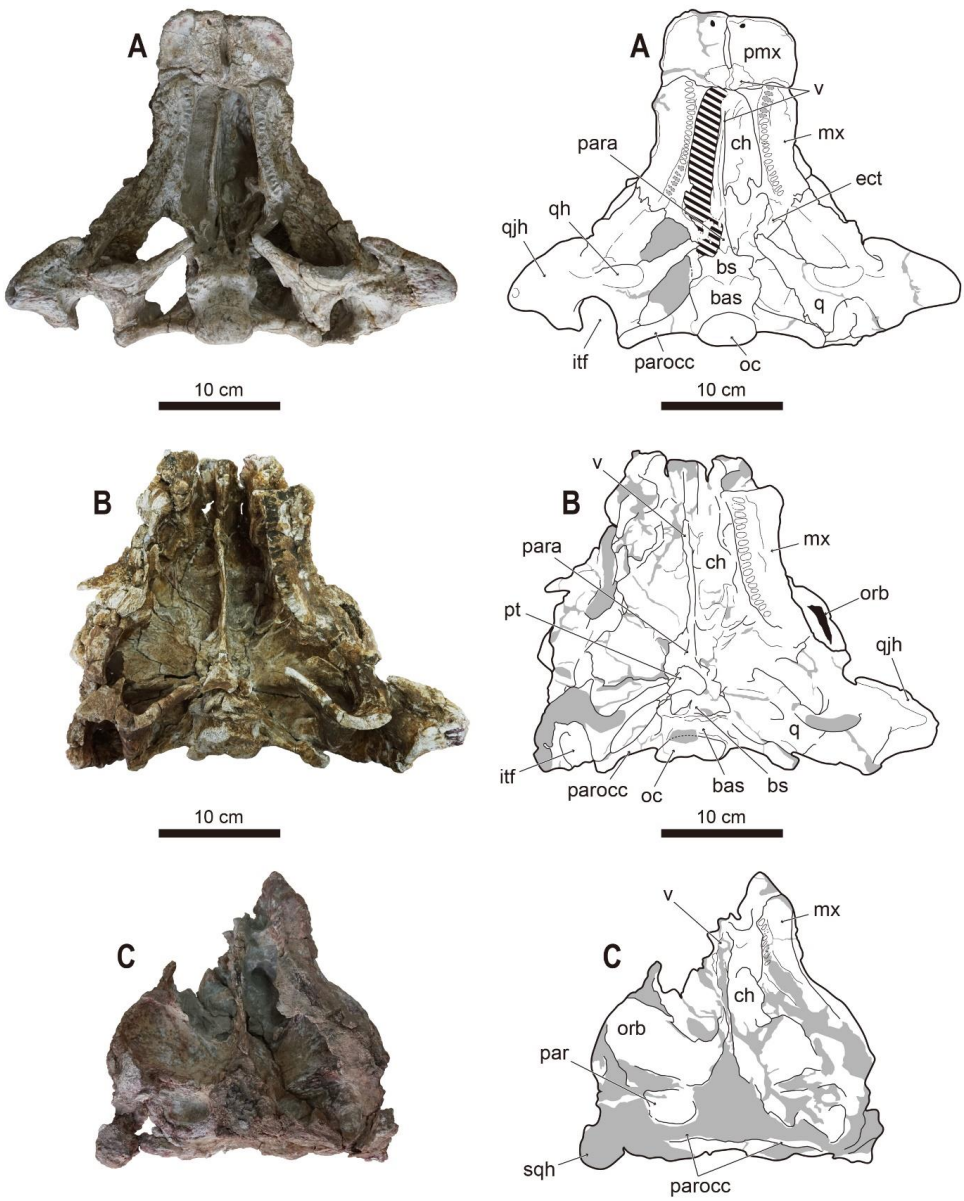

Figure 6. Photographs (A–C) and line drawings (A′–C′) of new skull specimens of *Talarurus plicatospineus* in palatal view. (A–A′) MPC-D 100/1354. (B–B′) MPC-D 100/1355. (C–C′) MPC-D 100/1356. Grey area indicates a damaged surface.

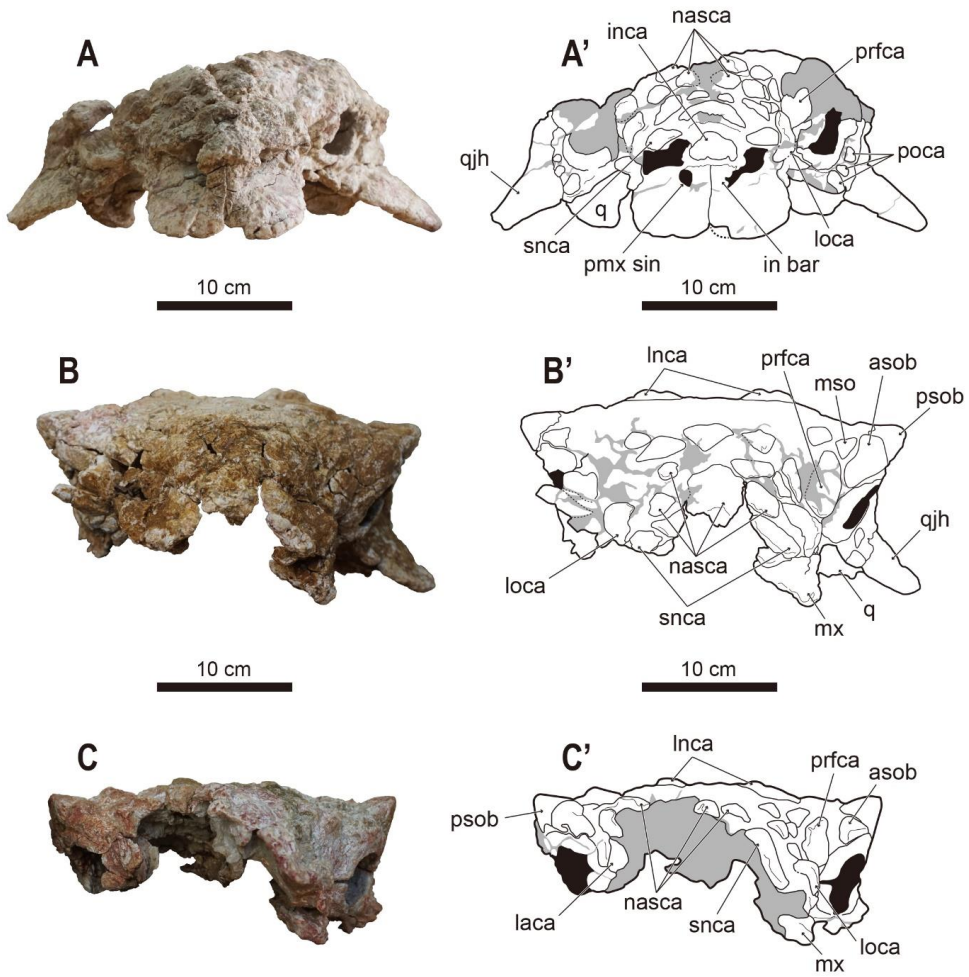

Figure 7. Photographs (A–C) and line drawings (A′–C′) of new skull specimens of *Talarurus plicatospineus* in anterior view. (A–A′) MPC-D 100/1354. (B–B′) MPC-D 100/1355. (C–C′) MPC-D 100/1356. Grey area indicates a damaged surface.

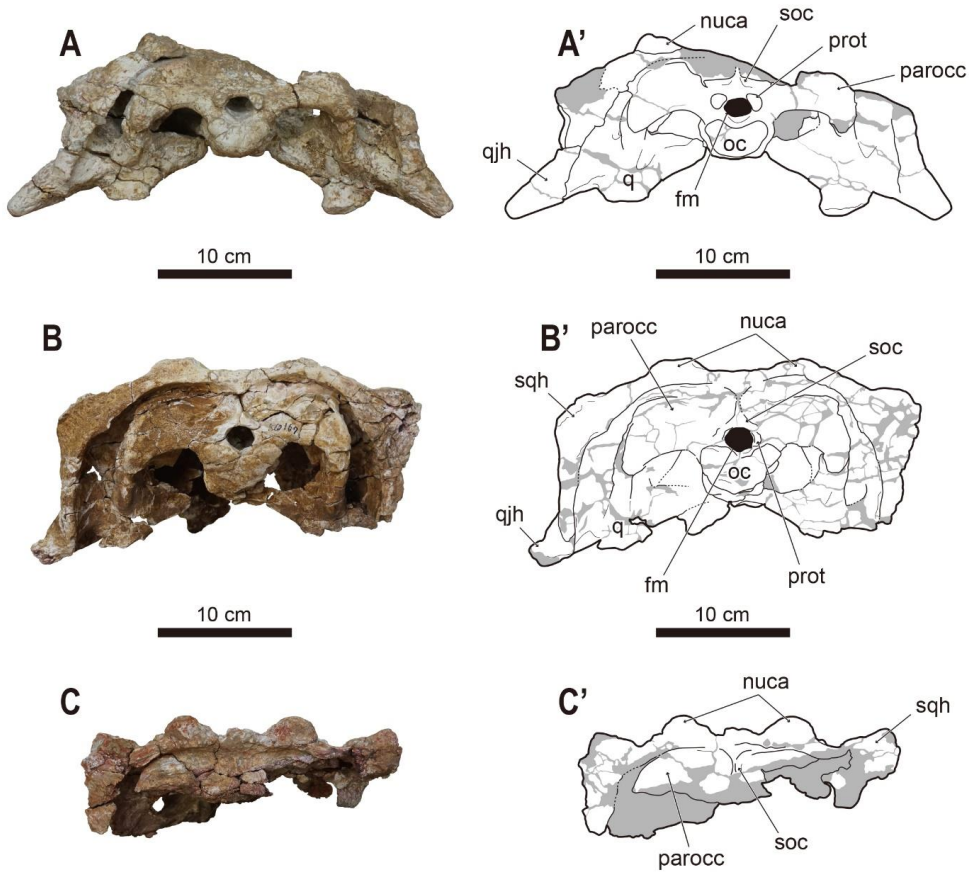

Figure 8. Photographs (A–C) and line drawings (A′–C′) of new skull specimens of *Talarurus plicatospineus* in occipital view. (A–A′) MPC-D 100/1354. (B–B′) MPC-D 100/1355. (C–C′) MPC-D 100/1356. Grey area indicates damaged surface.

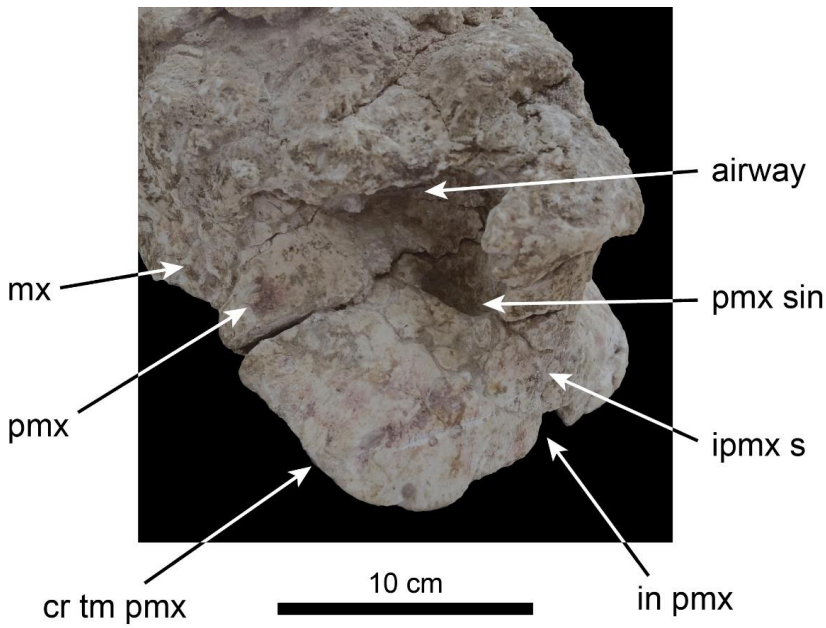

Figure 9. Rostrum of *Talarurus plicatospineus*, MPC-D 100/1354, in right oblique rostrodorsolateral view.

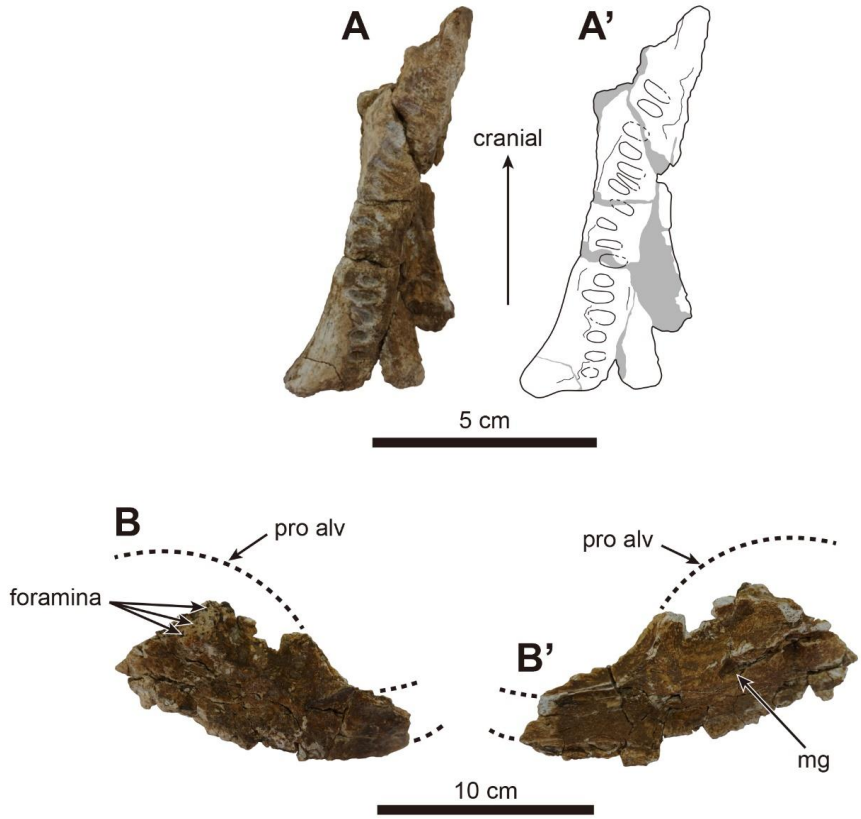

Figure 10. New maxilla and dentary specimens of *Talarurus plicatospineus*, MPC-D 100/1355. (A–A′) Photograph (A) and line drawing (A′) of the isolated right maxilla in palatal view. (B–B′) Partially preserved right dentary in external (B) and medial (B′) views. Grey area indicates a damaged surface.

Description. All three skulls are similar in size (Table 5). MPC-D 100/1354 is 301 mm in length and 372 mm in greatest width across the two quadratojugal horns. The preserved portion of MPC-D 100/1355 is 262 mm in length and 333 mm in greatest width. The preserved mandibular element of MPC-D 100/1355 is 137 mm in length and 75 mm in greatest height. The preserved portion of MPC-D 100/1356 is 249 mm in length and 265 mm in greatest width. In dorsal view, all skulls are trapezoidal in shape and broader than long (Fig. 5). Although MPC-D 100/1355 includes a few isolated postcranial elements, in this chapter, only the skull materials of *Talarurus* are being considered, and the postcranial elements of MPC-D 100/1355 will be presented elsewhere. The neuroanatomy of MPC-D 100/1354 was already fully described (Paulina-Carabajal et al., 2018).

Table 5. Measurements (mm) of the new skull specimens of *Talarurus plicatospineus* (MPC-D 100/1354, 100/1355, 100/1356). Tilde symbol (~) indicates that the measurement is given in terms of the specimen as preserved. 'L' refers to a structure from the left side, 'R' to the right side.

	MPC-D 100/1354	**MPC-D 100/1355**	**MPC-D 100/1356**
Craniocaudal length	301	~262	~249
Transverse width across supraorbitals	~194	302	265
Transverse width across squamosal horns	~306	290	263
Transverse width across quadratojugal horns	372	~333	~234
Orbit width	L: 34 R: ~33	L: 34 R: 49	L: 38 R: 45
Orbit height	L: 35 R: ~34	L: 31 R: 34	L: 33 R: ~35

Rostral region: The premaxillae are fused, although an interpremaxillary suture (*sensu* Vickaryous and Russell, 2003) is present (Figs. 6, 7, and 9). A premaxillary notch can be observed on the anterior tip. The anterior boundary of the combined premaxillae is straight transversely, and the broad internarial bar is oriented vertically. The exposed premaxilla-maxilla suture inclines posterodorsally. The palatal surfaces of the premaxillae are broad and rectangular. There are no premaxillary teeth. The external nares are triangular and face anterolaterally. A single paranasal aperture is present behind the internarial bar (Figs. 7 and 9). The external nares are rimmed dorsally by the elongate supranarial caputegulae. A single large internarial caputegulum protrudes anteriorly over the premaxillae (Figs. 3–5, 7). Around 20 caputegulae are present in the nasal region (Fig. 5). These caputegulae are relatively small, primarily irregular, flat or concave, and surrounded by a broad sulcus. The exposed maxillae are anteroposteriorly elongated and extend below the orbits. In palatal view (Figs. 6 and 10), the convex maxillary tooth row is situated medial to the buccal emargination. At least 23 alveoli are present in each maxilla, but no maxillary teeth are preserved. Two loreal caputegulae are present on each side (Figs. 3 and 4). The most anterior loreal caputegulum is large and rhomboid, whereas the posteriormost loreal caputegulum is elongate. Only one lacrimal caputegulum is present on each side (Figs. 3 and 4). This small, elongate ornament is located above the posterodorsal border of the maxilla. A large rhomboid “prefrontal” caputegulum is behind the loreal caputegulae, and an additional small prefrontal caputegulae is present along the

anteromedial border of the anterior supraorbital caputegulum (Fig. 5).

Temporal region: The frontoparietal caputegulae form a mosaic pattern (Fig. 5). Two large frontoparietal caputegulae are medially positioned on the skull roof. These ornamentations are transversely wide, primarily hexagonal, and are surrounded by smaller caputegulae. Only the posteriormost large frontoparietal caputegulum is preserved and triangular in the holotype. Three small medial supraorbital caputegulae are longitudinally arranged along the medial border of the supraorbital caputegulae (Fig. 5). The keeled supraorbital caputegulae have distinct apices (Figs. 3–5). The posterior supraorbital caputegulum is about four times larger than the anterior one, with shallow transverse grooves on the dorsal surface. The orbits face anterolaterally and tilt somewhat ventrally (Figs. 3, 4, 6, 7). The orbital rim thickens posteriorly. The triangular quadratojugal horns project lateroventrally (Figs. 3, 4, and 6–8). Proximally and anteriorly, each horn ends behind the orbit and does not contact the jugal, which results in a quadratojugal "neck" (*sensu* Arbour and Currie, 2016). Up to seven postocular caputegulae (*sensu* Arbour and Currie, 2016) are situated behind the orbit (Figs. 3 and 4). A wide transverse frontoparietal depression is present posteromedial to the posterior supraorbital caputegulae (Figs. 3–5). The rounded triangular squamosal horns project posterolaterally with dorsolateral keels and triangular bases (Figs. 3–5). A longitudinal furrow can be observed on the keel. Three caputegulae are present on each side of the dorsally raised nuchal shelf (Fig. 5). The high-relief lateral nuchal

caputegulum is four to five times larger than the surrounding nuchal ornamentations. The nuchal shelf is fused with the supraoccipital and the paroccipital processes in occipital view (Fig. 8).

Palatal region: The dorsoventrally thin rostral extension of the vomer is splayed and fused over the posteromedial region of the premaxillae (Fig. 6). The laterally thin osseous nasal septum (*sensu* Vickaryous and Russell, 2003) meets the skull roof dorsally and sagittally divides the rostrum. Posterolateral to the vomer is the pterygoid, but only a fragmentary right element is preserved in MPC-D 100/1355 (Fig. 6). A small, wedge-shaped left ectopterygoid is preserved in MPC-D 100/1354 (Fig. 6), which contributes to the anteromedial border of the supratemporal fenestra.

Occipital/Basicranial region: The parasphenoid tapers anteriorly into a triangular rostrum (*sensu* Vickaryous and Russell, 2003) (Fig. 6). The anteroposterior length of the basisphenoid and basioccipital are similar. Short, stout basipterygoid processes are present on the basisphenoid. Posterior to these processes is medially divided, rounded basal tubera. The ventral surface of the basioccipital is convex. Only the basioccipital contributes to the occipital condyle in MPC-D 100/1354 and 100/1355. However, the exoccipitals also form part of the condyle in the holotype (Maleev, 1956). The reniform occipital condyle is oriented posteroventrally. The ovoid foramen magnum is wider than high. A dorsoventral, sagittal nuchal ridge

(*sensu* Vickaryous et al., 2001) exists between the foramen magnum and the nuchal shelf. This medial ridge divides the supraoccipital region into two shallow fossae. Two small exoccipital protuberances project posteroventrally. The paraoccipital span does not reach the squamosal horns (Fig. 6). The lateral terminus of the paroccipital process is not fused to the squamosal condyle of the quadrates. Each quadrate is transversely broad (Figs. 6 and 8), and the pterygoid flange extends from the quadrate body more ventrally than in other ankylosaurids. In the lateral aspect, the quadrate curves anteriorly but is obscured by the quadratojugal horn (Figs. 3 and 4).

Mandibles: Only the partial right dentary is preserved in MPC-D 100/1355 (Fig. 10). It represents the first mandibular element ever found for *Talarurus*. The ramus tapers anteriorly and curves ventromedially. A predentary sulcus is present on the anterodorsal edge. No alveoli are preserved. The rugose lateral surface has a few foramina in the posterodorsal region. A shallow shelf is present along the dorsomedial portion of the mandibular ramus. The Meckelian groove (*sensu* Vickaryous and Russell, 2003) can also be observed on the medial surface.

Tarchia Maryañska, 1977

Type species. *Tarchia kielanae* Maryañska, 1977

Included species. Type species, *Tarchia teresae*, and *Tarchia tumanovae* sp. nov.

Revised generic diagnosis. An ankylosaurid distinguished by having the following unique set of characters (autapomorphies with an asterisk): a narrow internarial bar of the premaxillae (shared with *Tsagantegia*) (ambiguous in *Tarchia kielanae*); large, rhomboidal loreal caputegulum with a laterally extended posterior keel (shared with *Saichania*) (ambiguous in *Tar. kielanae*); subrectangular frontal caputegulae (shared with *Saichania*); a "neck" present at the base of the quadratojugal horn (shared with *Pinacosaurus mephistocephalus* and *Minotaurasaurus*) (ambiguous in *Tar. kielanae*); sigmoidal and peaked anteromedial supraorbital caputegulum*; posterolateral supraorbital caputegulum with a rounded anterior surface, and a flat, anteriorly-inclined posterior surface*; anteromedially poorly defined postorbital fossa that medially reaches the lateral nuchal caputegulae*; occiput visible in dorsal view (shared with *Minotaurasaurus* and *Zaraapelta*); foramen magnum taller than wide*. Differs from *Minotaurasaurus*, *Pinacosaurus grangeri*, *Saichania*, and *Zaraapelta* in having no postocular caputegulae (ambiguous in *Tar. kielanae*) and a posteroventrally oriented occipital condyle. Differs from *Minotaurasaurus*, *P. grangeri*, and *Zaraapelta* in having confluent supraorbital horns. Differs from *Minotaurasaurus* and *Saichania* in having a relatively tall braincase. Differs from *Minotaurasaurus*

and *Zaraapelta* in having a long nuchal crest. Differs from *Minotaurasaurus* in having relatively long paroccipital processes that laterally reach the squamosal horns. Differs from *Saichania* in having remodeled squamosal horns and anteroposteriorly short lateral nuchal caputegulae.

***Tarchia tumanovae* sp. nov.**

Etymology. Named in honor of Tatiana Tumanova for her contributions to understanding Mongolian ankylosaurs.

Type specimen. MPC-D 100/1353, a well-preserved skull, dorsal, sacral, caudal vertebrae, sixteen dorsal ribs, ilia, a partial ischium, free osteoderms, and tail club (Figs. 11–19).

Type locality and horizon. Upper Cretaceous (upper Campanian–lower Maastrichtian) Nemegt Formation, Hermiin Tsav, southern Gobi Desert, Mongolia.

Diagnosis. An ankylosaurid distinguished by having the following unique set of characters: a single relatively bulbous internarial caputegulum that does not reach the rostral tip of beak*; a nasofrontal sagittal furrow with a weak Z-shaped offset (shared with *Tarchia kielanae*); lateral nuchal caputegulae taller medially than laterally (shared with *Saichania*); vomerine keel extends below the alveolar ridge (shared with *Saichania*). Differs from *Minotaurasaurus*, *Pinacosaurus grangeri*, *Tar. kielanae*, *Tar. teresae*, and *Zaraapelta* in having a moderate-sized basioccipital foramen. Differs from *Minotaurasaurus*, *P. grangeri*, *Saichania*, and *Zaraapelta* in

having no postocular caputegulae and a posteroventrally oriented occipital condyle. Differs from *Minotaurasaurus*, *P. grangeri*, *Tar. teresae*, and *Zaraapelta* in having an anteriorly situated quadrate-quadratojugal region. Differs from *Minotaurasaurus*, *P. grangeri*, and *Zaraapelta* in having confluent supraorbital horns. Differs from *P. grangeri*, *Saichania*, and *Zaraapelta* in having a tall foramen magnum. Differs from *Saichania*, *Tar. kielanae* and *Zaraapelta* in having unfused quadrate to the exoccipital area. Differs from *Minotaurasaurus* and *Saichania* in having a relatively tall braincase. Differs from *Minotaurasaurus* and *Zaraapelta* in having subrectangular frontal caputegulae and a long nuchal crest. Differs from *Minotaurasaurus* in having narrow narial caputegulae and long paroccipital processes that reach the squamosal horns laterally. Differs from *Saichania* in having remodeled squamosal horns, anteroposteriorly short lateral nuchal caputegulae, and occiput visible in dorsal view. Differs from *Tar. teresae* by having an interpterygoid vacuity visible in occipital view.

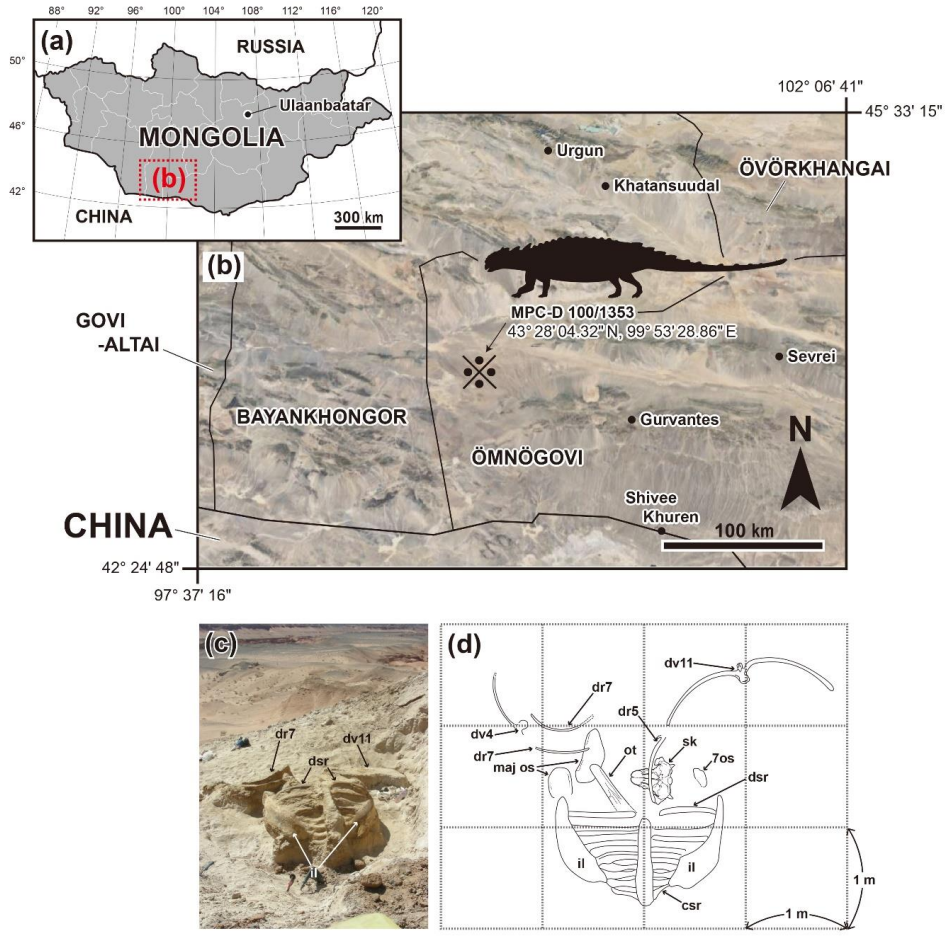

Figure 11. Map showing the locality where *Tarchia tumanovae* sp. nov. (MPC-D 100/1353) was discovered. (a) Map of Mongolia. (b) Enlarged map of the dotted lined rectangle of **(a)** marked with the fossil locality (※). (c) Photo of the excavation site. (d) Quarry map showing bone location.

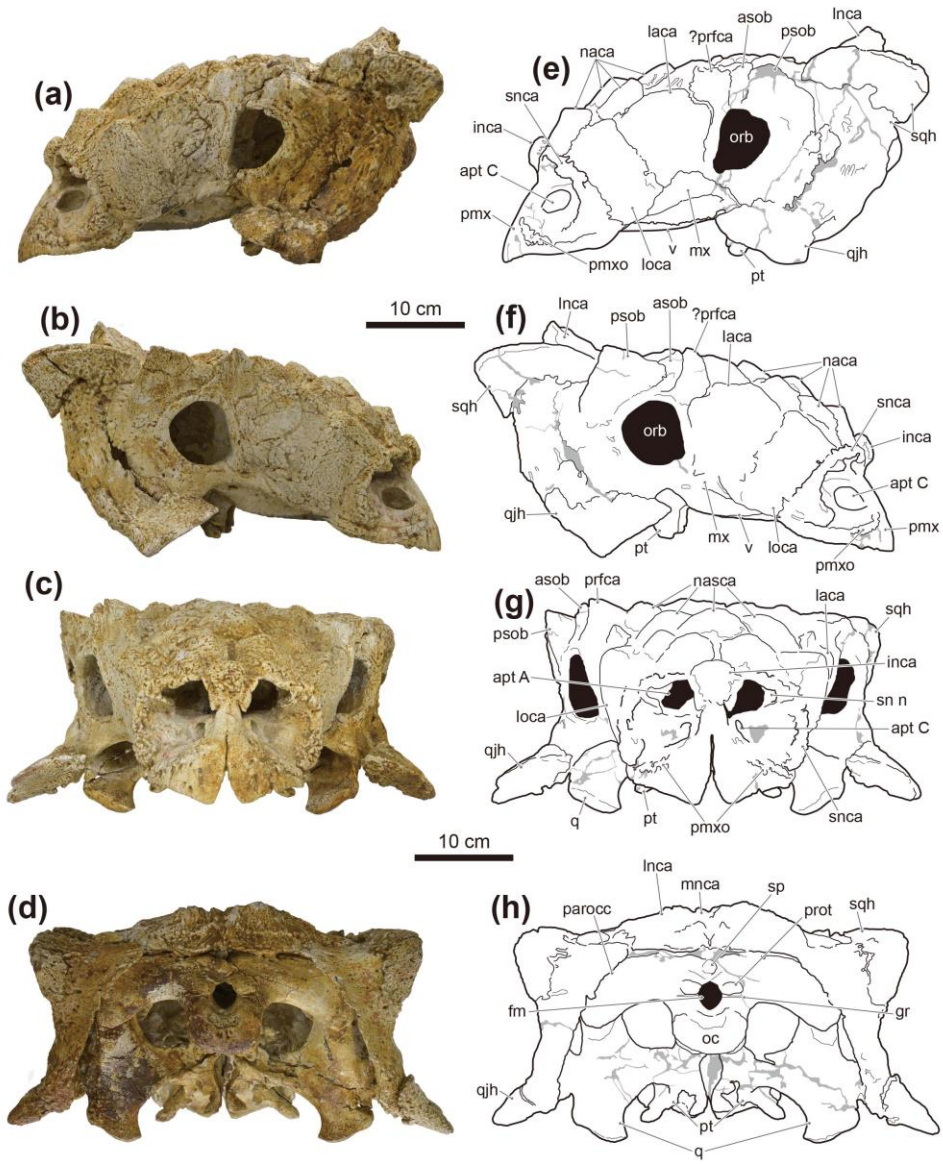

Figure 12. Photographs (a–d) and line drawings (e–h) of the skull of *Tarchia tumanovae* sp. nov. (MPC-D 100/1353). Photographs of the skull in (a) left lateral, (b) right lateral, (c) anterior, and (d) occipital views. Line drawings in (e) left lateral, (f) right lateral, (g) anterior, and (h) occipital views. Grey areas indicate damaged surfaces.

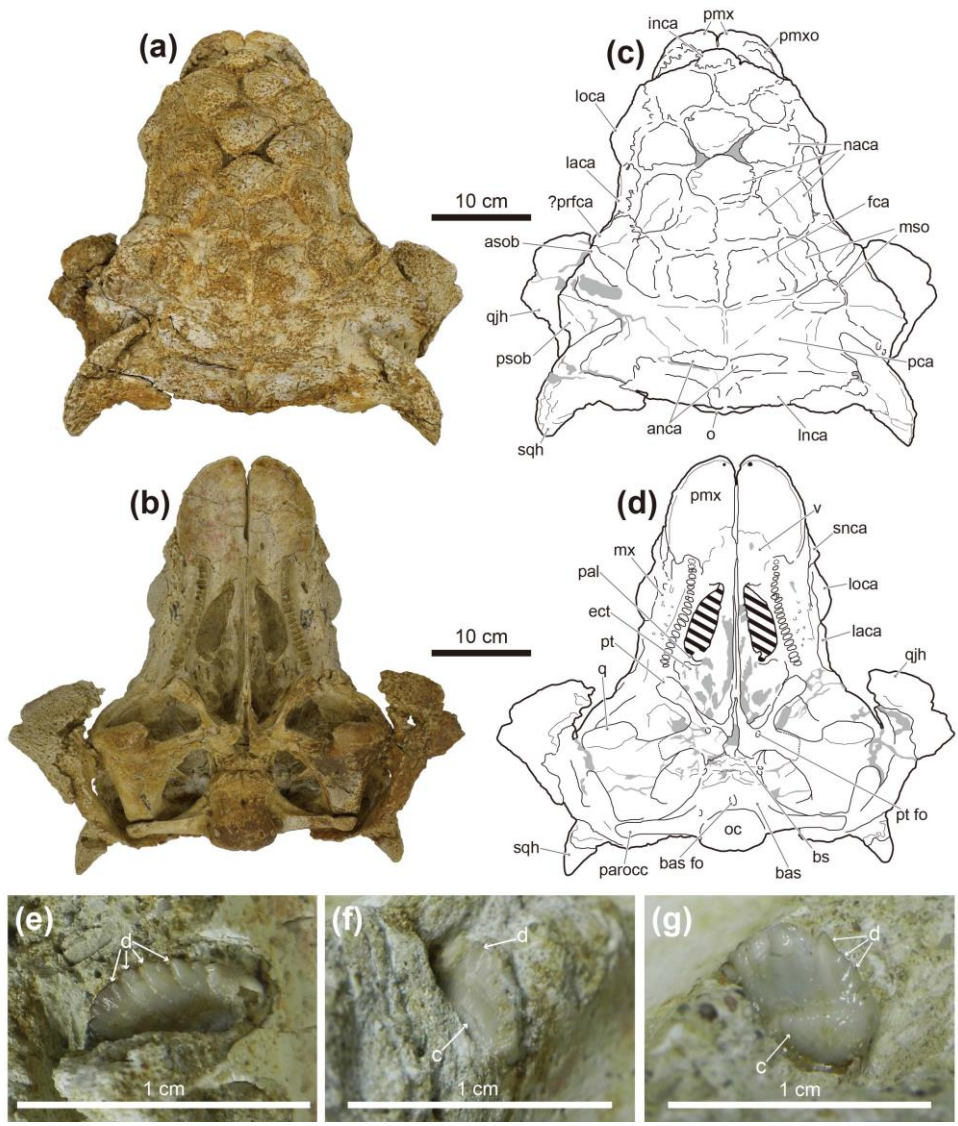

Figure 13. Photographs (a and b) and line drawings (c and d) of the skull, and photographs of the maxillary teeth (e–g) of *Tarchia tumanovae* sp. nov. (MPC-D 100/1353). Photographs of the skull in (a) dorsal and (b) palatal views. Line drawings in (c) dorsal and (d) palatal views. Grey areas indicate damaged surfaces, and solid diagonal lines indicate unremoved matrix. Photographs of (e) seventh left, (f) third right, and (g) eight right maxillary teeth in anterolabial view.

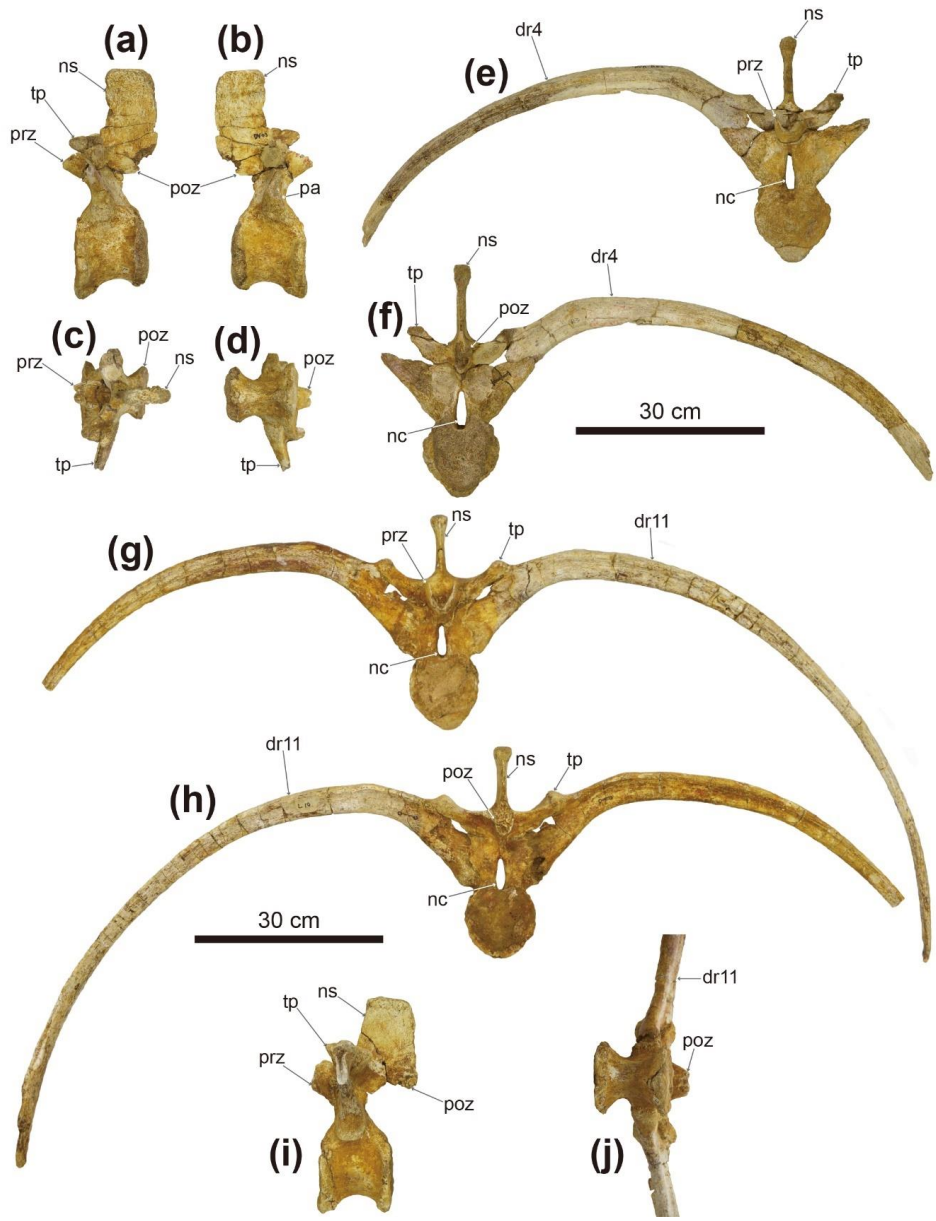

Figure 14. Photographs of dorsal vertebrae of *Tarchia tumanovae* sp. nov. (MPC-D 100/1353). The fourth dorsal vertebra in (a) left lateral, (b) right lateral, (c) dorsal, and (d) ventral views. Fourth dorsal vertebra with fused right rib in (e) anterior and (f) posterior views. The eleventh dorsal vertebra in (g) anterior, (h) posterior, (i) left lateral (with no ribs attached), and (j) ventral views.

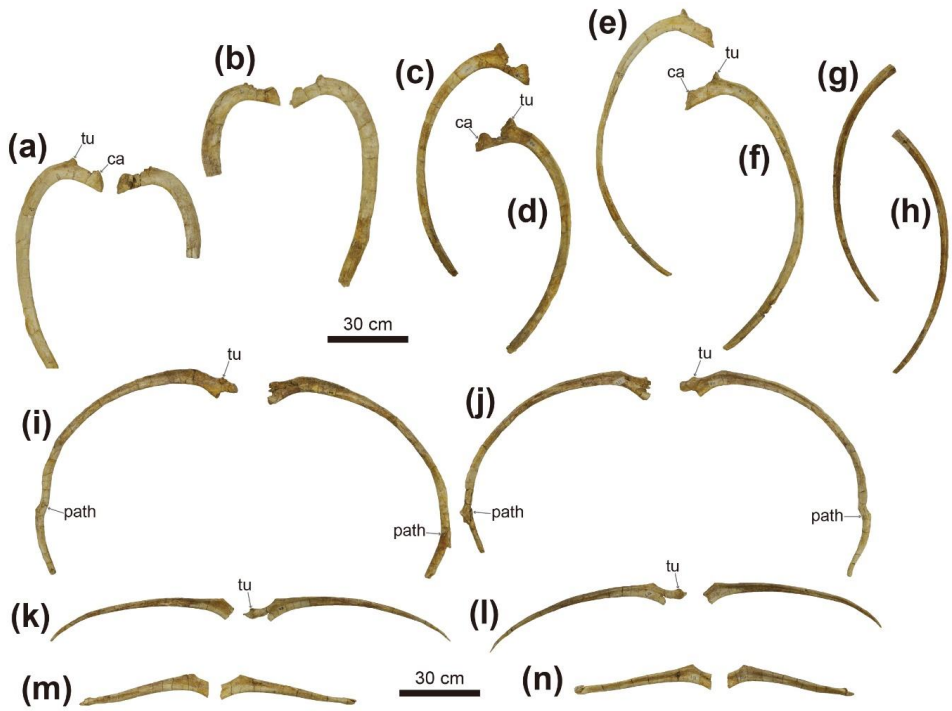

Figure 15. Photographs of dorsal (a–h) and dorsosacral ribs (i–p) of *Tarchia tumanovae* sp. nov. (MPC-D 100/1353). Both third dorsal ribs in (a) anterior and (b) posterior views. The fourth left dorsal rib in (c) anterior and (d) posterior views. The fifth left dorsal rib in (e) anterior and (f) posterior views. The sixth left dorsal rib in (g) anterior and (h) posterior views. Both first dorsosacral ribs in (i) anterior and (j) posterior views. Both second dorsosacral ribs in (k) anterior and (l) posterior views. Both third dorsosacral ribs in (m) anterior and (n) posterior views. Both third dorsosacral ribs in (o) anterior and (p) posterior views.

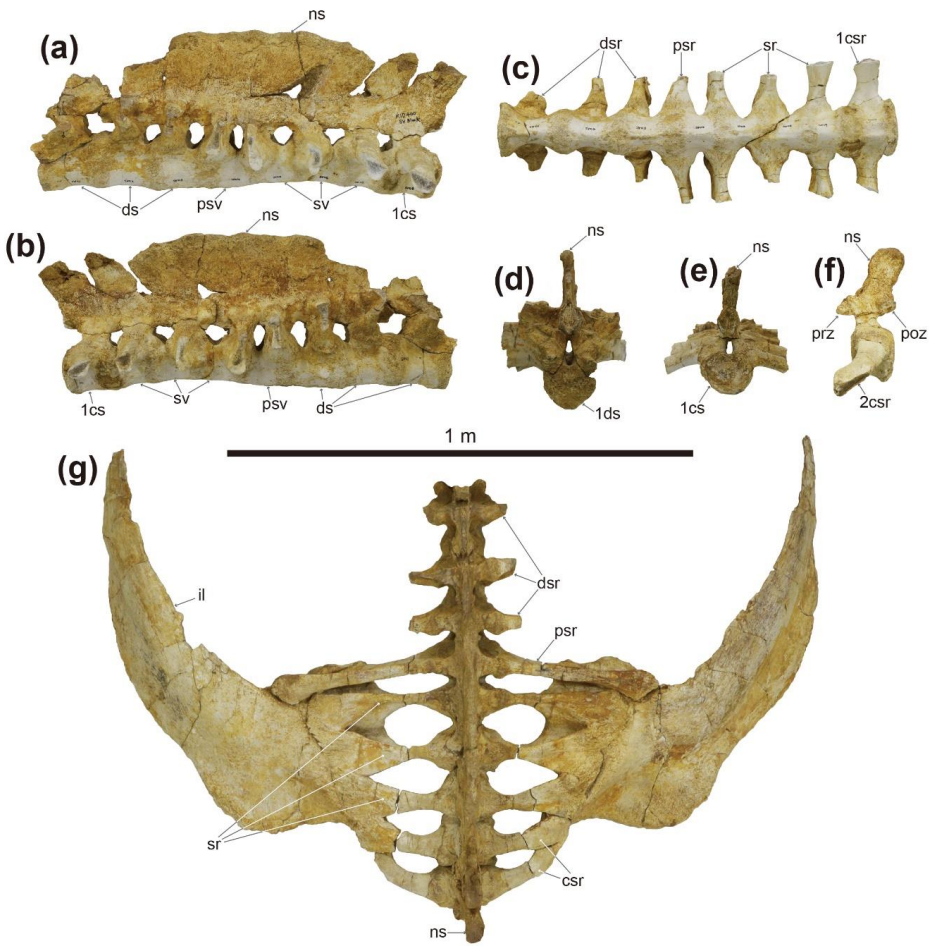

Figure 16. Photographs of the synsacrum (a–f) and ilia (g) of *Tarchia tumanovae* sp. nov. (MPC-D 100/1353). Synsacrum in (a) left lateral, (b) right lateral, (c) ventral, (d) anterior, and (e) posterior views. (f) Second caudosacral vertebra in left lateral view. (g) Synsacrum with the fused ilia in dorsal view.

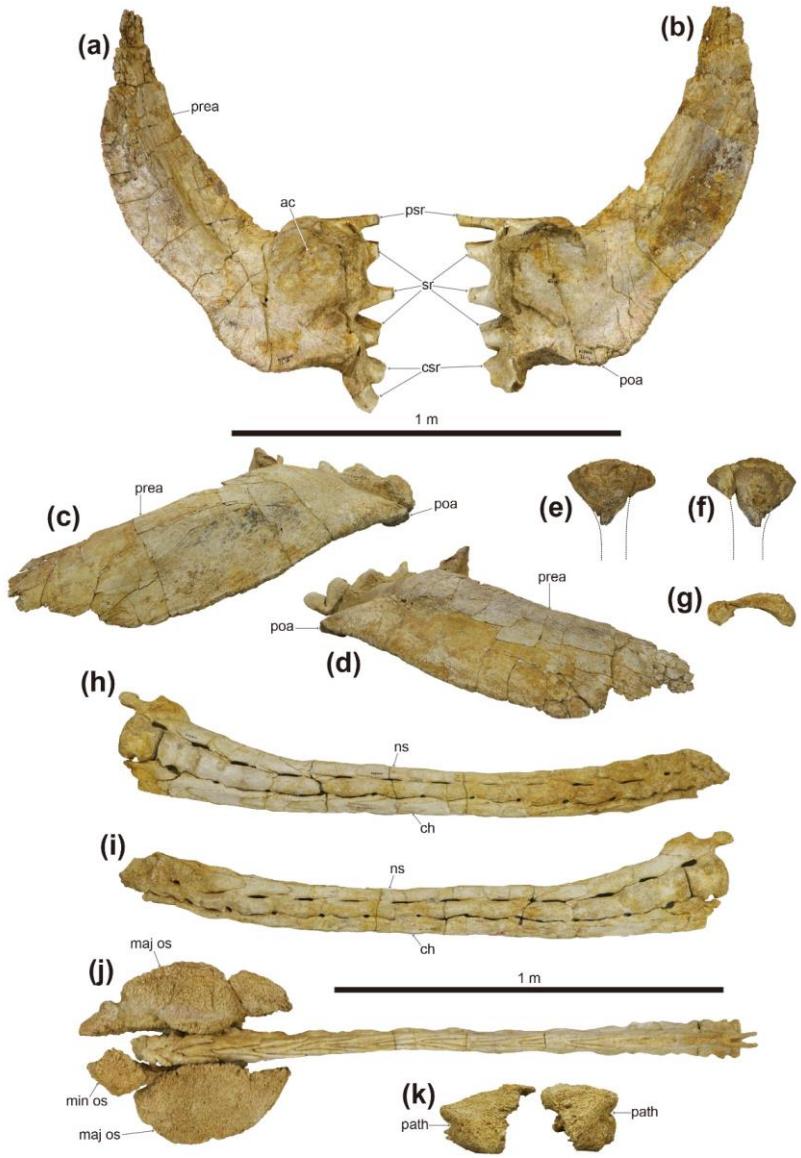

Figure 17. Photographs of both ilia (a–d), partial left ischium (e–g), and the tail club (h–k) of *Tarchia tumanovae* sp. nov. (MPC-D 100/1353). (a) Left and (b) right ilium in ventral view. (c) Right and (d) left ilium in lateral view. Left ischium in (e) lateral, (f) medial, and (g) proximal views. Tail club handle in (h) left lateral and (i) right lateral views. (j) Tail club handle and knob in dorsal view. (k) Tail club knob in proximal view.

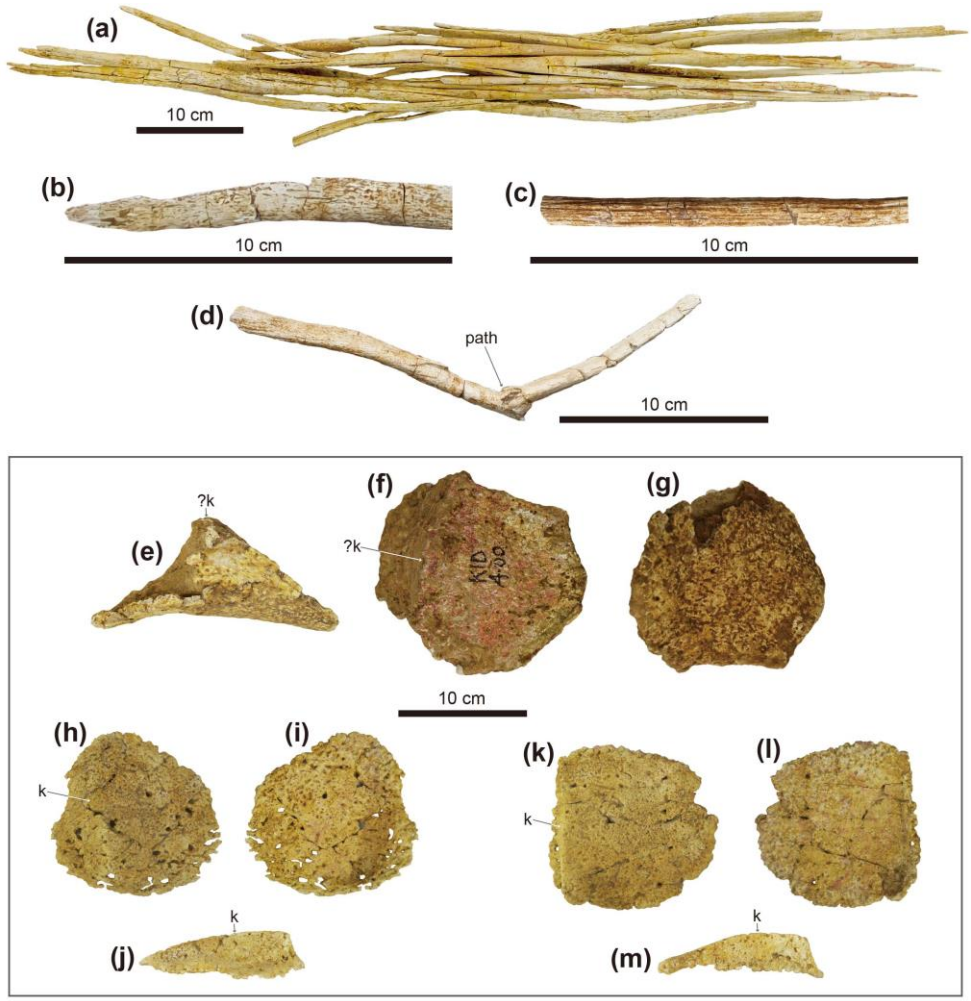

Figure 18. Photographs of ossified tendons from the tail knob handle (a–d) and dermal osteoderms (e–m) of *Tarchia tumanovae* sp. nov. (MPC-D 100/1353). (a) A bundle of ossified tendons from the tail knob handle. Close up photos of (b) an ossified tendon that is flattened and (c) a tendon elliptic in cross-section and longitudinal striae. (d) An ossified tendon with evidence of fracture healing. Type 2 osteoderm in (e) anterior, (f) oblique dorsolateral, and (g) ventral views. Two Type 7 osteoderms in (h and k) dorsal, (i and l) ventral, and (j and m) lateral views.

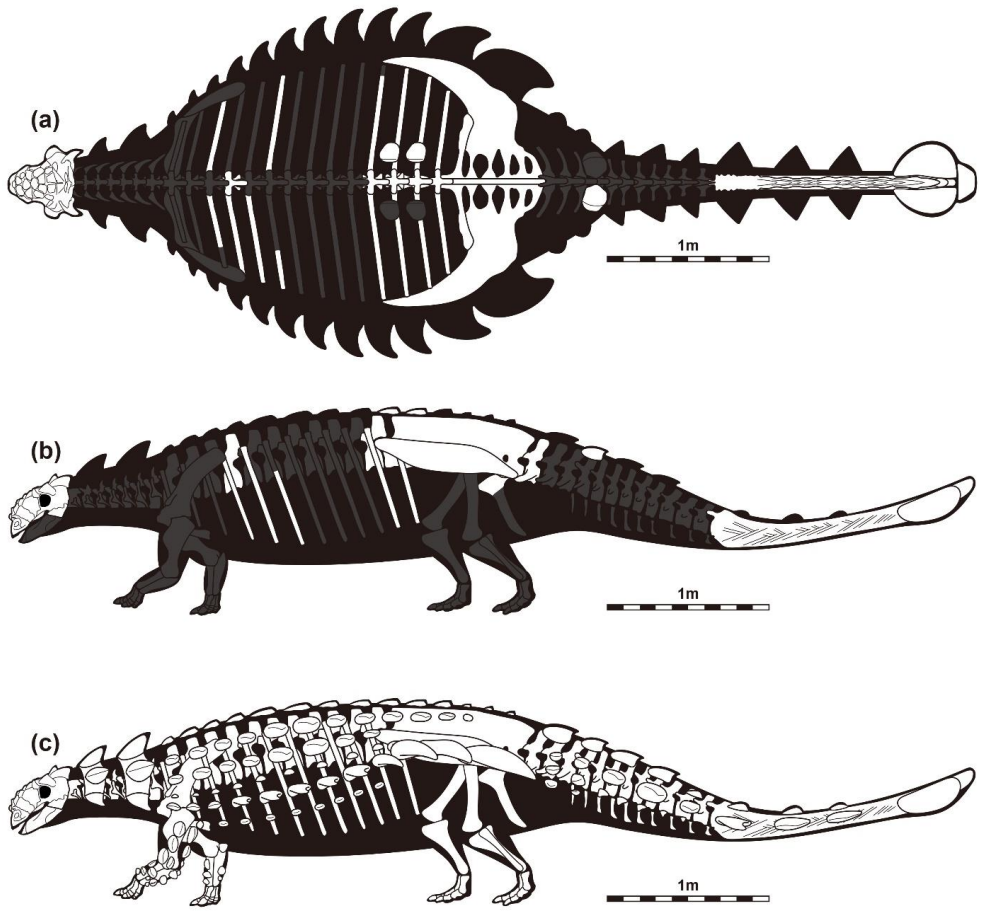

Figure 19. Skeletal diagram of *Tarchia tumanovae* sp. nov. (MPC-D 100/1353). (a) Dorsal and (b) left lateral views (white bones represent recovered elements). (c) Skeletal reconstruction with dermal armor.

Description. The shape of the skull is trapezoidal and broader than long in dorsal view (Fig. 13, see Tables 6–13 for measurements). All caputegulae are pitted externally. The neuroanatomy of MPC-D 100/1353 was fully described by Paulina-Carabajal et al. (2018).

Table 6. Measurements (mm) of the skull of *Tarchia tumanovae* sp. nov. (MPC-D 100/1353). The asterisk refers to incomplete measurement due to damage.

Element			**Measurements**
Skull dimension	Length	Rostral tip to squamosal horns	423.1
		Rostral tip to occipital condyle	402.4
	Width	Across supraorbitals	350.2
		Across squamosal horns	382.8
		Across quadratojugal horns	418.6*
Orbit dimension	Width		60.6
	Height		64.4

Table 7. Measurements (mm) of dorsal vertebrae of *Tarchia tumanovae* sp. nov. (MPC-D 100/1353).

	4th dorsal	**11th dorsal**
Centrum length	117.4	115.2
Width of anterior surface centrum	120	108.9
Height of the anterior surface of centrum	121.7	116.6
Width of the posterior surface of centrum	120.9	113.1
Height of the posterior surface of centrum	126.9	108
Total height	366.9	339.6

Table 8. Measurements (mm) of dorsosacral vertebrae of *Tarchia tumanovae* sp. nov. (MPC-D 100/1353). The asterisk refers to incomplete measurement due to damage.

	1st dorsosacral	**2nd dorsosacral**	**3rd dorsosacral**
Centrum length	133.2	114.3	119.3
Width of the anterior surface of centrum	112.3	96.4	89.5
Height of the anterior surface of centrum	116.3	107.4	98.4
Width of the posterior surface of centrum	96.4	89.5	98.4
Height of the posterior surface of centrum	107.4	98.4	83.5
Total height	252.5*	287.3*	340

Table 9. Measurements (mm) of the parasacral vertebra of *Tarchia tumanovae* sp. nov. (MPC-D 100/1353).

	parasacral
Centrum length	95.4
Width of the anterior surface of centrum	98.4
Height of the anterior surface of centrum	83.5
Width of the posterior surface of centrum	86.5
Height of the posterior surface of centrum	70.6
Total height	337

Table 10. Measurements (mm) of sacral vertebrae of *Tarchia tumanovae* sp. nov. (MPC-D 100/1353).

	1st sacral	**2nd sacral**	**3rd sacral**
Centrum length	102.4	89.5	84.5
Width of the anterior surface of centrum	86.5	82.5	74.6
Height of the anterior surface of centrum	70.6	76.5	86.5
Width of the posterior surface of centrum	82.5	74.6	107.4
Height of the posterior surface of centrum	76.5	86.5	95.4
Total height	323.1	308.2	304.2

Table 11. Measurements (mm) of caudosacral vertebrae of *Tarchia tumanovae* sp. nov. (MPC-D 100/1353). The asterisk refers to incomplete measurement due to damage.

	1st caudosacral	**2nd caudosacral**
Centrum length	129.2	93
Width of the anterior surface of centrum	107.4	123.5
Height of the anterior surface of centrum	95.4	112.4
Width of the posterior surface of centrum	112.3	115.5
Height of the posterior surface of centrum	92.4	103.8
Total height	294.2*	296.9

Table 12. Measurements (mm) of the tail club of *Tarchia tumanovae* sp. nov. (MPC-D 100/1353). The asterisk refers to incomplete measurement due to damage.

Element		Measurements
Tail club handle length	Length	1571.1
Tail club knob	Maximum width	549.5
	Maximum length	470.1
	Maximum height	170.3

Table 13. Measurements (mm) of ilia of *Tarchia tumanovae* sp. nov. (MPC-D 100/1353). The asterisk refers to incomplete measurement due to damage.

Element		Measurements
Right ilium	Length	930.9
	Length of preacetabular process	685.6
	Length of postacetabular process	188.7
Left ilium	Length	919.6
	Length of preacetabular process	680.4
	Length of postacetabular process	201
Left ischium	Length	17.2
	Proximal width	22.6

Rostral region: The premaxillae are fused dorsally, but the palatal surfaces are separate (Figs. 12 and 13). The rostral tip is protruded anteroventrally, and a premaxillary notch is present. The narrow internarial bar is oriented posterodorsally. A thin, rugose ossification is present below the external naris on each premaxilla. The anterior margin of the premaxillary ornamentation is convex, whereas the posterior margin is concave. The palatal surface of the premaxillae is shovel-like with a round anterior boundary. No premaxillary teeth are present. The subcircular external nares face anteriorly. The entrance to the airway (aperture A, *sensu* Hill et al., 2003) is large and subcircular. The airway is filled with a matrix. A supranarial notch is present on the medial wall of the maxillary region, lateral to the entrance to the airway. A short, medioventrally sharp intranasal process is present beneath the entrance of this aperture. A larger oval dorsolaterally-facing paranasal aperture (aperture C) is situated on the ventral wall of the external nares behind the internasal bar. The external nares are rimmed dorsomedially, dorsally, and laterally by supranarial caputegulae (*sensu* Blows, 2001). The dorsomedial and dorsal portion of the supranarial caputegulum is thin, whereas the wide ventrolateral part gives the caputegulum a boot-like appearance in lateral view. The anterior end of the nasals contacts the internasal bar anteromedially. A single medium-sized bulbous internarial caputegulum is situated above the contact between the internarial bar of the premaxillae and the anterior nasals and between the thin medial portion of the two supranarial caputegulae. Behind the internarial caputegulum, eleven pyramidal nasal caputegulae are present. Most of these

caputegulae are large and surrounded by a broad sulcus. The most medioposteriorly positioned pairs are transversely oriented pyramidal and rectangular, similar to the frontal caputegulae.

The maxillae are anteroposteriorly elongate, extending to below the orbits. In lateral view, the anterior portion of the maxillae is covered by the loreal caputegulum, whereas the posterior portion is exposed. The convex maxillary tooth row is situated medial to the buccal emargination in palatal view. Nineteen alveoli are present in each maxilla. A single loreal caputegulum is present on each side. The loreal caputegulum is large, rhomboid, and has a posterior keel that posterolaterally juts out. The lacrimal caputegulum is large and flat laterally and has a keeled edge on the dorsal margin. A single medium-sized possible prefrontal caputegulum is present on each side, forming the lateral margin of the skull. The left presumable prefrontal caputegulum is damaged, but the right is well preserved. This caputegulum is keeled dorsally and has a lateroposteriorly pointing apex in close contact with the anterior supraorbital caputegulum.

Temporal region: Paired, transversely oriented frontal caputegulae are pyramidal and rectangular (Figs. 13a, c). The nasofrontal sagittal furrow has a weak Z-shaped offset as in ZPAL MgD I/111 (holotype of *Tar. kielanae*). Although the parietal caputegulae are poorly defined, three shallow dorsal furrows diverge anteroposteriorly from each other at an angle of about 35°. Two medial supraorbital caputegulae are present on the right, whereas only the anteromedial one is

preserved on the left. The longitudinally oriented anteromedial caputegulum is sigmoidal. The transversally oriented posterolateral caputegulum has rounded anterior and flat, anteriorly-inclined posterior surfaces. The left supraorbital caputegulae have damaged apices, whereas the right ones are well preserved with a distinct apex. The anterior supraorbital caputegulum is narrow and keeled, with an anterolaterally directed apex. The posterior supraorbital caputegulum is laterally pointed and keeled dorsally and is about five times larger than the anterior supraorbital caputegulum. The orbits have a posteriorly thick orbital rim and face anterolaterally. The quadratojugal horns are triangular and project ventrolaterally (Figs. 12 and 13). A quadratojugal "neck" (*sensu* Arbour and Currie, 2016) is present at the base of the horns. Postocular caputegulae are absent. The squamosal horns are pyramidal and posteriorly recurved (Figs. 13a, c). These horns are divided into the upper external layer of the squamosal horn and the underlying squamosal horn proper (*sensu* Arbour et al., 2014b). The former is dorsolaterally keeled with a longitudinal furrow present on the posterior half of the keel. The narrow, sharp, and medially curved anterior portion of the caputegulae lies in a broad, deep postorbital fossa posterior to the supraorbital. The anterior tip of the right horn was slightly broken sometime after CT scanning of the braincase by Paulina-Carabajal et al. (2018). A narrow, deep sulcus separates the irregular ventral margin of the base of the external layer of the squamosal horn and the underlying squamosal horn proper. The surface of the external dermal layer is pitted, whereas the squamosal horn proper has a granular texture. The nuchal shelf

is dorsally uplifted and does not overhang the outer rim of the skull. Two nuchal caputegulae are present on each side. Both anterior and lateral nuchal caputegulae are elongate and transversely positioned. However, the lateral nuchal caputegulae are about four times larger than the anterior nuchal caputegulae, forming the posterior margin of the cranium. In occipital view, the nuchal shelf is not fused with the supraoccipital and paroccipital processes (Figs. 12d, h).

Palatal region: The rostral extension of the vomer is dorsoventrally thin, splayed, and fused with the posteromedial region of the premaxillae (Figs. 13b, d). The osseous nasal septum (*sensu* Vickaryous and Russell, 2003) extends dorsally but does not meet the skull roof. The vomerine keel ends ventral to the alveolar ridge. The palatine extends posteromedially from the maxilla and gently projects dorsally, forming a posteroventral secondary palate (*sensu* Vickaryous and Russell, 2003). The ectopterygoid is small and wedge-like. The pterygoid has a vertical anterior surface with a foramen pierced through the central body. The pterygoid flange projects anterolaterally and contacts the dorsally positioned ectopterygoid. The quadrate ramus contacts the posterolaterally positioned quadrate. The posterolateral edge of the quadrate ramus is damaged on both sides. The posteromedial margin of the main pterygoid body is not fused with the basipterygoid processes of the basisphenoid. The basipterygoid processes are divided from each other. An interpterygoid vacuity is present between the paired pterygoids.

Occipital/Basicranial region: The contact between the basisphenoid and the basioccipital forms a rugose transverse ridge in palatal view (Figs. 13b, d). A basioccipital foramen is present on the convex ventral surface of the basioccipital. The basioccipital and the exoccipitals are entirely fused and form a reniform occipital condyle oriented posteroventrally. The ovoid foramen magnum is taller than wide (Figs. 12d, h). A small hill-like process lies between the foramen magnum and the nuchal shelf. A horizontal groove is present below the paired exoccipital protuberances. The lateral terminus of the paroccipital process is long but not fused to the quadrate reaching laterally to the squamosal horns. The transversely broad quadrates are inclined anteroventrally toward the distal articular condyles in lateral view. The medial condyle of the quadrate is larger than the lateral condyle.

Teeth: Only the third and eighth right maxillary teeth and the seventh left maxillary tooth are preserved (Figs. 13e–g). Although these teeth are partially embedded within the sockets, up to eleven marginal denticles can be observed. Shallow vertical grooves are present between the denticles, and a shelf-like labial cingulum is also present.

Axial skeleton: Two isolated dorsal vertebrae with fused ribs (Fig. 14), probably presenting the fourth and eleventh dorsal vertebrae based on the length of the ribs, are preserved. Only the right rib is preserved on the fourth dorsal vertebra (Figs. 14e, f), whereas both ribs are present on the eleventh (Figs. 14g, h, j). These vertebrae have amphiplatyan spool-shaped centra, similar in length and height, and laterally constricted. A medial ridge is present on the ventral surface of the centrum. The tall and narrow neural arches are centrally located on the dorsal centra. Accordingly, the neural canals are dorsoventrally tall and laterally narrow. The transverse processes are angled about 45° dorsolaterally. The dorsally directed prezygapophyses extend beyond the anterior margin of the centrum. The postzygapophyses are directed ventrally and smaller than the prezygapophyses. Eight free dorsal ribs are preserved, including the three ribs fused to the free dorsal vertebrae (Figs. 14 and 15). These ribs have an anteroposteriorly expanded, flat dorsal surface with a dorsoventrally deep head. The rib is T-shaped in a proximal cross-section. The anterior dorsal ribs, especially the second dorsal ribs, are mediolaterally broader than the posterior ones. The articulated dorsal ribs are fused to the ventral side of the transverse processes. The fused dorsal ribs arc outward, resulting in a barrel-like trunk.

The synsacrum is well preserved and includes three dorsosacrals, one parasacral, three sacrals, and two caudosacral vertebrae (Fig. 16). These vertebrae are fused along the centra and the neural spines. The centra of these vertebrae are spool-shaped and laterally constricted. A single medial ridge is present on the

ventral surface of the centra of the dorsosacrals and the parasacral. Two medial ridges are present on the first and second sacrals and caudosacrals. The neural arches of the dorsosacrals are centrally located dorsal to the centra, whereas the neural arches of the parasacral and sacrals are shifted anteriorly, projecting beyond the anterior margin of the centra. The neural arches of the caudosacrals are also shifted anteriorly but not projected as much as in the parasacral and sacrals. The fused, laterally compressed neural spines are directed posterodorsally. All dorsosacral, parasacral, sacral, and caudosacral ribs are fused to the vertebrae, although the dorsosacral ribs were separated during preparation. The first pair of dorsosacral ribs are arced similar to the posterior dorsal ribs, whereas the second and third pairs are rod-like and much shorter in length. Bone healing is observed on both sides of the distal portion of the first dorsosacral ribs (Figs. 15i, j). In dorsal view, the ribs become shorter in mediolateral length from the parasacral to the second caudosacral. The parasacral ribs are slightly projected posterolaterally and contact the ilium. The sacral ribs are projected laterally, whereas the caudosacral ribs are projected anterolaterally. All sacral and caudosacral ribs are fused to the ilium—the ribs from the parasacral to caudosacrals project at a lower angle in the lateral view. The parasacral and the first sacral ribs have anteroposteriorly expanded dorsal and ventral surfaces, which give the ribs an I-shaped proximal cross-section (Figs. 16a, b). The cross-section of the proximal ribs becomes trapezoid from the second sacral to the second caudosacral (Figs. 16a, b).

Fourteen caudal vertebrae are fused into the handle (*sensu* Coombs, 1995)

of the tail club (Figs. 17h–j). The handle is slightly curved in a posterodorsal fashion. The first to second handle vertebrae are spool-shaped, similar in length and height, and laterally compressed. The centra are elongated from the third back, except the fourteenth handle vertebra is short and knob-like. The low neural spines are blade-like and decrease in height posteriorly. The paddle-like prezygapophyses project beyond the anterior margin of the centra and diverge at an angle of about 20º in dorsal view. These interlock with the distally elongate, wedge-like postzygapophyses of the adjacent vertebra. The small nub-like transverse processes are only present on the first to third handle vertebrae. The chevrons are elongated, blade-like, and fused onto the ventral surface of the centra. Well-preserved ossified tendons were uncovered along the lateral surfaces of the tail handle (Figs. 18a–d). These tendons are arranged in an imbricating pattern. Most of these tendons are flattened and periodically bifurcate into as many as four branches. Some tendons are elliptical in the cross-section with longitudinal striae on the external surfaces. A poorly healed pathology is preserved on one tendon. This tendon was fractured in the middle portion and fused at an angle of about 125º.

Appendicular skeleton: The ilia diverge at an angle of 27º from the body midline (Fig. 16). The long and blade-like preacetabular processes extend anterolaterally (Figs. 16g, 17a–d). The closed acetabulum is level with the medially positioned first and second sacral ribs. The short buttress-like postacetabular processes extend posterolaterally from the acetabulum. Only the proximal portion of the left ischium is preserved (Figs. 17e–g). The proximal margin of the ischium is convex.

Osteoderms: No cervical half-rings were preserved. A single isolated Type 2 osteoderm (*sensu* Arbour et al., 2013) is preserved (Figs. 18e–g). The external surfaces are damaged, whereas the medial surface is well preserved and smooth. It is polygonal in dorsal view, sharply keeled dorsally, and thin-walled. The surface texture of this osteoderm is pitted. Two isolated Type 7 osteoderms are sub-circular, dorsoventrally flattened, with a keel near one edge that tapers in height anteriorly (Figs. 18h–m). They are thin-walled, rugose externally with a slightly concave ventral surface. The distal end of the tail is enveloped with two major and one minor osteoderms, forming a tail club knob (Fig. 17j). The length and width of the tail club knob are nearly equal. The major osteoderms are hemispherical in dorsal view and dorsolaterally keeled; the right is slightly larger than the left. Pathological grooves are present along the lateral surfaces of the two major osteoderms (Fig. 17k). The minor osteoderm is a rhomboidal shape in dorsal view. The surface texture of the tail club knob is pitted, rugose, and spongy.

Ankylosauridae, gen. et sp. indet.

Studied specimen. MPC-D 100/1359 (Figs. 20–26), a nearly complete postcranial skeleton that lacks the tail but includes twelve dorsal vertebrae, ribs, pectoral girdles, forelimbs, pelvic girdles, hindlimbs, and free osteoderms.

Locality and horizon. Aeolian red sandstone deposit of the Upper Cretaceous (middle–upper Campanian) Baruungoyot Formation, Hermiin Tsav, southern Gobi Desert, Mongolia.

Remarks. The Joint Soviet-Mongolian Paleontological Expedition team first discovered and uncovered this specimen in 1972 or 1973 (Ligden Barsbold, personal communication May 20, 2020). They prepared it for excavation as a monolith but ran out of materials and time and abandoned it, intending to excavate it later. It was found by a Dinosaurs of the Gobi (Nomadic) Expedition in 1999, but it had no doubt been seen by many other expeditions in the meantime but not collected until the Korea-Mongolia International Dinosaur Expedition in 2008 (Fig. 20). Just before the excavation of MPC-D 100/1359, the sides of the specimen were still surrounded by a wooden crate, but loose plywoods covered the top. All of the intervening spaces had been filled in by loose, wind-blown sand. It is uncertain whether there was a skull and/or a tail club associated with the postcranial skeleton, although it's unlikely the skull was present because the cervical half-rings are missing.

The presence of a synsacrum, the horizontal rotation of the ilium, closed

acetabulum, absence of the pubis, and dermal armor on the lateral surface of the body clearly show that MPC-D 100/1359 belongs to Ankylosauria (Coombs and Maryañska, 1990; Carpenter, 2007). Furthermore, MPC-D 100/1359 contains ankylosaurid features such as a broad humerus, unguals that are wider than long, and a tridactyl pes (Coombs and Maryañska, 1990; Currie et al., 2011; Carpenter, 2012). A total of three ankylosaurid taxa – *Saichania chulsanensis*, *Tarchia kielanae*, and *Zaraapelta nomadis* – are known from the Baruungoyot Formation (Maryañska, 1977; Arbour et al., 2014b). *Saichania* is similar to MPC-D 100/1359 in having broad but irregular, plate-like, bony intercostal processes on the dorsal ribs and a robust ulna. However, *Saichania* differs from MPC-D 100/1359 by having fused dorsal ribs from the sixth dorsal vertebra, bony processes starting from the fifth rib, medially fused sternal plates, more robust humeri, a spur-like lateral process on the proximal end of the humerus, a pointed olecranon on the ulna, lateral and medial femoral condyles that have the same heights, and three rows of spine-like flank osteoderms (two rows of dorsoposteriorly bent osteoderms, and ventral to them, one row of dorsoanteriorly bent osteoderms) (Maryañska, 1977; Barrett et al., 1998; Arbour and Currie, 2016). No postcranial materials are known from *Tarchia kielanae* and *Zaraapelta* so comparisons to MPC-D 100/1359 are currently not possible (Maryañska, 1977; Arbour et al., 2014b; Penkalski and Tumanova, 2017). For these reasons, MPC-D 100/1359 must be considered an indeterminate ankylosaurid.

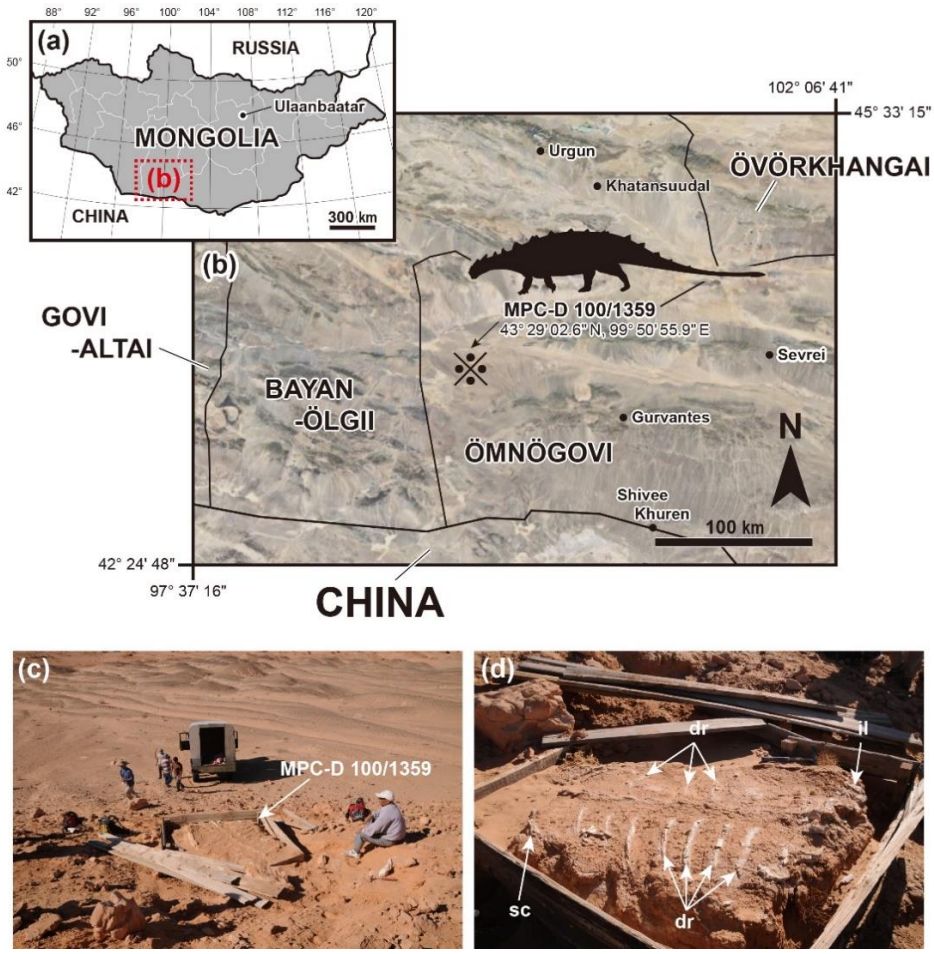

Figure 20. Map showing where the new ankylosaurid postcranial specimen (MPC-D 100/1359) was discovered. (a) Map of Mongolia. (b) Enlarged map of the rectangle with the dotted line in Fig. 20a. The fossil locality is marked by a symbol (※). (c) Photograph of the excavation site. (d) Close-up photograph of the exposed dorsal surface of the specimen.

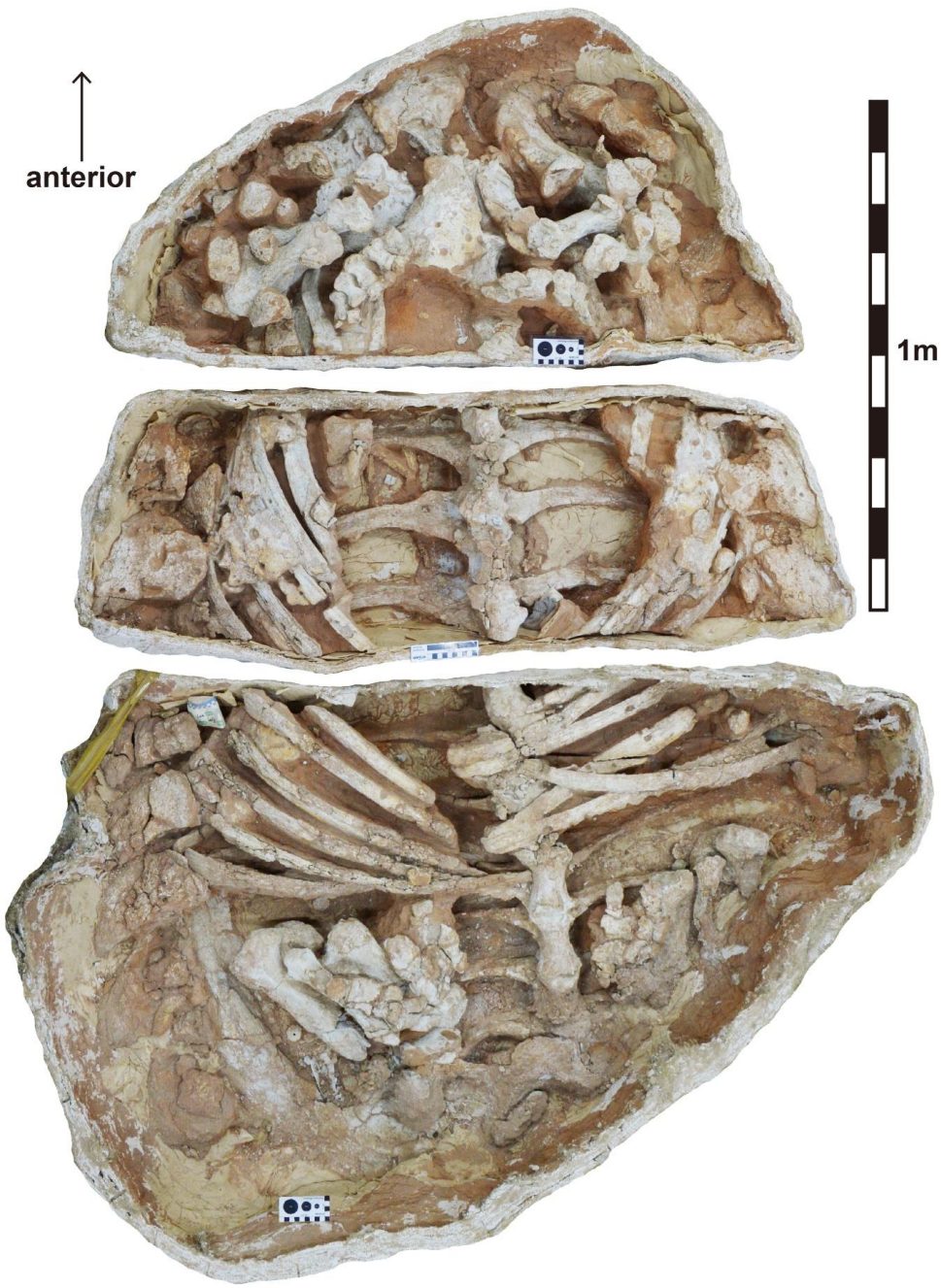

Figure 21. Photograph of the new ankylosaurid postcranial specimen (MPC-D 100/1359) in ventral view.

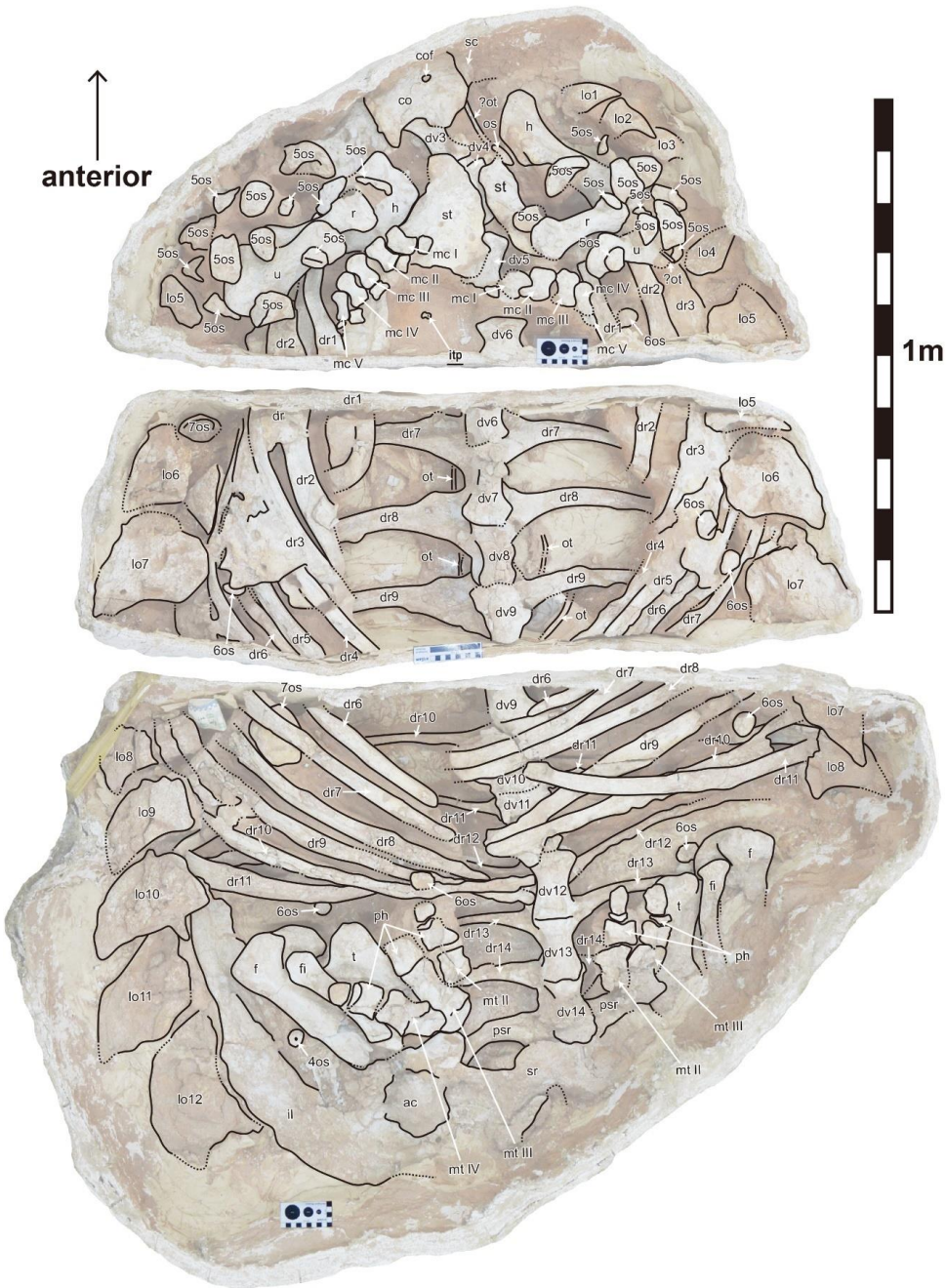

Figure 22. Line drawing of the new ankylosaurid postcranial specimen (MPC-D 100/1359) in ventral view.

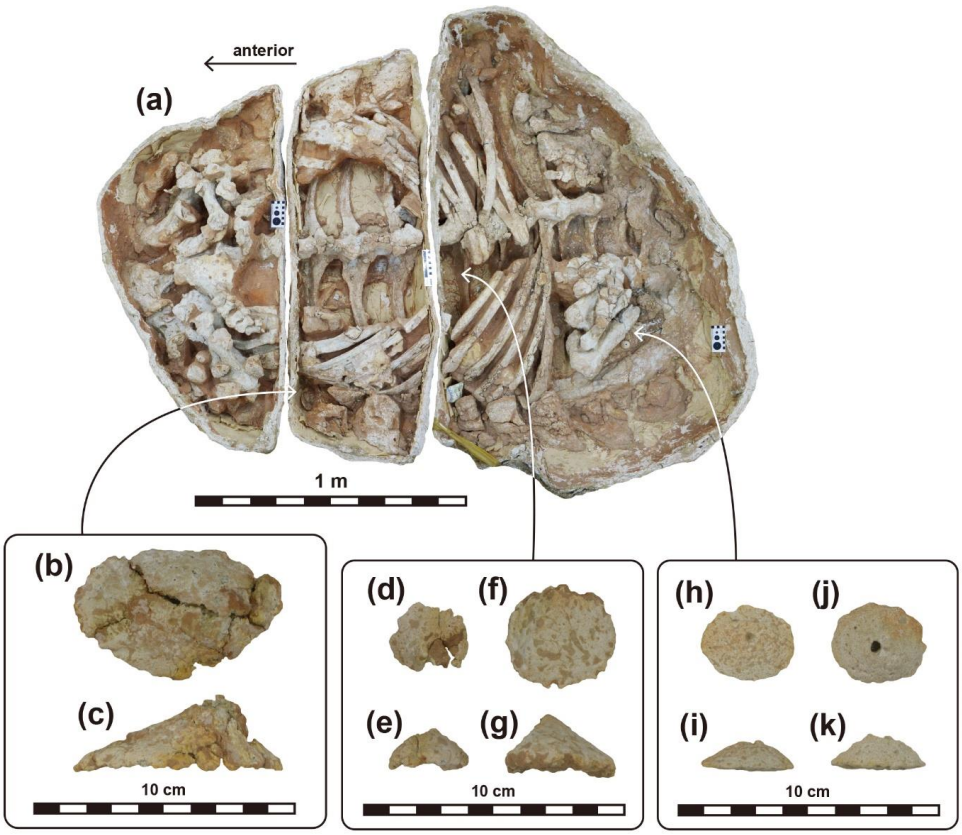

Figure 23. Selected osteoderms from the new ankylosaurid postcranial specimen (MPC-D 100/1359). (a) MPC-D 100/1359 in ventral view. Arrows indicate the areas where the selected osteoderms were collected. (b and c) Type 7 osteoderm in lateral (b) and dorsal (c) views. (d–k) Type 4 osteoderms in lateral (d, f, h, j) and dorsal (e, f, i, k) views.

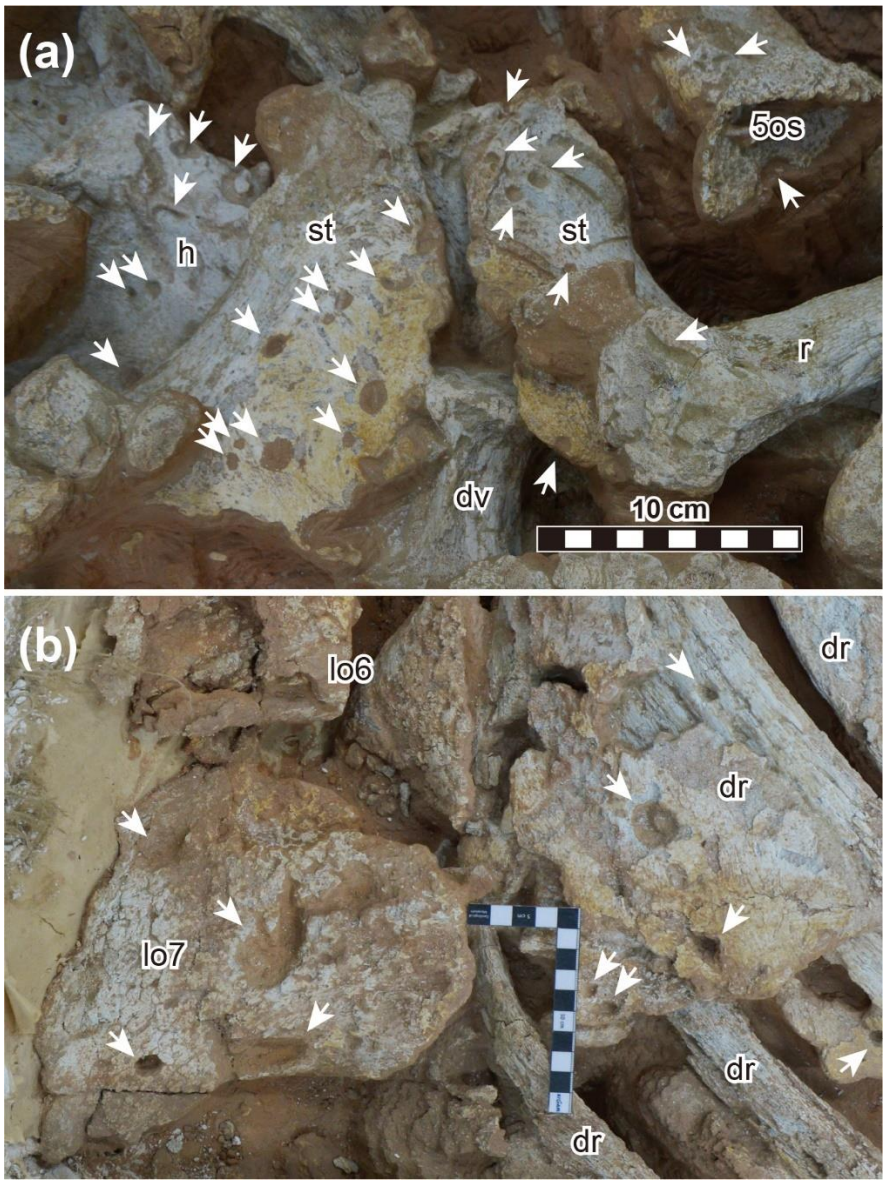

Figure 24. Feeding traces of dermestid beetles from the new ankylosaurid postcranial specimen (MPC-D 100/1359). (a) Close up photo of sternal plates. (b) Close up photo of the right lateral edge of the middle portion of the trunk. White arrows mark feeding traces.

Figure 25. Five isolated theropod phalanges (marked by white arrows) that were collected inside the ribcage of the new ankylosaurid postcranial specimen (MPC-D 100/1359).

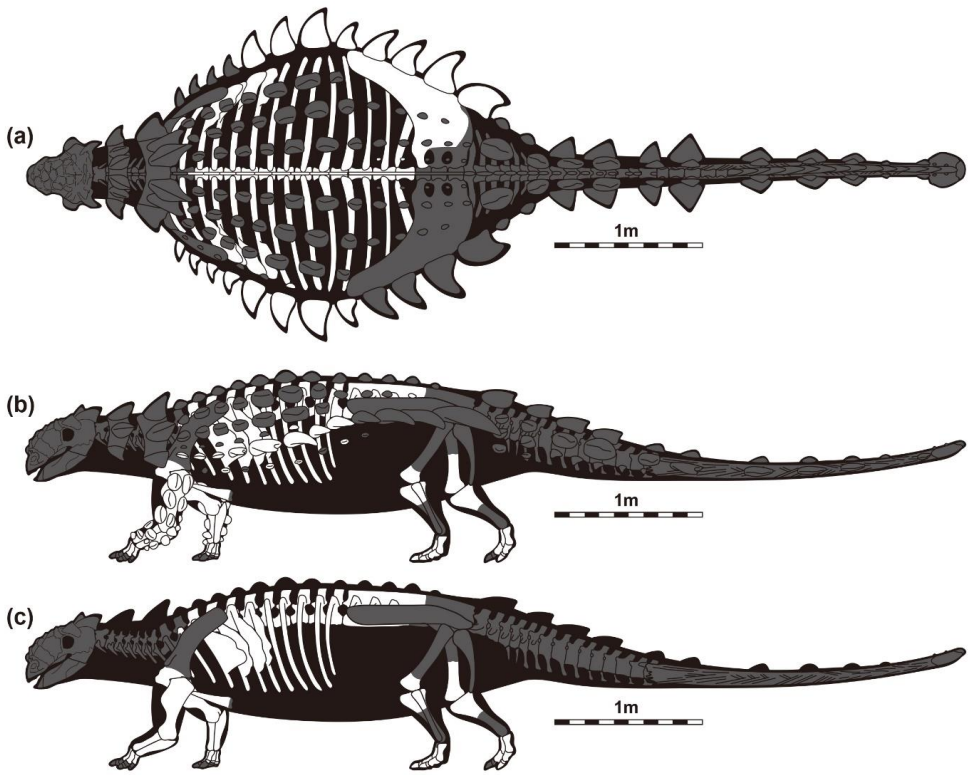

Figure 26. Skeletal diagram of the new ankylosaurid postcranial specimen (MPC-D 100/1359). (a) Dorsal view, (b) left lateral views with dermal armor, and (c) without dermal armor.

Description. The body lies horizontally in a "resting posture," with both forelimbs and hindlimbs folded and tucked underneath the torso (Figs. 21 and 22). The preserved trunk is 203 cm in length and 129 mm in greatest width (external osteoderms are excluded, see Tables 14-18 for detailed measurements). Feeding traces of dermestid beetles can be observed on the dorsal ribs, sternal plates, forelimbs, and dermal armor (Fig. 24). These circular borings are 5.5 to 36.25 mm in diameter. Five small, isolated theropod phalanges were also found inside the ribcage (Figs. 21, 22, and 24).

Table 14. Measurements (mm) of vertebrae of MPC-D 100/1359. The asterisk refers to incomplete measurement due to damage.

Element	Length of centrum	Width of the anterior surface of centrum	Width of the posterior surface of centrum
4th dorsal	116	4*	34*
5th dorsal	120	37*	24*
6th dorsal	111	51*	49*
7th dorsal	128	91	61*
8th dorsal	130	37*	79
9th dorsal	103	45*	53*
10th dorsal	-	75	8
11th dorsal	118*	79	-
12th dorsal	122*	72	34*
13th dorsal	128	68*	77
14th dorsal	115	77	77
15th dorsal	122	86	81
1st sacral	98*	76	-

Table 15. Measurements (mm) of pectoral girdle and forelimbs of MPC-D 100/1359. Asterisks refer to incomplete measurements due to damage.

Element		Measurements
Left scapula	Length	-
	Proximal height	91*
	Medial height	-
	Distal height	-
Left coracoid	Length	218
	Proximal height	129*
	Medial height	105*
	Distal height	91*
Left humerus	Length	322*
	Proximal width	169
	Medial width	46*
	Distal width	-
Right humerus	Length	372
	Proximal width	186
	Medial width	-
	Distal width	50*
Left ulna	Length	123*
	Proximal width	-
	Medial width	67*
	Distal width	94
Right ulna	Length	300
	Proximal width	158*
	Medial width	81
	Distal width	97
Left radius	Length	233
	Proximal width	91
	Medial width	50
	Distal width	91

(continued)

Element		Measurements
Right radius	Length	241
	Proximal width	50*
	Medial width	31*
	Distal width	88
Left sternum	Anteroposterior length	228*
	Mediolateral width	62*
Right sternum	Anteroposterior length	273
	Mediolateral width	225*

Table 16. Measurements (mm) of both manus of MPC-D 100/1359. Asterisks refer to incomplete measurements due to damage.

Element	Length	Proximal width	Distal width
Left metacarpal I	75	50*	57
Right metacarpal I	70	43	46
Left metacarpal II	70	56	63
Right metacarpal II	72	54	55
Left metacarpal III	75	58	30*
Right metacarpal III	79	53	46
Left metacarpal IV	73	42	33*
Right metacarpal IV	80	45	46
Left metacarpal V	25*	-	-
Right metacarpal V	65	38	28
Left manus phalanx I-1	36	26*	16*
Right manus phalanx I-1	31	33	36
Right manus phalanx II-1	26	34	40
Right manus phalanx III-1	27	37	46
Right manus phalanx IV-1	31	30	34
Right manus phalanx V-1	12	16	19

Table 17. Measurements (mm) of pelvic girdle and hindlimbs of MPC-D 100/1359. Asterisks refer to incomplete measurements due to damage.

Element		Measurements
Right illium	Length	769
	Length of preacetabular process	558
	Length of postacetabular process	55*
Left femur	Length	174*
	Proximal width	-
	Medial width	-
	Distal width	183
Right femur	Length	365*
	Proximal width	-
	Medial width	87*
	Distal width	179
Left tibia	Length	293*
	Proximal width	-
	Medial width	58*
	Distal width	101
Right tibia	Length	230
	Proximal width	-
	Medial width	62*
	Distal width	120
Left fibula	Length	210*
	Proximal width	74
	Medial width	39
	Distal width	-
Right fibula	Length	282
	Proximal width	71
	Medial width	41
	Distal width	50

Table 18. Measurements (mm) of both pedes of MPC-D 100/1359. Asterisks refer to incomplete measurements due to damage.

Element	Length	Proximal width	Distal width
Left metatarsal II	82	-	67
Right metatarsal II	73*	-	59
Left metatarsal III	126	-	60*
Right metatarsal III	127	65*	71
Right metatarsal IV	69	67	88
Left pes phalanx II-1	47	60*	65
Right pes phalanx II-1	58	72	55*
Left pes phalanx II-2	12	32	31
Right pes phalanx II-2	12	40	36
Left pes phalanx II-3	65	32*	34
Right pes phalanx II-3	37*	43	-
Left pes phalanx III-1	50	62	57
Right pes phalanx III-1	67	71	-
Left pes phalanx III-2	12	46	36
Left pes phalanx III-3	65	43	34
Right pes phalanx IV-1	39	68	70
Right pes phalanx IV-2	20	51	56
Right pes phalanx IV-3	45	54	29

Axial skeleton: The overall torso is dorsoventrally shallow and fusiform (Figs. 21 and 22). Twelve articulated dorsal vertebrae are present. However, it can be assumed that the two most anterior dorsal vertebrae are missing because fourteen dorsal ribs are preserved on each side. The dorsal centra are spool-shaped and longer than high or wide. Ossified tendons are present along the neural spines. The centra of the posterior dorsal vertebrae are a bit shorter in length, and the lateral surfaces are less concave than the anterior ones. No sacral vertebrae are preserved posterior to the dorsal vertebrae. Nine fused posterior dorsal vertebrae from the seventh to 15th are also fused with their ribs to form a long presacral rod. The dorsal ribs increase progressively in size posteriorly from the first to the 11th. These ribs each have a horizontally expanded, flat dorsal surface with a ventrally deep head, which gives the rib a T- or L-shaped proximal cross-section. These ribs also have irregular plate-like bony processes that extend posteriorly from the mid-shaft regions. The processes overlap the lateral surfaces of up to three following ribs. In the third to sixth dorsal ribs, these processes are co-ossified, forming a large lateral plate. The 12th to 14th dorsal ribs are rod-like, smaller, and anteroposteriorly narrower than the 11th. A parasacral rib (*sensu* Penkalski, 2018) is present posterior to the 14th dorsal ribs. These are also slender, similar to the 12th to 14th dorsal ribs, and the lateral portion is posteriorly arched where it contacts the ilium posterolaterally. The most anterior sacral rib is preserved on the right side only. This robust rib is horizontal and fused laterally to the ilium.

Appendicular skeleton: Only the left scapula and coracoid are preserved, and a suture line is observable between the two bones (Figs. 21 and 22). Although the preserved scapula is fragmentary, the coracoid is moderately complete. A hook-like sternal process is present on the ventral margin of the coracoid. The coracoid foramen is located near the glenoid fossa, which faces posterolaterally and is separated by an open suture from the scapula. The unfused sternal plates are large and triangular. The hourglass-shaped humeri are short and robust, and the maximum proximal width is about 50% of the total length. The deltopectoral crest extends distally to about the middle of the humerus and has a lateral process on the proximal edge, which can be observed on the left side. The crest extends more laterally than anteriorly. The humeral shaft is short and thick. Both rod-like radii are present. The expanded proximal and distal condyles of the radius are similar in size. Both robust ulnae are also preserved, and each has a blunt olecranon. The medial process of the ulna is prominent. Five metacarpals are preserved in a shallow arc on both sides. All metacarpals are robust, with expanded proximal articular surfaces and distal condyles. Metacarpals I to IV are similar in size, but metacarpal V is smaller than others. Five proximal phalanges (I-1 to V-1) are present on the right manus, but only the first proximal phalanx (I-1) is preserved on the left manus. The phalanges are wide distally than proximally.

An undistorted right ilium is preserved, which diverges at around 28° from the body's midline (Figs. 21 and 22). It is long with a blade-like preacetabular process extending anterolaterally. The closed acetabulum is level with the medially

positioned first sacral rib. A short buttress-like postacetabular process extends posterolaterally from the acetabulum. The femur is uncrushed but only preserved with posteriorly expanded distal condyles, of which the lateral condyle projects more ventrally than the medial one. The stout tibiae are straight, and each has an anteroposteriorly expanded proximal condyle. Both of the long and narrow fibulae are preserved, although the distal portion of the right one is missing. They are straight or slightly curved. Left metatarsals II to IV, and right metatarsals II and III are preserved. They are elongate and somewhat hour-glass shaped. Metatarsal III is only slightly longer than metatarsals II and IV. Pedal phalanges II-1 to -3, III-1, and IV-1 to -3 are preserved on the left side, whereas III-1 to -3 and IV-1 to -3 are present on the right side. The phalangeal count is 0-3-3-3-0. Based on the well-preserved unguals on the left pes, the unguals are longer than wide. The distal portion of the unguals on the right pes is poorly preserved.

Osteoderms: Large, dorsoposteriorly bent spine-like Type 1 osteoderms (*sensu* Arbour et al., 2013) are present in a row along the lateral side of the body (Figs. 21 and 22). The fifth to 12th lateral osteoderms are preserved on the right side, whereas the first to eighth are preserved on the left side. The most anterior Type 1 osteoderm is positioned above the forearm. The osteoderms increase in size from the first to the seventh. The eighth Type 1 osteoderm is about half the volume of the seventh one. Posteriorly from here, the osteoderms increase again in size from the eighth to the 12th. The most posterior osteoderm is lateral to the preacetabular

process of the ilium. A slightly compressed, keeled Type 7 osteoderm with a backswept tip was collected in the central region of the right side of the trunk, slightly dorsal to the lateral Type 1 osteoderms (Figs. 23b and 23c). Its dorsal surface is rugose. A total of six small, nodular Type 6 osteoderms are present on the ventral portion of the trunk (Figs. 21 and 22). Five of them are observable on the left side, whereas three can be seen on the right side. On the left side, one of these osteoderms is between the first and second dorsal ribs, whereas the other four are situated slightly ventromedially along with the large lateral Type 1 osteoderms. One is situated between the fifth and sixth dorsal ribs on the left side, whereas the other two are positioned near the distal tip of the ninth dorsal rib and behind the 11^{th} dorsal rib, respectively. Another single large flat Type 7 osteoderm (longitudinal length: about 125 mm, transverse width: about 100 mm) with a slightly concave ventral surface is present on the right side of the ribcage behind the seventh rib (Figs. 21 and 22). Only the ventral side of this osteoderm is observable at present. Three small, conical, and circular based Type 4 osteoderms with small neurovascular canals on the external surface are preserved: two within the ribcage and one beneath the pelvic region (Figs. 21, 22, and 23d–k). Medium-sized, trapezoidal or oval, keeled Type 5 osteoderms cover the lateral side of the forelimb: thirteen on the right and twelve on the left side (Figs. 21 and 22).

Comparisons to other Asian ankylosaurids

***Bissektipelta archibaldi*:** No overlapping portions are present between this taxon and MPC-D 100/1359.

***Chuanqilong chaoyangensis*:** This taxon is similar to MPC-D 100/1359 by having widely divergent ilia, a ventrally projected lateral condyle on the femur, and triangular unguals on the pes. However, it differs in having a gracile ulna (Han et al., 2014).

***Crichtonpelta benxiensis*:** This taxon is similar to MPC-D 100/1359 by having fifteen dorsal vertebrae, widely divergent ilia, and a ventrally projected lateral condyle on the femur. However, it differs by having eleven free dorsal vertebrae and four dorsosacral vertebrae (Lü et al., 2007).

***Gobisaurus domoculus*:** No comparable postcranial materials are described in scientific literature.

***Jinyunpelta sinensis*:** There are no noticeable differences between this taxon and MPC-D 100/1359 because of the limited postcranial materials described in the scientific literature.

***Liaoningosaurus paradoxus*:** This taxon is similar to MPC-D 100/1359 by having widely divergent ilia, triangular pedal unguals. However, it differs by having lateral and medial condyles on the femur in the same horizon and a pedal phalangeal count 0-3-4-5-0 (Xu et al., 2001).

***Minotaurasaurus ramachandrani*:** No postcranial materials are described in scientific literature.

***Pinacosaurus grangeri*:** This taxon is similar to MPC-D 100/1359 by having seven free dorsal vertebrae, widely divergent ilia, and Type 1 osteoderms present along the flanks and the preacetabular process of the ilium. However, it differs by having a preserved pair of fused sternal plates with long narrow lateral processes on the posterolateral edge, a gracile ulna, both lateral and medial condyles on the femur extending to the same level, some specimens having a pedal phalangeal count of 0-3-3/4-3/4-0, a hoof-like ungual phalanx III-4 on the pes, and up to eighteen Type 1 osteoderms on each side of the flank and up to seven on each side of the pelvic region (Maleev, 1954; Maryañska, 1971; Currie et al., 2011; Burns et al., 2015).

***Pinacosaurus mephistocephalus*:** This taxon is similar to MPC-D 100/1359 by having widely divergent ilia (Godefroit et al., 1999). There are no noticeable differences between this taxon and MPC-D 100/1359 because of the limited postcranial materials described in the scientific literature.

***Saichania chulsanensis*:** Comparison with this taxon is mentioned in the 'remarks' section.

***Shamosaurus scutatus*:** There are no noticeable differences between this taxon and MPC-D 100/1359 because of the limited postcranial materials described in the scientific literature.

***Talarurus plicatospineus*:** This taxon is similar to MPC-D 100/1359 in having a robust ulna and a lateral condyle on the femur that more projects ventrally than the medial one. However, it differs by having four dorsosacral vertebrae (Gilmore, 1933; Maleev, 1952b; 1956; Maryañska, 1977).

***Tarchia kielanae*:** See 'remarks' section.

***Tarchia teresae*:** No postcranial materials are described in the scientific literature.

***Tsagantegia longicranialis*:** No postcranial materials are known from this taxon.

***Zaraapelta nomadis*:** See 'remarks' section.

MPC 100/1305: This specimen is a nearly complete skeleton without a skull from the Djadokhta Formation (Campanian). This specimen is considered an indeterminate ankylosaurid herein (see chapter II-2.3). MPC 100/1305 is similar to MPC-D 100/1359 by having a robust ulna, a ventrally projected lateral condyle on the femur, a pedal phalangeal count of 0-3-3-3-0, and large Type 1 osteoderms laterally placed to the preacetabular process of the ilium. However, it differs by having ten free dorsal vertebrae, four dorsosacral vertebrae, fused pair of sternal plates with an anterior notch and a smooth lateral margin, and Type 5 osteoderms laterally placed between the forearm and the ilia (Carpenter et al., 2011).

ZMNH M8718: This specimen was excavated from the Chaochuan Formation (Albian–Cenomanian) and formally known as "*Zhejiangosaurus lishuiensis*" (Lü et al., 2007; Arbour and Currie, 2016). ZMNH M8718 includes dorsosacral and sacral vertebrae, fourteen caudal vertebrae, both ilia, a single pubis, complete hindlimbs and pes, and some unidentified bone fragments (Lü et al., 2007). It is similar to MPC-D 100/1359 by having a widely divergent ilium, a slightly ventrally projected lateral condyle on the femur. However, it differs by having six dorsosacral vertebrae, a pedal phalangeal count of 0-3-4-5-0, and a hoof-like ungual phalanx III on the pes (Lü et al., 2007; Arbour and Currie, 2016).

Preservation of MPC-D 100/1359

Few bones of MPC-D 100/1359 are distorted, and none are dislocated from the death posture, which suggests there was no post-mortem transportation. Feeding traces of dermestid beetles are present on the bone surfaces (Fig. 24). Because rapid and deep burial prevents the activity of dermestid beetles, Fanti et al. (2012) suggested that the presence of these traces might be evidence of the exposure of the body, allowing the development of a dermestid colony within the carcass. Some dorsal osteoderms (Type 4 and 7) are preserved inside the ribcage and the pelvic region (Figs. 21, 22, and 23d–k), which seem to have sunk into the body during decomposition before the final burial. On the other hand, the spine-like osteoderms on the flanks and pelvic area are preserved in place with feeding traces of dermestid beetles present on the ventral surfaces. This preservation difference implies that the lower part of the body of MPC-D 100/1359, slightly beneath the lateral osteoderms, was exposed and scavenged by beetles before the sediments finally covered the rest of the body. The five isolated theropod phalanges collected inside the trunk must have entered the ribcage from above before the final burial of this specimen (Figs. 21, 22, and 25).

Several ankylosaur specimens preserved in a similar “resting posture” to MPC-D 100/1359 were previously reported from the Djadokhta (Campanian) and Baruungoyot (middle–upper Campanian) formations of Mongolia (Maleev, 1954; Tverdochlebov and Zybin, 1974; Maryañska, 1977; Currie, 1989; Currie et al.,

2011), and the Bayan Mandahu Formation (Campanian) of China (Godefroit et al., 1999; Currie et al., 2011). Because all of these specimens were discovered in rock units deposited in semiarid to arid climates in eolian environments, it was interpreted that they were buried alive in dust storms or rainstorm episodes (Jerzykiewicz et al., 1993; Loope et al., 1998). MPC-D 100/1359 also perished *in situ*, possibly due to famine, dust storms, or any other possible number of reasons.

V. PHYLOGENETIC ANALYSES

V-1. Phylogenetic placement of *Talarurus plicatospineus*

The phylogenetic analysis resulted in 60 most parsimonious trees (tree length = 276 steps, consistency index = 0.547, and retention index = 0.56). The strict consensus tree (Fig. 27) shows that *Talarurus* is a sister to the clade that includes derived Asian taxa, such as *Saichania* (including *Tar. teresae*), *Tar. kielanae* (including *Minotaurasaurus*), and *Zaraapelta*. The clade that includes *Talarurus*, *Saichania*, *Tar. kielanae*, and *Zaraapelta* shares only one synapomorphy: the presence of small postocular caputegulae posterolateral to the orbit (character 50, state 1). Two North American taxa, *Akainacephalus* and *Nodocephalosaurus*, appear to be basal to this clade.

The phylogenetic placement of *Talarurus* has always been problematic. In Hill et al. (2003), *Talarurus* was recovered as a sister taxon to the clade that includes derived ankylosaurines such as *Ankylosaurus*, *Euoplocephalus*, *Nodocephalosaurus*, *Saichania*, *Shanxia*, "*Tarchia gigantea*" (now partially *Tar. teresae*), and *Tianzhenosaurus*. A similar result was obtained in a more recent analysis of Arbour and Evans (2017), which placed *Talarurus* outside of the clade that includes the derived ankylosaurines, such as *Ankylosaurus*, *Ano. lambei*, *Dyoplosaurus*, *Euoplocephalus*, *Saichania*, *Sc. Cutleri*, *Tar. kielanae*, *Ziapelta*, and *Zuul*. Vickaryous et al. (2004) placed *Talarurus* within the derived clade of Asian

ankylosaurines, including *Pinacosaurus*, *Saichania*, and *Tianzhenosaurus*. The result of Thompson et al. (2012) is similar to that of Vickaryous et al. (2004) and placed *Talarurus* within the clade that includes *Saichania*, "*Tar. gigantea*," and *Tianzhenosaurus*. In more recent analyses (Arbour and Currie, 2016; Zheng et al., 2018), however, *Talarurus* was positioned within the derived clade of North American Ankylosaurini. The results from this study (Fig. 27) are somewhat similar to those of Vickaryous et al. (2004) and Thompson et al. (2012).

North American ankylosaurines are known from the middle to late Campanian to Late Maastrichtian (Arbour and Currie, 2016; Penkalski and Tumanova, 2017; Penkalski, 2018; Wiersma and Irmis, 2018). Because the temporal range of these taxa does not go below the Santonian–Campanian boundary, earlier researchers speculated that the paleobiogeographic dispersal of derived ankylosaurids between Asia and western North America must have occurred during or earlier than the Campanian (Sullivan, 1999; Arbour et al., 2014a; Wiersma and Irmis, 2018). However, the placement of two North American taxa, *Akainacephalus* and *Nodocephalosaurus*, basal to *Talarurus* in the cladogram in this study, suggests that migration occurred before the Cenomanian (Fig. 28). The paleobiogeographic dispersal of ankylosaurines might have happened at least twice, one earlier than the Cenomanian and the other during or before the Campanian. The migration of ankylosaurines from Asia to western North America may be concordant with the records of other dinosaurs such as tyrannosauroids (Loewen et al., 2013), therizinosaurids (Zanno, 2010), caenagnathids (Funston et

al., 2018), and hadrosauroids (Prieto-Márquez, 2010).

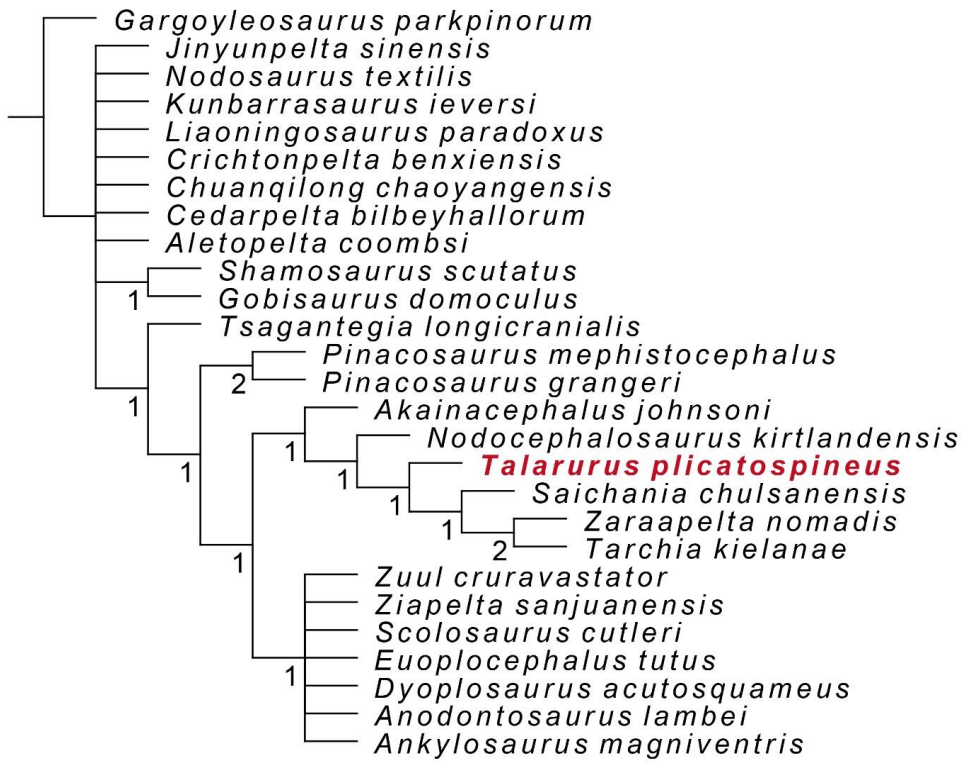

Figure 27. Strict consensus of 60 most parsimonious trees. Values beneath nodes indicate Bremer support.

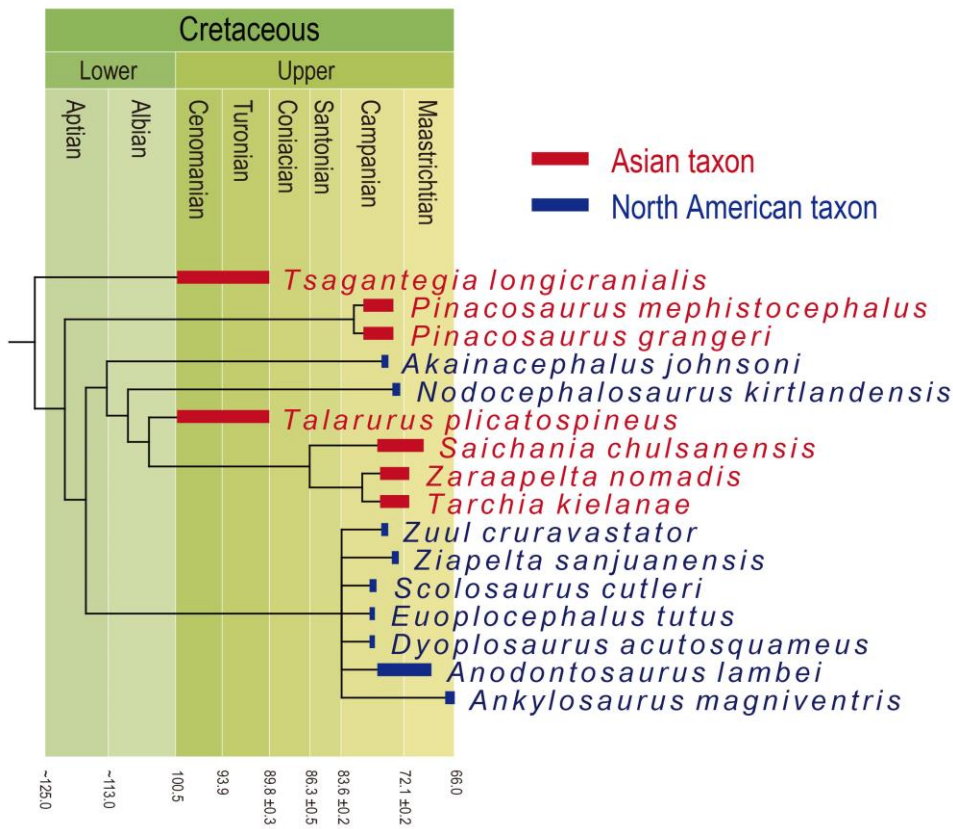

Figure 28. Time-scaled strict consensus tree of the 60 most parsimonious trees.

V-2. Phylogenetic placement of *Tarchia tumanovae* sp. nov.

The phylogenetic analysis resulted in a single most parsimonious tree (tree length = 32 steps, consistency index = 0.813, and retention index = 0.769) (Fig. 29). *Tar. tumanovae* is a sister to the clade that includes *Tar. kielanae* and *Tar. teresae*. *Tar. kielanae* and *Tar. teresae* share only one synapomorphy: moderate-sized basioccipital foramen (character 10: state 1). The three *Tarchia* species share five synapomorphies: a "neck" present at the base of the quadratojugal horn (7:1) (ambiguous in *Tar. kielanae*); tall foramen magnum (9:1); tall braincase (15:1); posteroventrally oriented occipital condyle (17:1); no postocular caputegulae (21:0) (ambiguous in *Tar. kielanae*). *Saichania*, *Zaraapelta*, and *Minotaurasaurus* were recovered as successive outgroups to the clade containing three *Tarchia* species.

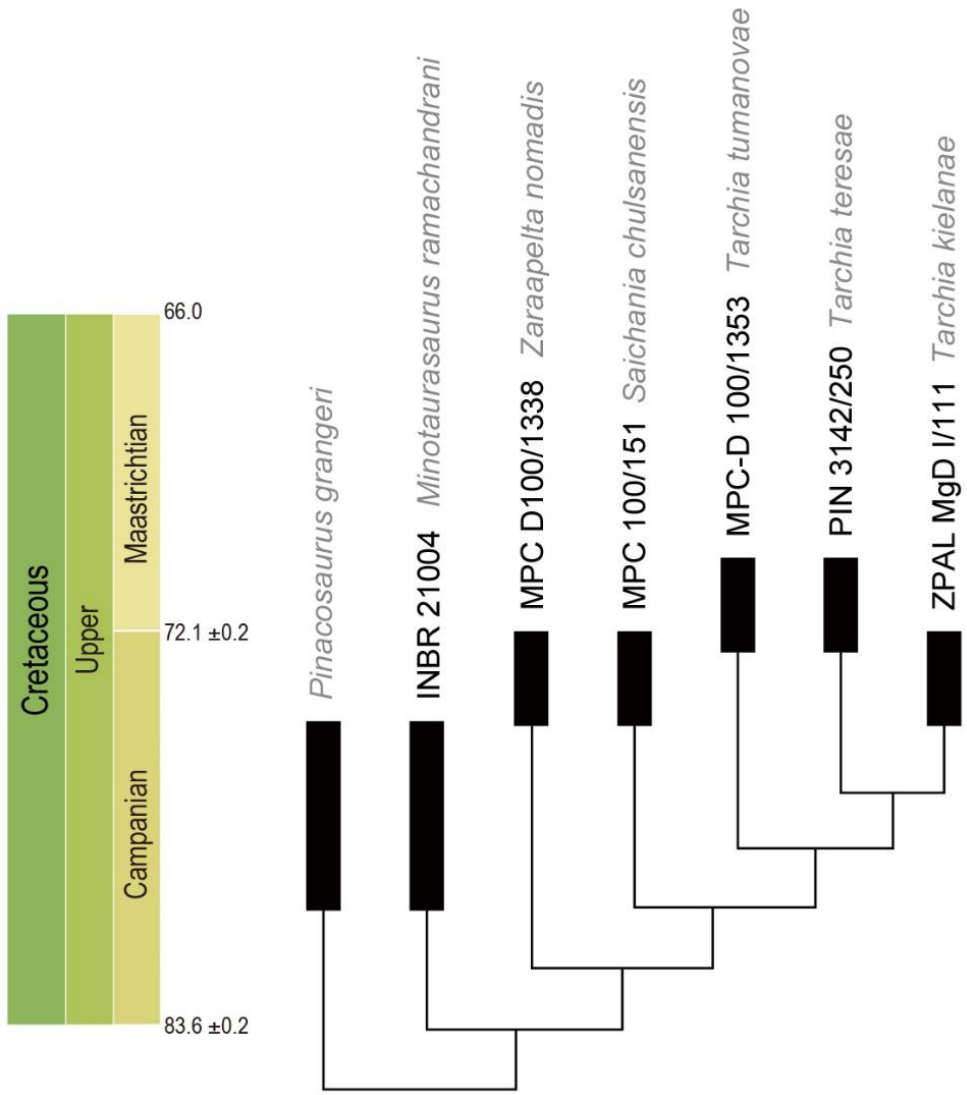

Figure 29. The single most-parsimonious tree produced by phylogenetic analysis, using implied character weighting with a k-value of 3.

VI. DISCUSSION

VI-1. Paleoecology of *Talarurus* and *Tsagantegia*

Only two ankylosaur taxa, *Talarurus* and *Tsagantegia*, are known from the Bayanshiree Formation (Maleev, 1952b; Tumanova, 1987, 1993). The skulls of the two taxa are similar in size (up to 301 mm and 300 mm in length, respectively). Nevertheless, the rostra of both taxa are quite different from each other in shape (Figs. 30–32). In lateral view, the palatal surface of the premaxilla slopes down anteriorly in *Talarurus*, resulting in a ventrally pointing rostral tip. However, *Tsagantegia* is horizontal like the skull roof, and the rostral tip protrudes anteroventrally. In palatal view, the palatal surface of the premaxilla of *Talarurus* is broad and sub-rectangular, with a transversely straight anterior boundary. In contrast, the snout of *Tsagantegia* is somewhat shovel-shaped, with a rounded anterior boundary.

The rostral differences between these two taxa may be evidence of niche partitioning. A similar case can be observed in modern mammals such as the white (*Ceratotherium*) and black rhinoceros (*Diceros*). Both genera are distributed in central to southern Africa and are similar in size, measuring up to 4 m in length and weighing up to 3,500 kg (Steele, 1960; Nowak, 1991). The white rhinoceros has a broad rectangular muzzle, whereas the muzzle of the black rhinoceros protrudes and is rounded (Groves, 1972; Hillman-Smith and Groves, 1994). The rostral

differences provide a direct clue to the feeding habits of these two rhinocerotid taxa. Being a bulk feeder, the white rhinoceros consumes low-lying vegetation (Groves, 1972). In contrast, the black rhinoceros, a selective feeder, prefers high-growing shrubs (Hillman-Smith and Groves, 1994). The white rhinoceros might be the modern equivalent of *Talarurus*, with the black rhinoceros analogous to *Tsagantegia*. Like the white rhinoceros, the broad muzzle of *Talarurus* would have enhanced cropping vegetation along a flat surface. Similar niche-related rostral morphologies are also known in ungulates and ground sloths (Janis and Ehrhardt, 1988; Solounias and Moelleken, 1993; Solounias et al., 1988; Susana Bargo et al., 2006).

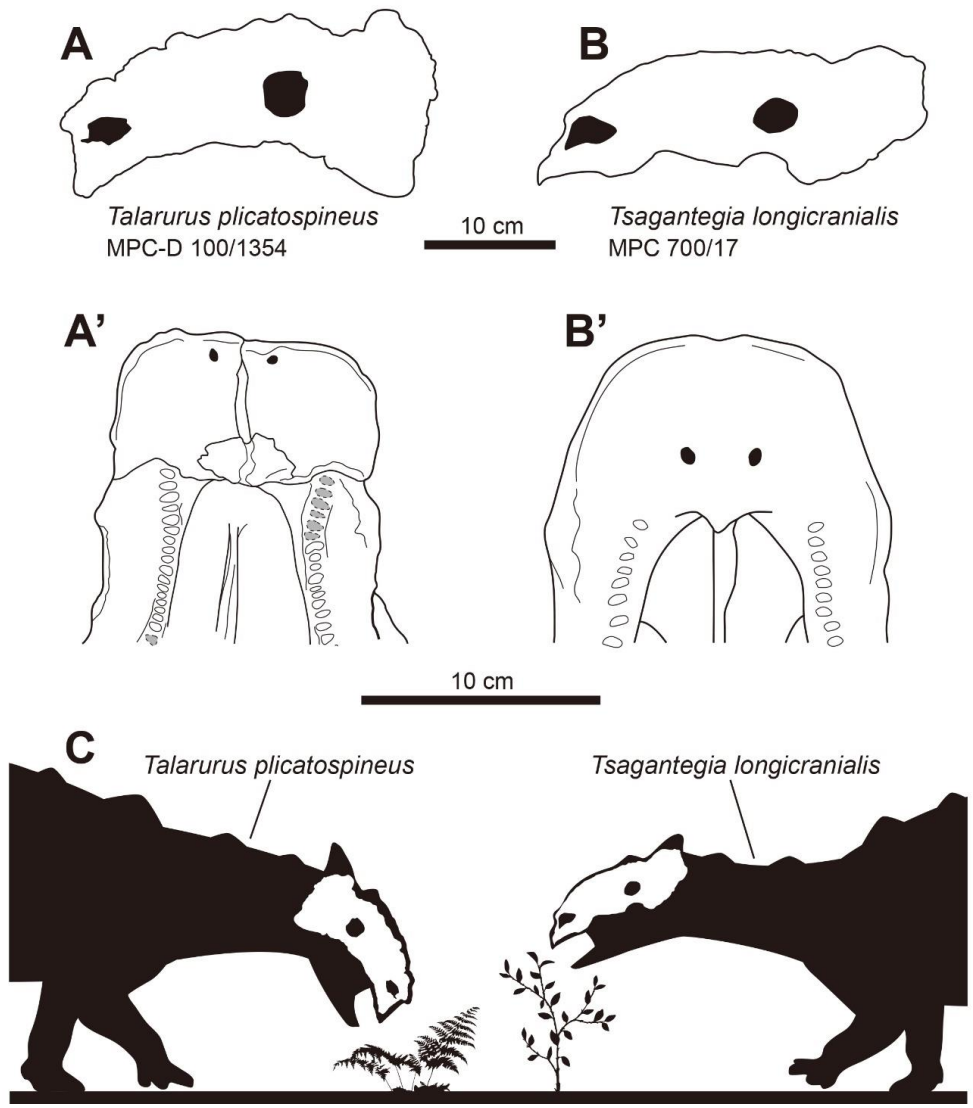

Figure 30. Skull (in left lateral view) and muzzle (in palatal view) comparisons of *Talarurus plicatospineus* (A–A') to *Tsagantegia longicranialis* (B–B'), and (C) a hypothesized illustration for the different feeding heights between the two taxa.

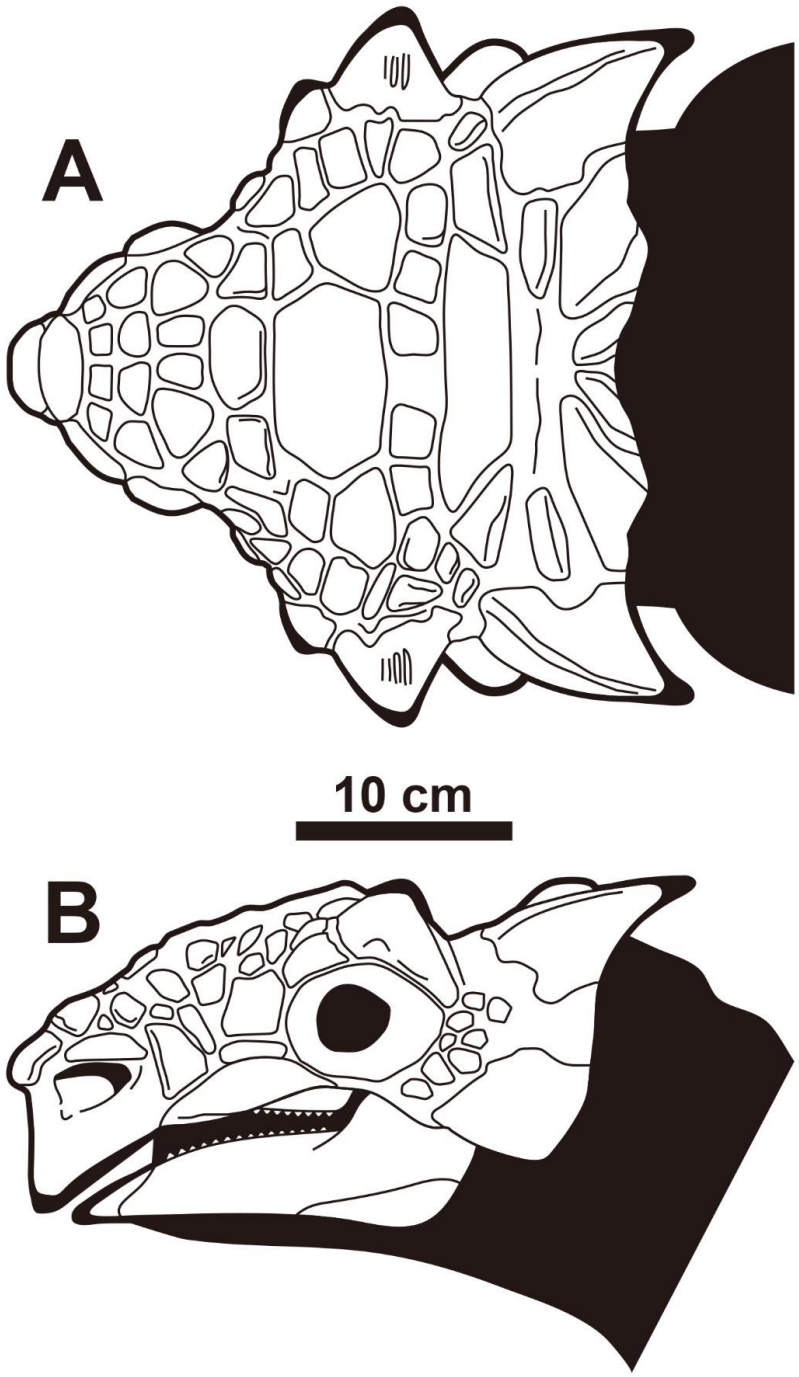

Figure 31. Skull reconstruction of *Talarurus plicatospineus*. (A) Dorsal and (B) left lateral views.

Figure 32. Head reconstruction of *Talarurus plicatospineus*. Drawn by Jed Taylor.

VI-2. Squamosal horn remodeling in ankylosaurines

The squamosal horns of MPC-D 100/1353 are divided into the external layer of the squamosal horn and the underlying squamosal horn propers (Figs. 12a, b, e, f). These two layers are tightly fused in the holotype of *Zaraapelta* (MPC-D 100/1338) (Arbour et al., 2014b). In the holotype of *Minotaurasaurus* (INBR 21004), only the anterior end of the original osteodermal horn is present above the squamosal horn proper (Miles and Miles, 2009), whereas in the holotype of *Tar. teresae* (PIN 3142/250), the external layers are partially preserved (Tumanova, 1977; Penkalski and Tumanova, 2017). Arbour et al. (2014) hypothesized that the external dermal layer might have fused to the squamosal horn proper during ontogeny, based on MPC-D 100/1338. However, Penkalski and Tumanova (2017) suggested that MPC-D 100/1338 is immature, and the external layer might have resorbed during ontogeny, disappearing entirely in skeletally mature individuals. The divided state and shape of the squamosal horns in MPC-D 100/1353 is somewhat between MPC-D 100/1338 and INBR 21004. Moreover, the irregular ventral margin of the base of the external dermal layer in MPC-D 100/1353 may represent resorption. If this is the case, ankylosaurines underwent extreme ontogenetic remodeling of the squamosal horns, as Penkalski and Tumanova (2017) proposed. Nonetheless, histological analysis of ankylosaurine specimens is needed to support this hypothesis further.

VI-3. Evidence of agonistic behavior in ankylosaurines

Fracture healing can be observed on both sides of the first dorsosacral ribs of MPC-D 100/1353 in the anterolateral part of the pelvic area (Figs. 15i, j). Arbour et al. (2020) suggested that the localized injuries on the pelvic area in ankylosaurines are likely caused by intraspecific combat inflicted by the tail club knob. This idea was supported by the fact that there was no relationship between tail club knob size and predator body mass, and concentrated pathologies observed in free caudal vertebrae, tail club knobs, and pelvic osteoderms confined to mature individuals (Arbour and Currie, 2011; Arbour et al., 2020). A poorly healed ossified tendon on the tail knob handle is present in the holotype of *Tar. tumanovae* (Fig. 18d), which is a possible injury due to active tail use during combat (Fig. 33).

The tail club knob of the holotype also has pathologies. Grooves are present along each lateral surface of the two major osteoderms (Fig. 17k). Moreover, the tail club knob is asymmetric in dorsal view, the left major osteoderm being shorter in mediolateral width than the right (Fig. 17j). Similar asymmetric bone growth has been observed on the postorbital horn of a male Dall sheep (*Ovis dalli dalli*), which impact each other with their heads at intraspecific combat (Hoef and Bunch, 1992). As in the horn asymmetry in Dall sheep, the reduced size of the left major osteoderm in MPC-D 100/1353 could result from tail club strikes. Asymmetry of the tail club knob was noticed in three ankylosaur specimens from North America, ROM 788 (*Platypelta*), ROM 75860 (holotype of *Zuul*), and UALVP 16247 (Ankylosauridae indet.) (Arbour, 2009; Arbour and Currie, 2011;

Arbour and Evans, 2017). UALVP 16247 is similar to MPC-D 100/1353 by having the left major osteoderm smaller in volume than the right (Arbour, 2009). However, the left major osteoderm is larger than the right in ROM 788 and ROM 75860 (Arbour and Currie, 2011; Arbour and Evans, 2017). Modern African elephants (*Loxodonta*) show tusk asymmetry due to side preferences in tusk use in stripping bark, digging root, and agonist interactions (Capstick, 1977; Marais and Hadaway, 2008; Bielert et al., 2018). Comparable to the tusk asymmetry in African elephants, tail asymmetry may relate to side preferences in tail use among ankylosaurine taxa or individuals. Pathologies found on the pelvic area and tail of MPC-D 100/1353 provide additional evidence of agonistic behavior in ankylosaurines. Laterally wide trunks of ankylosaurines could have protected vital organs from being ruptured during conspecific tail club strikes (Carpenter, 1997).

Figure 33. Life reconstruction of *Tarchia tumanovae* sp. nov. Drawn by Yusik Choi.

VI-4. Niche shifting in Mongolian ankylosaurids

Sub-rectangular broad muzzles are a morphological character of low-level bulk feeders, whereas anteriorly protruded shovel-shaped muzzles are selective feeders in ankylosaurines (Carpenter, 1982; Ősi et al., 2017; see chapter III-4). Similar dietary adaptations based on rostral shape are also known in mammalian herbivores, such as ungulates and ground sloths (Janis and Ehrhardt, 1988; Solounias et al., 1988; Solounias and Moelleken, 1993; Susana Bargo et al., 2006). Based on these examples, both *Tarchia* species from the Nemegt Formation were probably selective feeders (Fig. 34).

Bulk feeding ankylosaurines were present before the Baruungoyot and the Nemegt "age" (middle Campanian–lower Maastrichtian) based on known skull specimens (Fig. 34). On the other hand, all ankylosaurines from the Nemegt and the Baruungoyot formations were adapted for selective feeding. These dietary shifts in ankylosaurines probably relate to habitat change, the shift from semi-arid (Bayanshiree Formation) and arid (Djadokhta and Baruungoyot formations) to more humid climates (Nemegt Formation) (Jerzykiewicz, 2000; Ősi et al., 2017). Climate-driven habitat change alters the plant communities in the environment (Feeley et al., 2020), and niche shifting in ankylosaurids might have responded to this. Recently, Jerzykiewicz et al. (2021) proposed that Djadokhta, Baruungoyot, and Nemegt Formations are coeval, and the Nemegt Gobi Basin can be visualized as an ephemeral lake surrounded by semi-arid alluvial plains and arid dune fields. If this is the case, the dietary difference between these Mongolian taxa may result

from habitat differentiation within the same basin.

Tar. teresae and *Tar. tumanovae* coexisted with other megaherbivores, such as saurolophine hadrosaurids (*Barsboldia* and *Saurolophus angustirostris*) (Rozhdestvensky, 1952; Maryañska and Osmólska, 1981), ornithomimosaurs (*Deinocheirus*) (Osmólska and Roniewicz, 1970; Lee et al., 2014), sauropods (*Nemegtosaurus* and *Opisthocoelicaudia*) (Nowinski, 1971; Borsuk-Białynicka, 1977), and therizinosaurs (*Therizinosaurus*) (Maleev, 1954). Among these herbivores, the derived hadrosaurids are bulk feeders based on rostral morphology and dental microwear (Carrano et al., 1999; Williams et al., 2009). Recent phylogenic and biogeographic analyses suggest that saurolophine hadrosaurids immigrated from North America to Mongolia (Central Asia) in the post-Djadokhta "age" (Campanian) (Tsogtbaatar et al., 2015; Kobayashi et al., 2021), and this record is concordant with the niche shift in Mongolian ankylosaurs. The invasion of new bulk-feeding dinosaurs, which caused interspecific competition for limited resources, possibly drove selection pressure on the diets of ankylosaurs.

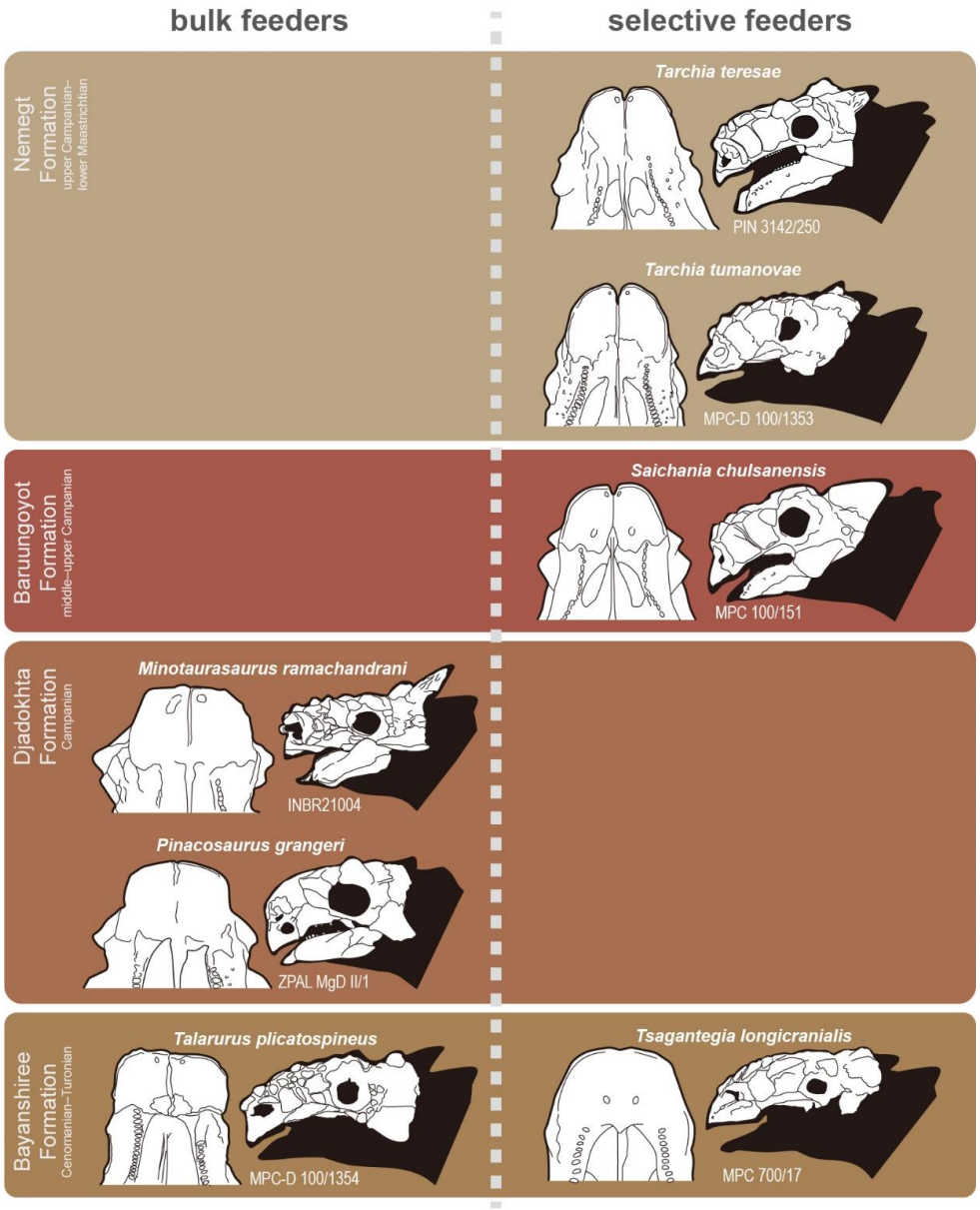

Figure 34. Skull (in left lateral view) and beak (in palatal view) comparisons of Mongolian ankylosaurines and their dietary categories through time.

VI-5. Postcranial evolution of ankylosaurids

MPC-D 100/1359 has nine sacrodorsal vertebrae (Figs. 21 and 22), the highest number known for ankylosaurs. Three to four sacrodorsals is the typical number for ankylosaurids, except *Anodontosaurus lambei*, which has five sacrodorsals (Maleev, 1954; Lü et al., 2007; Arbour and Currie, 2013; Penkalski and Blows, 2014; Penkalski, 2014; 2018; Wiersma and Irmis, 2018) (Fig. 35). Furthermore, the presence of broad but irregular, plate-like, bony intercostal processes is rare on the mid-shafts of the dorsal ribs. This feature is shared only with *Saichania* from the Baruungoyot Formation (Maryañska, 1977). The extensively fused vertebral series with unique dorsal ribs must have reduced the flexibility of the trunk. This character has been interpreted as possibly important in the evolution of bracing against tail movements (Arbour and Zanno, 2013; Tschopp and Mateus, 2013). However, it is unclear why Asian ankylosaurids had less flexible trunks than North American taxa. Although no ankylosaurid tail has been described from the Baruungoyot Formation in detail, an almost complete tail (ZPAL MgD I/113) from the Nemegt Formation (upper Campanian–lower Maastrichtian) suggests that some Asian ankylosaurids had more elongate tails than those of North American taxa (Arbour et al., 2013). The high rigidity of the trunk in some Asian ankylosaurids might have functioned as a buttress for the long tail.

The phalangeal pedal formula of MPC-D 100/1359 (0-3-3-3-0) is the same as those of one *Pinacosaurus grangeri* specimen (MPC 100/1320) and MPC 100/1305 (Ankylosauridae indet.) from the Djadokhta Formation (Campanian) but

differs from that of earlier Asian ankylosaurids such as *Liaoningosaurus* (0-3-4-5-0) and the majority of *P. grangeri* specimens (0-3-4-4-0 and 0-3-3-4-0) as well as North American ankylosaurid taxa (0-3-4-3/4-0) (Coombs, 1986; Arbour et al., 2009; Carpenter et al., 2011; Currie et al., 2011; Burns et al., 2015; Wiersma and Irmis, 2018) (Fig. 35). Although phalangeal pedal formulae can differ between individuals within the same species, as in *P. grangeri* (Currie et al., 2011), the phalangeal formula shows that the pedal phalanges, especially the second and third digits, of Asian ankylosaurids decreased in number through time. A decrease in the number of phalanges is recognized in the manus of sauropods to support their greater body masses (Christiansen, 1997). It is possible that this transition also occurred in the pedes of Asian ankylosaurs in correlation with the ventrally projected lateral condyles of the femora, which are considered as adaptations for weight-bearing (Carpenter et al., 2011) and have been observed in several Asian specimens (e.g., *Chuanqilong*, *Crichtonpelta*, *Talarurus*, MPC 100/1305, and ZMNH M8718) (Maleev, 1954; Lü et al., 2007a, 2007b; Carpenter et al., 2011; Han et al., 2014). Furthermore, the reduced number of pedal phalanges resulted in less mobility of the limbs (Christiansen, 1997). This feature might have also functioned as a less-flexible buttress for a long tail like the highly rigid trunk.

MPC-D 100/1359 is the fourth ankylosaurid specimen described with *in situ* flank osteoderms. The previously described specimens are MPC 100/1305 and PIN 614 (*P. grangeri*) from the Djadokhta Formation and MPC 100/151 (holotype of *Saichania*) from the Baruungoyot Formation (Maleev, 1954; Maryañska, 1977;

Carpenter et al., 2011). Both MPC 100/151 and PIN 614 have spine-like Type 1 osteoderms on the flanks as in MPC-D 100/1359. Instead of Type 1 osteoderms, however, keeled rhomboid Type 5 osteoderms are present on the sides of MPC 100/1305 (Carpenter et al., 2011) (Fig. 35), suggesting that there were at least two forms of flank armor within Asian ankylosaurids.

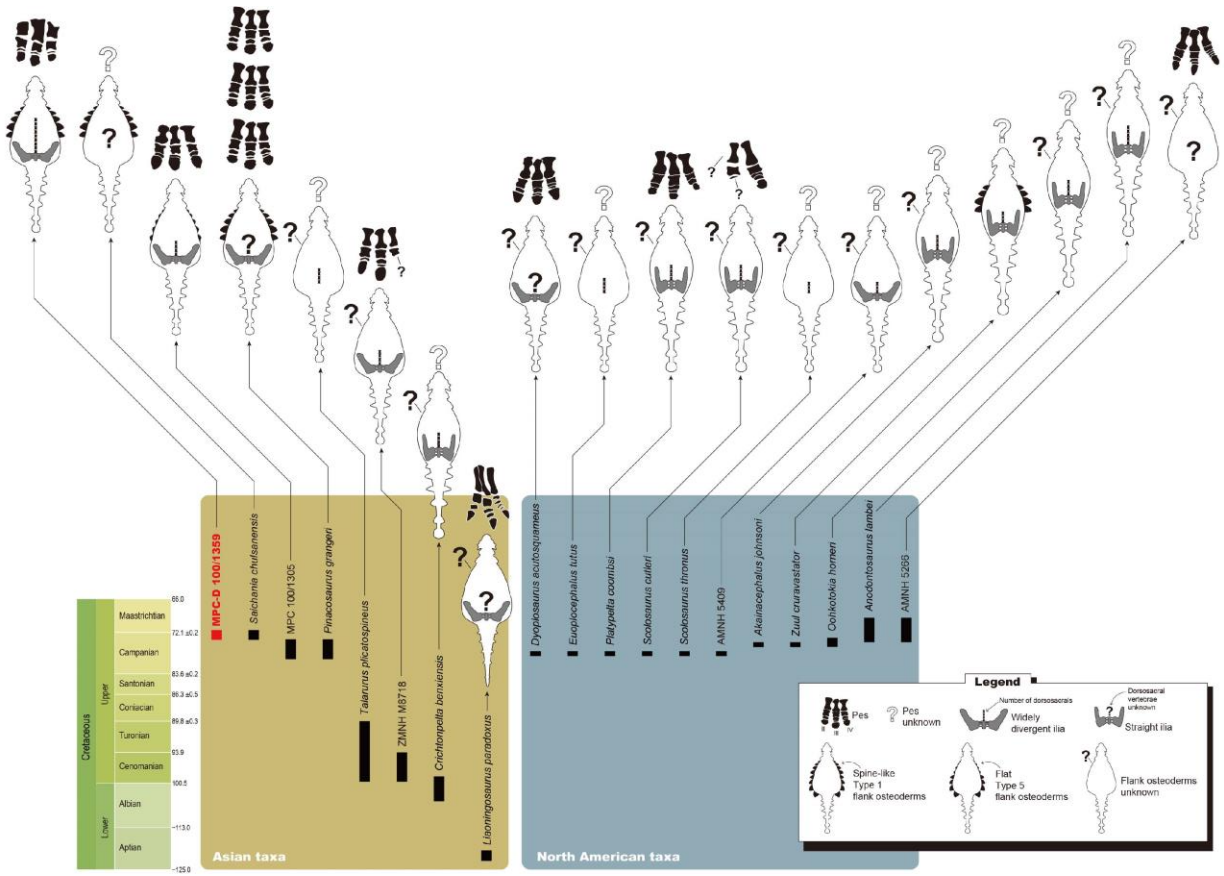

Figure 35. The temporal range of all known ankylosaurids with either well-preserved sacral rods and pelvic girdles, pedes, or flank osteoderms.

VI-6. Digging ability of ankylosaurids

A few authors have previously remarked that ankylosaurids show adaptations for digging. Maleev (1954) first hypothesized that "*Syrmosaurus viminicaudus*" (= *P. grangeri*) dug with anteroposterior body movements and covered up the lateral sides of their bodies with sediments using both fore- and hind limbs to leave the dorsal parts of their bodies exposed, similar to modern horned lizards (*Phrynosoma*). Maryañska (1977) supported this hypothesis based on the dorsoventrally flattened body shape and keeled dermal armor on lateral sides of the body of *Saichania*. Furthermore, Coombs (1978) concluded that digging habits were possible for ankylosaurids by reconstructing their forelimb muscles. No one has discussed the possibility of whether ankylosaurids were adapted for digging ever since.

Most ankylosaurids, including MPC-D 100/1359, show characteristics of digging, such as large acromion processes on the scapulae, robust humeri with well-developed deltopectoral crests, radii shorter than humeri, short and robust ulnae with well-developed olecranon processes, manus shorter than radii (terminal phalanges excluded), short and wide metacarpals and proximal phalanges, low intermembral indices (<70), and short or absent pubic symphyses (Hildebrand, 1974; 1985; Vizcaíno et al., 1999; Heckert et al., 2010; Lyson et al., 2016). Although the forelimb characters are also generally assumed to be related to weight-bearing (Coombs, 1978), low intermembral indices and the reduction or absence of pubic symphyses are considered two of the most indicative features of

digging (Coombs, 1983). Ankylosaurids also have dorsoventrally flattened and fusiform bodies with anteroposteriorly broadened dorsal ribs. It is an adaptation linked to counteracting the transverse bending force caused by the digging movements of the forelimbs (Lyson et al., 2016; Venkadesan et al., 2020). Additionally, the extensive fusion of vertebrae and dorsal ribs and the decreased numbers of pedal phalanges observed in MPC-D 100/1359 are related to digging. The high rigidity of the trunk may have stabilized the body during digging with forelimbs. The reduction of mobility in the hind limbs – caused by the decreased number of pedal phalanges – may have been suitable for anchoring ankylosaurs when they were digging (Hildebrand, 1985).

Coombs (1978) concluded that the ankylosaurid manus does not show special modifications for digging behaviors because the hoof-like manual unguals of ankylosaurids are different from the long, deep, and claw-like unguals of most digging animals. However, bony ungual length or curvature may not correlate well with the ecology of animals (Birn-Jeffery et al., 2012). The metacarpals of ankylosaurid forefeet, including those of MPC-D 100/1359, are arranged in a shallow arc (Figs. 21 and 22) that can increase the stiffness of the forefeet (Maryañska, 1977; Currie et al., 2011; Venkadesan et al., 2020). This shape gives the manus a shovel or trowel-like appearance. Even though ankylosaurids did not have claw-like unguals, therefore, it seems that they may have been able to dig soft substrate with the stiff trowel-like manus (Fig. 36).

Tumanova (1987) rejected the possibility of digging in ankylosaurids

because of their large body sizes. However, body size cannot be used to disqualify digging abilities in ankylosaurs because similar-sized, large animals such as mylodontid ground sloths could dig (Bargo et al., 2000). Although mylodontids were capable of dwelling in underground spaces (Dondas et al., 2009), it is doubtful that ankylosaurids could have done the same. To date, no paleoburrows attributable to ankylosaurs have been reported from ankylosaurid-bearing strata. Moreover, the stiffened elongated tail of ankylosaurids would not suit dwelling in underground spaces.

Anatomical features discussed in this paper could be good supporting evidence for the surface digging ability of ankylosaurids. By taking advantage of digging, ankylosaurids may have been able to dig out roots for food, dig wells to reach subsurface water, or dig into the sediments to find supplementary minerals to consume as modern African elephants (*Loxodonta*) do today (Haynes, 2012).

It was long assumed that ankylosaurids might have hunkered down to defend their relatively soft undersides from predators (Fastovsky and Weishampel, 2012). As crouching down in the shallow pits, they might protect their limbs and vulnerable belly parts and anchor their bodies to avoid getting turned over by large predators. Extant horned lizards (*Phrynosoma*) have a similar flat body and lateral fringe scales to those of ankylosaurids, which makes it difficult for predators to detect their silhouettes when partially buried or at rest on flat substrates (Sherbrooke and Montanucci, 1988; Sherbrooke, 2003; Vitt and Caldwell, 2013). Ankylosaurids may have utilized a similar strategy.

Figure 36. Life reconstruction of the new ankylosaurid specimen (MPC-D 100/1359). Drawn by Yusik Choi.

VII. TAXONOMIC REVIEW OF MONGOLIAN ANKYLOSAURS

VII-1. Introduction

In 1933, Charles Whitney Gilmore described and figured out the first ankylosaur species from Mongolia, *Pinacosaurus grangeri*. Since then, several taxa have been described in the scientific literature. Although some are now considered invalid, such as "*Amtosaurus magnus*" (Kurzanov and Tumanova, 1978; now regarded as ?Ornithischia indet.), "*Maleevus disparoserratus*" (Maleev, 1952a; = "*Pinacosaurus disparoserratus*"), "*Tarchia gigantea*" (Tumanova, 1977; now partially *Tarchia teresae*), and "*Tarchia giganteus*" (Maleev, 1956; now regarded as Ankylosauridae indet.), now there are ten valid species of ankylosaurs from Mongolia (Table 1). This review discusses the current understanding of the history and taxonomy of these taxa.

VII-2. Systematic paleontology

Dinosauria Owen, 1842; *sensu* Padian and May, 1993

Ornithischia Seeley, 1887; *sensu* Padian and May, 1993

Thyreophora Nopcsa, 1915; *sensu* Sereno, 1986

Ankylosauria Osborn, 1923; *sensu* Carpenter, 2007

Ankylosauridae Brown, 1908; *sensu* Sereno, 1998

Shamosaurinae Tumanova, 1983; *sensu* Arbour and Currie, 2016

Phylogenetic definition. All ankylosaurids closer to *Shamosaurus scutatus* than to *Ankylosaurus magniventris*.

Included taxa. *Gobisaurus domoculus* and *Shamosaurus scutaus* (type species).

Shamosaurus Tumanova, 1983

Type species. *Shamosaurus scutatus* Tumanova, 1983

Generic diagnosis. Genus monotypic, as for the type species.

Shamosaurus scutatus Tumanova, 1983

Type specimen. PIN 3779/2, skull (Tumanova, 1983: figs. 1 and 2), mandibles (Tumanova, 1987: fig. 12) (Figs. 1 and 2), and partial postcranial skeleton (Tumanova, 2000: figs. 2 and 3) (Figs. 37 and 38).

Type locality and horizon. Lower Cretaceous (Aptian–Albian) Zuunbayan Formation, Khamryn-Us, Mongolia.

Referred specimens. PIN 3779/1, partial skull (Tumanova, 1983: fig. 1c) (Zuunbayan Formation, Khamryn-Us, Mongolia).

Revised diagnosis. An ankylosaurid distinguished by the following unique set of characters (autapomorphies with an asterisk): a longitudinal furrow on the dorsal surface of the premaxilla (shared with *Zhongyuansaurus*); large, dome-like nasal area*; rugose, amorphous frontonasal ornamentation (shared with *Gobisaurus*); quadratojugal horns with a centrally positioned apices (shared with *Gobisaurus*); boss-like, short squamosal horns (shared with *Gobisaurus* and *Zhongyuansaurus*). Further differs from *Gobisaurus* in having a longer maxillary tooth row relative to skull length and a dorsally more prominent nuchal crest.

Discussion. The holotype of *Sh. scuatus* (PIN 3779/2) (Figs. 37 and 38) was collected by the Soviet-Mongolian Expedition in 1977 (Tumanova, 1983). Although the holotype includes a cranium, mandibles, and partial postcranial elements, the original description by Tumanova (1983) only contained information on the skull, and figures of mandibles and postcranial elements were not included. The mandibles of the holotype were later figured by Tumanova (1987), and a left scapulocoracoid and two dorsal vertebrae were described by Tumanova (2000). Recently, Arbour and Currie (2016) added a description of two cervical half rings to the holotype. Another partial skull (PIN 3997/1), discovered from the same locality as the holotype, was also included in the study of Tumanova (1983). This

skull is slightly larger than the holotype skull and has a more prominent nuchal crest. It is possible that PIN 3997/1 is from a more mature individual than the holotype.

A partial mandible (PIN 3101) was collected from the Lower Cretaceous (Aptian–Albian) Khovboor Beds, Khovboor, Mongolia, and was mentioned as a referred specimen of *Shamosaurus* in Tumanova (1987) with no specific reasoning. Since diagnostic features are absent on the mandible of *Shamosaurus*, it seems more appropriate to classify PIN 3101 as an indeterminate ankylosaur rather than *Shamosaurus*.

Tumanova (1983) suggested that *Shamosaurus* and *Saichania chulsanensis* belong to Shamosaurinae, which was a sister group to the clade that includes "*Amtosaurus magnus*," *P. grangeri*, "*Syrmosaurus*" (synonym of *Pinacosaurus*), *Talarurus*, and "*Tarchia gigantea*." Later, *Shamosaurus* was recovered as a sister taxon to the clade that includes "polacanthines" (which consists of *Gastonia burgei*, *Mymoorapelta*, and *Polacanthus*) and derived ankylosaurids such as *Ankylosaurus*, *Euoplocephalus*, *P. grangeri*, *Saichania*, "*Tar. gigantea*," and *Tsagantegia* (Kirkland, 1998). However, Carpenter (2001) placed *Shamosaurus* as a sister taxon to the clade that consists of *Ankylosaurus*, *Euoplocephalus*, *P. grangeri*, *Saichania*, and "*Tar. gigantea*". On the other hand, in Hill et al. (2003)'s analysis, *Shamosaurus* and *Tsagantegia* formed a clade, a sister group to the clade that comprises the derived ankylosaurines such as *Ankylosaurus*, *Euoplocephalus*, *Nodocephalosaurus*, *Saichania*, *Shanxia*, "*Tar. gigantea*,"

Tianzhenosaurus. A similar result was obtained in a more recent analysis by Burns et al. (2011). In a cladogram of Vickaryous et al. (2004), *Shamosaurus* was recovered as a sister taxon to *Gobisaurus*, and the two formed a clade that is a sister group to the derived ankylosaurines, which includes *Ankylosaurus*, *Euoplocephalus*, *P. grangeri*, *Pinacosaurus mephistocephalus*, *Saichania*, *Talarurus*, "*Tar. gigantea*," *Tianzhenosaurus*, and *Tsagantegia*. Arbour and Currie (2016) obtained a similar result. However, Thompson et al. (2012) found *Shamosaurus* in a basal position within the Ankylosauridae, and Wiersma and Irmis (2018) also had a similar result. In this dissertation, *Shamosaurus* formed a clade with *Gobisaurus* as in Vickaryous et al. (2004) and Arbour and Currie (2016). Unfortunately, this clade was resolved in a polytomy with *Aletopelta*, *Cederpelta*, *Chuangilong*, *Crichtonpelta*, *Jinyunpelta*, *Kunbarrasaurus*, *Liaoningosaurus*, *Nodosaurus*, and the clade that includes the ankylosaurines (Fig. 27).

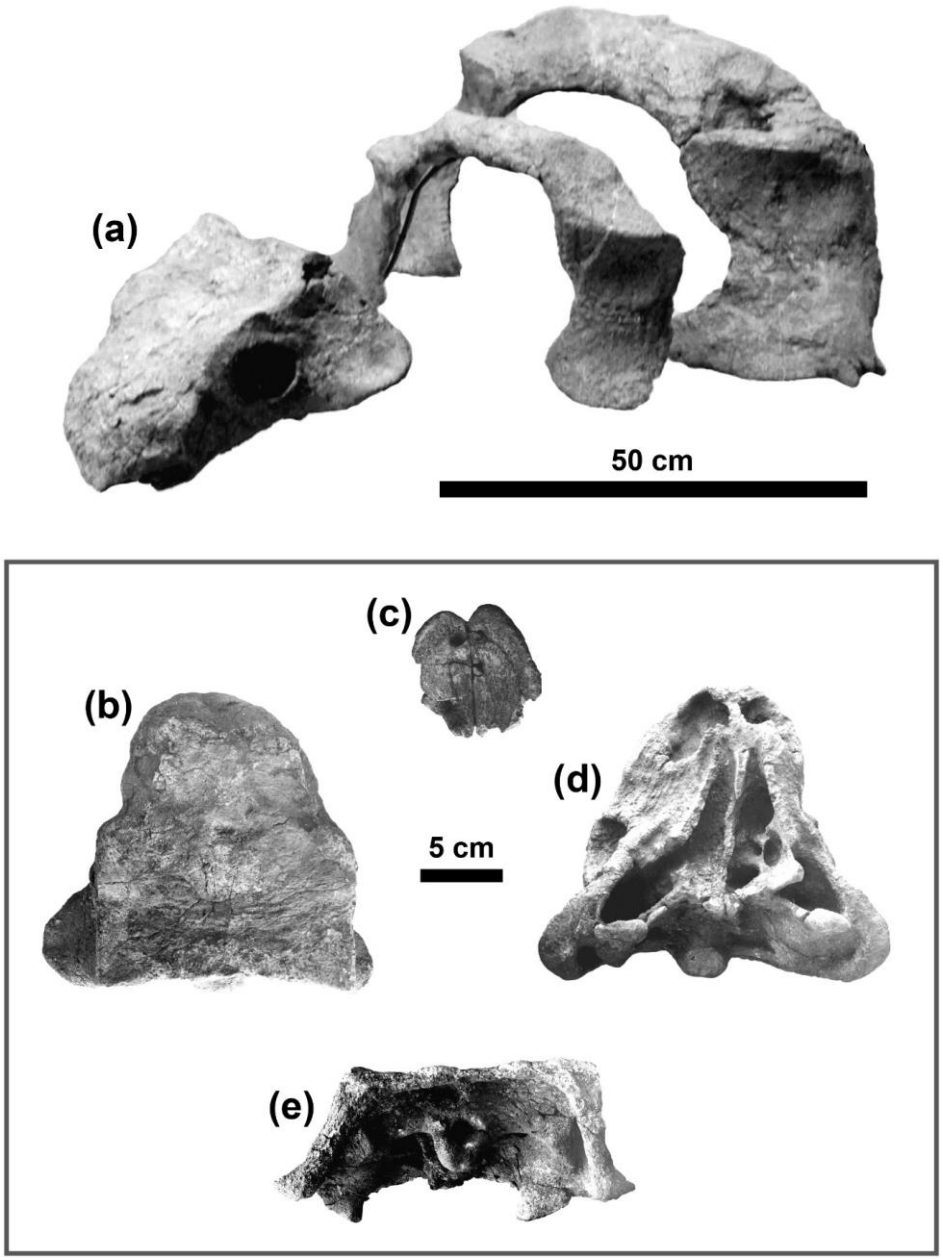

Figure 37. Photographs of the holotype of *Shamosaurus scuatus* (PIN 3779/2). (a) Skull, 1st and 2nd cervical half rings in left oblique anterolateral view. (b) Skull in dorsal view. (c) Rostral beak in palatal view. Skull in (d) palatal and (d) occipital views. Courtesy of Tatiana Tumanova.

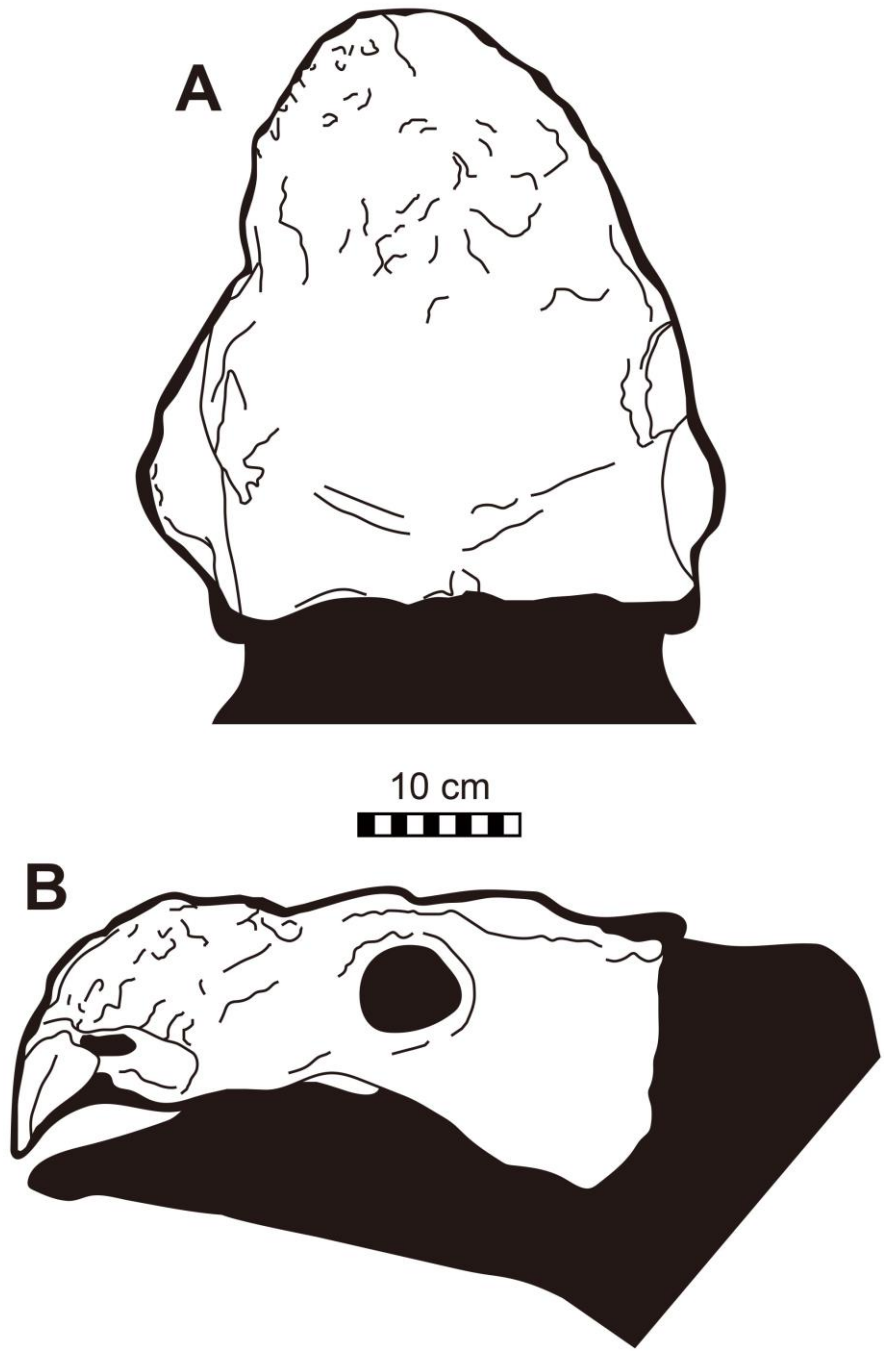

Figure 38. Line drawings of the holotype skull of *Shamosaurus scutatus* (PIN 3779/2). (A) Dorsal and (B) left lateral views.

Ankylosaurinae Nopcsa, 1918; *sensu* Sereno, 1998

Phylogenetic definition. All ankylosaurids closer to *Ankylosaurus magniventris* than to *Shamosaurus scutatus*.

Included taxa. *Akainacephalus johnsoni*, *Ankylosaurus magniventris* (type species), *Anodontosaurus inceptus*, *Ano. lambei*, *Euoplocephalus tutus*, *Dyoplosaurus acutosquameus*, *Minotaurasaurus ramachandrani*, *Nodocephalosaurus kirtlandensis*, *Oohkotokia horneri*, *Pinacosaurus grangeri*, *Pinacosaurus mephistocephalus*, *Platypelta coombsi*, *Saichania chulsanensis*, *Scolosaurus cutleri*, *Sc. thronus*, *Shanxia tianzhenensis*, *Talarurus plicatospineus*, *Tarchia kielanae*, *Tar. teresae*, *Tianzhenosaurus youngi*, *Tsagentegia longicranialis*, *Zaraapelta nomadis*, *Ziapelta sanjuanensis*, and *Zuul cruravastator*.

Minotaurasaurus Miles and Miles, 2009

Type species. *Minotaurasaurus ramachandrani* Miles and Miles, 2009

Generic diagnosis. Genus monotypic, as for the type species.

Minotaurasaurus ramachandrani Miles and Miles, 2009

Type specimen. INBR 21004, complete skull and mandibles (Miles and Miles, 2009: figs. 1–10) (Figs. 39 and 40).

Type locality and horizon. No locality and stratigraphic data were provided in the original description by Miles and Miles (2009), but it was collected from the Upper Cretaceous (Campanian) Djadokhta Formation, southern Gobi Desert, Mongolia (Dingus et al., 2008; Penkalski and Tumanova, 2017).

Revised diagnosis. An ankylosaurid distinguished by the following unique set of characters (autapomorphies with an asterisk): premaxillary ornamentation present (shared with *Jinyunpelta*, *Saichania*, and *Tarchia*); paranasal aperture B (*sensu* Hill et al., 2003) present (shared with *Pinacosaurus*); two pairs of paranasal aperture C (*sensu* Hill et al., 2003) present*; two pairs of small bulbous internarial caputegulae*; large, wide, and arched supranarial caputegulae*; numerous small lacrimal and loreal caputegulae present (shared with *Zaraapelta*); lacrimal incisure present (shared with *Pinacosaurus grangeri*); large, sharply pointed, pyramidal prefrontal caputegulae (shared with *P. grangeri* and *Zaraapelta*); ridge-like frontal caputegulae*; a frontal sagittal furrow with a Z-shaped offset*; anterior and posterior supraorbital caputegulae with distinct apices (shared with *P. grangeri* and *Zaraapelta*); a "neck" present at the base of the quadratojugal horn (shared with *Pinacosaurus*, *Tarchia*, and *Talarurus*); well defined postorbital fossa (shared with *Zaraapelta*); narrow, cone shaped squamosal horns*; short, narrow nuchal crest (shared with *Pinacosaurus mephistocephalus*); occiput visible in dorsal view (shared with *Tarchia* and *Zaraapelta*); short paroccipital processes*. Differs from *Saichania*, *Tar. kielanae*, and *Zaraapelta* in having unfused quadrate to the exoccipital area. Differs from *Saichania* and *Tarchia* in having a small basioccipital

foramen. Differs from *Saichania* and *Tar. teresae* in having anteroposteriorly long mandibular caputegulae. Differs from *Tarchia* in having postocular caputegulae, a low braincase, wide foramen magnum, and ventrally oriented occipital condyle.

Discussion. The holotype (INBR 21004) (Figs. 39 and 40) is a purchased specimen from the Tucson Gem, Mineral, & Fossil Show (Arizona, USA) and is now in the private collection of V.S. Ramachandran (Miles and Miles, 2009; Arbour et al., 2014b), therefore not accessible. Penkalski and Tumanova (2017) mentioned a new specimen (MAE 98 179) from Ukhaa Tolgod, southern Gobi Desert, which includes a skull, axis, and first cervical half ring, could be assigned to this taxon. However, this specimen is currently undescribed.

Arbour et al. (2014) considered *Minotaurasaurus* as a synonym of *Tar. kielanae*, due to the presence of the accessory postorbital ossification surrounded by a furrow in both taxa. However, based on new stratigraphic information and detailed morphologic comparisons to *Saichania* and *Tar. kielanae*, Penkalski and Tumanova (2017) concluded that *Minotaurasaurus* was distinct and valid.

In Thompson et al. (2012)'s analysis, *Minotaurasaurus* formed a clade with *P. grangeri*, a sister taxon to the derived ankylosaurids *Nodocephalosaurus*, *Saichania*, *Talarurus*, "*Tar. gigantea*," and *Tianzhenosaurus*. In contrast, *Minotaurasaurus* formed a clade with *Shanxia* and *Tar. kielanae*, which was a sister group to the clade that includes *Akainacephalus* and *Nodocephalosaurus* (Wiersma and Irmis, 2018). In this dissertation, *Minotaurasaurus* was recovered as a sister taxon to the clade that includes *Saichania*, *Tarchia*, and *Zaraapelta* (Fig.

29).

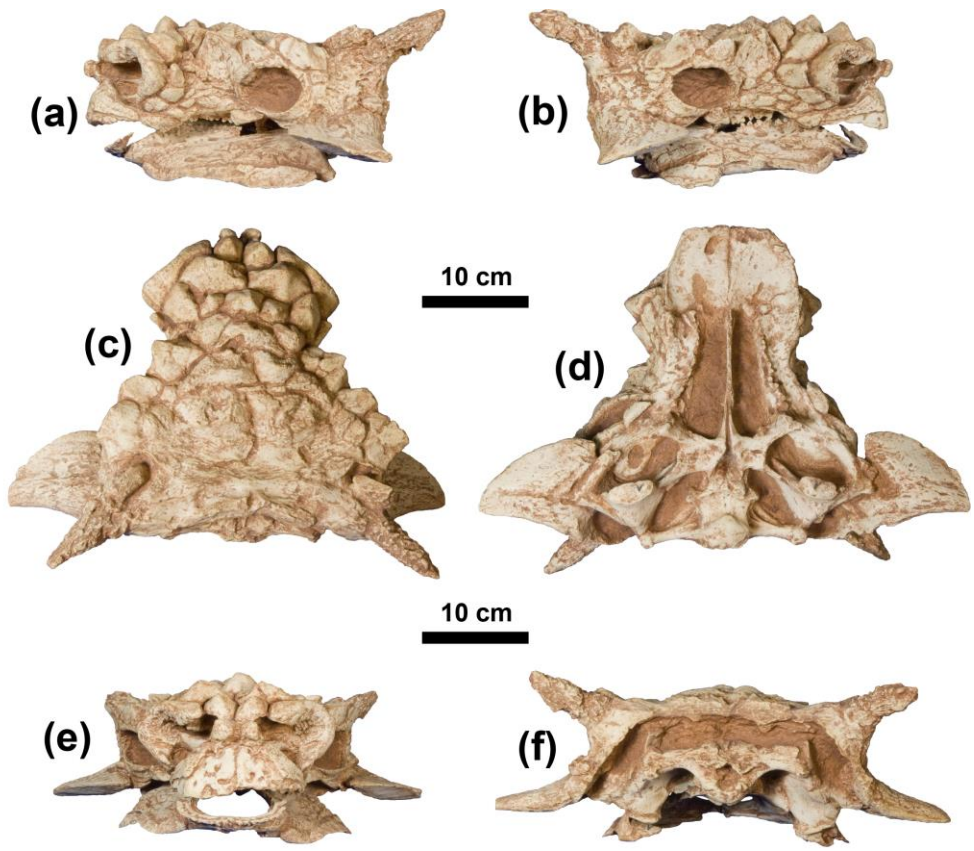

Figure 39. Photographs of the cast of the holotype of *Minotaurasaurus ramachandrani* (INBR 21004). (a) Left lateral, (b) right lateral, (c) dorsal, (d) palatal (mandible excluded), (e) anterior, and (f) occipital views. Courtesy of Lawrence Witmer.

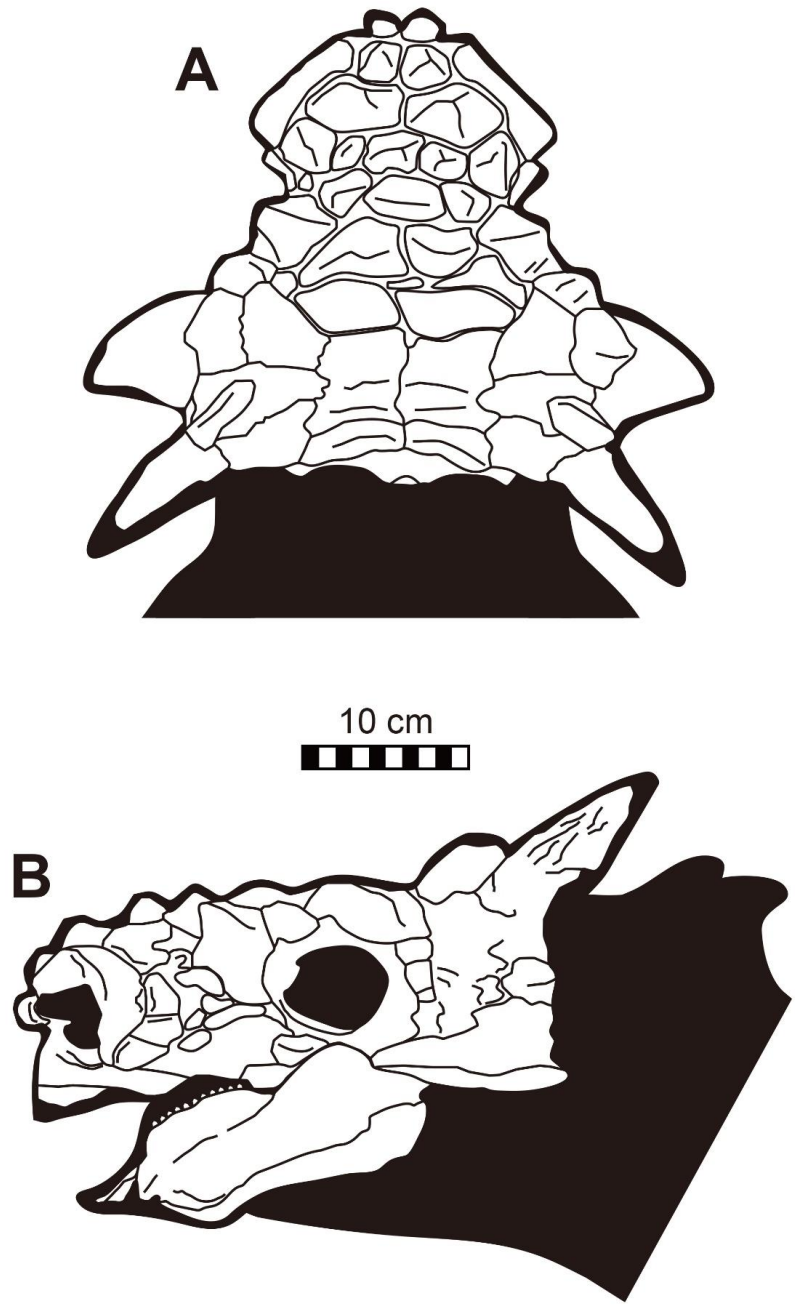

Figure 40. Line drawings of the holotype skull of *Minotaurasaurus ramachandrani* (INBR 21004). (A) Dorsal and (B) left lateral views.

Pinacosaurus Gilmore, 1933

= *Syrmosaurus* Maleev, 1952a

Type species. *Pinacosaurus grangeri* Gilmore, 1933

Included species. Type species and *Pinacosaurus mephistocephalus*.

Revised generic diagnosis. An ankylosaurid distinguished by the following unique set of characters: paranasal aperture B (*sensu* Hill et al., 2003) present (shared with *Minotaurasaurus*); a "neck" present at the base of the quadratojugal horn (shared with *Minotaurasaurus*, *Tarchia*, and *Talarurus*). Differs from *Jinyunpelta*, *Minotaurasaurus*, *Saichania*, and *Tarchia* in having no premaxillary ornamentation. Differs from *Minotaurasaurus* in having narrow supranarial caputegulae and broad paroccipital span.

Pinacosaurus grangeri Gilmore, 1933

= *Pinacosaurus ninghsiensis* Young, 1935

= *Syrmosaurus viminocaudus* Maleev, 1952a

= *Syrmosaurus viminicaudus* Maleev, 1954b (emended spelling)

Type specimen. AMNH 6523, skull, mandibles, atlas, axis, and free osteoderms (Gilmore, 1933: figs. 1–3).

Type locality and horizon. Upper Cretaceous (Campanian) Djadokhta Formation, Bayan Zag, southern Gobi Desert, Mongolia.

Referred specimens. 1) From Djadokhta Formation, Bayan Zag, Mongolia– PIN 614, an almost complete postcranial skeleton of an adult. ZPAL MgD II/1, skull (Maryañska, 1971: fig. 1, pls. 6 and 7) (Figs. 41 and 42) with an almost complete skeleton of a juvenile (Maryañska, 1977: pls. 22–25). ZPAL MgD II/9, sacral vertebrae, caudal vertebrae including tail club handle, fragments of the shoulder girdle, almost complete right manus, pelvic girdle, femur, tibia, and pes (Maryañska, 1977: pls. 24–25). ZPAL MgD II/31, tail club handle.

2) From Djadokhta Formation, Alagteeg, Mongolia–MPC 100/1307, right pes (Currie et al., 2011: fig. 9). MPC 100/1308, both distal ends of tibiae and pedes (Currie et al., 2011: fig. 8). MPC 100/1309, left pes. MPC 100/1310, left humerus (Currie et al., 2011: fig. 4A), radius, ulna, one carpal, five metacarpals (Currie et al., 2011: fig. 6), and five proximal manual phalanges. MPC 100/1311, tibia, fibula, two tarsals, three left pedal phalanges. MPC 100/1312, fragments of pedal phalanges. MPC 100/1313, pedal phalanges. MPC 100/1314, distal ends of the right radius and ulna, plus most of the manus. MPC 100/1315, nine manual phalanges of a juvenile, and four manual phalanges of an adult. MPC 100/1316, distal ends of tibiae and fibulae, and pedes (Currie et al., 2011: fig. 11). MPC 100/1317, partial manual phalanx and unidentified bone fragments. MPC 100/1318, right manus. MPC 100/1319, left pes. MPC 100/1320, distal ends of tibia and fibula, and right pes (Currie et al., 2011: fig. 10B). MPC 100/1321, skull and assorted bones. MPC 100/1322, two quadrates, coracoid, right ulna, ischium, and three femora of at least two individuals (Currie et al., 2011: fig. 4B). MPC

100/1323, right radius and ulna (Currie et al., 2011: figs. 4C and D), manus, and two pedes (possibly same individual as MPC 100/1326, according to Currie et al. (2011)). MPC 100/1324, eight vertebrae, coracoid, free osteoderms, and others (possibly same individual as MPC 100/1325 or 100/1326, according to Currie et al. (2011)). MPC 100/1325, right manus hand (possibly the same individual as MPC 100/1326, according to Currie et al. (2011)). MPC 100/1326, forearm (Currie et al., 2011: fig. 4E), manus, and associated tail. MPC 100/1327, left tibia and pes. MPC 100/1328, left pes. MPC 100/1329, vertebral centra, manual ungual, and pedes. MPC 100/1330, cervical half rings, vertebrae, and pes. MPC 100/1331, complete right pes. MPC 100/1332, scapula, coracoid, and ribs. MPC 100/1333, ilia, both humeri, radii, ulnae, both manus, and one pes of a large individual. MPC 100/1334, tibia, fibulae, and pes of two individuals. MPC 100/1335, skull, two arms, and leg. MPC 100/1336, free osteoderms. MPC 100/1337, right manus. MPC 100/1338, partial manus. MPC 100/1339, both radii, ulnae, manus, tibiae (Currie et al., 2011: fig. 7B), fibulae (Currie et al., 2011: fig. 7A), and pedes (Currie et al., 2011: fig. 10A). MPC 100/1340, right radius, distal ulna, and manus. MPC 100/1341, distal ends of both radii, ulnae, and manus. MPC 100/1342, left tibia, fibula, and pes. MPC 100/1343, left partial femur, tibia, fibula, and both pedes. MPC 100/1344, skull, cervical vertebrae, articulated dorsal vertebrae, tail, scapula, right humerus, both femora, and second cervical ring. MPC 100/1345, thoracic rib and cervical half ring. MPC 100/1346, coracoid and right humerus. MPC 100/1347, right frontal. MPC 100/1358, right metacarpus (Currie et al., 2011: fig. 5). PIN 3144,

basicranium, four articulated cervical vertebrae, a dorsal centrum, two sacral centra, seven free caudal centra, left coracoid and scapula, both humeri, right ulna and radius, right partial ilium, left femur, left tibia, and cervical half ring segments of a juvenile (Burns et al., 2015: figs. 2–13).

3) From Djadokhta Formation, Ukhaa Tolgod, Mongolia–MPC 100/1014, nearly complete skull and mandibles (Hill et al., 2003: figs. 2–8). MPC 100/1386, nearly complete skull (Hill et al., 2015: figs. 1 and 2), mandibles (Hill et al., 2015: fig. 1), articulated hyobranchial apparatus (Hill et al., 2015: figs. 1 and 3), partial postcranial including left radius (Hill et al., 2015: fig. 6), first cervical half ring, and free osteoderms (Hill et al., 2015: fig. 7).

4) From Upper Cretaceous (Campanian) Bayan Mandahu Formation, Inner Mongolia, China–IVPP no catalog number, upper jaw fragment, partial right mandible, 23 vertebrae, right scapula, right humerus, radius or ulna, ilium, partial ischia, right femur, both tibiae, fibula, two metatarsals, cervical half ring fragments, and free osteoderms (holotype of "*Pinacosaurus ninghsiensis*" (Young, 1935: pls. 1–3)). IVPP V16283, partial skull of a juvenile. IVPP V16346, an incomplete skull of a sub-adult (Burns et al., 2011, fig. 6B). IVPP V16853, complete skull and cervical half rings of a juvenile (Burns et al., 2011, fig. 2). IVPP V16854, an almost complete skeleton of a juvenile (Burns et al., 2011, fig. 6A). IVPP V16855, skull and skeleton of a juvenile.

Revised diagnosis. An ankylosaurid distinguished by the following unique set of characters (autapomorphy with an asterisk): notch present medial to the supranarial caputegulae*; lacrimal incisure present (shared with *Minotaurasaurus*); sharply pointed, pyramidal prefrontal caputegulae (shared with *Minotaurasaurus* and *Zaraapelta*); anterior and posterior supraorbital caputegulae with distinct apices (shared with *Minotaurasaurus* and *Zaraapelta*). Differs from *Jinyunpelta*, *Minotaurasaurus*, *Saichania*, and *Tarchia* in having no premaxillary ornamentation. Differs from *Minotaurasaurus* in having narrow supranarial caputegulae and broad paroccipital span.

Discussion. It is the first ankylosaur taxon from Mongolia reported in the scientific literature. The holotype (AMNH 6523) was discovered from Bayan Zag during the Central Asiatic Expeditions in 1923 and belonged to an adult individual (Gilmore, 1933). The skull is dorsoventrally and lateromedially crushed, and based on this specimen, Gilmore (1933) concluded that *P. grangeri* closely resembles *Euoplocephalus* and *Dyoplosaurus*. Although, as mentioned by Maryañska (1971), the reconstructions of the holotype skull in this original description are not quite accurate. Maleev (1952a, 1954b) described a new ankylosaur, "*Syrmosaurus viminicaudus*," based on an almost complete postcranial skeleton (PIN 614) from Bayan Zag, the same location where the holotype of *P. grangeri* was uncovered. This taxon was later regarded as a synonym of *P. grangeri* by Maryañska (1971). Since the only adult specimens collected from the type locality were the skull material of the holotype and the postcranial of PIN 614, Coombs (1971) suspected

that the two might be the same individual. This hypothesis was never tested afterward. Well-preserved juvenile specimens of *P. grangeri* were also recovered from Bayan Zag during the Polish-Mongolian Expedition in 1964, and Maryañska (1971, 1977) described these materials in detail. Among these specimens, ZPAL MgD II/1 contains an almost complete skull (Figs. 41 and 42) and a postcranial skeleton. Due to the poor preservation of the holotype, the current diagnosis and description of *P. grangeri* are mainly based on this specimen. Additional two hundred and eighty-five specimens of juvenile to sub-adult *P. grangeri* were discovered by the Joint Soviet-Mongolian Paleontological Expedition in 1969 and 1970 from the Djadokhta Formation, Alagteeg, Mongolia (Tverdochlebov and Zybin, 1974; Maryañska, 1977; Fastovsky and Watabe, 2000; Currie et al., 2011; Burns et al., 2015). Most of these were fragmentary, and only eighty-three specimens were considered informative and cataloged (Burns et al., 2015). Among the cataloged specimens, only one individual (PIN 3144) was described in detail by Burns et al. (2015). From 1995 to 1996, more than thirty juvenile skeletons of *P. grangeri* were collected from Alagteeg during the Mongolian-Japanese Joint Paleontological Expedition (Suzuki and Watabe, 2000; Watabe and Suzuki, 2000), but none of these are currently described. In 2001, and between 2003 and 2007, the "Dinosaur of the Gobi" Nomadic Expeditions uncovered over forty *P. grangeri* specimens from Alagteeg (Currie et al., 2011). The majority of the specimens collected during this expedition are manus and pes elements, and Currie et al. (2011) described the complete feet morphology of *P. grangeri* based on these finds.

P. grangeri specimens were also collected from Ukhaa Tolgod during the American Museum expeditions between 1990 and 2005. Two of the skulls (MPC 100/1014 and MPC 100/1386) from this area were described by Hill et al. (2003, 2015). Young (1935) described a new species, "*Pinacosaurus ningheiensis*," based on a nearly complete skeleton with no given catalog number from the Upper Cretaceous (Campanian) Bayan Mandahu Formation in the northwest of Ninghsia Province, China. This taxon was later regarded as a synonym of *P. grangeri* by Maryañska (1971). Additional specimens of *P. grangeri* from the Bayan Mandahu Formation were later described and discussed by Burns et al. (2011).

MPC 100/1305, a nearly complete skeleton lacking a skull from the Djadokhta Formation, was considered a possible *Pinacosaurus* by Arbour and Currie (2013). Only two ankylosaurine taxa are currently known from the Djadokhta Formation, *Minotaurasaurus ramachandrani* and *P. grangeri* (Gilmore, 1933; Maryañska, 1971; Hill et al., 2003; Dingus et al., 2008; Miles and Miles, 2009; Currie et al., 2011; Burns et al., 2015; Penkalski and Tumanova, 2017). As mentioned above, the holotype of *Minotaurasaurus* lacks any postcranial elements, so the comparison of MPC 100/1305 to this taxon is not possible (Miles and Miles, 2009). Whereas MPC 100/1305 differs from *P. grangeri* by having seven free dorsal vertebrae, a convex dorsal margin on the scapular blade, a coracoid with a straight anterior margin, a fused pair of sternal plates with an anterior notch and a smooth lateral margin, a lateral process on the proximal edge of the deltopectoral crest of humerus, a more prominent distal condyle on the radius than the proximal

one, a robust ulna, and a ventrally projected lateral condyle on the femur (Carpenter et al., 2011; Currie et al., 2011; Burns et al., 2015). Therefore, it is certain that MPC 100/1305 is not *P. grangeri* but possibly *Minotaurasaurus*. However, new *Minotaurasaurus* specimens with both cranial and postcranial portions are needed further to clarify the taxonomic identification of MPC 100/1305.

In a cladogram of Kirkland (1998), *P. grangeri* was recovered as a sister taxon to the clade that includes the derived ankylosaurines such as *Ankylosaurus*, *Euplocephalus*, *Saichania*, and "*Tar. gigantea.*" However, *P. grangeri* was a sister taxon to *Euplocephalus* and formed a clade with *Saichania* and "*Tar. gigantea*" (Carpenter, 2001). Vickaryous et al. (2004) positioned *P. grangeri* within the derived Asian ankylosaurines, consisting of *P. mephistocephalus*, *Saichania*, *Talarurus*, and *Tianzhenosaurus*. Thompson et al. (2012) result is similar and placed *P. grangeri* as a sister taxon to *Minotaurasaurus*, within the clade that comprises *Ankylosaurus*, *Euoplocephalus*, *Nodocephalosaurus*, *Saichania*, *Talarurus*, "*Tar. gigantea*," and *Tianzhenosaurus*. In contrast, in a phylogenetic analysis by Hill et al. (2003), *P. grangeri* was recovered as a basal ankylosaurid, sister to the ankylosaurines, which is similar to that of Wiersma and Irmis (2018). In this dissertation, *P. grangeri* formed a clade with *P. mephistocephalus*, and this clade was recovered as a sister to the clade, which included the derived ankylosaurines (Fig. 27).

Generally, *P. grangeri* is positioned as a sister taxon to *P.*

mephistocephalus (Burns et al., 2011; Arbour et al., 2014b; Arbour and Currie, 2016). However, in some cases, the relationship between the two species is not supported (Vickaryous et al., 2004; Thompson et al., 2012; Wiersma and Irmis, 2018). Unfortunately, the morphological data of *P. grangeri* are primarily based on juvenile specimens, which may cause the instability of its phylogenetic position (Maryañska, 1971, 1977; Godefroit et al., 1999; Hill et al., 2003; Burns et al., 2011; Arbour and Currie, 2016).

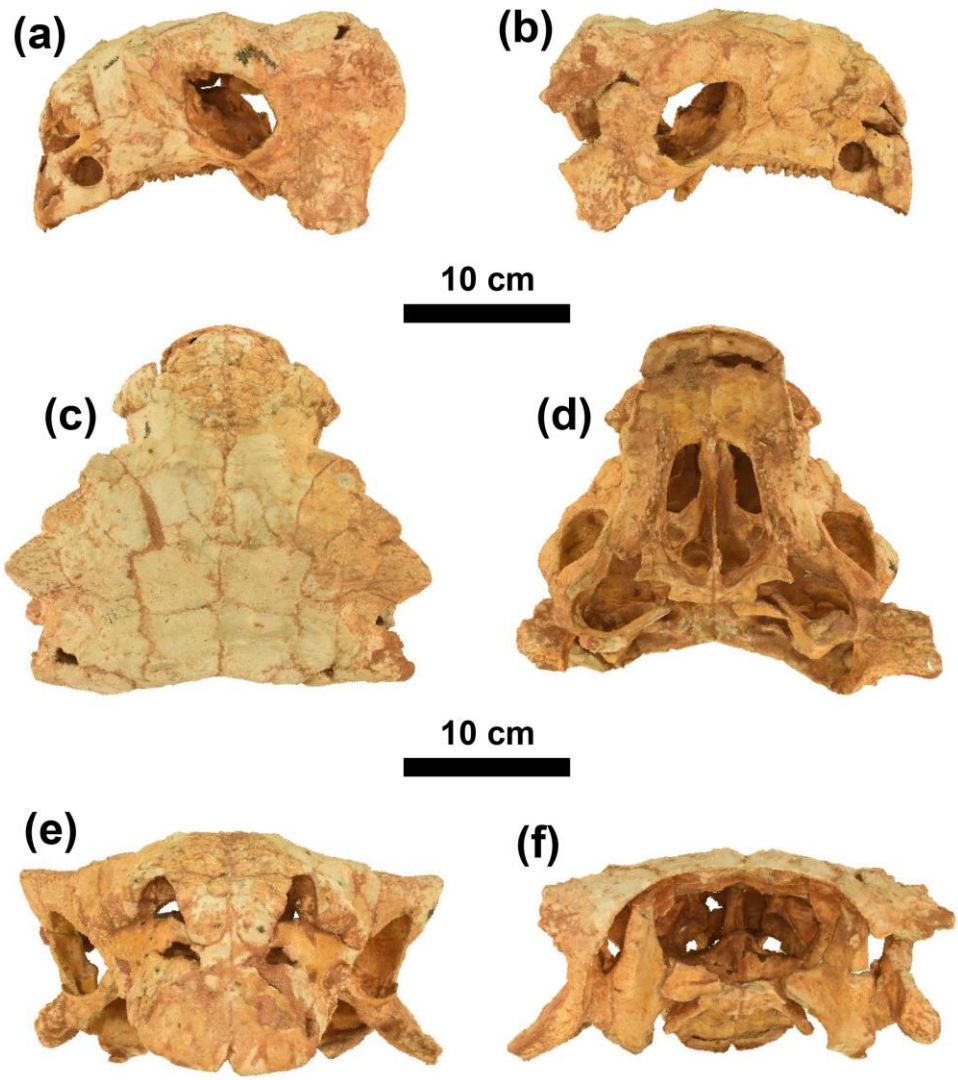

Figure 41. Photographs of a skull of a juvenile *Pinacosaurus grangeri* (ZPAL MgD II/1). (a) Left lateral, (b) right lateral, (c) dorsal, (d) palatal, (e) anterior, and (f) occipital views. Braincase portion is excluded. Courtesy of Tomasz Szczygielski.

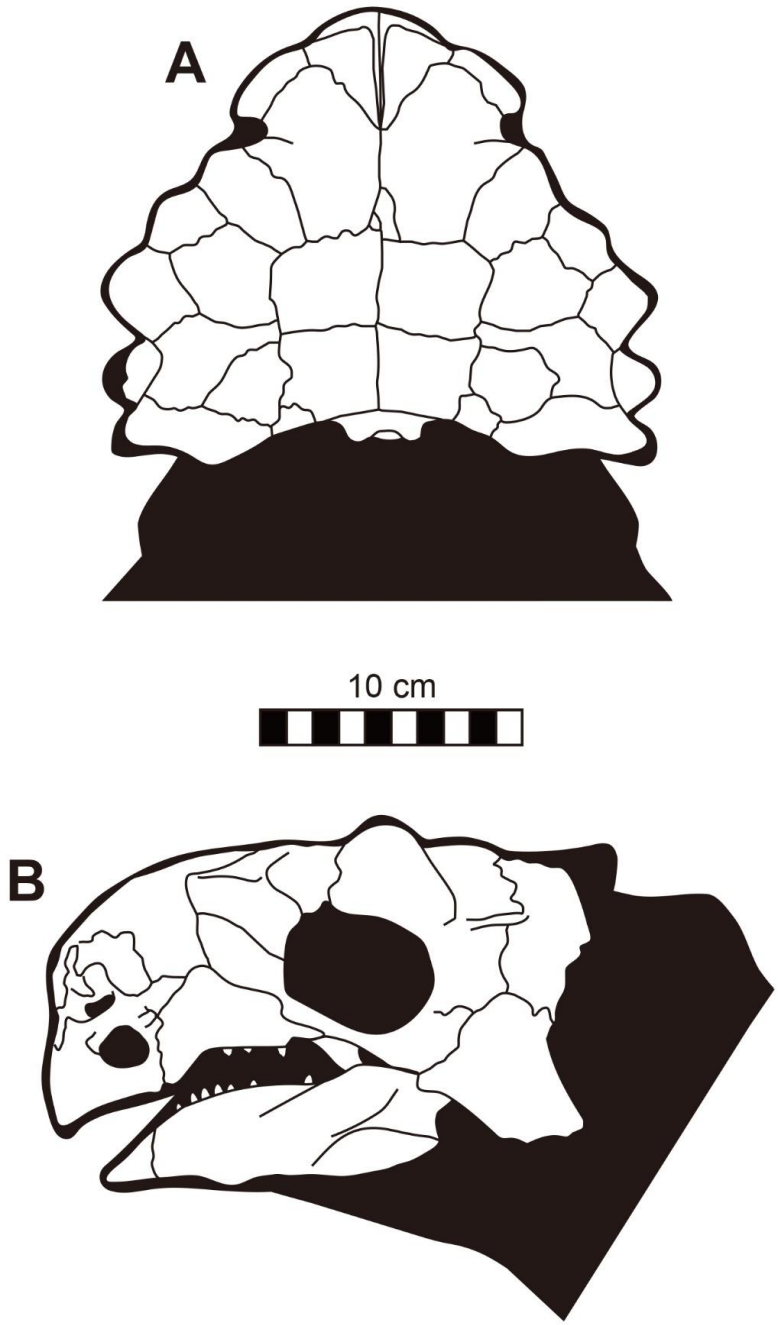

Figure 42. Line drawings of a skull of a juvenile *Pinacosaurus grangeri* (ZPAL MgD II/1). (A) Dorsal and (B) left lateral views.

Saichania Maryañska, 1977

Type species. *Saichania chulsanensis* Maryañska, 1977

Generic diagnosis. Genus monotypic, as for the type species.

Saichania chulsanensis Maryañska, 1977

Type specimen. MPC 100/151, complete skull (Figs. 43 and 44), mandibles, seven cervical vertebrae, ten dorsal vertebrae, ribs, both scapulocoracoids, sternal plates, humerus, ulna, radius, manus, first and second cervical half rings, and free osteoderms (Maryañska, 1977: figs. 4–9 and 11, pls. 28–36).

Type locality and horizon. Upper Cretaceous (middle–upper Campanian) Baruungoyot Formation, Khulsan, southern Gobi Desert, Mongolia.

Referred specimens. 1) From Baruungoyot Formation, Khulsan, Mongolia– PIN no catalog number, a skull with an almost complete postcranial skeleton.

2) From Baruungoyot Formation, Hermiin Tsav II, Mongolia–PIN 3142/251, skull, mandibles, and complete skeleton (Tumanova, 1987: pl. 2 (hyoids and the distal portion of the tail are figured)). ZPAL MgD I/114, skull roof fragment and free osteoderms.

Revised diagnosis. An ankylosaurid distinguished by the following unique set of characters (autapomorphy with an asterisk): vertically positioned single flat internarial caputegulum (shared with *Tarchia teresae*); large, rhomboidal loreal

caputegulum with a laterally extended posterior keel (shared with *Tarchia*); a straight frontal sagittal furrow (shared with *Tarchia teresae*); subrectangular frontal caputegulae (shared with *Tarchia*); conical postocular caputegulae (shared with *Oohkotokia*); a single small exit for cnn. IX–XII*. Differs from *Pinacosaurus grangeri*, *Minotaurasaurus*, *Tarchia*, and *Zaraapelta* in having a moderate size basioccipital foramen. Differs from *Minotaurasaurus*, *P. grangeri*, *Tar. teresae*, and *Zaraapelta* in having an anteriorly situated quadrate-quadratojugal region. Differs from *Pinacosaurus*, *Minotaurasaurus*, and *Tarchia* in having no "neck" on quadratojugal horns. Differs from *P. grangeri*, *Minotaurasaurus*, and *Zaraapelta* in having laterally flat prefrontal caputegulae and confluent supraorbitals. Differs from *Minotaurasaurus*, *Tarchia*, and *Zaraapelta* in having no remodeled squamosal horns, anteroposteriorly wide lateral nuchal caputegulae, and an invisible occiput in dorsal view. Differs from *P. grangeri* and *Minotaurasaurus* in having no lacrimal incisure. Differs from *Minotaurasaurus* and *Tarchia* in having no postorbital fossa and fully keeled squamosal horns. Differs from *Minotaurasaurus* and *Tar. teresae* in having fused quadrate to the exoccipital area. Differs from *Minotaurasaurus* and *Zaraapelta* in having a pair of loreal and lacrimal caputegulae. Differs from *Minotaurasaurus* in having narrow supranarial caputegulae, mediolaterally long lateral nuchal caputegulae, and broad paroccipital span. Differs from *Tarchia* in having a relatively low occiput, ventrally oriented occipital condyle, and a wide foramen magnum. Differs from *Zaraapelta* in having well-defined nuchal caputegulae.

Discussion. The holotype of *Saichania* (MPC 100/151) (Figs. 43 and 44) was found in Khulsan during the Polish-Mongolian Expedition in 1970 and was excavated in the following year (Kielan-Jaworowska, 2013). The holotype was described by Maryañska (1977) in detail. Maryañska (1977) also referred to two additional specimens from Khulsan (PIN no catalog number) and Hermiin Tsav II (ZPAL MgD I/114). These are not currently figured nor described in the scientific literature. An additional skeleton with a skull from Hermiin Tsav II (PIN 3142/251) was referred by Tumanova (1987), but only the hyoids and the distal portion of the tail were described.

The phylogenetic positions of *Saichania* were mainly within the derived ankylosaurines. In a cladogram of Kirkland (1998), *Saichania* was placed as a sister taxon to "*Tar. gigantea*" and included in a clade with *Ankylosaurus* and *Euoplocephalus*. Hill et al. (2003) result is also similar, but the clade that comprises *Saichania* and "*Tar. gigantea*" was resolved in a polytomy with *Ankylosaurus*, *Euoplocephalus*, *Nodocephalosaurus*, *Shanxia*, and *Tianzhenosaurus*. On the other hand, *Saichania* was placed inside the clade that includes *Euoplocephalus, P. grangeri*, and "*Tar. gigantea*" (Carpenter, 2001). Vickaryous et al. (2004) positioned *Saichania* within the clade that consists of only Asian ankylosaurines, although the phylogenetic placement of *Saichania* and *Talarurus* was unresolved with the clade that includes *P. grangeri*, *P. mephistocephalus*, and *Tianzhenosaurus*. A similar result by Thompson et al. (2012) showed that *Saichania* and "*Tar. gigantea*" form a clade that is a sister

group to the clade comprising *Talarurus* and *Tianzhenosaurus*. Arbour and Currie (2016) regarded *Saichania* as a sister taxon to the clade of *Tar. kielanae* and *Zaraapelta*, whereas Penkalski and Tumanova (2017) to the clade of *Tar. kielanae* and *Tar. teresae*. However, Wiersma and Irmis (2018) suggested that *Saichania* is a basal taxon to the derived ankylosaurines. In the first analysis in this dissertation, *Saichania* was recovered as a sister to the clade, which included *Zaraapelta* and *Tarchia kielanae* (Fig. 27). In the second analysis, *Saichania* was recovered as a sister to the clade that contains the three *Tarchia* species (Fig. 29).

Penkalski and Tumanova (2017) referred to ZPAL MgD I/42 (one free caudal vertebra and a tail club, from Altan Uul IV) as *Saichania* with no specific reasoning. In ZPAL MgD I/42, the prezygapophyses of the tail club handle diverge at an angle of about 22–26 º, and the tail club knob is narrow. Based on PIN 3142/251, *Saichania* has caudal prezygapophyses that diverge at about 16–24º with a narrow tail club knob, similar to ZPAL MgD I/42. Although ZPAL MgD I/42 was collected from the Nemegt Formation, all other specimens of *Saichania* are from the Baruungoyot Formation. The referral of ZPAL MgD I/42 to *Saichania* extends the stratigraphic range of this taxon. However, since *Saichania* differentiates from other ankylosaurs only by cranial characteristics, it is challenging to assign ZPAL MgD I/42 to *Saichania* just by the tail morphology. New articulated specimens, including cranial and postcranial skeletons from the Nemegt Formation, are needed to clarify further the taxonomic identification of ZPAL MgD I/42. It is reasonable to refer to this specimen as Ankylosaurinae indet.

Two new ankylosaur taxa, *Shanxia tianzhenensis* (Barrett et al., 1998) and *Tianzhenosaurus youngi* (Pang and Cheng, 1998), were reported from the Upper Cretaceous Huiquanpu Formation, Shanxi, China. Sullivan (1999) suggested that *Shanxia* and *Tianzhenosaurus* may be junior synonyms to *Saichania* based on similar overall skull morphology. Upchurch and Barrett (2000) agreed that *Tianzhenosaurus* might be a synonym for *Saichania* but rejected the suggestion that *Shanxia* was synonymous with *Saichania*, based on the squamosal horn and nuchal caputegulum shape. Arbour and Currie (2016) agreed with Sullivan (1999) and considered the differences between these taxa, either individual or taphonomic variation.

However, additional characters distinguish between *Saichania*, *Shanxia*, and *Tianzhenosaurus*. *Shanxia* differs from *Saichania* in having remodeled squamosal horns and a single opening for cnn. IX–XII and the jugular vein, no basioccipital condyle, and a caudoventrally oriented occipital condyle. In contrast, *Tianzhenosaurus* differs from *Saichania* in having no premaxillary ornamentation, a caudodorsally tilted single flat internarial caputegulum, dorsoventrally narrow external nares, laterally exposed maxillae, flat nasal caputegulae, loreal caputegulum with no posterior keel, postocular caputegulae along the posterior rim of the orbit, relatively short squamosal horns, and occipitally overhanging nuchal crests. Because of these differences, both *Shanxia* and *Tianzhenosaurus* should be considered valid genera.

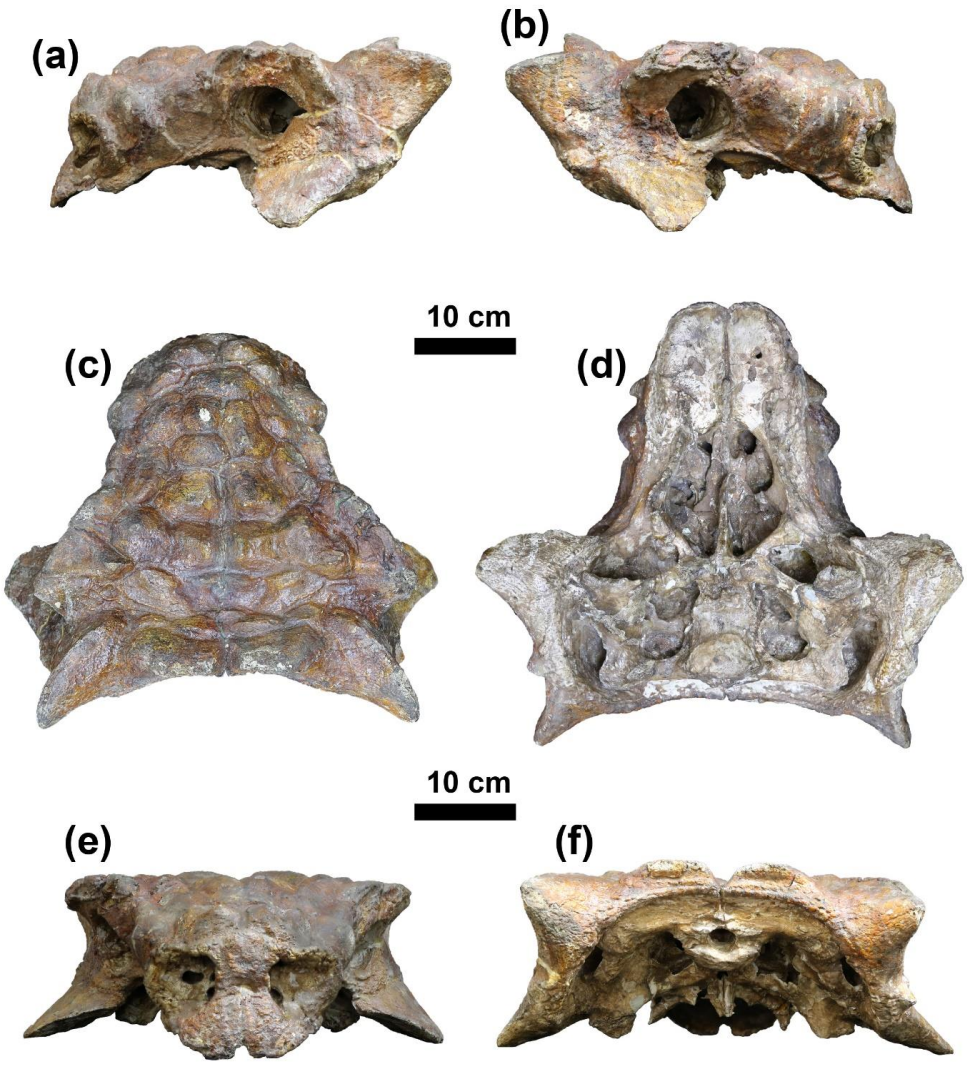

Figure 43. Photographs of the holotype skull of *Saichania chulsanensis* (MPC 100/151). (a) Left lateral, (b) right lateral, (c) dorsal, (d) palatal, (e) anterior, and (f) occipital views. Courtesy of Badamkhatan Zorigt.

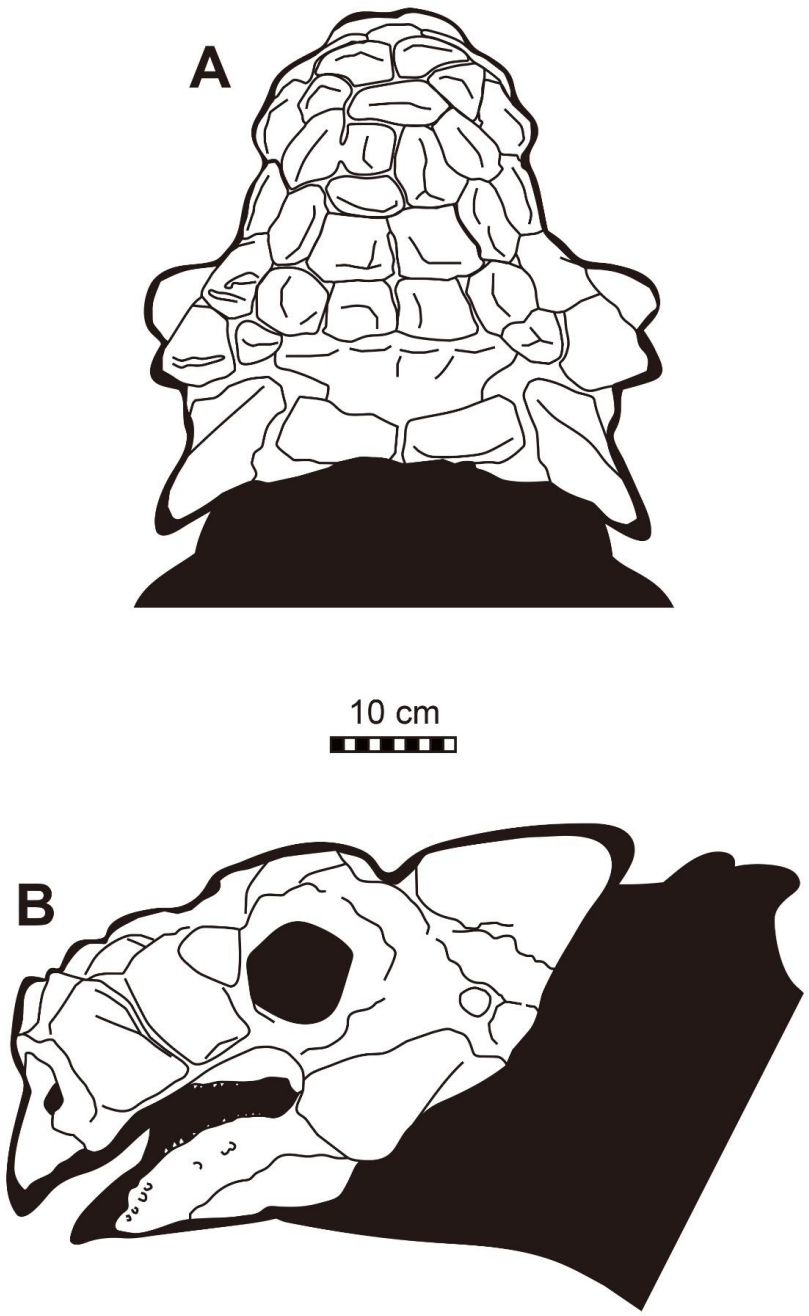

Figure 44. Line drawings of the holotype skull of *Saichania chulsanensis* (MPC 100/151). (A) Dorsal and (B) left lateral views.

Talarurus Maleev, 1952b

Type species. *Talarurus plicatospineus* Maleev, 1952b

Generic diagnosis. Genus monotypic, as for the type species.

Talarurus plicatospineus Maleev, 1952b

Type specimen. PIN 557/91, posterior portion of the skull (Maleev, 1956: figs. 1–3) (Figs. 45 and 46).

Type locality and horizon. Upper Cretaceous (Cenomanian–Turonian) Bayanshiree Formation, Bayan Shiree, eastern Gobi Desert, Mongolia.

Referred specimens. 1) From Bayanshiree Formation, Bayan Shiree, Mongolia–KID 151, two partial basicranials. MPC-D 100/1354, nearly complete skull (Figs. 3–9). MPC-D 100/1355, skull lacking the nasal area, plus partial left mandible, one partial cervical half ring, one dorsal vertebra, one dorsal rib piece, and two caudal vertebrae (Figs. 3–8, and 10). MPC-D 100/1356, skull lacking the nasal area (Figs. 3–8). PIN 557, partial postcranial skeletons of at least six individuals (Maleev, 1952b: figs. 1–3, 1956: figs. 4–32).

2) From Bayanshiree Formation, Baynshin Tsav, Mongolia–PIN 3780/1, skull roof with occipital section and braincase (Tumanova, 1987: fig. 5).

Revised diagnosis. See chapter IV-1.

Discussion. In 1948, at least six individuals and a partial skull of *Talarurus* were

first collected from Bayan Shiree by the Joint Soviet-Mongolian Paleontological Expedition (Maleev, 1952b; Maryañska, 1977). These specimens were cataloged under PIN 557, and based on these materials, Maleev (1952b, 1956) described and distinguished *Talarurus* as a distinct taxon. However, Maryañska (1977) excluded the postcranial materials and only included the skull as the holotype (Figs. 45 and 46). A new partial skull specimen (PIN 3780/1) from Baynshin Tsav was later described by Tumanova (1987). Between 1995 and 1998, the Mongolia-Japan Joint Paleontological Expeditions discovered possible *Talarurus* specimens from Bayan Shiree (Matsumoto et al., 2010), but none of these are currently studied. The most recent discoveries of *Talarurus* were collected from Bayan Shiree and Shine Us Khudag by the Korea-Mongolia International Dinosaur Expedition in 2007. These specimens are three relatively well-preserved skulls (MPC-D 100/1354, 100/1355, 100/1356), which are part of the studied materials in this dissertation (see chapter IV-1).

Arbour and Currie (2016) referred to KID 154 (dorsal neural arch from Bayan Shiree), 162 (distal tibia and fibula, phalanges, and miscellaneous bone fragments, from Shine Us Khudag), 185 (Arbour and Currie (2016) referred this specimen as a partial coracoid from Bayan Shiree, but this is a proximal right humerus), 186 (miscellaneous bone fragments from Bayan Shiree), and 187 (one free caudal vertebra and possible tail club knob fragments from Bayan Shiree), as *Talarurus*. Two ankylosaur taxa, *Talarurus* and *Tsagentegia*, are currently known from the Bayanshiree Formation. Since both *Talarurus* and *Tsagentegia* are

diagnosed only by cranial characteristics with similar size (skulls up to about 301 mm and 300 mm in length, respectively), it is impossible to assign these fragmentary materials to a specific taxon. Therefore, it seems more appropriate to classify these specimens as Ankylosaurine indet., not *Talalrurus*, for now.

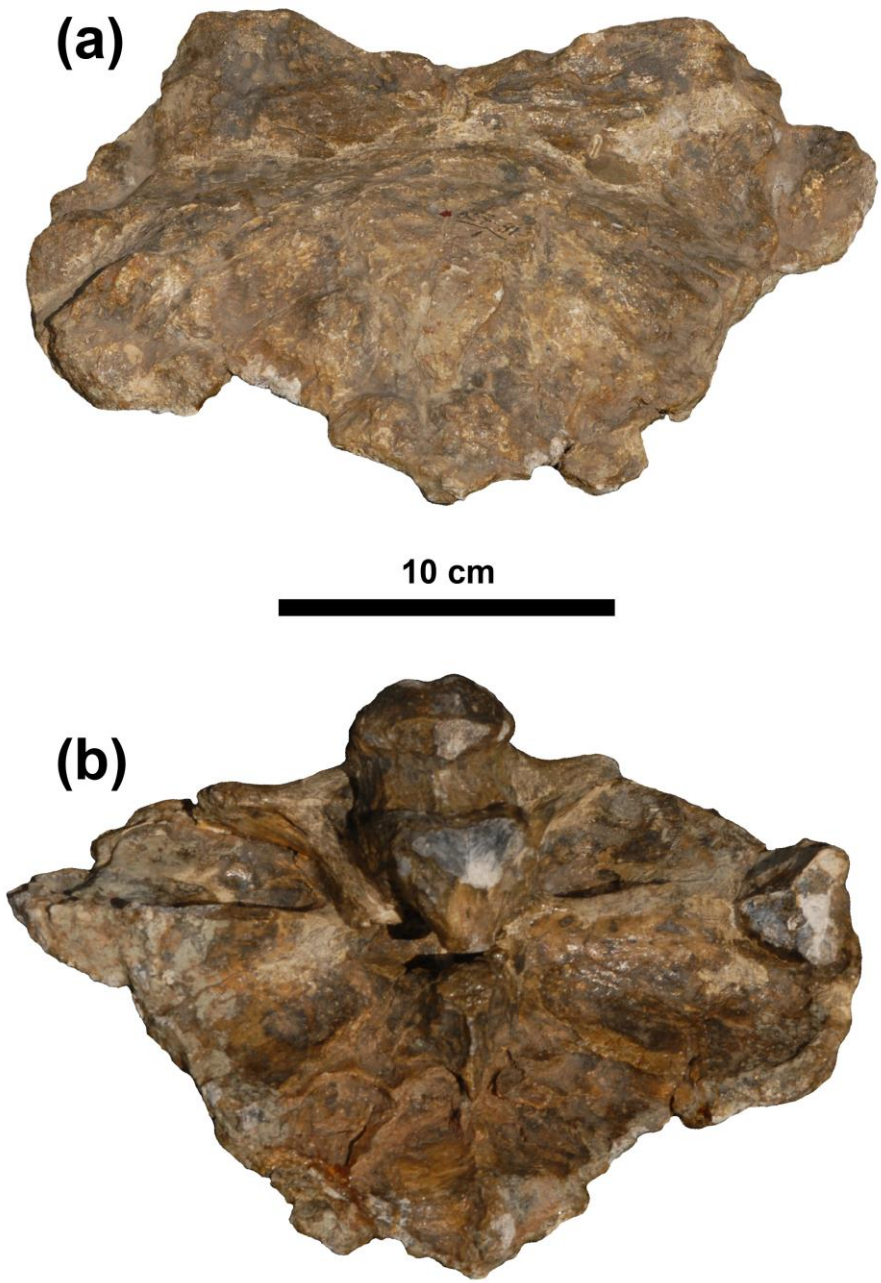

Figure 45. Photographs of the holotype skull of *Talarurus plicatospineus* (PIN 557/91). (a) Dorsal and (b) palatal views. Courtesy of Tatiana Tumanova.

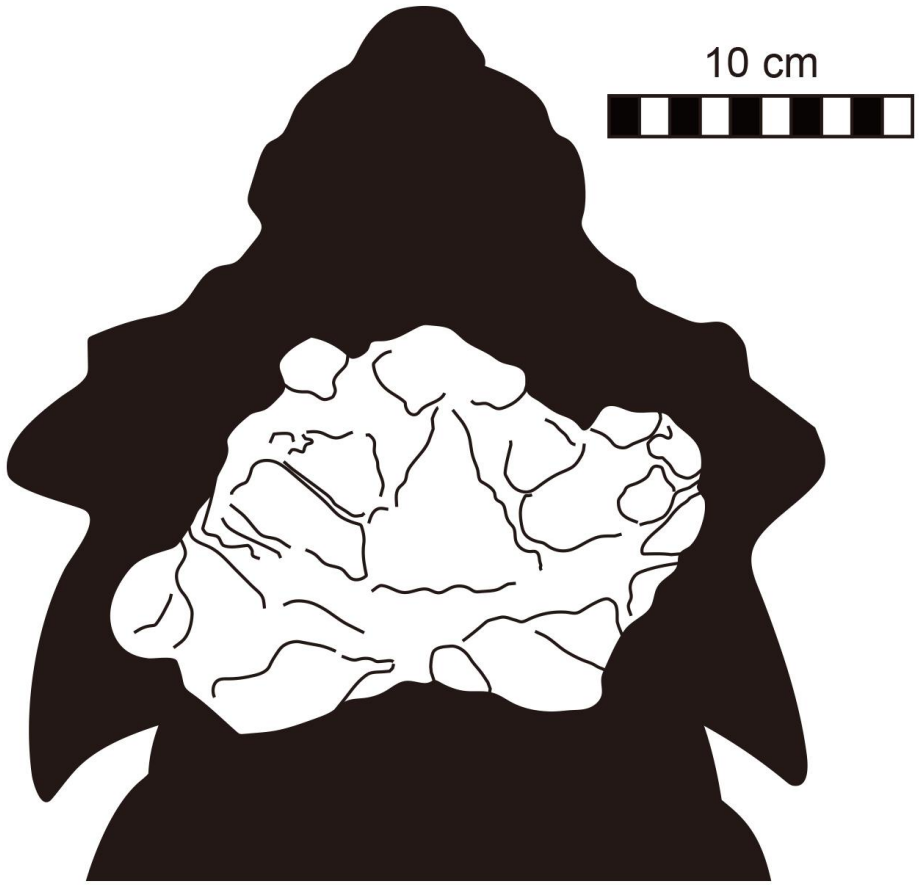

Figure 46. Line drawing of the holotype skull of *Talarurus plicatospineus* (PIN 557/91) in dorsal view.

Tarchia Maryańska, 1977

Type species. *Tarchia kielanae* Maryańska, 1977

Included species. Type species, *Tarchia teresae*, and *Tarchia tumanovae* sp. nov.

Revised generic diagnosis. See chapter IV-1.

Tarchia kielanae Maryańska, 1977

Type specimen. ZPAL MgD I/111, a posterior portion of skull roof, occipital portion, and braincase (Maryańska, 1977: pl. 27) (Figs. 47 and 48).

Type locality and horizon. Upper Cretaceous (middle–upper Campanian) Baruungoyot Formation, Khulsan, southern Gobi Desert, Mongolia.

Referred specimens. ZPAL MgD I/114, fragmentary skull and osteoderms (Baruungoyot Formation, Hermiin Tsav II) (Penkalski and Tumanova, 2017: fig. 5D).

Revised diagnosis. An ankylosaurid distinguished by the following unique set of characters (autapomorphy with an asterisk): a nasofrontal sagittal furrow with a weak Z-shaped offset (shared with *Tarchia tumanovae* and *Zaraapelta*); lateral nuchal caputegulae taller laterally than medially (shared with *Tarchia teresae*); jugular vein and cnn. IX-XI exit through one single opening and two separate exits for cn. XII*; large basioccipital foramen (shared with *Tar. teresae*). Differs from *Minotaurasaurus*, *Pinacosaurus grangeri*, *Saichania*, and *Zaraapelta* in having a

posteroventrally oriented occipital condyle. Differs from *Pinacosaurus grangeri*, *Saichania*, and *Zaraapelta* in having a tall foramen magnum. Differs from *Minotaurasaurus* and *Saichania* in having a relatively tall braincase. Differs from *Minotaurasaurus* in having mediolaterally long lateral nuchal caputegulae and broad paroccipital span. Differs from *Saichania* in having remodeled squamosal horns, anteroposteriorly short lateral nuchal caputegulae, and occiput visible in dorsal view.

Discussion. The holotype of *Tar. kielanae* (ZPAL MgD I/111) (Figs. 47 and 48) was discovered by the Polish-Mongolian Expedition in 1970 and was described by Maryañska (1977). A second specimen (ZPAL MgD I/114) was mentioned in Penkalski and Tumanova (2017). However, both specimens are partial skull elements.

Tar. kielanae was regarded as a junior synonym of "*Tar. gigantea*" by Coombs and Maryañska (1990). Arbour et al. (2014) later redefined *Tar. kielanae* as a separate species. However, Arbour et al. (2014) considered *Minotaurasaurus* a synonym of *Tar. kielanae*, due to the presence of an accessory postorbital ossification between the posterior supraorbital caputegulum and the squamosal horn. Penkalski and Tumanova (2017) later separated the two taxa based on stratigraphic positions and cranial differences such as the nuchal caputegulae and braincase. The accessory osteoderm was considered a feature present in both *Minotaurasaurus* and *Tar. kielanae*. However, this structure is more likely an external dermal layer fused to the squamosal horn proper during ontogeny (see

chapter V-4).

Tar. kielanae was placed as a sister taxon to *Zaraapelta* in the results of Arbour et al. (2014) and Arbour and Currie (2016). However, both results were based on the assumption that *Minotaurasaurus* was *Tar. kielanae*. Later in a limited cladistic analysis by Penkalski and Tumanova (2017), *Tar. kielanae* formed a clade with *Tar. teresae*, and this group was recovered as sister to *Saichania*. In the first analysis in this dissertation, *Tar. kielanae* was recovered as a sister to *Zaraapelta* (Fig. 27). In the second analysis, *Tar. kielanae* was recovered as a sister to *Tar. teresae* (Fig. 29).

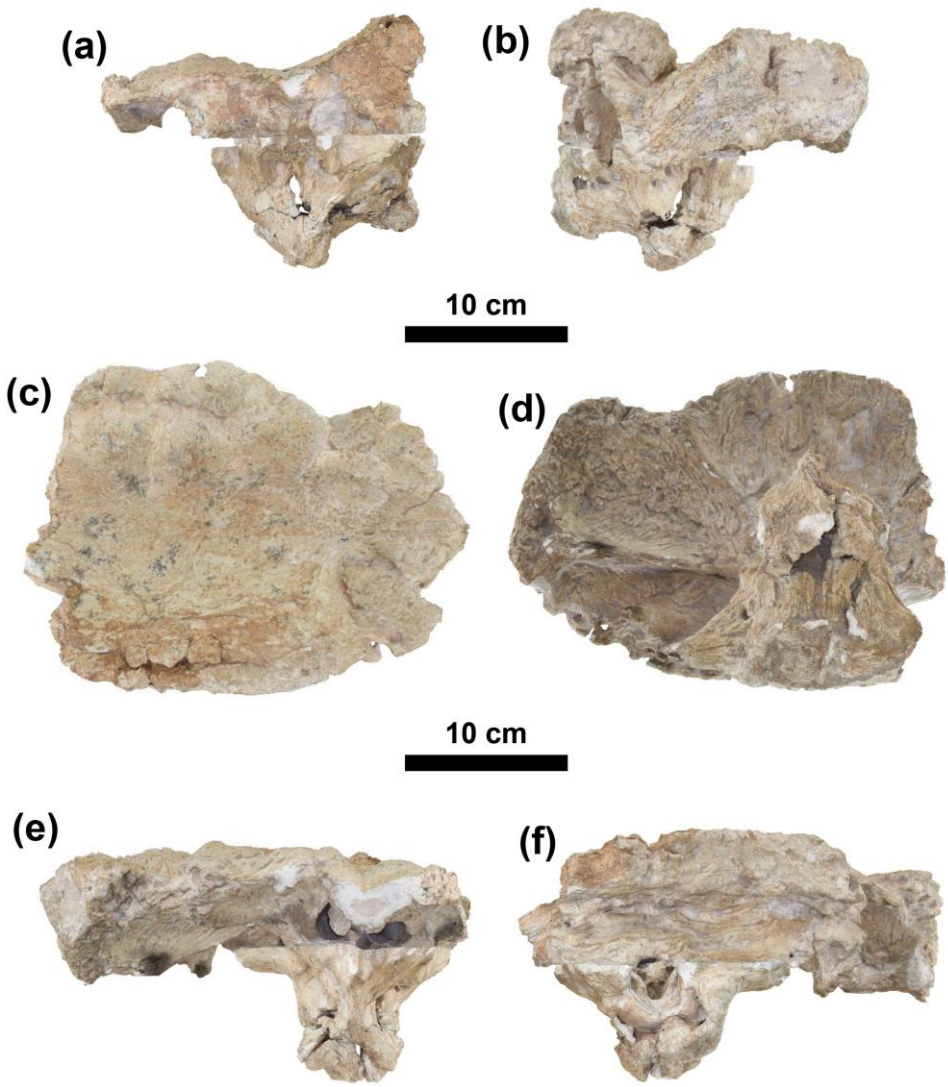

Figure 47. Photographs of the holotype skull of *Tarchia kielanae* (ZPAL MgD I/111). (a) Left lateral, (b) right lateral, (c) dorsal, (d) palatal, (e) anterior, and (f) occipital views. Courtesy of Tomasz Szczygielski.

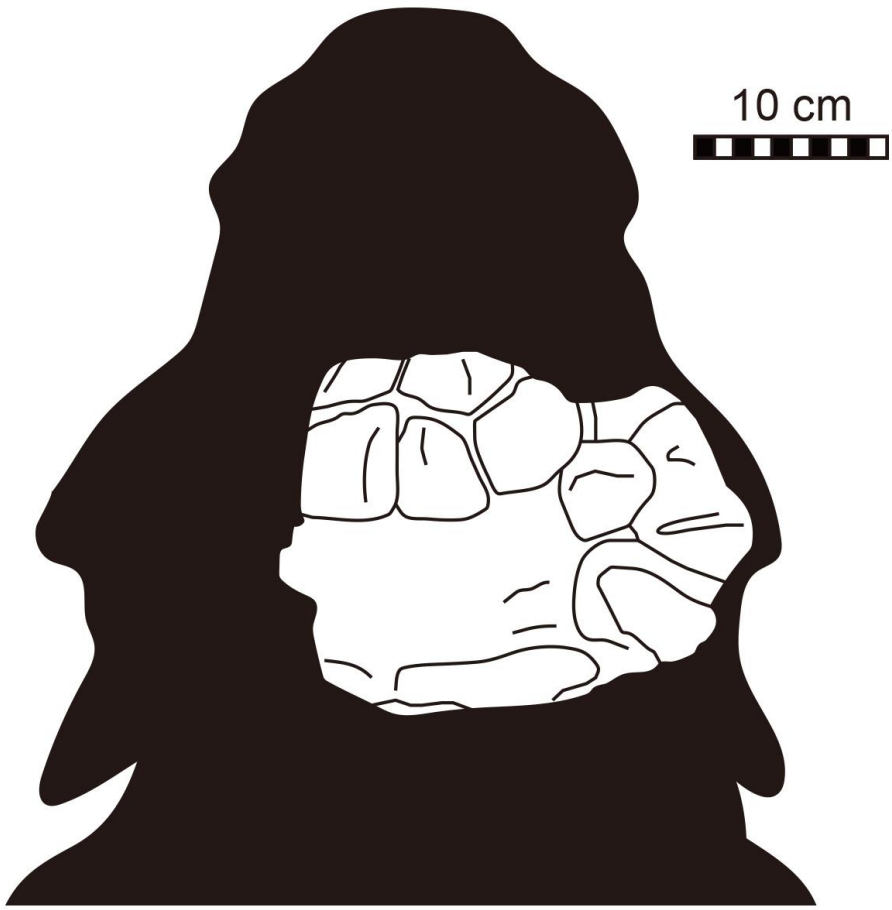

Figure 48. Line drawing of the holotype skull of *Tarchia kielanae* (ZPAL MgD I/111) in dorsal view.

Tarchia teresae Penkalski and Tumanova, 2017

Type specimen. PIN 3142/250, complete skull and mandibles (Tumanova, 1977: figs. 1–3) (Figs. 49 and 50), and postcranial material.

Type locality and horizon. Upper Cretaceous (upper Campanian–lower Maastrichtian) Nemegt Formation, Hermiin Tsav I, southern Gobi Desert, Mongolia.

Revised diagnosis. An ankylosaurid distinguished by the following unique set of characters: vertically positioned single flat internarial caputegulum (shared with *Saichania*); a straight frontal sagittal furrow (shared with *Saichania*); lateral nuchal caputegulae taller laterally than medially (shared with *Tarchia kielanae*); large basioccipital foramen (shared with *Tar. kielanae*). Differs from *Minotaurasaurus*, *Pinacosaurus grangeri*, *Saichania*, and *Zaraapelta* in having no postocular caputegulae and a posteroventrally oriented occipital condyle. Differs from *Minotaurasaurus*, *P. grangeri*, and *Zaraapelta* in having confluent supraorbital horns. Differs from *Minotaurasaurus*, *Saichania*, and *Zaraapelta* in having a relatively tall braincase. Differs from *Saichania*, *Tar. kielanae*, and *Zaraapelta* in having unfused quadrate to the exoccipital area. Differs from *Minotaurasaurus* and *Saichania* in having a relatively tall braincase. Differs from *Minotaurasaurus* and *Zaraapelta* in having subrectangular frontal caputegulae and a mediolaterally long nuchal crest. Differs from *Saichania* and *Tarchia tumanovae* in having an anteriorly situated quadrate-quadratojugal region. Differs from *Minotaurasaurus* in

having relatively long paroccipital processes. Differs from *Saichania* in having a quadratojugal horn neck, remodeled squamosal horns, anteroposteriorly short lateral nuchal caputegulae, and squamosal horns encircled by a prominent basal sulcus. Differs from *Tar. tumanovae* in having an interpterygoid vacuity invisible in occipital view.

Discussion. The holotype of *Tar. teresae* (PIN 3142/250) (Figs. 49 and 50) was discovered by the Polish-Mongolian Expedition in 1973 but wasn't assigned to a new taxon (Tumanova, 1977). Tumanova (1977) first described the specimen as "*Tar. gigantea*". Although PIN 3142/250 also contains postcranial elements, only the cranium and mandibles were figured and described in detail. The postcranial portion of PIN 3142/250 is still unstudied.

Arbour et al. (2014) reassigned PIN 3142/250 as *Saichania* based on similarities of the shape of cranial caputegulae. Later Penkalski and Tumanova (2017) suggested that PIN 3142/250 was distinct due to the significant differences in stratigraphic positions and the quadrate-exoccipital complex and assigned it as a new taxon.

A recent cladistic analysis by Penkalski and Tumanova (2017) placed *Tar. teresae* as a sister taxon to *Tar. kielanae*, and both taxa were recovered as a sister group to *Saichania*. In this dissertation, *Tar. teresae* formed a clade with *Tar. kielanae*, and this clade was recovered as a sister to *Tar. tumanovae* (Fig. 29).

Penkalski and Tumanova (2017) referred to ZPAL MgD I/43 (caudal vertebrae including tail club, from Altan Uul IV) as *Tar. teresae* with no specific

reasoning. In ZPAL MgD I/43, the prezygapophyses of the tail club handle diverge at an angle of about 20–25 º, and the tail club knob is wide. Since the postcranium of the holotype has not been described, a comparison to ZPAL MgD I/43 is currently not possible. However, the overall morphology of ZPAL MgD I/43 is somewhat similar to the holotype of *Tar. tumanovae* (MPC-D 100/1353). Therefore, it seems more appropriate to classify this specimen as ?*Tar. tumanovae* rather than *Tar. teresae*.

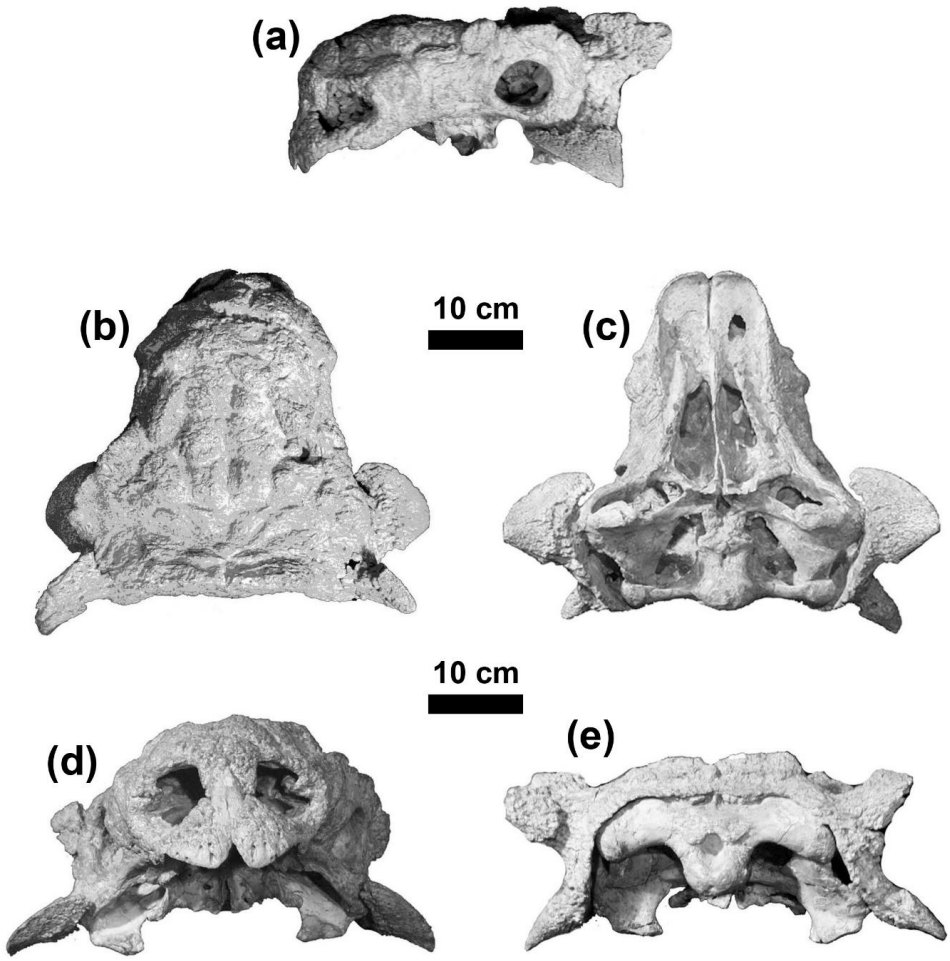

Figure 49. Photographs of the holotype skull of *Tarchia teresae* (PIN 3142/250). (a) Left lateral, (b) dorsal, (c) palatal, (d) anterior, and (e) occipital views. Courtesy of Tatiana Tumanova.

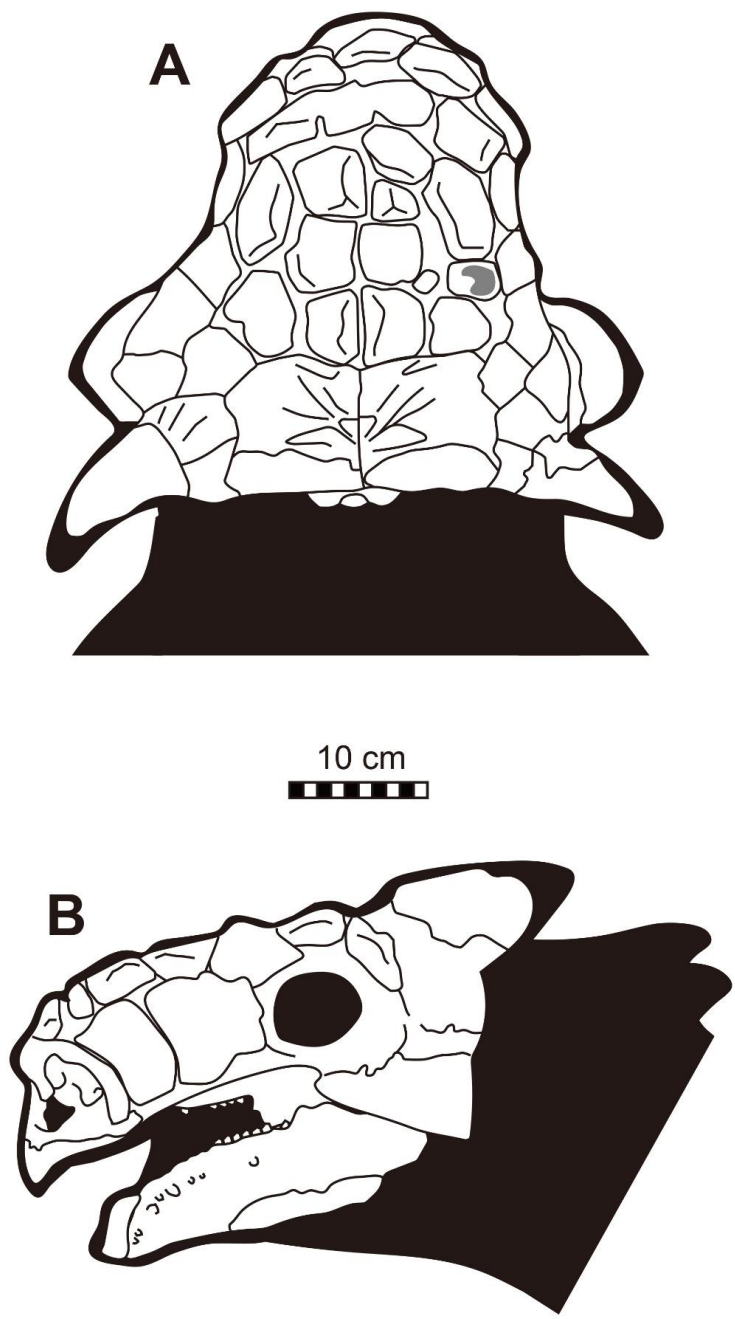

Figure 50. Line drawings of the holotype skull of *Tarchia teresae* (PIN 3142/250). (A) Dorsal and (B) left lateral views.

Tarchia tumanovae sp. nov.

Type specimen. MPC-D 100/1353, a well-preserved skull, dorsal, sacral, caudal vertebrae, sixteen dorsal ribs, ilia, a partial ischium, free osteoderms, and tail club.

Type locality and horizon. Upper Cretaceous (upper Campanian–lower Maastrichtian) Nemegt Formation, Hermiin Tsav, southern Gobi Desert, Mongolia.

Diagnosis. See chapter IV-1.

Discussion. The holotype of *Tar. tumanovae* sp. nov. (MPC-D 100/1353) was found from Hermiin Tsav during the Korea-Mongolia International Dinosaur Expedition in 2008. The holotype is described in this dissertation (see chapter V). The neuroanatomy of the holotype was fully described by Paulina-Carabajal et al. (2018) before. However, Paulina-Carabajal et al. (2018) misclassified this specimen as *Tarchia teresae* based on the similarities of the quadrate-exoccipital complex.

Tsagantegia Tumanova, 1993

Type species. *Tsagantegia longicranialis* Tumanova, 1993

Generic diagnosis. Genus monotypic, as for the type species.

Tsagantegia longicranialis Tumanova, 1993

Type specimen. MPC 700/17, skull (Tumanova, 1993: fig. 1) (Figs. 51 and 52).

Type locality and horizon. Upper Cretaceous (Cenomanian–Turonian) Bayanshiree Formation, Tsagan-Teg, eastern Gobi Desert, Mongolia.

Revised diagnosis. An ankylosaurid distinguished by the following unique set of characters (autapomorphy with an asterisk): a narrow internarial bar of the premaxillae (shared with *Tarchia*); a caudodorsally tilted single flat internarial caputegulum (shared with *Tianzhenosaurus*); two pairs of small nasal caputegulae surrounded by much larger two pairs of rhomboid caputegulae*; flat, plate-like postocular caputegulae situated ventroposterior to the orbital rim (shared with *Tianzhenosaurus*); tear shape, laterally tapering lateral nuchal caputegulae*. Differs from *Minotaurasaurus*, *Pinacosaurus mephistocephalus*, *Talarurus*, and *Tarchia* in having no "neck" at the base of the quadratojugal horns. Differs from *Minotaurasaurus*, *Saichania*, and *Tarchia* in having no premaxillary ornamentation and flat nasofrontal caputegulae. Differs from *Minotaurasaurus*, *Tarchia*, and *Zaraapelta* in having occiput unvisible in dorsal view. Differs from *Minotaurasaurus*, *Pinacosaurus grangeri*, and *Zaraapelta* in having flat prefrontal caputegulae. Differs from *Minotaurasaurus*, *Talarurus*, and *Zaraapelta* in having a pairs of large loreal and lacrimal caputegulae. Differs from *Minotaurasaurus* and *P. grangeri* in having no lacrimal incisure. Differs from *Saichania* and *Tarchia* in having flat loreal caputegulae. Differs from *Minotaurasaurus* in having narrow

supranarial caputegulae, flat frontal caputegulae, and a wide paroccipital span. Differs from *Saichania* in having anteroposteriorly short lateral nuchal caputegulae. Differs from *Tarchia* in having a wider than tall foramen magnum. Differs from *Tarchia tumanovae* in having an interpterygoid vacuity invisible in occipital view.

Discussion. The holotype of *Tsagantegia* (MPC 700/17) (Figs. 51 and 52) was collected by the Soviet-Mongolian Expedition in 1983 and was described by Tumanova (1993) in detail. No additional specimens of this taxon have been reported in scientific literature.

In a cladogram of Kirkland (1998), *Tsagantegia* was placed basal to the clade that includes the derived ankylosaurines, such as *Ankylosaurus*, *Euoplocephalus, P. grangeri*, *Saichania*, and "*Tar. gigantea*". A similar result was obtained by Vickaryous et al. (2004), placing *Tsagantegia* on the basal to the clade that includes *Ankylosaurus*, *Euoplocephalus, P. grangeri,* and *P. mephistocephalus*, *Saichania, Talarurus*, "*Tar. gigantea*," and *Tianzhenosaurus*. Hill et al. (2003) regarded *Tsagantegia* as a clade with *Shamosaurus*. This clade was a sister group to the derived ankylosaurines, such as *Ankylosaurus*, *Euoplocephalus*, *Nodocephalosaurus*, *Saichania, Shanxia*, "*Tar. gigantea*," and *Tianzhenosaurus*. Arbour and Evans (2017) regarded it as a sister taxon to the clade, which included *Nodocephalosaurus* and *Talarurus*. The phylogenetic placement of *Tsagantegia* as a basal Ankylosaurine is also supported in recent analyses (Thompson et al., 2012; Arbour and Currie, 2016; Wiersma and Irmis, 2018). However, *Tsagantegia* was recovered as a derived ankylosaurine and closely related to the North American

Ankylosaurini (Zheng et al., 2018). In this dissertation, *Tsagantegia* was recovered as a sister to the derived ankylosaurines (Fig. 27).

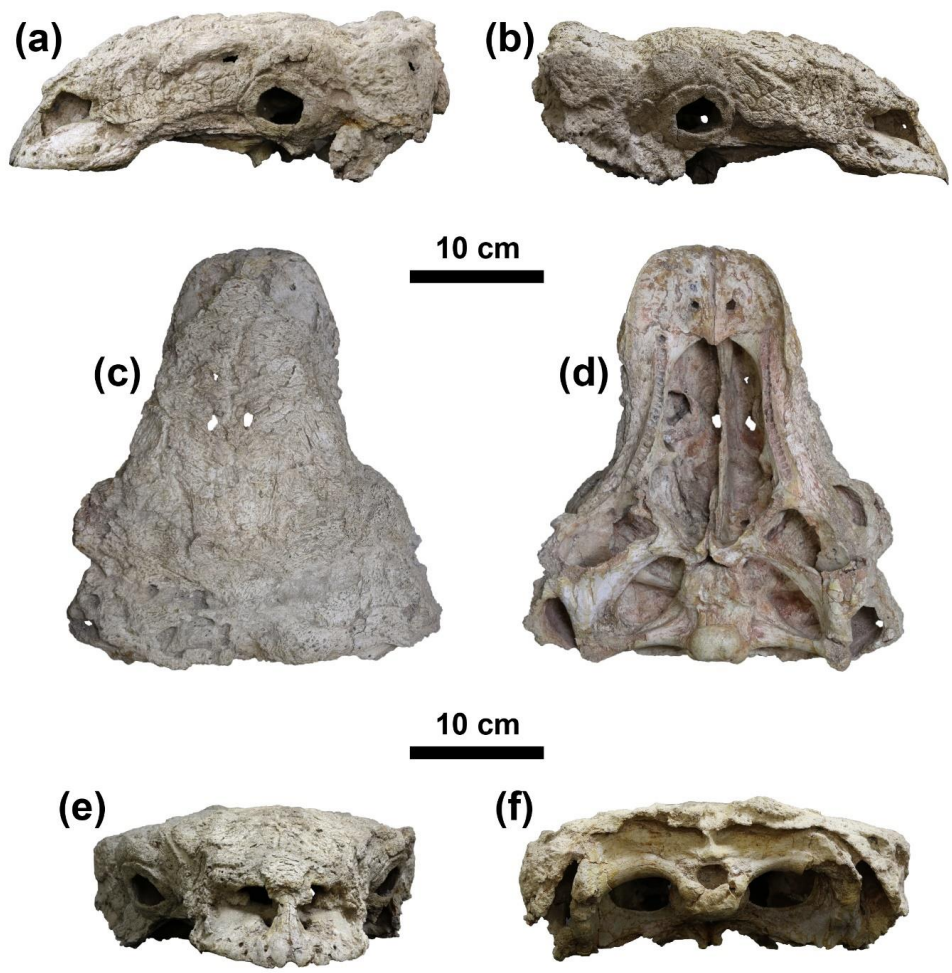

Figure 51. Photographs of the holotype skull of *Tsagantegia longicranialis* (MPC 700/17). (a) Left lateral, (b) right lateral, (c) dorsal, (d) palatal, (e) anterior, and (f) occipital views. Courtesy of Badamkhatan Zorigt.

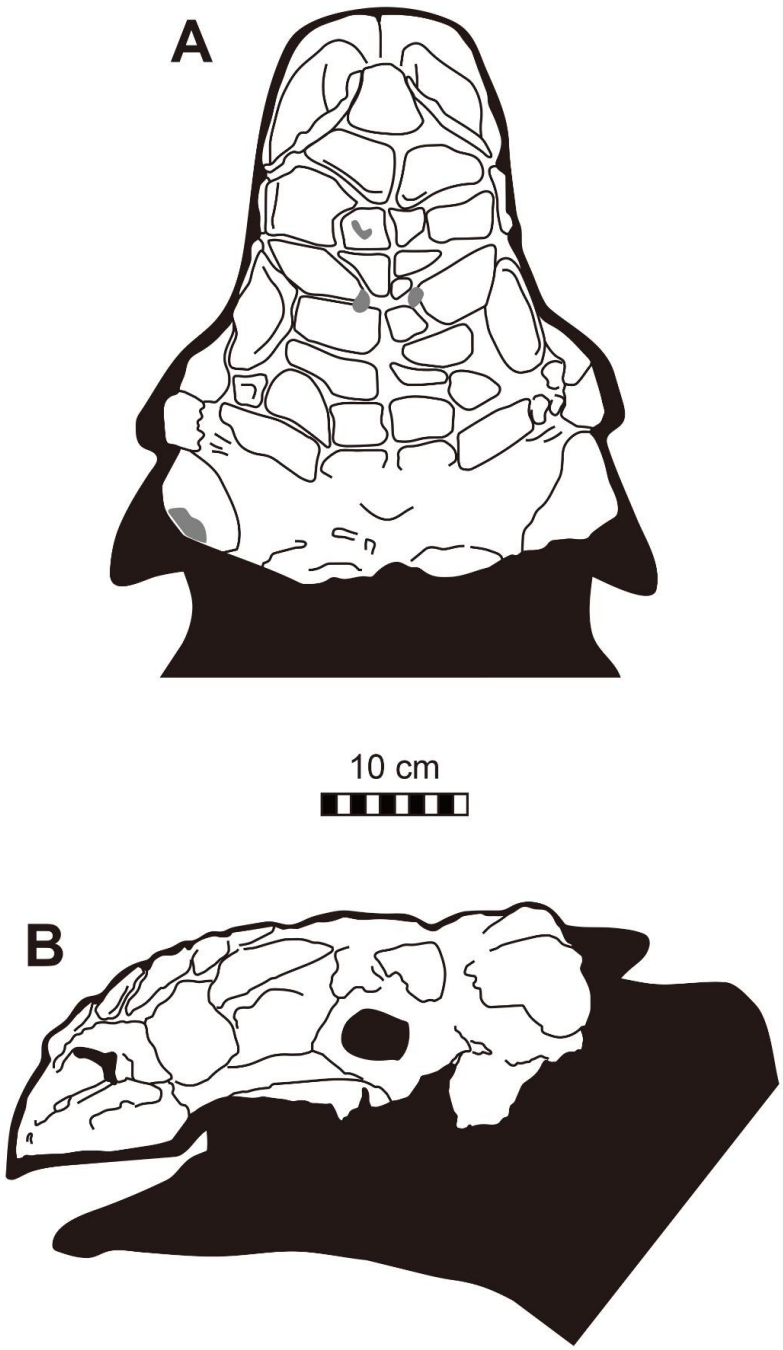

Figure 52. Line drawings of the holotype skull of *Tsagantegia longicranialis* (MPC 700/17). (A) Dorsal and (B) left lateral views.

Zaraapelta Arbour et al., 2014b

Type species. *Zaraapelta nomadis* Arbour et al., 2014b

Generic diagnosis. Genus monotypic, as for the type species.

Zaraapelta nomadis Arbour et al., 2014b

Type specimen. MPC D100/1338, skull lacking the rostrum (Arbour et al., 2014b: figs. 8–11) (Figs. 53 and 54).

Type locality and horizon. Upper Cretaceous (middle–upper Campanian) Baruungoyot Formation, Hermiin Tsav, southern Gobi Desert, Mongolia.

Revised diagnosis. An ankylosaurid distinguished by the following unique set of characters (autapomorphies with an asterisk): numerous small lacrimal and loreal caputegulae present (shared with *Minotaurasaurus*); large, sharply pointed, pyramidal prefrontal caputegulae (shared with *Minotaurasaurus* and *Pinacosaurus grangeri*); subrectangular frontal caputegulae (shared with *Saichania* and *Tarchia*); a nasofrontal sagittal furrow with a weak Z-shaped offset (shared with *Tarchia kielanae* and *Tarchia tumanovae*); anterior and posterior supraorbital caputegulae with distinct apices (shared with *Minotaurasaurus* and *Pinacosaurus grangeri*); plate-like postocular caputegulae covering the entire postocular region*; anteromedially poorly defined postorbital fossa that medially does not reach the nuchal crest*; occiput visible in dorsal view (shared with *Minotaurasaurus* and

Tarchia). Differs from *Minotaurasaurus*, *Pinacosaurus*, *Saichania*, *Talarurus*, *Tarchia*, and *Tsagantegia* in having no distinct nuchal caputegulae. Differs from *Minotaurasaurus*, *Pinacosaurus*, *Saichania*, *Tarchia*, and *Talarurus* in having no "neck" present at the base of the quadratojugal horns. Differs from *Minotaurasaurus* and *Tarchia teresae* in having fused quadrate to the exoccipital area. Differs from *Minotaurasaurus* in having a broad paroccipital span. Differs from *Saichania* in having remodeled squamosal horns. Differs from *Tar. tumanovae* in having an interpterygoid vacuity invisible in occipital view.

Discussion. The holotype of *Zaraapelta* (MPC D100/1338) (Figs. 53 and 54) was discovered by the "Dinosaur of the Gobi" Nomadic Expedition in 2000 and was described in detail by Arbour et al. (2014). No additional specimens of this taxon have been reported in scientific literature.

In most phylogenetic analyses (Arbour et al., 2014b; Arbour and Currie, 2016; Arbour and Evans, 2017; Zheng et al., 2018), *Zaraapelta* was recovered as a sister taxon to *Tarchia kielanae*. However, in a limited cladistic analysis of Penkalski and Tumanova (2017), *Zaraapelta* was placed basal to the clade, including *Saichania*, *Tar. kielanae*, and *Tar. teresae*. On the other hand, Wiersma and Irmis (2018) regarded *Zaraapelta* as a basal ankylosaurine. In the first analysis in this dissertation, *Zaraapelta* was recovered as a sister to *Tar. kielanae* (Fig. 27). In the second analysis, *Zaraapelta* was recovered as a sister to the clade that included *Saichania* and *Tarchia* (Fig. 29).

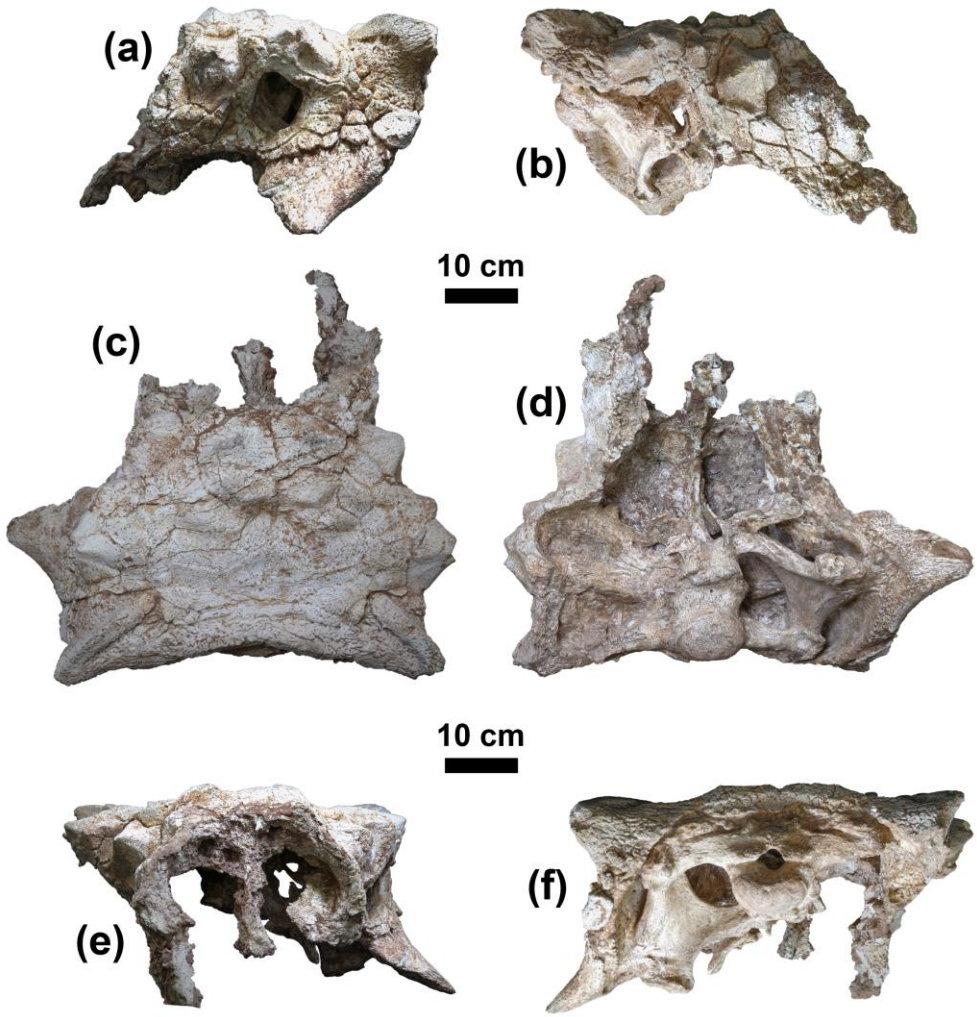

Figure 53. Photographs of the holotype skull of *Zaraapelta nomadis* (MPC D100/1338). (a) Left lateral, (b) right lateral, (c) dorsal, (d) palatal, (e) anterior, and (f) occipital views. Courtesy of Badamkhatan Zorigt.

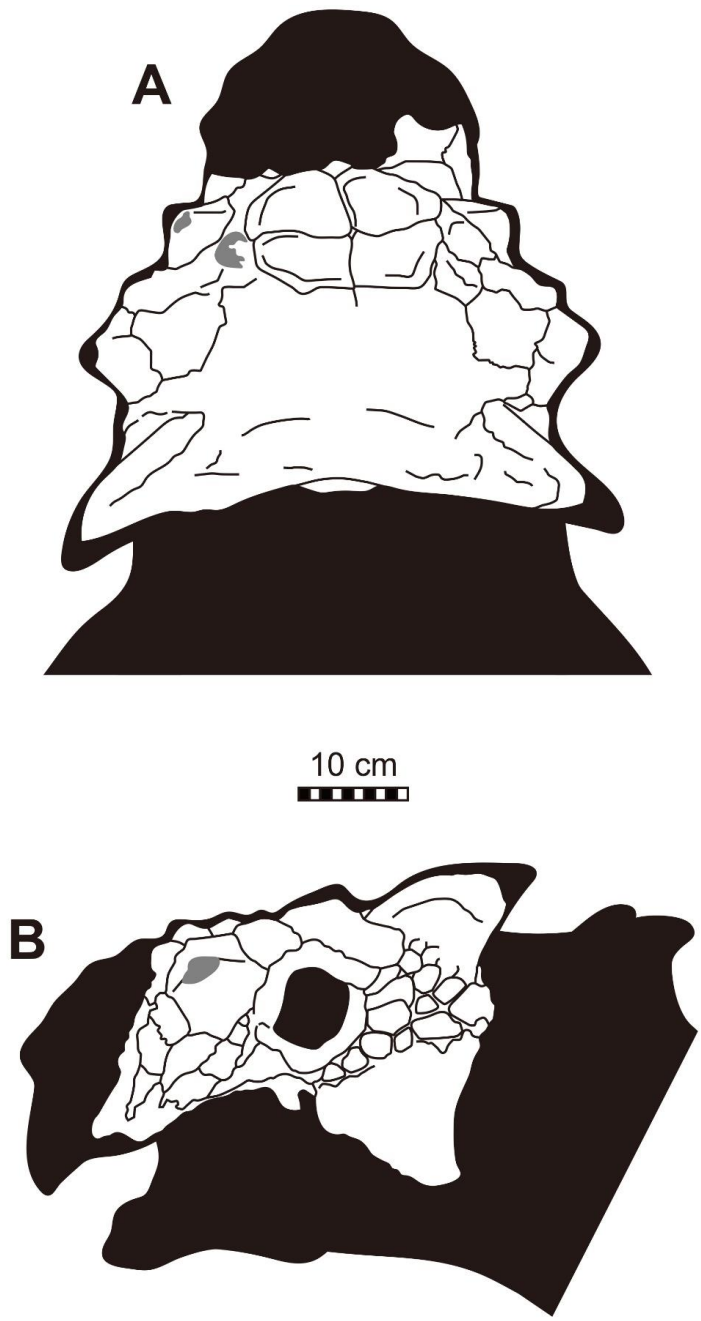

Figure 54. Line drawings of the holotype skull of *Zaraapelta nomadis* (MPC D100/1338). (A) Dorsal and (B) left lateral views.

VIII. CONCLUSIONS

The following conclusions are addressed based on the newly discovered ankylosaur specimens and taxonomic review of previously reported ankylosaur specimens of Mongolia:

1. The cladistic analysis result showed that *Talarurus* is a sister taxon to the clade that includes the Late Cretaceous ankylosaurines of Mongolia. This analysis also suggests that there was a dispersal event of ankylosaurines from Asia to western North America before the Cenomanian.

2. The rostral morphology of *Talarurus* is different from that of *Tsagantegia*, suggesting possible niche partitioning among these taxa during the Bayanshiree “time” (Cenomanian–Turonian). The former was probably a bulk feeder, while the latter was a selective feeder.

3. A new ankylosaurid dinosaur, *Tarchia tumanovae* sp. nov., has been named from the Upper Cretaceous (upper Campanian–lower Maastrichtian) Nemegt Formation of Mongolia.

4. The squamosal horns of some ankylosaurids underwent extreme ontogenetic remodeling.

5. Localized pathologies on the dorsosacral ribs and the tail prove the agonistic behavior in *Tar. tumanovae* sp. nov.

6. *Tar. tumanovae* sp. nov. had an anteriorly protruded shovel-shaped beak, a morphological character of selective feeders. Ankylosaurid diets shifted from low-level bulk feeding to selective feeding during the Baruungoyot and the Nemegt “age” (middle Campanian–lower Maastrichtian). This ankylosaurid niche shifting might have responded to habitat change and competition with other bulk-feeding herbivores, such as hadrosaurids.

7. Asian ankylosaurids evolved rigid bodies with a decreased number of pedal phalanges, especially the second and third digits, through time.

8. At least two forms of flank armor within Ankylosauridae were recognized, one with spine-like osteoderms and the other with keeled rhomboidal osteoderms.

9. Unique anatomical features related to digging are present in Ankylosauridae, such as dorsoventrally flattened and fusiform body shapes, extensively fused series of vertebrae, anteroposteriorly broadened dorsal ribs, a robust humerus with a well-developed deltopectoral crest, a short and robust ulna with a well-developed olecranon process, a trowel-like manus, and decreased numbers of pedal phalanges. Ankylosaurids were likely to dig the substrate, taking advantage of it for self-defense and survival.

10. PIN 3101, a partial mandible from the Lower Cretaceous (Aptian–Albian) Khovboor Beds, is reclassified as an indeterminate ankylosaur rather than *Shamosaurus*.

11. MPC 100/1305, a nearly complete skeleton lacking a skull from the upper Cretaceous (Campanian) Djadokhta Formation, is not *Pinacosaurus grangeri* but possibly *Minotaurasaurus*.

12. ZPAL MgD I/42, one free caudal vertebra and a tail club from the upper Cretaceous Nemegt Formation, is reclassified as an indeterminate ankylosaur.

13. *Shanxia tianzhenensis* and *Tianzhenosaurus youngi* from the Upper Cretaceous Huiquanpu Formation should be valid taxa.

14. KID 154 (dorsal neural arch), 162 (distal tibia and fibula, phalanges, and miscellaneous bone fragments), 185 (proximal right humerus), 186 (miscellaneous bone fragments), and 187 (one free caudal vertebra and possible tail club knob fragments) from the upper Cretaceous (Cenomanian–Turonian) Bayanshiree Formation, is reclassified as an indeterminate ankylosaur.

15. ZPAL MgD I/43, caudal vertebrae including a tail club from the upper Cretaceous Nemegt Formation, is reclassified as ?*Tar. tumanovae*.

REFERENCES

Alifanov, V.R., 1993a. New lizards of the family Macrocephalosauridae (Sauria) from the Upper Cretaceous of Mongolia and some critical comments on the classification of Teiidae (*sensu* Estes, 1983a). Paleontological Zhurnal 27, 57–74.

Alifanov, V.R., 1993b. Some peculiarities of the Cretaceous and Palaeogene lizard faunas of the Mongolian People's Republic. Kaupia. Darmstadter Beiträge zur Naturgeschichte 3, 9–13.

Alifanov, V.R.,1993c. Upper Cretaceous lizards of Mongolia and the first inter-American contact. Paleontological Zhurnal 27, 79–85.

Alifanov, V.R., 2000. The fossil record of Cretaceous lizards from Mongolia. In: Benton, M.J., Shishkin, M.A., Unwin, D.M., Kurochkin, E.N. (Ed.), The Age of Dinosaurs in Russia and Mongolia. Cambridge University Press, Cambridge, 368–389.

Alifanov, V.R., 2003. Two new dinosaurs of the infraorder Neoceratopsia (Ornithischia) from the Upper Cretaceous of the Nemegt Depression, Mongolian People's Republic. Paleontological Zhurnal 37, 524–534.

Alifanov, V.R., 2008. The tiny horned dinosaur *Gobiceratops minutus* gen. et sp. nov. (Bagaceratopidae, Neoceratopsia) from the Upper Cretaceous of Mongolia. Paleontological Zhurnal 42, 621–633.

Alifanov, V.R., Barsbold, R., 2009. *Ceratonykus oculatus* gen. et sp. nov., a new dinosaur (? Theropoda, Alvarezsauria) from the Late Cretaceous of Mongolia. Paleontological Zhurnal 43, 94–106.

Arbour, V.M., 2009. Estimating impact forces of tail club strikes by ankylosaurid dinosaurs. PLoS ONE 4, e6738. DOI: 10.1371/journal.pone.0006738.

Arbour, V.M., Currie, P.J., 2011. Tail and pelvis pathologies of ankylosaurian dinosaurs. Historical Biology 23, 375–390.

Arbour, V.M., Currie, P.J., 2013a. *Euoplocephalus tutus* and the diversity of ankylosaurid dinosaurs in the Late Cretaceous of Alberta, Canada, and Montana, USA. PLoS ONE 8, e62421. DOI: 10.1371/journal.pone.0062421.

Arbour, V.M., Currie, P.J., 2013b. The taxonomic identity of a nearly complete ankylosaurid dinosaur skeleton from the Gobi Desert of Mongolia. Cretaceous Research 46, 24–30.

Arbour, V.M., Currie, P.J., 2015. Ankylosaurid dinosaur tail clubs evolved through stepwise acquisition of key features. Journal of Anatomy 227, 514–523.

Arbour, V.M., Currie, P.J., 2016. Systematics, phylogeny and palaeobiogeography of the ankylosaurid dinosaurs. Journal of Systematic Palaeontology 14, 385–444.

Arbour, V.M., Evans, D.C., 2017. A new ankylosaurine dinosaur from the Judith River Formation of Montana, USA, based on an exceptional skeleton with soft tissue preservation. Royal Society Open Science 4, 161086. DOI:

10.1098/rsos.161086.

Arbour, V.M., Mallon, J.C., 2017. Unusual cranial and postcranial anatomy in the archetypal ankylosaur *Ankylosaurus magniventris*, FACETS 2, 764–794.

Arbour, V.M., Zanno, L.E., 2018. The evolution of tail weaponization in amniotes. Proceedings of the Royal Society B 285, 20172299. DOI: 10.1098/rspb.2017.2299.

Arbour, V.M., Burns, M.E., Sissons, R.L., 2009. A redescription of the ankylosaurid dinosaur *Dyoplosaurus acutosquameus* Parks, 1924 (Ornithischia: Ankylosauria) and a revision of the genus. Journal of Vertebrate Paleontology 29, 1117–1135.

Arbour, V.M., Lech-Hernes, N.L., Guldberg, T.E., Hurum, J.H., Currie, P.J., 2013. An ankylosaurid dinosaur from Mongolia with in situ armour and keratinous scale impressions. Acta Palaeontologica Polonica 58, 55–64.

Arbour, V.M., Burns, M.E., Sullivan, R.M., Lucas, S.G., Cantrell, A.K., Fry, J., Suazo, T.L., 2014a. A New Ankylosaurid Dinosaur from the Upper Cretaceous (Kirtlandian) of New Mexico with Implications for Ankylosaurid Diversity in the Upper Cretaceous of Western North America. PLoS ONE 9, e108804. DOI: 10.1371/journal.pone.0108804.

Arbour, V.M., Currie, P.J., Badamgarav, D., 2014b. The ankylosaurid dinosaurs of the Upper Cretaceous Baruungoyot and Nemegt formations of Mongolia. Zoological Journal of the Linnean Society 172, 631–652.

Arbour, V., Zanno, L.E., Evans, D., 2020. Evidence for intraspecific combat, rather

than antipredator defense, as the selective pressure underlying the evolution of ankylosaurine tail clubs. The Society of Vertebrate Paleontology 80th Annual Meeting, Program and Abstracts, 64.

Averianov, A.O., Lopatin, A.V., 2019. Sauropod diversity in the Upper Cretaceous Nemegt Formation of Mongolia–a possible new specimen of *Nemegtosaurus*. Acta Palaeontologica Polonica 64, 313–321.

Bargo, M.S., Vizcaíno, S.F., Archuby, F.M., Blanco, R.E., 2000. Limb bone proportions, strength and digging in some Lujanian (Late Pleistocene–Early Holocene) mylodontid ground sloths (Mammalia, Xenarthra). Journal of Vertebrate Paleontology 20, 601–610.

Barrett, P.M., 2005. The diet of ostrich dinosaurs (Theropoda: Ornithomimosauria). Palaeontology 48, 347–358.

Barrett, P.M., You, H., Upchurch, P., Burton, A., 1998. A new ankylosaurian dinosaur (Ornithischia: Ankylosauria) from the Upper Cretaceous of Shanxi Province, People's Republic of China. Journal of Vertebrate Paleontology 18, 376–384.

Barsbold, R., 1971. Certain large gastropods from the Upper Cretaceous deposits of South-Western Mongolia. The Joint Soviet Mongolian Paleontological Expedition Transaction 3, 14–19.

Barsbold, R., 1972. Biostratigraphy and Freshwater Molluscs of the Upper Cretaceous of the Gobi part of the Peoples' Republic of Mongolia. Nauka, Moscow, p. 88. [In Russian]

Barsbold, R., 1974. Saurornithoididae, a new family of small theropod dinosaurs from central Asia and North America. Palaeontologia Polonica 30, 5–22.

Barsbold, R., 1976. New data on *Therizinosaurus* (Therizinosauridae, Theropoda). Trudy Sovmestnaya Sovetsko-Mongol'skaya Paleontologicheskaya Ekspeditsii 15, 28–39. [In Russian]

Barsbold, R., 1981. Toothless carnivorous dinosaurs of Mongolia. Trudy Sovmestnaya Sovetsko-Mongol'skaya Paleontologicheskaya Ekspeditsia 3, 68–75. [In Russian]

Barsbold, R., 1983. Carnivorous dinosaurs from the Cretaceous of Mongolia. Trudy Sovmestnaya Sovetsko-Mongol'skaya Paleontologicheskaya Ekspeditsii 19, 1–120. [In Russian]

Barsbold, R., 1986a. Coelurosaurian Oviraptors. In: Vorobyeva, E.I. (Ed.), Herpetologische Untersuchungen in der Mongolischen Volksrepublik. Akademia Nauk SSSR, 210–223. [In Russian]

Barsbold, R., 1986b. Thieving dinosaurs oviraptors. Trudy Sovmestnaya Sovetsko-Mongol'skaya Paleontologicheskaya Ekspeditsii 22, 210–223. [In Russian]

Barsbold, R., 1988a. A new Late Cretaceous ornithomimid from the Mongolian People's Republic. Paleontologičeskij žurnal 1984, 124–127.

Barsbold, R., 1988b. About the bone crest and the horn cover of the carnivorous-oviraptors dinosaurs. Trudy Sovmestnaya Sovetsko-Mongol'skaya Paleontologicheskaya Ekspeditsii 34, 77–80. [In Russian]

Barsbold, R., Osmólska, H., Watabe, M., Currie, P.J., Tsogtbaatar, K., 2000. A new

oviraptorosaur (Dinosauria, Theropoda) from Mongolia: the first dinosaur with a pygostyle. Acta Palaeontologica Polonica 45, 97–106.

Bell, A.K., Chiappe, L.M., Erickson, G.M., Suzuki, S., Watabe, M., Barsbold, R., Tsogtbaatar, K., 2010. Description and ecologic analysis of *Hollanda luceria*, a Late Cretaceous bird from the Gobi Desert (Mongolia). Cretaceous Research 31, 16–26.

Bell, P.R., 2011. Cranial Osteology and Ontogeny of *Saurolophus angustirostris* from the Late Cretaceous of Mongolia with comments on *Saurolophus osborni* from Canada. Acta Palaeontologica Polonica 56, 703–722.

Bell, P.R., Currie, P.J., Lee, Y.-N., 2012. Tyrannosaur feeding traces on *Deinocheirus* (Theropoda:?Ornithomimosauria) remains from the Nemegt Formation (Late Cretaceous), Mongolia. Cretaceous Research 37, 186–190.

Bell, P.R., Evans, D.C., Eberth, D.A., Fanti, F., Tsogtbaatar, Kh., Ryan, M.J., 2018. Sedimentological and taphonomic observations on the “Dragon's Tomb” *Saurolophus* (Hadrosauridae) bonebed, Nemegt Formation (Upper Cretaceous), Mongolia. Palaeogeography, Palaeoclimatology, Palaeoecology 494, 75–90.

Benton, M.J., Shishkin, M.A.,Unwin,D.M., Kurochkin, E.N., 2000. Mongolian place names and stratigraphic terms. In: Benton, M.J., Shishkin, M.A., Unwin, D.M., Kurochkin, E.N. (Ed.), The age of dinosaurs in Russia and Mongolia. Cambridge University Press, Cambridge, 22–28.

Bever, G.S., Brusatte, S.L., Carr, T.D., Xu, X., Balanoff, A.M., Norell, M.A., 2013.

The Braincase Anatomy of the Late Cretaceous Dinosaur *Alioramus* (Theropoda: Tyrannosauroidea). Bulletin of the American Museum of Natural History 376, 1–72.

Bielert, C., Costo, N., Gallup, A., 2018. Tuskedness in African elephants – an anatomical investigation of laterality. Journal of Zoology 304, 169–174.

Birn-Jeffery, A.V., Miller, C.E., Naish, D., Rayfield, E.J., Hone, D.W.E., 2012. Pedal claw curvature in birds, lizards and Mesozoic dinosaurs–complicated categories and compensating for mass-specific and phylogenetic control. PLoS One 7, e50555. DOI: 10.1371/journal.pone.0050555.

Blows, W.T., 2001. Dermal armor of the polacanthine dinosaurs. In: Carpenter, K. (Ed.), The Armored Dinosaurs. Indiana University Press, Bloomington, 363–385.

Borsuk-Białynicka, M., 1977. A new camarasaurid sauropod *Opisthocoelicaudia skarzynskii* gen. n., sp. n. from the Upper Cretaceous of Mongolia. Palaeontologia Polonica 37, 5–64.

Borsuk-Białynicka, M., 1978. *Eopelobates leptocolaptus* sp. n. - the first upper Cretaceous pelobatid frog from Asia. Palaeontologia Polonica 38, 57–63.

Borsuk-Białynicka, M., 1984. Anguimorphs and related lizards from the Late Cretaceous of the Gobi Desert, Mongolia. Palaeontologia Polonica 46, 1–105.

Borsuk-Białynicka, M., 1985. Carolinidae, a new family of xenosaurid-like lizards from the Upper Cretaceous of Mongolia. Acta Geologica Polonica 30,

151–176.

Borsuk-Białynicka, M., 1988. *Globaura venusta* gen et sp. n and *Eoxanta lacertifrons* gen. et sp. n. - non-teiid lacertoids from the Late Cretaceous of Mongolia. Acta Palaeontologica Polonica 33, 211–248.

Borsuk-Białynicka, M., Moody, S.M., 1984. Priscagaminae, a new subfamily of the Agamidae (Sauria) from the Late Cretaceous of the Gobi Desert. Acta Palaeontologica Polonica 29, 51–81.

Brown, B., 1908. The Ankylosauridae, a new family of armored dinosaurs from the Upper Cretaceous. Bulletin of the American Museum of Natural History 24, 187–201.

Brusatte, S.L., Carr, T.D., Erickson, G.M., Bever, G.S., Norell, M.A., 2009. A long-snouted, multihorned tyrannosaurid from the Late Cretaceous of Mongolia. PNAS 106, 17261–17266.

Brusatte, S.L., Carr, T.D., Norell, M.A., 2012. The Osteology of *Alioramus*, A Gracile and Long-Snouted Tyrannosaurid (Dinosauria: Theropoda) from the Late Cretaceous of Mongolia. Bulletin of the American Museum of Natural History 366, 1–197.

Burns, M.E., Currie, P.J., Sissons, R., Arbour, V.M., 2011. Juvenile specimens of *Pinacosaurus grangeri* Gilmore, 1933 (Ornithischia: Ankylosauria) from the Late Cretaceous of China, with comments on the specific taxonomy of *Pinacosaurus*. Cretaceous Research 32, 174–186.

Burns, M.E., Tumanova, T.A., Currie, P.J., 2015. Postcrania of juvenile

Pinacosaurus grangeri (Ornithischia: Ankylosauria) from the Upper Cretaceous Alagteeg Formation, Alag Teeg, Mongolia: implications for ontogenetic allometry in ankylosaurs. Journal of Paleontology 89, 168–182.

Capstick, P.H., 1977. Death in the long grass: a big game hunter's adventures in the African bush. Macmillan, London, 320 pp.

Carpenter, K., 1982. Skeletal and dermal armor reconstruction of *Euoplocephalus tutus* (Ornithischia: Ankylosauridae) from the Late Cretaceous Oldman Formation of Alberta. Canadian Journal of Earth Sciences 19, 689–697.

Carpenter, K., 1992. Tyrannosaurids (Dinosauria) of Asia and North America. In: Mateer, N.J., Chen, P.J. (Ed.), Aspects of Nonmarine Cretaceous Geology, Proceedings of the First International Symposium of IGCP 245 Nonmarine Cretaceous Correlations, Ocean Press, Beijing, 250–268.

Carpenter, K., 1997. Agnostic behavior in pachycephalosaurs (Ornithischia: Dinosauria): a new look at head butting behavior. Contributions to Geology, University of Wyoming 32, 19–25.

Carpenter, K., 2001. Phylogenetic analysis of the Ankylosauria. In: Carpenter, K. (Ed.), The armored dinosaurs. Indiana University Press, Bloomington, 455–483.

Carpenter, K., 2007. Ankylosauria. In: Currie, P.J., Padian, K. (Ed.), Encyclopedia of dinosaurs. Academic Press, Cambridge, 16–20.

Carpenter, K., 2012. Ankylosauria. In: Brett-Surman, M.K., Holtz, T.R. Jr., Farlow, J.O. (Ed.), The Complete Dinosaur (2nd edition). Indiana University Press,

Bloomington, 505–526.

Carpenter, K., Hayashi, S., Kobayashi, Y., Maryañska, T., Barsbold, R., Sato, K., Obata, I., 2011. *Saichania chulsanensis* (Ornithischia, Ankylosauridae) from the Upper Cretaceous of Mongolia. Palaeontographica, Abteilung A: Palaeozoology–Stratigraphy 294, 1–61.

Carr, T.D., 1999. Craniofacial ontogeny in Tyrannosauridae (Dinosauria, Coelurosauria). Journal of Vertebrate Paleontology 19, 497–520.

Carrano, M.T., Janis, C.M., Sepkoski, J.J., Jr., 1999. Hadrosaurs as ungulate parallels: Lost lifestyles and deficient data. Acta Palaeontologica Polonica 44, 237–261.

Cau, A., Madzia, D., 2018. Redescription and affinities of *Hulsanpes perlei* (Dinosauria, Theropoda) from the Upper Cretaceous of Mongolia. PeerJ 6, e4868. DOI: 10.7717/peerj.4868.

Chiappe, L.M., Norell, M.A., Clark, J.M., 1998. The skull of a relative of the stem-group bird *Mononykus*. Nature 392, 275–278.

Chiappe, L.M., Norell, M.A., Clark, J.M., 2002. The Cretaceous, short-armed Alvarezsauridae: *Mononykus* and its kin. In: Chiappe, L.M., Witmer, L.M. (Ed.), Mesozoic Birds Above the Heads of Dinosaurs. University of California Press, Berkeley, 87–120.

Chkhikvadze, V.M., Shuvalov, V.F., 1980. The problem of the origin of the three-clawed turtles. Soobshcheniya Akudemii Nauk Gruzinskoy 100, 501–503. [In Russian]

Christiansen, P., 1997. Locomotion in sauropod dinosaurs. Gaia 14, 45–75.

Clemens, W.A., Lillegraven, J.A., Lindsay, E.H., Simpson, G.G., 1979. Where, when, and what-a survey of known Mesozoic mammal distribution. In: Lillegraven, J.A., Kielan-Jaworowska, Z., Clemens, W.A. (Ed.), Mesozoic mammals-the first two-thirds of mammalian history. University of California Press, Berkeley, 7–58.

Conrad, J.L., Rieppel, O., Gauthier, J.A., Norell, M.A., 2011. Osteology of *Gobiderma pulchrum* (Monstersauria, Lepidosauria, Reptilia). Bulletin of the American Museum of Natural History 362, 88 pp.

Coombs, M.C., 1983. Large mammalian clawed herbivores: a comparative study. Transactions of the American Philosophical Society 73, 1–96.

Coombs, W.P. Jr., 1971. The Ankylosauria. Ph.D. dissertation, Columbia University, New York, 487 pp.

Coombs, W.P. Jr., 1978. Forelimb muscles of the Ankylosauria (Reptilia, Ornithischia). Journal of Paleontology 52, 642–657.

Coombs, W.P. Jr., 1986. A juvenile ankylosaur referable to the genus *Euoplocephalus* (Reptilia, Ornithischia). Journal of Vertebrate Paleontology 6, 162–173.

Coombs, W.P. Jr., 1995. Ankylosaurian tail clubs of middle Campanian to early Maastrichtian age from western North America, with description of a tiny tail club from Alberta and discussion of tail orientation and tail club function. Canadian Journal of Earth Sciences 32, 902–912.

Coombs, W.P. Jr., Maryañska, T., 1990. Ankylosauria. In: Weishampel, D.B., Dodson, P., Osmolska, H. (Ed.), The Dinosauria. University of California Press, Berkeley, 456–483.

Currie, P.J., 1989. Long distance dinosaurs. Natural History 6, 60–65.

Currie, P.J., 2000. Theropods from the Cretaceous of Mongolia. In: Benton, M.J., Shishkin, M.A., Unwin, D.M., Kurochkin, E.N. (Ed.), The Age of Dinosaurs in Russia and Mongolia. Cambridge University Press, Cambridge, 434–455.

Currie, P.J., Badamgarav, D., Koppelhus, E., 2003. The First Late Cretaceous Footprints from the Nemegt Locality in the Gobi of Mongolia. Ichnos 10, 1–13.

Currie, P.J., Badamgarav, D., Koppelhus, E.B., Sissons, R., Vickaryous, M.K., 2011. Hands, feet, and behaviour in *Pinacosaurus* (Dinosauria: Ankylosauridae). Acta Palaeontologica Polonica 56, 489–504.

Currie, P.J., Funston, G.F., Osmólska, H., 2015. New Specimens of the Crested Theropod Dinosaur *Elmisaurus rarus* from Mongolia. Acta Palaeontologica Polonica 61, 143–157.

Currie, P.J., Wilson, J.A., Fanti, F., Mainbayar, B., Tsogtbaatar, K., 2018. Rediscovery of the type localities of the Late Cretaceous Mongolian sauropods *Nemegtosaurus mongoliensis* and *Opisthocoelicaudia skarzynskii*: Stratigraphic and taxonomic implications. Palaeogeography, Palaeoclimatology, Palaeoecology 494, 5–13.

Czepiński, Ł., 2019. Ontogeny and variation of a protoceratopsid dinosaur *Bagaceratops rozhdestvenskyi* from the Late Cretaceous of the Gobi Desert. Historical Biology, DOI: 10.1080/08912963.2019.1593404.

Danilov, I.G., Hirayama, R., Sukhanov, V.B., Suzuki, S., Watabe, M., Vitek, N.S., 2014. Cretaceous soft-shelled turtles (Trionychidae) of Mongolia: new diversity, records and a revision. Journal of Systematic Palaeontology 12, 799–832.

Dewaele, L., Tsogtbaatar, K., Barsbold, R., Garcia, G., Stein, K., Escuillié, F., Godefroit, P., 2015. Perinatal specimens of *Saurolophus angustirostris* (Dinosauria: Hadrosauridae), from the Upper Cretaceous of Mongolia. PLoS ONE 10, e0138806. DOI: 10.1371/journal.pone.0138806.

Dingus, L., Loope, D.B., Dashzeveg, D., Swisher, C.C., Minjin, C., Novacek, M.J., Norell, M., 2008. The geology of Ukhaa Tolgod (Djadokhta Formation, Upper Cretaceous, Nemegt Basin, Mongolia). American Museum Novitates 3616, 1–40.

Dondas, A., Isla F.I., Carballido, J.L., 2009. Paleocaves exhumed from the Miramar Formation (Ensenadan Stage-age, Pleistocene), Mar del Plata, Argentina. Quaternary International 210, 44–50.

Dong, Z., 1993. An ankylosaur (ornithischian dinosaur) from the Middle Jurassic of the Junggar Basin, China. Vertebrata PalAsiatica 31, 257–266.

Dzik, J., 1975. Spiroboloid millipedes from the Late Cretaceous of the Gobi Desert, Mongolia. In: Kielan-Jaworowska, Z. (Ed.), Results of the Polish-

Mongolian Palaeontological Expeditions, Part VI. Polish Academy of Sciences, Warsaw, 17–23.

Eberth, D.A., 2018. Stratigraphy and paleoenvironmental evolution of the dinosaur-rich Baruungoyot–Nemegt succession (Upper Cretaceous), Nemegt Basin, southern Mongolia. Palaeogeography, Palaeoclimatology, Palaeoecology 494, 29–50.

Eberth, D.A., Badamgarav, D., Currie, P.J., 2009a. The Baruungoyot–Nemegt transition (Upper Cretaceous) at the Nemegt type area, Nemegt Basin, south-central Mongolia. Journal of the Paleontological Society of Korea 25, 1–15.

Eberth, D.A., Kobayashi, Y., Lee, Y.-N., Mateus, O., Therrien, F., Zelenitsky, D.K., Norell, M.A., 2009b. Assignment of *Yamaceratops dorngobiensis* and associated redbeds at Shine Us Khudag (eastern Gobi, Dorngobi Province, Mongolia) to the redescribed Javkhlant Formation (Upper Cretaceous). Journal of Vertebrate Paleontology 29, 295–302.

Efimov, M.B., 1983. Revision of the fossil crocodiles of Mongolia. Trudy Sovmestnaya SovetskoeMongol'skaya Paleontologicheskaya Ekspeditsia 24, 76–95. [In Russian]

Efremov, I.A., 1949. Preliminary results of the work of the first Mongolian Paleontological Expedition of the Academy of Sciences USSR, 19461. Trudy Mongolskoy Komissii AN SSSR 38, 8–27. [In Russian]

Elzanowski, A., 1974. Preliminary note on the palaeognathous bird from the Upper

Cretaceous of Mongolia. Results of the Polish-Mongolian Palaeontological Expeditions, Part V. Polish Academy of Sciences, Warsaw, 103–109.

Elzanowski, A., 1977. Skulls of *Gobipteryx* (Aves) from the Upper Cretaceous of Mongolia. Palaeontologia Polonica 37, 153–165.

Elzanowski, A., 1981. Embryonic bird skeletons from the Late Cretaceous of Mongolia. Palaeontologia Polonica 42, 147–179.

Evans, D.C., Brown, C.M., Ryan, M.J., Tsogtbaatar, K., 2011. Cranial ornamentation and ontogenetic status of *Homalocephale calathocercos* (Ornithischia: Pachycephalosauria) from the Nemegt Formation, Mongolia. Journal of Vertebrate Paleontology 31, 84–92.

Evans, D.C., Hayashi, S., Chiba, K., Watabe, M., Ryan, M.J., Lee, Y.-N., Currie, P.J., Tsogtbaatar, K., Barsbold, R., 2018. Morphology and histology of new cranial specimens of Pachycephalosauridae (Dinosauria: Ornithischia) from the Nemegt Formation, Mongolia. Palaeogeography, Palaeoclimatology, Paleoecology 494, 121–134.

Fanti, F., Cantelli, L., Angelicola, L., 2018. High-resolution maps of Khulsan and Nemegt localities (Nemegt Basin, southern Mongolia): Stratigraphic implications. Palaeogeography, Palaeoclimatology, Palaeoecology 494, 14–28.

Fanti, F., Currie, P.J., Badamgarav, D., 2012. New specimens of *Nemegtomaia* from the Baruungoyot and Nemegt formations (Late Cretaceous) of Mongolia. PLoS ONE 7, e31330. DOI: 10.1371/journal.pone.0031330.

Fastovsky, D.E., Watabe, M., 2000. Sedimentary environment of Alag Teg (Djadochta Age), central Gobi, Mongolia. Hayashibara Museum of Natural Sciences Research Bulletin 1, 137.

Fastovsky, D.E., Weishampel, D.B., 2012. Dinosaurs: A Concise Natural History, 2nd edition. Cambridge University Press, Cambridge, 424 pp.

Feeley, K.J., Bravo-Avila, C., Fadrique, B., Perez, T.M., Zuleta, D., 2020. Climate-driven changes in the composition of New World plant communities. Nature Climate Change 10, 965–970.

Fowler, D.W., Woodward, H.N., Freedman, E.A., Larson, P.L., Horner, J.R., 2011. Reanalysis of "*Raptorex kriegsteini*": a juvenile tyrannosaurid dinosaur from Mongolia. PLoS ONE 6, e21376. DOI: 10.1371/journal.pone.0021376.

Funston, G.F., Mendonca, S.E., Currie, P.J., Barsbold, R., 2018. Oviraptorosaur anatomy, diversity and ecology in the Nemegt Basin. Palaeogeography, Palaeoclimatology, Palaeoecology 494, 101–120.

Gao, K., Norell, M.A., 1998. Taxonomic revision of *Carusia* (Reptilia: Squamate) from the Late Cretaceous of the Gobi Desert and phylogenetic relationships of anguimorphan lizards. American Museum Novitates 3230, 1–51.

Gilmore, C.W., 1933a. Two new dinosaurian reptiles from Mongolia with notes on some fragmentary specimens. American Museum Novitates 679, 1–20.

Gilmore, C.W., 1933b. On the dinosaurian fauna of the Iren Dabasu Formation.

Bulletin of the American Museum of Natural History 67, 23–78.

Gilmore, C.W., 1943. Fossil lizards of Mongolia. Bulletin of the American Museum of Natural History 81, 361–384.

Godefroit, P., Pereda-Suberbiola, X., Li, H., Dong, Z.-M., 1999. A new species of the ankylosaurid dinosaur *Pinacosaurus* from the Late Cretaceous of Inner Mongolia (P. R. China). Bulletin de l'Institut Royal des Sciences Naturelles de Belgique 69 (Suppl. B), 17–36.

Goloboff, P.A., Farris, J.S., Nixon, K.C., 2008. TNT, a free program for phylogenetic analysis. Cladistics 24, 774–786.

Gradziński, R., 1970. Sedimentation of dinosaur-bearing Upper Cretaceous deposits of the Nemegt Basin, Gobi desert. Palaeontologia Polonica 21, 147–229.

Gradziński, R., Jerzykiewicz, T., 1974a. Sedimentation of the Barun Goyot Formation. Palaeontologia Polonica 30, 111–146.

Gradziński, R., Jerzykiewicz, T., 1974b. Dinosaur- and mammal-bearing aeolian and associated deposits of the Upper Cretaceous in the Gobi Desert (Mongolia). Sedimentary Geology 12, 249–278.

Gradziński, R., Kielan-Jaworowska, Z., Maryańska, T., 1977. Upper Cretaceous Djadokhta, Barun Goyot and Nemegt formations of Mongolia, including remarks on previous subdivisions. Acta Geologica Polonica 27, 281–318.

Groves, C.P., 1972. *Ceratotherium simum*. Mammalian Species 8, 1–6.

Gubin, Y.M., 1993. Cretaceous anurans of Mongolia. Paleontological Zhurnal 27,

51–56.

Han, F., Zheng, W., Hu, D., Xu, X., Barrett, P.M., 2014. A new basal ankylosaurid (Dinosauria: Ornithischia) from the Lower Cretaceous Jiufotang Formation of Liaoning Province, China. PLoS ONE 9, e104551. DOI: 10.1371/journal.pone.0104551.

Hanai, T., Tsuihiji, T., 2018. Description of Tooth Ontogeny and Replacement Patterns in a Juvenile *Tarbosaurus bataar* (Dinosauria: Theropoda) Using CT-Scan Data. The Anatomical Record 302, 1210–1225.

Haynes, G., 2012. Elephants (and extinct relatives) as earth-movers and ecosystem engineers. Geomorphology 157–158, 99–107.

Heckert, A.B., Lucas, S.G., Rinehart, L.F., Celeskey, M.D., Spielmann, J.A., Hunt, A.P., 2010. Articulated skeletons of the aetosaur *Typothorax coccinarum* Cope (Archosauria: Stagonolepididae) from the Upper Triassic Bull Canyon Formation (Revueltian: Early–Mid Norian), Eastern New Mexico, USA. Journal of Vertebrate Paleontology 30, 619–642.

Hicks, J.F., Brinkman, D.L., Nichols, D.J., Watabe, M., 1999. Paleomagnetic and palynologic analyses of Albian to Santonian strata at Bayn Shireh, Burkhant, and Khuren Dukh, eastern Gobi Desert, Mongolia. Cretaceous Research 20, 829–850.

Hill, R.V., Witmer, L.M., Norell, M.A., 2003. A new specimen of *Pinacosaurus grangeri* (Dinosaur: Ornithischia) from the Late Cretaceous of Mongolia: ontogeny and phylogeny of ankylosaurs. American Museum Novitates

3395, 1–29.

Hildebrand, M., 1974. Analysis of vertebrate structure. John Wiley and Sons, New Jersey, 656 pp.

Hildebrand, M., 1985. Digging of quadrupeds. In: Hildebrand, M., Bramble, D.M., Liem, K.F., Wake, D.B. (Ed.), Functional vertebrate morphology. Harvard University Press, Massachusetts, 89–109.

Hillman-Smith, A.K., Groves, C.P., 1994. *Diceros bicornis*.Mammalian Species 455, 1–8.

Hoef, M., Bunch, T.D., 1992. Cranial asymmetry in a Dall sheep ram (*Ovis dalli dalli*). Journal of Wildlife Diseases 28, 330–332.

Hurum, J.H., 2001. Lower jaw of *Gallimimus bullatus*. In: Tanke, D.H., Carpenter, K. (Eds.), Mesozoic Vertebrate Life. Indiana University Press, Bloomington, 34–41.

Hurum, J.H., Sabath, K., 2003. Giant theropod dinosaurs from Asia and North America: Skulls of *Tarbosaurus bataar* and *Tyrannosaurus rex* compared. Acta Palaeontologica Polonica 48, 161–190.

Ishigaki, S., 2010. Theropod trampled bedding plane with laboring trackways from the Upper Cretaceous Abdrant Nuru fossil site, Mongolia. Hayashibara Museum of Natural Sciences Research Bulletin 3, 133–141.

Janis, C.M., Ehrhardt, D., 1988. Correlation of relative muzzle width and relative incisor width with dietary preference in ungulates. Zoological Journal of the Linnean Society 92, 267–284.

Jerzykiewicz, T., 2000. Lithostratigraphy and sedimentary settings of the Cretaceous dinosaur beds of Mongolia. In: Benton, M.J., Shishkin, M.A., Unwin, D.M., Kurochkin, E.N. (Ed.), The Age of Dinosaurs in Russia and Mongolia. Cambridge University Press, Cambridge, 279–296.

Jerzykiewicz, T., Russell, D.A., 1991. Late Mesozoic stratigraphy and vertebrates of the Gobi Basin. Cretaceous Research 12, 345–377.

Jerzykiewicz, T., Currie, P.J., Eberth, D.A., Johnston, P.A., Koster, E.H., Zheng, J.-J., 1993. Djadokhta Formation correlative strata in Chinese Inner Mongolia: an overview of the stratigraphy, sedimentary geology, and paleontology and comparisons with the type locality in the pre-Altai Gobi. Canadian Journal of Earth Sciences 30, 2180–2195.

Jerzykiewicz, T., Currie, P.J., Fanti, F., Lefeld, J., 2021. Lithobiotopes of the Nemegt Gobi Basin. Canadian Journal of Earth Sciences, 1–23. DOI: 10.1139/cjes-2020-0148.

Karczewska, J., Ziembiúska-Tworzydło, M., 1970. Upper Cretaceous Charophyta from the Nemegt Basin, Gobi Desert. Palaeontologia Polonica 21, 121–144.

Karczewska, J., Ziembińska-Tworzydło, M., 1983. Age of the Upper Cretaceous Nemegt Formation (Mongolia) on charophytan evidence. Acta Palaeontologica Polonica 28, 137–146.

Karhu, A.A., Rautian, A.S., 1996. A new family of Maniraptora (Dinosauria: Saurischia) from the Late Cretaceous of Mongolia. Paleontological Zhurnal 30, 583–592.

Khosatzky, L.I., 1999. Turtles - trionychids of the Cretaceous of Mongolia. Voprosy Paleontologii 11, 141–149. [In Russian]

Khosatzky, L.I., Młynarski, M., 1971. Chelonians from the Upper Cretaceous of the Gobi Desert, Mongolia. Palaeontologia Polonica 25, 131–144.

Kielan-Jaworowska, Z., 1969. Preliminary data on the Upper Cretaceous eutherian mammals from Bayn Dzak, Gobi Desert. Palaeontologia Polonica 30, 23–44.

Kielan-Jaworowska, Z., 1974a. Multituberculate succession in the Late Cretaceous of the Gobi Desert (Mongolia). Palaeontologia Polonica 30, 23–44.

Kielan-Jaworowska, Z., 1974b. Migrations of the Multituberculata and the Late Cretaceous connections between Asia and North America. Annals of The South African Museum 64, 231–244.

Kielan-Jaworowska, Z., 1975a. Preliminary description of two new eutherian genera from the Late Cretaceous of Mongolia. Palaeontologia Polonica 33, 5–16.

Kielan-Jaworowska, Z., 1975b. Evolution of the therian mammals in the Late Cretaceous of Asia. Part I. Deltatheridiidae. Palaeontologia Polonica 33, 103–132.

Kielan-Jaworowska, Z., 2013. In Pursuit of Early Mammals. Indiana University Press, Indiana, 253 pp.

Kielan-Jaworowska, Z., Trofimov, B.A., 1980, Cranial morphology of the Cretaceous eutherian mammal *Barunlestes*. Acta Palaeontologica Polonica

25, 167–185.

Kielan-Jaworowska, Z., Novacek, M.J., Trofimov, B.A., Dashzeveg, D., 2000. Mammals from the Mesozoic of Mongolia. In: Benton, M.J., Shishkin, M.A., Unwin, D.M., Kurochkin, E.N. (Ed.), The Age of Dinosaurs in Russia and Mongolia. Cambridge University Press, Cambridge, 573–626.

Kielan-Jaworowska, Z., Hurum, J.H., Badamgarav, D., 2003. An extended range of the multituberculate Kryptobaatar and distribution of mammals in the Upper Cretaceous of the Gobi Desert. Acta Geologica Polonica 48, 273–278.

Kim, B., Yun, H., Lee, Y.-N., 2019. The postcranial skeleton of *Bagaceratops* (Ornithischia: Neoceratopsia) from the Baruungoyot Formation (Upper Cretaceous) in Hermiin Tsav of southwestern Gobi, Mongolia. Journal of the Geological Society of Korea 55, 179–190. [In Korean with English abstract]

Kim, S.-H., Lee, Y.-N., Park, J.-Y., Lee, S., Winkler, D.A., Jacobs, L.L., Barsbold, R., 2022. A new species of Osteoglossomorpha (Actinopterygii: Teleostei) from the Upper Cretaceous Nemegt Formation of Mongolia: Paleobiological and paleobiogeographic implications. Cretaceous Research 135, 105214.

Kirkland, J.I., 1998. A polacanthine ankylosaur (Ornithischia: Dinosauria) from the Early Cretaceous (Barremian) of eastern Utah. New Mexico Museum of Natural History and Science Bulletin 14, 271–281.

Kjansep-Romaschkina, N.P., 1975. Some Late Jurassic and Cretaceous Charophyta from Mongolia. The Joint Soviet Mongolian Paleontological Expedition Transaction 2, 181–204.

Kobayashi, Y., Barsbold, R., 2006. Ornithomimids from the Nemegt Formation of Mongolia. Journal of the Paleontological Society of Korea 22, 195–207.

Kobayashi, Y., Takasaki, R., Kubota, K., Fiorillo, A.R., 2021. A new basal hadrosaurid (Dinosauria: Ornithischia) from the latest Cretaceous Kita-ama Formation in Japan implies the origin of hadrosaurids. Scientific Reports 11, 8547. DOI: 10.1038/s41598-021-87719-5.

Konzhukova, E.D., 1954. New fossil crocodilian from Mongolia. Trudy Paleontologicheskogo Instituta ANSSSR 48, 171–194.

Kundrát, M., Janáček, J., 2007. Cranial pneumatization and auditory perceptions of the oviraptorid dinosaur *Conchoraptor gracilis* (Theropoda, Maniraptora) from the Late Cretaceous of Mongolia. Naturwissenschaften 94, 769–778.

Kurochkin, E.N., 1988a. Cretaceous birds of Mongolia and their phylogenetic significance. Trudy Sovmestnaya Sovetsko-MongoIskaya Paleontologicheskaya Ekspeditsia 34, 33–42. [In Russian]

Kurochkin, E.N., 1988b. Finding of dinosaur eggs in the Lower Cretaceous of Mongolia. Sovemestnaya Sovetsko-Mongolskaya Paleontologicheskaya Ekspeditsia, Trudy 34, 72–77. [In Russian]

Kurochkin, E.N., 1999. A new large enantiornithid from the Upper Cretaceous of Mongolia (Aves, Enantiornithes). Trudy Zoologicheskogo Instituta RAN

277, 130–141. [In Russian]

Kurochkin, E.N., 2000. Mesozoic birds of Mongolia and the former USSR. In: Benton, M.J., Shishkin, M.A., Unwin, D.M., Kurochkin, E.N. (Ed.), The Age of Dinosaurs in Russia and Mongolia. Cambridge University Press, Cambridge, 533–559.

Kurochkin, E.N., Chatterjee, S., Mikhailov, K.E., 2013. An embryonic enantiornithine bird and associated eggs from the cretaceous of Mongolia. Paleontological Zhurnal 47, 1252–1269.

Kurumada, Y., Aoki, S., Aoki, K., Kato, D., Saneyoshi, M., Tsogtbaatar, K., Windley, B.F., Ishigaki, S., 2020. Calcite U–Pb age of the Cretaceous vertebrate-bearing Bayn Shire Formation in the Eastern Gobi Desert of Mongolia: usefulness of caliche for age determination. Terra Nova. DOI: 10.1111/ter.12456.

Kurzanov, S., Bannikov, A., 1983. A new sauropod from the Upper Cretaceous of Mongolia. Paleontological Zhurnal 17, 90–96.

Kurzanov, S.M., 1976. A new late Mesozoic carnosaur from Nogon-Tsav, Mongolia]. The Joint Soviet-Mongolian Paleontological Expedition Transactions 3, 93–104. [In Russian]

Kurzanov, S.M., 1981. On an unusual theropod from the Upper Cretaceous of Mongolia. Trudy Sovmestnaya Sovetsko-Mongol'skaya Paleontologicheskaya Ekspeditsii 15, 39–50. [In Russian]

Kurzanov, S.M., 1987. Avimidae and the problem of the origin of birds. Trudy

Sovmestnaya Sovetsko-MongoIskaya Paleontologicheskaya Ekspeditsia 31, 92 pp. [In Russian]

Kurzanov, S.M., 1990. A new Late Cretaceous protoceratopsid genus from Mongolia. Journal of Paleontology 24, 85–91.

Kurzanov, S.M., Osmólska, H., 1991. *Tochisaurus nemegtensis* gen. et sp. n., a now troodontid (Dinosauria, Theropoda) from Mongolia. Palaeontologia Polonica 36, 69–76.

Kurzanov, S.M., Tumanova, T.A., 1978. The structure of the endocranium in some Mongolian ankylosaurs. Paleontological Zhurnal 1978, 90–96.

Lee, H.-J., Lee, Y.-N., Adams, T.L., Currie, P.J., Kobayashi, Y., Jacobs, L.L., Koppelhus, E.B., 2018. Theropod trackways associated with a *Gallimimus* foot skeleton from the Nemegt Formation, Mongolia. Palaeogeography, Palaeoclimatology, Palaeoecology 494, 160–167.

Lee, S., Park, J.-Y., Lee, Y.-N., Kim, S.-H., Lü, J., Barsbold, R., Tsogtbaatar, K., 2019a. A new alvarezsaurid dinosaur from the Nemegt Formation of Mongolia. Scientific Reports 9, 15493. DOI: 10.1038/s41598-019-52021-y.

Lee, S., Lee, Y.-N., Chinsamy, A., Lü, J., Barsbold, R., Tsogtbaatar, K., 2019b. A new baby oviraptorid dinosaur (Dinosauria: Theropoda) from the Upper Cretaceous Nemegt Formation of Mongolia. PLoS ONE 14, e0210867. DOI: 10.1371/journal.pone.0210867.

Lee, Y.-N., Barsbold, R., Currie, P.J., Kobayashi, Y., Lee, H.-J., Godefroit, P., Escuillie, F., Chinzorig, T., 2014. Resolving the long-standing enigmas of

the giant ornithomimosaur *Deinocheirus mirificus*. Nature 515, 257–260.

Lee, Y.-N., Lee, H.-J., Kobayashi, Y., Paulina-Carabajal, A., Barsbold, R., Fiorillo, A.R., Tsogtbaatar, K., 2019. Unusual locomotion behaviour preserved within a crocodyliform trackway from the Upper Cretaceous Bayanshiree Formation of Mongolia and its palaeobiological implications. Palaeogeography, Palaeoclimatology, Palaeoecology 533, 109239. DOI: 10.1016/j.palaeo.2019.109239.

Lillegraven, J.A., McKenna, M.C., 1986. Fossil mammals form the "Mesaverde" Formation (Late Cretaceous, Judithian) of the Bighorn and Wind River Basins, Wyoming, with definitions of Late Cretaceous North American land-mammal "Ages". American Museum Novitates 2840, 1–68.

Loewen, M.A., Irmis, R.B., Sertich, J.J.W., Currie, P.J., Sampson, S.D., 2013. Tyrannt Dinosaur Evolution Tracks the Rise and Fall of Late Cretaceous Oceans. PLoS ONE 8, e79420. DOI: 10.1371/journal.pone.0079420.

Longrich, N.R., Currie, P.J., Dong, Z.-M., 2010. A new oviraptorid (Dinosauria: Theropoda) from the Upper Cretaceous of Bayan Mandahu, Inner Mongolia. Palaeontology 53, 945–960.

Loope, D.B., Dingus, L., Swisher, C.C. III., Minjin, C., 1998. Life and death in a Late Cretaceous dune field, Nemegt basin, Mongolia. Geology **26**, 27–30.

Lü, J., Ji, Q., Gao, Y., Li, Z., 2007a. A new species of the ankylosaurid dinosaur *Crichtonsaurus* (Ankylosauridae : Ankylosauria) from the Cretaceous of Liaoning Province, China. Acta Geologica Sinica 81, 883–897.

Lü, J., Jin, X., Sheng, Y., Li, Y., Wang, G., Azuma, Y., 2007b. New nodosaurid dinosaur from the Late Cretaceous of Lishui, Zhejiang Province, China. Acta Geologica Sinica 81, 344–350.

Lü, J.-C., Tomida, Y., Azuma, Y., Dong Z.-M., Lee, Y.-N., 2004. New oviraptorid dinosaur (Dinosauria: Oviraptorosauria) from the Nemegt Formation of Southwestern Mongolia. Bulletin of the National Science Museum of Tokyo, Series C 30, 95–130.

Lü, J.-C., Tomida, Y., Azuma, Y., Dong Z.-M., Lee, Y.-N., 2005. *Nemegtomaia* gen. nov., a replacement name for the oviraptorosaurian dinosaur *Nemegtia* Lü et al., 2004, a preoccupied name. Bulletin of the National Science Museum of Tokyo, Series C 31, 51 pp.

Lyson, T.R., Rubidge, B.S., Scheyer, T.M., de Queiroz, K., Schachner, E.R., Smith, R.M.H., Botha-Brink, J., Bever, G.S., 2016. Fossorial origin of the turtle shell. Current Biology 26, 1887–1894.

Makovicky, P.J., Kobayashi, Y., Currie, P.J., 2004. Ornithomimosauria. In: Weishampel, D.B., Dodson, P., Osmólska, H. (Ed.), The Dinosauria, second edition. University of California Press, Berkeley, 137–150.

Maidment, S.C.R., Strachan, S.J., Ouarhache, D., Scheyer, T.M., Brown, E.E., Fernandex, V., Johanson, Z., Raven, T.J., Barrett, P.M., 2021. Bizarre dermal armour suggests the first African ankylosaur. Nature Ecology and Evolution 5, 1576–1581.

Maleev, E.A., 1952a. A new family of armored dinosaurs from the Upper

Cretaceous of Mongolia. Doklady Akademii Nauk SSR 87, 131–134. [In Russian]

Maleev, E.A., 1952b. A new ankylosaur of the Upper Cretaceous of Mongolia. Doklady Akademii Nauk SSSR 87, 273–276. [In Russian]

Maleev, E.A., 1954a. New tortoise-like saurian from Mongolia. Priroda 3, 106–108. [In Russian]

Maleev, E.A., 1954b. The armored dinosaurs of the Cretaceous Period in Mongolia (Family Syrmosauridae). Trudy Paleontologicheskogo Instituta Akademiy Nauk SSSR 48, 142–170. [In Russian]

Maleev, E.A., 1955. Giant carnivorous dinosaurs of Mongolia. Doklady Akademii Nauk SSSR 104, 634–637. [In Russian]

Maleev, E.A., 1956. Armored dinosaurs of the Upper Cretaceous of Mongolia, Family Ankylosauridae. Trudy Palaeontologicheskoi Instytuta, Akademiia Nauk SSSR 62, 51–91. [In Russian]

Maleev, E.A., 1965. The carnosaur dinosaur brain. Paleontological Zhurnal 2, 141–143. [In Russian]

Maleev, E.A., 1974. Gigantic carnosaurs of the family Tyrannosauridae. Trudy Sovmestnaya Sovetsko-Mongol'skaya Paleontologicheskaya Ekspeditsia 1, 132–191. [In Russian]

Marais, J., Hadaway, D., 2008. Great tuskers of Africa. Penguin Books, Johannesburg, 240 pp.

Marsh, O.C., 1890. Additional characters of the Ceratopsidae, with notice of new

Cretaceous dinosaurs. American Journal of Science 39, 418–426.

Martinson, G.G., 1975. To the question about principles of stratigraphy and correlation of Mesozoic continental deposits. The Joint Soviet Mongolian Paleontological Expedition Transaction 13, 7–24.

Martinson, G.G., 1982. Late Cretaceous mollusks of Mongolia. Trudy Sovmestnaya Sovetsko-Mongol'skaya Paleontologicheskaya Ekspeditsia 17, 5–76. [In Russian]

Martinson, G.G., Kolesnikov, C.M., 1974. Cretaceous limnetic Mollusca from fossiliferous rock tables in Mongolia. The Joint Soviet Mongolian Paleontological Expedition Transaction 1, 235–256.

Maryañska, T., 1969. Remains of armoured dinosaurs from the Uppermost Cretaceous in Nemegt Basin, Gobi Desert. Palaeontologia Polonica 21, 23–34.

Maryañska, T., 1971. New data on the skull of *Pinacosaurus grangeri* (Ankylosauria). Palaeontologia Polonica 25, 45–53.

Maryañska, T., 1977. Ankylosauridae (Dinosauria) from Mongolia. Palaeontologia Polonica 37, 85–151.

Maryañska, T., 2000. Sauropods from Mongolia and the former Soviet Union. In: Benton, M.J., Shishkin, M.A., Unwin, D.M., Kurochkin, E.N. (Ed.), The Age of Dinosaurs in Russia and Mongolia. Cambridge University Press, Cambridge, 456–461.

Maryañska, T., Osmólska, H., 1975. Protoceratopsidae (Dinosauria) of Asia.

Palaeontologia Polonica 33, 133–181.

Maryañska, T., Osmólska, H., 1979. Aspects of hadrosaurian cranial anatomy. Lethaia 12, 265–273.

Maryañska, T., Osmólska, H., 1981a. Cranial anatomy of *Saurolophus augustirostris* with comments on the Asian Hadrosauridae (Dinosauria). Palaeontologia Polonica 42, 5–24.

Maryañska, T., Osmólska, H., 1981b. First lambeosaurine dinosaur from the Nemegt Formation, Upper Cretaceous, Mongolia. Acta Palaeontologica Polonica 26, 5–24.

Matsumoto, Y., Hashimoto, R., Sonoda, T., Fujiyama, Y., Mifune, B., Kawahara, Y., Saneyoshi, M., 2010. Report of the preparation works for Mongolian specimens in Hayashibara Museum of Natural Sciences: 1999–2008. Hayashibara Museum of Natural Sciences Research Bulletin 3, 167–185.

Mikhailov, K.E., 2000. Eggs and eggshells of dinosaurs and birds from the Cretaceous of Mongolia. In: Benton, M.J., Shishkin, M.A., Unwin, D.M., Kurochkin, E.N. (Ed.), The Age of Dinosaurs in Russia and Mongolia. Cambridge University Press, Cambridge, 560–572.

Miles, C.A., Miles, C.J., 2009. Skull of *Minotaurasaurus ramachandrani*, a new Cretaceous ankylosaur from the Gobi Desert. Current Science 96, 65–70.

Młynarski, M., 1972. *Zangerlia testudinimorpha* n. gen., n. sp., a primitive land tortoise from the Upper Cretaceous of Mongolia. Palaeontologia Polonica 27, 85–92.

Młynarski, M., Narmandach, P., 1972. New turtle remains from the Upper Cretaceous of the Gobi Desert, Mongolia. Palaeontologia Polonica 27, 95–101.

Montanari, S., Higgins, P., Norell, M.A., 2013. Dinosaur eggshell and tooth enamel geochemistry as an indicator of Mongolian Late Cretaceous paleoenvironments. Palaeogeography, Palaeoclimatology, Palaeoecology 370, 158–166.

Nakajima, J., Kobayashi, Y., Chinzorig, T., Tanaka, T., Takasaki, R., Tsogtbaatar, K., Currie, P.J., Fiorillo, A.R., 2018. Dinosaur tracks at the Nemegt locality: paleobiological and paleoenvironmental implications. Palaeogeography, Palaeoclimatology, Palaeoecology 494, 147–159.

Newbrey, M.G., Brinkman, D.B., Winkler, D.A., Freeman, E.A., Neuman, A.G., Fowler, D.W., Woodward, H.N., 2013. Teleost centrum and jaw elements from the Upper Cretaceous Nemegt Formation (Campanian–Maastrichtian) of Mongolia and a re-identification of the fish centrum found with the theropod *Raptorex kreigsteini*. In: Arratia, G., Schultze, H.-P., Wilson, M.V.H. (Ed.), Mesozoic Fishes 5 – Global Diversity and Evolution. Verlag Dr. Friedrich Pfeil, München, 291–303.

Nessov, L.A., Borkin, L.Y., 1983. New records of bird bones from the Cretaceous of Mongolia and central Asia. Trudy Zoologicheskogo Instituta Akademii Nauk SSSR 116, 108–112. [In Russian]

Nopcsa, F., 1915. The dinosaurs of the Transylvanian parts of Hungary.

Mitteilungen Jahrbuch Ungarische Geologische Reichsanstalt 23, 1–26. [In German]

Nopcsa, F., 1918. *Leipsanosaurus* n. gen. a new thyreophoran from the Gosau. Földtani Közlöny 48, 324–328. [In German]

Norell, M.A., Makovicky, P.J., Currie, P.J., 2001. The beaks of ostrich dinosaurs. Nature 412, 873–874.

Norell, M.A., Makovicky, P.J., Bever, G.S., Balanoff, A.M., Clark, J.M., Barsbold, R., Rowe, T., 2009. A Review of the Mongolian Cretaceous Dinosaur *Saurornithoides* (Troodontidae: Theropoda). American Museum Novitates 3654, 1–63.

Norman, D.B., 1984. A systematic reappraisal of the reptile order Ornithischia. In: Reif, W.-E., Westphal, F. (Ed.), Third symposium on Mesozoic terrestrial ecosystems, short papers. Attempto Verlag, Tübingen, Germany, 157–162.

Norman, D.B., Sues, H.-D., 2000. Ornithopods from Kazakhstan, Mongolia and Siberia. In: Benton, M.J., Shishkin, M.A., Unwin, D.M., Kurochkin, E.N. (Ed.), The Age of Dinosaurs in Russia and Mongolia. Cambridge University Press, Cambridge, 462–479.

Novas, F.E., 1996. Alvarezsauridae, Cretaceous basal birds from Patagonia and Mongolia. Memoirs of the Queensland Museum 39, 675–702.

Novojilov, N.I., 1954. Leaf-footed crustaceans of the Upper Jurassic and Cretaceous of Mongolia. Trudy Paleontologic'eskogo Instituta Akademii Nauk SSSR 48, 7–119.

Nowak, R.M., 1991. Walker's Mammals of the World, fifth edition-Volume II. Johns Hopkins University Press, Maryland, 1614 pp.

Nowinski, A., 1971. *Nemegtosaurus mongoliensis* n. gen., n. sp. (Sauropoda) from the uppermost Cretaceous of Mongolia. Palaeontologia Polonica 25, 57–81.

Olshevsky, G., 1995a. The origin and evolution of the tyrannosaurids, Part 1. Kyoryugaku Saizensen 9, 92–119.

Olshevsky, G., 1995b. The origin and evolution of the tyrannosaurids, Part 2. Kyoryugaku Saizensen 10, 75–99.

Osborn, H.F., 1923. Two Lower Cretaceous dinosaurs of Mongolia. American Museum Novitates 95, 1–10.

Osmólska, H., 1981. Coossified tarsometatarsi in theropod dinosaurs and their bearing on the problem of bird origins. Palaeontologica Polonica 42, 79–95.

Osmólska, H., 1987. *Borogovia gracilicrus* gen. et sp. n., a new troodontid dinosaur from the Late Cretaceous of Mongolia. Acta Palaeontologica Polonica 32, 133–150.

Osmólska, H., 1996. An unusual theropod dinosaur from the Late Cretaceous Nemegt Formation of Mongolia. Acta Palaeontologica Polonica 41, 1–38.

Osmólska, H., Roniewicz, E., 1970. Deinocheiridae, a new family of theropod dinosaurs. Palaeontologica Polonica 21, 5–19.

Osmólska, H., Roniewicz, E., Barsbold, R., 1972. A new dinosaur, *Gallimimus bullatus* n. gen., n. sp. (Ornithomimidae) from the Upper Cretaceous of Mongolia. Palaeontologia Polonica 27, 103–143.

Owen, R., 1842. Report on British fossil reptiles. Reports of the British Association for the Advancement of Science 11, 60–204.

Owocki, K., Kremer, B., Cotte, M., Bocherens, H., 2020. Diet preferences and climate inferred from oxygen and carbon isotopes of tooth enamel of *Tarbosaurus bataar* (Nemegt Formation, Upper Cretaceous, Mongolia). Palaeogeography, Palaeoclimatology, Palaeoecology 537, 109190. DOI: 10.1016/j.palaeo.2019.05.012.

Ősi, A., Prondvai, E., Mallon, J., Bodor, E.R., 2017. Diversity and convergences in the evolution of feeding adaptations in ankylosaurs (Dinosauria: Ornithischia). Historical Biology 29, 539–570.

Padian, K., 1992. A proposal to standardize tetrapod phalangeal formula designations. Journal of Vertebrate Paleontology 12, 260–262.

Padian, K., May, C., 1993. The earliest dinosaurs. New Mexico Museum of Natural History and Science, Bulletin 3, 379–381.

Pang, Q., Cheng, Z., 1998. A new ankylosaur of Late Cretaceous from Tianzhen, Shanxi. Progress in Natural Science 8, 326–334.

Paulina-Carabajal, A., Lee, Y.-N., Kobayashi, Y., Lee, H.-J., Currie, P.J., 2018. Neuroanatomy of the ankylosaurid dinosaurs *Tarchia teresae* and *Talarurus plicatospineus* from the Upper Cretaceous of Mongolia, with comments on endocranial variability among ankylosaurs. Palaeogeography, Palaeoclimatology, Palaeoecology 494, 135–146.

Pawlicki, P., Bolechała, P., 1987. X-ray microanalysis of fossil dinosaur bone: age

differences in the calcium and phosphorus content of *Gallimimus bullatus* bones. Folia Histochemica et Cytobiologica 25, 241–244.

Penkalski, P., 2014. A new ankylosaurid from the Late Cretaceous Two Medicine Formation of Montana, USA. Acta Palaeontologica Polonica 59, 617–634.

Penkalski, P., 2018. Revised systematics of the armoured dinosaur *Euoplocephalus* and its allies. Neues Jahrbuch für Geologie und Paläontologie – Abhandlungen 287, 261–306.

Penkalski, P., Blows, W.T., 2013. *Scolosaurus cutleri* (Ornithischia: Ankylosauria) from the Upper Cretaceous Dinosaur Park Formation of Alberta, Canada. Canadian Journal of Earth Sciences 50, 171–182.

Penkalski, P., Tumanova, T., 2017. The cranial morphology and taxonomic status of *Tarchia* (Dinosauria: Ankylosauridae) from the Upper Cretaceous of Mongolia. Cretaceous Research 70, 117–127.

Perle, A., 1977. On the first discovery of *Alectrosaurus* (Tyrannosauridae, Theropoda) in the Late Cretaceous of Mongolia. Shinzhlekh Ukhaany Akademi Geologiin Khureelen 3, 104–113. [In Russian]

Perle, A., 1982. On a new finding of the hind limb of *Therizinosaurus* sp. from the Late Cretaceous of Mongolia. Problemy Mongol'skoi Geologii 5, 94–98. [In Russian]

Perle, A., Maryańska, T., Osmólska, H., 1982. *Goyocephale lattimorei* gen. et sp. n., a new flat-headed pachycephalosaur (Ornithischia, Dinosauria) from the Upper Cretaceous of Mongolia. Acta Palaeontologica Polonica 27, 115–

127.

Perle, A., Norell, M.A., Chiappe, L.M., Clark, J.M., 1993. Flightless bird from the Cretaceous of Mongolia. Nature 362, 623–626.

Perle, A., Chiappe, L.M., Rinchen, B., Clark, J.M., Norell, M.A., 1994. Skeletal morphology of *Mononykus olecranus* (Theropoda: Avialae) from the Late Cretaceous of Mongolia. American Museum Novitates 3105, 1–29.

Prieto-Márquez, A., 2010. Global historical biogeography of hadrosaurid dinosaurs. Zoological Journal of the Linnean Society 159, 435–525.

Phil, S., James, R.H., 2010. Hip heights of the gigantic theropod dinosaurs *Deinocheirus mirificus* and *Therizinosaurus cheloniformis*, and implications for museum mounting and paleoecology. Bulletin of Gunma Museum of Natural History 14, 1–10.

Rougier, G.W., Davis, B.M., Novacek, M.J., 2015. A deltatheroidan mammal from the Upper Cretaceous Baynshiree Formation, eastern Mongolia. Cretaceous Research 52, 167–177.

Rozhdestvenskii, A.K., 1970. Giant claws of enigmatic Mesozoic reptiles. Paleontological Zhurnal 4, 117–125. [In Russian]

Rozhdestvensky, A.K., 1952. A new representative of the duck-billed dinosaurs from the Upper Cretaceous of Mongolia. Doklady Akademii Nauk SSSR 86, 405–408. [In Russian]

Rozhdestvensky, A.K., 1971. Study of dinosaurs of Mongolia and their role in continental Mesozoic subdivision. Trudy Sovmestnaya Sovetsko-

Mongol'skaya Paleontologicheskaya Ekspeditsii 3, 21–32. [In Russian]

Rozhdestvensky, A.K., 1974. A history of dinosaur fauna from Asia and other continents and some problems on the paleogeography. Trudy Sovmestnaya Sovetsko-Mongol'skaya Paleontologicheskaya Ekspeditsia 1, 68–75. [In Russian]

Russell, D. A., Dong, Z., 1993. The affinities of a new theropod from the Alxa Desert, Inner Mongolia, People's Republic of China. Canadian Journal of Earth Sciences 30, 2107–2127.

Sabath, K., 1991. Upper Cretaceous amniotic eggs from the Gobi Desert. Acta Palaeontologica Polonica 36, 151–192.

Saveliev, S.V., Alifanov, V.R., 2007. A new study of the brain of the predatory dinosaur *Tarbosaurus bataar* (Theropoda, Tyrannosauridae). Paleontological Zhurnal 41, 281–289.

Seeley, H.G., 1887. On the classification of the fossil animals commonly named Dinosauria. Proceedings of the Royal Society of London 43, 165–171.

Senter, P., 2005. Function in the stunted forelimbs of *Mononykus olecranus* (Theropoda), a dinosaurian anteater. Paleobiology 31, 373–381.

Sereno, P.C., 1986. Phylogeny of the bird-hipped dinosaurs (Order Ornithischia). National Geographic Research 2, 234–256.

Sereno, P.C., 1998. A rationale for phylogenetic definitions, with application to the higher-level taxonomy of Dinosauria. Neues Jahrbuch für Geologie und Paläontologie Abhandlungen 210, 41–83.

Sereno, P.C., Tan, L., Brusatte, S.L., Kriegstein, H.J., Zhao, X., Cloward, K., 2009. Tyrannosaurid skeletal design first evolved at small body size. Science 326, 418–422.

Sherbrooke, W.C., 2003. Introduction to Horned Lizards of North America. University of California Press, Berkeley, 191 pp.

Sherbrooke, W.C., Montanucci, R.R., 1988. Stone mimicry in the round-tailed horned lizard, *Phrynosoma modestum* (Sauria: Iguanidae). Journal of Arid Environments 14, 275–284.

Shuvalov, V.F., Chkhikvadze, V.M., 1975. New data on Late Cretaceous turtles from southern Mongolia. In: Kramarenko, N.N. (Ed.), Iskopayemaya fauna i flora Mongolia, Sovmestnaya Sovetsko-Mongolskaya Paleontologicheskaya Ekspeditsia, Trudy 2, 214–229. [In Russian]

Shuvalov, V.F., Chkhikvadze, V.M., 1979. On stratigraphic and systematic position of some freshwater turtles from new Cretaceous localities in Mongolia. Trudy Sovmestnoy Sovetsko-Mongol'skoy Paleontologicheskoy Ekspeditsii 8, 58–76. [In Russian]

Sochava, A.V., 1969. Dinosaur eggs from the Upper Cretaceous of the Gobi Desert. Paleontological Zhurnal 4, 353–361. [In Russian]

Sochava, A.V., 1975. Stratigraphy and lithology of the Upper Cretaceous sediments in southern Mongolia. Trudy Sovmestnaya Sovetsko-Mongol'skaya Paleontologicheskaya Ekspeditsia 13, 113–182. [In Russian]

Solounias, N., Moelleken, S.M.C., 1993. Dietary adaptation of some extinct

ruminants determined by premaxillary shape. Journal of Mammalogy 74, 1059–1071.

Solounias, N., Teaford, M., Walker, A., 1988. Interpreting the diet of extinct ruminants: the case of a non-browsing giraffid. Paleobiology 14, 287–300.

Stankevitch, Z.E., Khand, E., 1976. Ostracoda of Upper Cretaceous, barungoyotian suite from Trans-Altaian Gobi (Mongolia). The Joint Soviet Mongolian Paleontological Expedition Transaction 3, 159–161.

Steele, N.A., 1960. Meeting of rhinos of two species. Lammergeyer 1, 40–41.

Stettner, B., Person, W.S., Currie, P.J., 2018. A giant sauropod footprint from the Nemegt Formation (Upper Cretaceous) of Mongolia. Palaeogeography, Palaeoclimatology, Palaeoecology 494, 147–159.

Storrs, G.W., Efimov, M.B., 2000. Mesozoic crocodyliforms of north–central Eurasia. In: Benton, M.J., Shishkin, M.A., Unwin, D.M., Kurochkin, E.N. (Ed.), The Age of Dinosaurs in Russia and Mongolia. Cambridge University Press, Cambridge, 402–419.

Sues, H.-D., 2019. The Rise of Reptiles: 320 Million Years of Evolution. Johns Hopkins University Press, Baltimore, 400 pp.

Sukhanov, V.B., 2000. Mesozoic turtles of Middle and Central Asia. In: Benton, M.J., Shishkin, M.A., Unwin, D.M., Kurochkin, E.N. (Ed.), The Age of Dinosaurs in Russia and Mongolia. Cambridge University Press, Cambridge, 309–367.

Sukhanov, V.B., Narmandakh, P., 1975. Cherepakhi gruppy *Basilemys* (Chelonia,

Dermatemydidae) v Azii [New turtles of the group of *Basilemys* (Chelonia, Dermatemydidae)]. Trudy Sovmestnaya Sovetsko-MongoIskaya Paleontologicheskaya Ekspeditsia 2, 94–101 [In Russian].

Sullivan, R.M., 1999. *Nodocephalosaurus kirtlandensis*, gen. et sp. nov., a new ankylosaurid dinosaur (Ornithischia: Ankylosauria) from the Upper Cretaceous Kirtland Formation (upper Campanian), San Juan Basin, New Mexico. Journal of Vertebrate Paleontology 19, 126–139.

Sullivan, R.M., 2006. A taxonomic review of the Pachycephalosauridae (Dinosauria: Ornithischia). New Mexico Museum of Natural History and Science, Bulletin 35, 347–366.

Susana Bargo, M., Toledo, N., Vizcaino, S.F., 2006. Muzzle of South American Pleistocene Ground Sloths (Xenarthra, Tardigrada). Journal of Morphology 267, 248–263.

Suzuki, S., Narmandakh, P., 2004. Change of the Cretaceous turtle faunas in Mongolia. Hayashibara Museum of Natural Sciences Research Bulletin 2, 7–14.

Suzuki, S., Watabe, M., 2000. Report on the Japan-Mongolia Joint Paleontological Expedition to the Gobi desert, 1998. Hayashibara Museum of Natural Sciences Research Bulletin 1, 83–98.

Szczechura, J., Błaszyk, J., 1970. Fresh-water Ostracoda from the Upper Cretaceous of Nemegt Basin. Palaeontologia Polonica 21, 107–118.

Thompson, R.S., Parish, J.C., Maidment, S.C.R., Barrett, P.M., 2012. Phylogeny of

the ankylosaurian dinosaurs (Ornithischia: Thyreophora). Journal of Systematic Palaeontology 10, 301–312.

Tschopp, E., Mateus, O., 2013. Clavicles, interclavicles, gastralia, and sterna ribs in sauropod dinosaurs: new reports from Diplodocidae and their morphological, functional and evolutionary implications. Journal of Anatomy 222, 321–340.

Tsogtbaatar, K., Weishampel, D.B., Evans, D.C., Watabe, M., 2015. A new hadrosauroid (*Plesiohadros djadokhtaensis*) from the Late Cretaceous Djadokhtan Fauna of southern Mongolia. In: Eberth, D.A., Evans, D.C. (Ed.), Hadrosaurs. Indiana University Press, Bloomington, 108–135.

Tsogtbaatar, K., Weishampel, D.B., Evans, D.C., Watabe, M., 2019. A new hadrosauroid (Dinosauria: Ornithopoda) from the Late Cretaceous Baynshire Formation of the Gobi Desert (Mongolia). PLoS ONE 14, e0208480. DOI: 10.1371/journal.pone.0208480.

Tsuihiji, T., Watabe, M., Tsogtbaatar, K., Tsubamoto, T., Barsbold, R., Suzuki, S., Lee, A.H., Ryan, C.R., Kawahara, Y., Witmer, L.M., 2011. Cranial osteology of a juvenile specimen of *Tarbosaurus bataar* (Theropoda, Tyrannosauridae) from the Nemegt Formation (Upper Cretaceous) of Bugin Tsav, Mongolia. Journal of Vertebrate Paleontology 31, 497–517.

Tsuihiji, T., Watabe, M., Tsogtbaatar, K., Barsbold, R., 2016. Dentaries of a caenagnathid (Dinosauria: Theropoda) from the Nemegt Formation of the Gobi Desert in Mongolia. Cretaceous Research 63, 148–153.

Tsuihiji, T., Andres, B., O'Connor, P.M., Watabe, M., Tsogtbaatar, K., Mainbayar, B., 2017. Gigantic pterosaurian remains from the Upper Cretaceous of Mongolia Journal of Vertebrate Paleontology 37, e1361431. DOI: 10.1080/02724634.2017.1361431.

Tumanova, T.A., 1977. New data on the ankylosaur *Tarchia gigantea*. Paleontological Zhurnal 4, 92–100. [In Russian]

Tumanova, T.A., 1983. The first ankylosaurs from the Lower Cretaceous of Mongolia. In: Tatarinov, L.P., Barsbold, R., Vorobyeva, E., Luvsandanzan, B., Trofimov, B.A., Reshetov, Y.A., Shishkin, M.A. (Eds.), Iskopayemyye reptilii mongolii. Trudy Sovmestnaya Sovetsko-Mongol'skaya Paleontologicheskaya Ekspeditsiya 4, 110–118. [In Russian]

Tumanova, T.A., 1987. The armored dinosaurs of Mongolia. The Joint Soviet Mongolian Paleontological Expedition Transaction 32, 1–76. [In Russian]

Tumanova, T.A., 1993. A new armored dinosaur from Southeastern Gobi. Paleontologicheskii Zhurnal 27, 92–98. [In Russian]

Tumanova, T.A., 2000. Armoured dinosaurs from the Cretaceous of Mongolia. In: Benton, M.J., Shishkin, M.A., Unwin, D.M., Kurochkin, E.N. (Ed.), The Age of Dinosaurs in Russia and Mongolia. Cambridge University Press, Cambridge, 517–532.

Turner, A.H., 2015. A Review of *Shamosuchus* and *Paralligator* (Crocodyliformes, Neosuchia) from the Cretaceous of Asia. PLoS ONE 10, e0118116. DOI: 10.1371/journal.pone.0118116.

Tverdochlebov, V.P., Zybin, J.I., 1974. Genesis of the Upper Cretaceous sediments with dinosaur remains at Tugrikin-us and Alag-Taag localities. Sovmestnaâ Sovetsko-Mongolskaâ Paleontologičeskaâ Ekspediciâ, Trudy 1, 314–319. [In Russian]

Upchurch, P., Barrett, P.M., 2000. The taxonomic status of *Shanxia tianzhenensis* (Ornithischia, Ankylosauridae); a response to Sullivan (1999). Journal of Vertebrate Paleontology 20, 216–217.

Vasiliev, V.G., Volkhonin, V.C., Grishin, G.L., Ivanov, A.K., Marinov, I.A., Mokshancev, K. B., 1959. Geological structure of the People's Republic of Mongolia (Stratigraphy and Tectonics). Gostoptekhizdat, Leningrad, 494 pp. [In Russian]

Venkadesan, M., Yawar, A., Eng, C.M., Dias, M.A., Singh, D.K., Tommasini, S.M., Haims, A.H., Bandi, M.M., Mandre, S., 2020. Stiffness of the human foot and evolution of the transverse arch. Nature 579, 97–100.

Vickaryous, M.K., Russell, A.P., 2003. A redescription of the skull of *Euoplocephalus tutus* (Archosauria: Ornithischia): a foundation for comparative and systematic studies of ankylosaurian dinosaurs. Zoological Journal of the Linnean Society 137, 157–186.

Vickaryous, M.K., Maryañska, T., Weishampel, D.B., 2004. Ankylosauria. In: Weishampel, D.B., Dodson, P., Osmólska, H. (Ed.), The Dinosauria, second edition. University of California Press, Berkeley and Los Angeles, California, 363–392.

Vickaryous, M.K., Russell, A.P., Currie, P.J., Zhao, X.-J., 2001. A new ankylosaurid (Dinosauria: Ankylosauria) from the Lower Cretaceous of China, with comments on ankylosaurian relationships. Canadian Journal of Earth Sciences 38, 1767–1780.

Vitt, L.J., Caldwell, J.P., 2013. Herpetology: An Introductory Biology of Amphibians and Reptiles, 4th edition. Academic Press, Cambridge.

Vizcaíno, S.F., Fariña, R.A., Mazzetta, G., 1999. Ulnar dimensions and fossoriality in armadillos and other South American mammals. Acta Theriologica 44, 309–320.

Watabe, M., Suzuki, S. 2000. Report on the Japan-Mongolia Joint Paleontological expedition to the Gobi desert, 1996. Hayashibara Museum of Natural Sciences Research Bulletin 1, 58–68.

Watabe, M., Tsuihiji, T., Suzuki, S., Tsogtbaatar, K., 2009. The first discovery of pterosaurs from the Upper Cretaceous of Mongolia. Acta Palaeontologica Polonica 54, 231–242.

Watabe, M., Tsogtbaatar, K., Sullivan, R.M., 2011. A new pachycephalosaurid from the Baynshire Formation (Cenomanian-late Santonian), Gobi Desert, Mongolia. New Mexico Museum of Natural History and Science, Bulletin 53, 489–497.

Weishampel, D.B., Fastovsky, D.E., Watabe, M., Varrichio, D., Jackson, F., Tsogtobaatar, K., Barsbold, R., 2008. New oviraptorid embryos from Bugin-Tsav, Nemegt Formation (Upper Cretaceous), Mongolia, with

insights into their habitat and growth. Journal of Vertebrate Paleontology 28, 1110–1119.

Wiersma, J.P., Irmis, R.B., 2018. A new southern Laramidian ankylosaurid, *Akainacephalus johnsoni* gen. et sp. nov., from the upper Campanian Kaiparowits Formation of southern Utah, USA. PeerJ 6, e5016. DOI: 10.7717/peerj.5016.

Williams, V.S., Barrett, P.M., Purnell, M.A., 2009. Quantitative analysis of dental microwear in hadrosaurid dinosaurs, and the implications for hypotheses of jaw mechanics and feeding. PNAS 106, 11194–11199.

Wilson, J.A., 2005. Redescription of the Mongolian sauropod *Nemegtosaurus mongoliensis* Nowinski (Dinosauria: Saurischia) and comments on late cretaceous sauropod diversity. Journal of Systematic Palaeontology 3, 283–318.

Xu, X., Wang, X.-L., You, H.-L., 2001. A juvenile ankylosaur from China. The Science of Nature 88, 297–300.

Young, C.C., 1935.On a new nodosaurid from Ninghsia. Palaeontologica Sinica, Series C 11, 5–27.

Zanno, L.E., 2010. A taxonomic and phylogenetic re-evaluation of Therizinosauria (Dinosauria: Maniraptora). Journal of Systematic Palaeontology 8, 503–543.

Zheng, W., Jin, X., Azuma, Y., Wang, Q., Miyata, K., Xu, X., 2018. The most basal ankylosaurine dinosaur from the Albian–Cenomanian of China, with

implications for the evolution of the tail club. Scientific Reports 8, 3711. DOI: 10.1038/s41598-018-21924-7.

Zhou, Z., 1995. Is *Mononykus* a bird?. The Auk 112, 958–963.

APPENDIX 1. Institutional abbreviations

AMNH American Museum of Natural History, New York, USA

HBV Geoscience Museum, Shijiazhuang University of Economics (previously Hebei College of Geology), Shijiazhuang, Hebei, China

INBR Victor Valley Museum, California, USA

IVPP Institute of Vertebrate Paleontology and Paleoanthropology, Beijing, China

KID Korea-Mongolia International Dinosaur Expedition–Mongolian Paleontological and Geological Institute, Mongolian Academy of Sciences, Ulaanbaatar, Mongolia

MAE Mongolian American Museum Expedition–Mongolian Paleontological and Geological Institute, Mongolian Academy of Sciences, Ulaanbaatar, Mongolia

MPC Mongolian Paleontological and Geological Institute, Mongolian Academy of Sciences, Ulaanbaatar, Mongolia

PIN Paleontological Institute, Russian Academy of Sciences, Moscow, Russia

ROM Royal Ontario Museum, Toronto, Ontario, Canada

UALVP The University of Alberta Laboratory for Vertebrate Paleontology, Edmonton, Alberta, Canada

ZMNH Zhejiang Museum of Natural History, Hangzhou, Zhejiang, People's Republic of China

ZPAL Zaklad Paleobiologii (Institute of Paleobiology)–Polish Academy of Sciences, Warsaw, Poland.

APPENDIX 2. Abbreviations used in figures

3os	Type 3 osteoderm
4os	Type 4 osteoderm
5os	Type 5 osteoderm
6os	Type 6 osteoderm
7os	Type 7 osteoderm
ac	acetabulum
anca	anterolateral nuchal caputegulum
apt A	aperture A
apt B	aperture B
apt C	aperture C
asob	anterior supraorbital caputegulum
bas	basioccipital
bas fo	basioccipital foramen
bs	basisphenoid
c	cingulum
ca	capitulum
ch	channel
che	chevron
co	coracoid
cof	coracoid foramen
cr tm pmx	premaxillary tomial crest
cs	caudosacral vertebra
csr	caudosacral rib
d	denticle
dr	dorsal rib
ds	dorsosacral vertebra
dsr	dorsosacral rib
dv	dorsal vertebra
ect	ectopterygoid
en	external naris
f	femur
fca	frontal caputegulum
fi	fibula
fm	foramen magnum
fpca	frontoparietal caputegulum
gr	groove
h	humerus
il	ilium
in bar	internarial bar
in pmx	premaxillary notch
inca	internarial caputegulum
ipmx s	interpremaxillary suture
itf	infratemporal fenestra
itp	isolated theropod phalanx
k	keel
laca	lacrimal caputegulum
lnca	lateral nuchal caputegulum
lo	lateral osteoderm
loca	loreal caputegulum
maj os	major osteoderm
mc	metacarpal
mg	Meckalian groove
min os	minor osteoderm
mnca	medial nuchal caputegulum
mso	middle supraorbital caputegulae
mt	metatarsal
mx	maxilla
nasca	nasal caputegulum
nc	neural canal
ns	neural spine
nuca	nuchal caputegulum

nuch nuchal shelf
oc occipital condyle
orb orbit
ot ossified tendon
pa parapophysis
pal palatine
par parietal
para parasphenoid
parocc paroccipital process
path pathology
pca parietal caputegulum
ph phalanx
pmx premaxilla
pmx sin premaxillary sinus
pmxo premaxillary ornamentation
poa postacetabular process
poca postocular caputegulum
poz postzygapophysis
prea preacetabular process
prfca prefrontal caputegulum
pro alv alveolar border
prot protuberance
prz prezygapophysis
psob posterior supraorbital caputegulum
psr parasacral rib
psv parasacral vertebra
pt pterygoid
pt fo pterygoid foramen
q quadrate
qh quadrate head
qjh quadratojugal horn
r radius
sc scapula
sn n supranarial notch
snca supranarial caputegulum
socc supraoccipital
sp small process between the foramen magnum and the nuchal shelf
sqh squamosal horn
sr sacral rib
st sternal plate
sv sacral vertebra
t tibia
tp transverse process
tu tuberculum
u ulna
v vomer

APPENDIX 3. Data matrix related to chapter V-1

Gargoyleosaurus parkpinorum

0110000001111000000?221011000101??001?210??110121100000012?0111100?010
?0100101011111110??000010101????1???0?0????????????????????????????0???????
???211001????122221??2100??10202??2???

Akainacephalus johnsoni

11110100?12100010??222120001111?11120211?1110?212010?10110101100001?
?11111000?11110?110???????1?00111110001111O?0?1?00110?1?11111100?00??1
00???1011010????23??1?0231???1110??1222

Aletopelta coombsi

??
???????????111?????????????0???0?0?????????????????1??????0?????????????11
11??1?2??????2????1???3?1???

Ankylosaurus magniventris

11110100?11?112101?2310101111101110l1?210?111012120102111111111000011l
1111111011110O1?211111???1111111??000011311???01110010????0?????011010
0???2010111???122?????22100??????1??12

Anodontosaurus lambei

11110100?11111110?123101011111111011121011110121211021111111110000111

1111111011110 01?21111????????1110?00?11111???????????1110011?101001??

????0101111 2?122??????220???????????23

Cedarpelta bilbeyhallorum

11100?00?01?0?0????10000?00?100?1000?1?0??1?0????000??101?11110??0???0

1?1111011??1????00??????1??????1100??0?0???11?????????????????011010???

?10101??????????????????????????????

Chuanqilong chaoyangensis

?1?1???101?111?????????????

????1111?0???111????1??101???????000?1????0100001?11100011?0000100??221

1?11102??2?????0?????0????????00

Crichtonpelta benxiensis

111101???????????1?1000000011????000?211011?012110101111110???11000?1?0

11111?????????????????????1101111110010?0????00101111010?11100?1?1??0000??

??20101110????????????????????????????

Dyoplosaurus acutosquameus

??1??????????????????2?10??????????????11?1???0?????1021?????????????????????

????????????????1????????????????0100111?1????????????110011?101????0??2201

?111121122??????????1111??12211

Euoplocephalus tutus

1111010011111111101123101011111111101112111111012120102111111111000011111111101111101121111??0111111110000011111011011100101111001111010010001?120101111211222112022 10?111???12?12

Gobisaurus domoculus

11100110?01101010??100000000101?1000?110?111012120100111?011110000??00110100?1????????1???????????11????????11????????????????????0????0?0000??

?1?????????????????????0??????????00

Liaoningosaurus paradoxus

??

??????????0111??????????0??0???01010????0?0??00?1110001100100 00?102?00?111000????????????????????????

Kunbarrasaurus ieversi

111000????????0????2???????1101?10???210??1??????00???001111110???1??01

001010?1?11?????11?0??01??????10?????0??1???????????0010???0?00?000????

??????????121????11100111O2?1212??

Nodocephalosaurus kirtlandensis

111??????????????????2?21???1?1???1011?22????1012120?0??1??11???????????1?

111??????????????????????????????0??

???????2222120????0???????????

Nodosaurus textilis

??

??????????????????????111111???000?0????????????111??1101?????????1111?1

?011?12????2??????000?0312???

Pinacosaurus grangeri

111101001111110101?01000200?1111011?20221011001211O1??1111111110000111

011011101111100111111O??01?11111100?001111101001l?10?0111100111101001

00101201011112112222????02210101020?12212

Pinacosaurus mephistocephalus

11110100??????101???0?010???11???0?1?211?1100222101??1?0??????????????

???????1?10???1111101????????11????011111????1111??0?11100????????10?10?

??????????122????022100???1???????

Jinyunpelta sinensis

11100001111??011??1000???011????000?21?0??????1?0??????????????????????

??????1????0101??????01??1?11??????0?1?1??????1??1????100?1??0?00?1?101?

???1?????????????????1????1???11

Saichania chulsanensis

1111000111111111??22221101110111011121101110121211011111111111000111

01111111111110112111101111112?11?????????????1??1?110?01???????????10100

101??????????122????0222000??10??????

Scolosaurus cutleri

11110?????????1??1?23101?1111????011?211??1101212110211111111107???????1

11111???????????111???????1???100?00111111011?1110??0?11100110102001????

1????11?12112222?????2210111110112212

Shamosaurus scutatus

11100110?011?1010??100000000101?1000?110?11101212010111010111110011?

0011011??1111000?11??

????????????1???????2210????????????

Talarurus plicatospineus

11110000111110011102311110211111?10110221011 10?22211021111111110???01?

?11{0 1}1010??11?????????????????11?0111000001111101101111000?111001111010

0100101201011 11??12????????2?0?????0??????

Tarchia kielanae

11110001111?1?111??222212021111?1122?221?11012222110101010111110000?01

01111111111110112111 10??

????????????????????????????????????

Tsagantegia longicranialis

11100000?11111000??2210100111110101 1?210?1110121?0101111111111110001?0

01111?10?????????11??0??

????????????????????????????????????

Zaraapelta nomadis

111?00???????????02?22????2?1???1?221220?11101212110001111111111001?1??

1111110???

??????????????????????????????????

Ziapelta sanjuanensis

1111010??11??1110??2310101111111??011?211?11101???01021??????1?0?0?1???1

111??0?????????1???

?????????2???????220????????????

Zuul cruravastator

11110100?110?1110??2310101111111?1012?21111110121211021111111110000 1?0

0111111?1111000?001000??0???1?1??0?0?011111?????????????1??0011?????????

???????????122????1?????1112??12211

APPENDIX 4. Character statements related to chapter V-2

Below is the character from Penkalski and Tumanova (2017), which is modified in this study.

Character 5. Remodeled squamosal horns

0: absent

1: present

Below are the two new characters that are added in this study.

Character 22. Skull in lateral view

0: quadrate-quadratojugal region normal

1: quadrate-quadratojugal region anteriorly situated

Character 23. Skull in occipital view

0: interpterygoid vacuity non-visible

1: interpterygoid vacuity visible

APPENDIX 5. Data matrix related to chapter V-2

Pinacosaurus grangeri **ZPAL MgD I/111**

01?11?01001?01?10000?00 11121??11210??1011?1???

INBR 21004

01211011?00111010010100

MPC D100/1338

012111010011??01?1?110?

MPC 100/151

10000100011000000101111

MPC-D 100/1353

11121?11111000101011011

PIN 3142/250

11121?11121000101011000

국문초록

갑옷공룡(Ankylosauria)은 사족보행인 초식 공룡의 한 무리로 골편(骨片, osteoderm)들이 융합된 두개골(頭蓋骨, skull)과 몸통의 배측면(背側面, dorsolateral)에 골편들이 부시상(副矢狀, parasagittal)으로 덮고 있는 것이 특징이다. 2007년과 2008년 사이에 한국-몽골 국제공룡탐사에 의해 갑옷공룡 표본들이 고비사막에서 추가로 발견됐다. 본 표본들은 상부 백악기 Cenomanian–Turonian 바얀시레층(Bayanshiree Formation), middle–upper Campanian 바룬고욧층(Baruungoyot Formation), 그리고 upper Campanian–lower Maastrichtian 네메겟층(Nemegt Formation)에서 발견됐다. 바얀시레(Bayan Shiree)의 바얀시레층에서 산출된 새로운 두개골 표본 세 개를 통해 *Talarurus plicatospineus*의 정의를 재정립할 수 있었다. 힐멘자프(Hermiin Tsav)의 네메겟층에서 산출된 두개골을 포함한 부분적인 두후골격(頭後骨格, postcranial)은 새로운 분류군으로 확인돼 *Tarchia tumanovae*로 명명됐다. 힐멘자프의 바룬고욧층에서 산출된 새로운 두후골격 표본은 불분명한 안킬로사우루스과(Ankylosauridae)로 분류됐다. 계통발생 분석(phylogenetic analysis) 결과는 *Talarurus*속이 *Saichania chulsanensis*, *Tarchia kielanae*, 그리고 *Zaraapelta nomadis*를 포함한 아시아의 파생된 안킬로사우루스아과(Ankylosaurinae)의 자매 분류군(sister taxon)임을 보여준다. 또한 안킬로사우루스아과의 아시아에서 북아메리카 대륙으로의 이주(移住, migration)가 Cenomanian 이전에 있었음을 보여준다. *Talarurus*속과 바얀시레층의 또 다른 안킬로사우루스과인 *Tsagantegia*속 사이의 주둥이 형태 차이는 이들의 생태지위 분할(niche partitioning)을 시사한다. *Tar. tumanovae*의 인골뿔(鱗骨–, squamosal horn)은

외피층(外皮層, external dermal layer)과 그 밑에 있는 진정인골뿔(眞情鱗骨–, squamosal horn proper)로 나뉜다. 외피층의 불규칙한 복면(腹面, ventral) 가장자리는 흡수된 표면을 나타낼 수 있으며, 이는 일부 안킬로사우루스아과의 인골뿔이 극단적인 개체발생적(ontogenetic) 변화를 겪었음을 시사한다. 또한 배천추(背薦椎, dorsosacral vertebra)의 늑골(肋骨, rib) 부위와 꼬리의 국소적 골절 흔적은 이들의 세력투쟁행위(agonistic behavior)의 증거를 제공한다. *Tar. tumanovae*의 비대칭인 꼬리곤봉(tail club)은 이런 행위로 인한 뼈의 비정상적인 성장 때문인 것으로 보인다. 더 나아가, 안킬로사우루스과(Ankylosauridae)의 섭식방법은 상부 백악기 middle Campanian–early Maastrichtian 중에 대량섭식(bulk-feeding)에서 선택적 섭식(selective feeding)으로 바뀐 것으로 보인다. 안킬로사우루스과의 이런 생태지위 변화는 서식지 변화와 다른 대량섭식 초식 공룡과의 경쟁 때문인 것으로 여겨진다. 아시아의 안킬로사우루스과는 후두골격이 뻣뻣해지고 뒷발의 지골(趾骨, pedal phalanges) 수가 줄어드는 방향으로 진화했다. 안킬로사우루스과에는 두 가지 형태의 측면(側面, flank) 갑옷, 하나는 가시형(spine-like)의 골편, 그리고 다른 하나는 용골(龍骨, keel)이 발달한 능형(菱形, rhomboid)의 골편이 있음이 확인됐다. 안킬로사우루스과에서는 땅파기와 관련된 독특한 해부학적 특징들도 확인됐다. 땅파기와 관련된 특징들로는 배복(背腹, dorsoventral) 방향으로 납작한 방추형(紡錘形, fusiform)의 몸통, 광범위하게 융합된 척추, 전후(前後, anteroposteriorly) 방향으로 넓은 늑골, 잘 발달된 삼각흉근능선(三角胸筋稜線, deltopectoral crest)을 가진 강건한 상완골(上腕骨, humerus), 잘 발달된 주두돌기(肘頭突起, olecranon process)를 가진 짧은 척골(尺骨, ulna), 모종삽형(trowel-like) 앞발, 그리고 지골 수가 줄어든 뒷발이 있다. 비록 굴착형(fossorial) 동물은 아니었지만, 안킬로사우루스과는 자기 방어와 생존을 위해 땅을 잘 파헤쳤을 것으로

보인다. 더 나아가, 본 학위논문에서는 몽골에서 알려진 10종의 갑옷공룡에 대한 분류학적 리뷰를 실시하였다.

주요어: 안킬로사우루스과, 안킬로사우루스아과, *Talarurus plicatospineus*, *Tarchia tumanovae*, 생태지위 분할, 몽골
학번: 2017-34699

감사의 글

무엇보다 저의 지도교수님이신 이융남 교수님께 감사드립니다. 교수님께서는 저에게 공룡을 연구할 수 있는 아주 소중한 기회를 주셨습니다. 덕분에 세 살배기 때부터 꿔온 꿈을 이루게 됐습니다. 교수님의 가르침을 받아 화석을 단순히 분류하고 기재하는 데 그치지 않고 현생 생물과의 비교를 통해 고생물의 생태와 진화 과정을 밝혀내는 연구를 할 수 있었습니다. 교수님이 아니셨다면 저는 학위과정 동안 양질의 논문들을 게재하지 못했을 것이라 장담합니다. 더 나아가, 교수님께서는 제게 훌륭한 학자보다는 좋은 사람이 되라고 하셨습니다. 교수님의 가르침 평생 잊지 않고 살아가겠습니다. 아시아 공룡연구의 권위자이신 이융남 교수님의 지도를 받을 수 있어서 영광이었습니다. 앞으로도 연구를 계속하면서 학자로서의 자질을 습득하고 성장해 나가는 모습을 보여드리겠습니다. 교수님의 자랑스러운 제자가 되도록 노력하겠습니다.

지도교수님께서 이끄셨던 한국-몽골 국제공룡탐사팀이 아니었더라면 이 학위논문에 포함돼 있는 귀중한 화석들을 연구할 수 없었을 겁니다. 국제공룡탐사에 참여하신 모든 선배 학자 분들께 특별히 감사드립니다. 특히 갑옷공룡 화석 발굴에 참여하신 Rinchen Barsbold 박사님(Mongolian Academy of Sciences), Louis Jacobs 교수님(Southern Methodist University), Philip Currie 교수님과 Eva Koppelhus 박사님(University of Alberta), Michael Ryan 교수님(Carleton University), Yoshitsugu Kobayashi 교수님(Hokkaido University), Octávio Mateus 교수님(Universidade Nova de Lisboa), Phil Bell 박사님(University of New England), 김남수 교수님(연세대학교), 이항재 관장님(지질자원연구원

지질박물관), 송교영 박사님(지질자원연구원), Michael Polcyn 연구원님(Southern Methodist University), 그리고 Robin Sissons 연구원님(University of Alberta)께 감사드립니다. 갑옷공룡 화석들을 깔끔하게 처리해주신 Clive Coy 연구원님(University of Alberta)과 김도권 주무관님(화성시청)에게도 감사드립니다.

연구를 하는 동안에도 많은 선배 학자 분들의 도움을 받았습니다. Tatiana Tumanova 박사님(Russian Academy of Sciences), Lawrence Witmer 교수님(Ohio University), Badamkhatan Zorigt 박사님(Mongolian Academy of Sciences), Tomasz Szczygielski 박사님(Polish Academy of Sciences), 그리고 Jelle Wiersma 연구원님(James Cook University)은 여러 갑옷공룡에 관한 문헌과 사진들을 공유해주셨습니다. Junpei Kimura 교수님(서울대학교)의 비교해부학 수업은 공룡의 습성과 생태를 추정하는데 큰 도움이 됐습니다. 학술지에 투고한 논문 원고들을 심사해주신 James Kirkland 박사님(Utah Geological Survey), Alexander Averianov 박사님(Russian Academy of Sciences), Jingmai O'Connor 박사님(Field Museum), Paul Penkalski 박사님(University of Pennsylvania), 그리고 본 학위논문을 심사해주신 정해명 교수님(서울대학교), 이성주 교수님(경북대학교), 허영숙 교수님(서울대학교), 우주선 교수님(서울대학교)은 건설적인 비판을 해주셨고 조언과 격려도 아끼지 않으셨습니다. 덕분에 논문의 질을 많이 향상할 수 있었습니다. 이 은혜 잊지 않겠습니다.

Institute of Paleontology (Mongolian Academy of Sciences) 소속의 Khishigjav Tsogtbaatar 박사님, Badamkhatan Zorigt 박사님, Ligden Barsbold 필드매니저님, Idersaikhan Damdinsuren 연구원님, Ganzorig Bayasgaa 연구원님, 그리고 S. Baaskaa 연구원님에게도 감사드립니다. 이분들 덕분에 '공룡의 땅'인 고비사막 한가운데서 즐거운 마음으로 공룡

화석들을 발굴할 수 있었습니다. 잔인한 더위 속에서 목숨을 잃지 않을 수 있었던 건 이분들 덕분입니다.

학위논문에 들어간 갑옷공룡 복원도들은 최유식 작가님과 Jed Taylor 작가님이 그려주셨습니다. 비늘과 골편 하나하나에 쏟아부은 정성에 몹시 감탄했습니다. 멋진 복원도들 덕분에 연구결과를 매스컴을 통해 널리 소개할 수 있었습니다. 정말 고맙습니다.

학위과정을 마무리하는 데 친애하는 연구실 동료들을 빼먹으면 섭섭합니다. 특히 이성진, 김수환, 윤한상, 김뇌헌, 손민영(University of Minnesota), 김도현, 그리고 김현욱 학우에게 깊은 감사 드립니다. 이성진 학우는 칠칠치 못한 저를 매번 도와주고 어려운 부탁도 흔쾌히 들어주는 그릇 큰 친구입니다. 항상 솔직하고 건설적인 의견을 주는 든든한 아군입니다. 김수환 학우는 무더운 고비사막 한가운데서도 유머를 잃지 않는 유쾌한 녀석입니다. 걱정거리가 있으면 진솔하게 얘기를 나눌 수 있는 믿음직스러운 동생입니다. 윤한상 학우는 실없는 농담에도 크게 웃어주는 넓은 마음의 소유자입니다. 먼 곳에 갈 때 함께 가주고, 먹을 게 있으면 항상 나눠주는 의리 있는 사나이입니다. 김뇌헌 학우는 저의 지루하고도 긴 이야기를 매번 불만 없이 들어주는 점잖은 동생입니다. 짜증 날 법도 한 연구실 형들의 장난에도 항상 웃어주는 착하디 착한 녀석입니다. 손민영 학우는 고생물학에 대한 열정 하나만큼은 최고인 동료입니다. 저에게 영감을 많이 제공해주는 은혜로운 존재입니다. 천하장사인 김도현 학우는 아마도 연구실에서 가장 든든한 동생일 겁니다. 항상 형들의 말을 귀담아 들어주는 고마운 친구입니다. 김현욱 학우는 화석 분류, 그림 그리기, 글쓰기, 야구, 연극 등 못하는 게 없는 팔방미인입니다. 저에게 매번 웃음을 선물해주는 위트 있는 동생입니다. 그들이 있어서 연구실에서의 하루하루가 너무 즐거웠습니다. 연구실 동생들에게 특별한 빚을 졌습니다.

고생물 연구를 하는 다른 동료들에게도 감사를 표하고 싶습니다. 정종윤 학우(전남대학교), 전주완 학우(Chinese Academy of Sciences)와는 연구와 관련된 아이디어들을 적극적으로 논의했습니다. 게다가 이 둘은 제게 연구에 참고할 만한 사진과 그림 자료들을 제공해줬습니다. 최병도 박사님(국립대구과학관)은 지난 16년 동안 진화에 대한 지식을 아낌없이 알려준 소중한 친구입니다. 제가 진화에 대해 알고 있는 거의 모든 건 이 친구가 알려준 거나 다름없습니다. 학부 새내기 때 그저 공룡 학명이나 외우고 다니던 시시한 저를 성선택과 생태적지위 분할에 관심 갖게 해 준 장본인입니다. 진심으로 고맙습니다.

가족의 사랑과 믿음이 지금의 저를 만들었습니다. 공룡 박사라는 저의 정신 나간 꿈을 끝까지 응원하고 지원해주신 아버지, 어머니, 그리고 항상 밝은 미래를 향해 전진하는 동생에게 언제나 고맙습니다. 한때 저의 담당 편집자였던 사랑스럽고 귀여운 아내, 그리고 아직 엄마 뱃속에서 자라고 있는 조그마한 무민이 덕분에 저는 요즘 너무나도 즐겁고 행복한 나날들을 보내고 있습니다. 이 학위논문을 이들에게 바칩니다. 사랑합니다.

Cretaceous ankylosaurs of Mongolia

: implications for paleobiogeography, paleoecology, and evolution, with a taxonomic review of Mongolian armored dinosaurs

지도 교수 이 융 남

이 논문을 이학박사 학위논문으로 제출함

2022년 8월

서울대학교 대학원
지구환경과학부
박 진 영

박진영의 이학박사 학위논문을 인준함

2022년 8월

위 원 장 정 해 명 (인)

부위원장 이 융 남 (인)

위 원 이 성 곤 (인)

위 원 허 영 숙 (인)

위 원 우 주 선 (인)